Hydraulic drivetrains for wind turbines

Radial piston digital machines

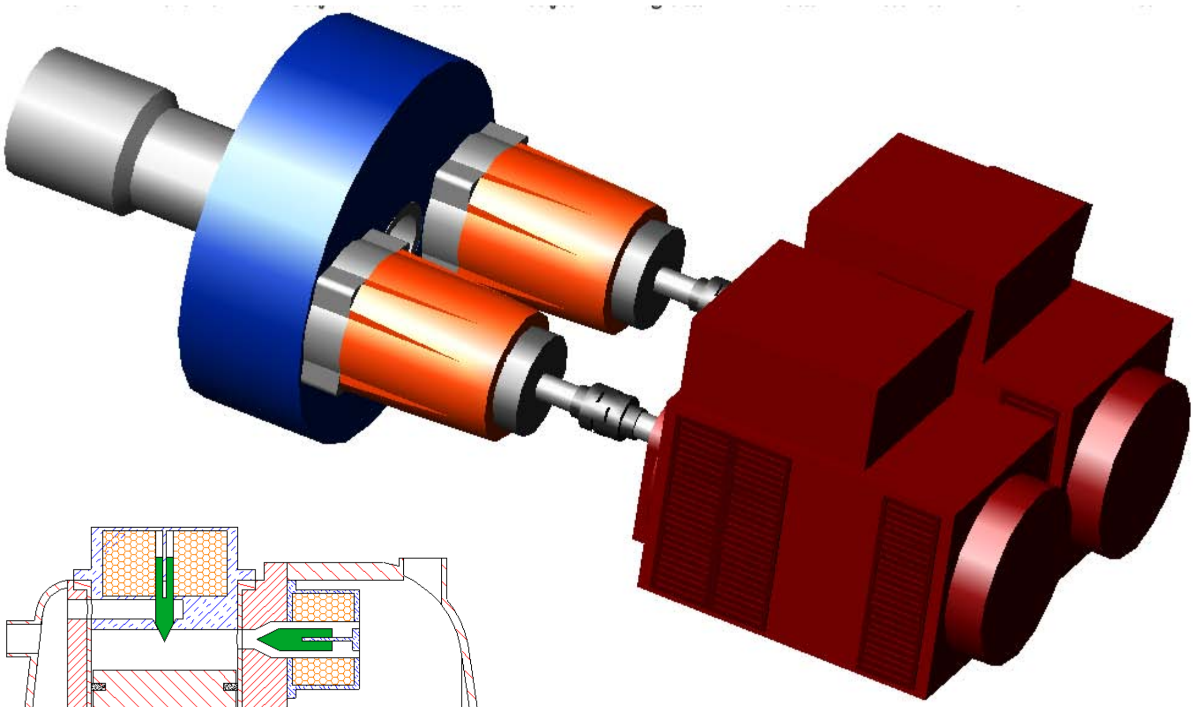

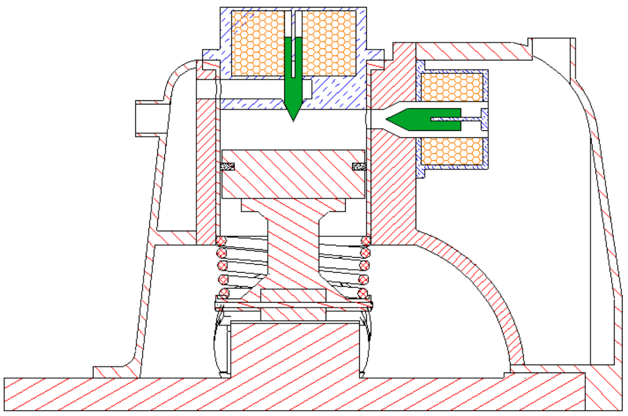

Ivan G. Piña Rodriguez

M.Sc. Sustainable Energy Technologies

Sustainable Electrical Engineering

2010-2012

TU Delft Delft University of Technology

Hydraulic drivetrains for wind turbines

M.Sc. Thesis

Graduation project for
M.Sc. in Sustainable Energy Technology
Delft University of Technology

Thursday 5th July 2012 at 14:45 hrs

By:
Ivan Gustavo Piña Rodriguez

At:
Electric Power Processing
Sustainable Electrical Engineering
Faculty of Electrical Engineering, Mathematics and Computer Science

To my family, for my people…

Preface

If the iron is blunt, and one does not sharpen the edge,
he must use more strength, but wisdom helps one to succeed.
Ec 10,10

Two years ago, when I decided to pursue a Master in Science degree I was conscious that this would be a new challenge in my professional life. Enlightening, intense and short are three different adjectives that can accurately represent my feelings about this ending chapter. Still, none of them can represent the past two years of my life as well as complete satisfaction. This period will be remembered for me with joy as time of large personal and professional growth. In fact, I am very pleased with the results, personal satisfaction and experiences that I've already collected.

On the other hand, being abroad my homeland brought me sobriety and the capacity to look from different perspective all things that are needed back there. My personal believes and previous formation gave me, some time ago, the need of being an active player in my medium. But my studies at Delft University of Technology, gave me confidence that today I am better prepared than two years ago to face future challenges when playing an actor roll in my society.

The key to successfully close this chapter of my life is related with the outstanding mental, physical and environmental health that I had enjoyed in the past two years. I believe that this optimal environment does not come from luck or destiny; but it is a personal gift given by my Lord, the almighty God. This is why I want to thank Him for this valuable gift.

The completion of this degree required the communal interaction of several people and institutions. Therefore I want to use this opportunity to thank all them for their support. In the front line is my family, who always had and will encourage me to accept and overcome important challenges; then, I want to thank to the Government of my home country (Mexico), who through the Consejo Nacional de Ciencia y Tecnología (CONACYT) gave a scholarship that gave me economical certainty.

Finally, I want to offer special thanks to my graduation project advisor, Dr. Ir. Henk Polinder, who took me under his personal supervisory and gave me freedom to be my own director in this graduation project. Also I want to thank the graduation committee members for their support and feedback: Prof. Dr. Ir. Gijs van Kuik, Prof. Dr. Ir. Bram Ferreira and Ir. Niels Diepeveen. I also thank, in general to members of the Electrical Power Processing department (section of Sustainable Electrical Engineering) in the Faculty of Electrical Engineering, Mathematics and Computer Science at Delft University of Technology for being my second home in the past nine months.

Delft, The Netherlands
June 2012
Ivan Gustavo Piña Rodriguez

Table of Contents

List of Symbols

$(\hat{\imath} \quad \hat{\jmath} \quad \hat{k})$ Unity vectors
A_R swept rotor area
A_p cross section of the moving piston
A_u area of the orifice through which the fluid is passing
$C_{d,u}$ discharge coefficient
C_p power coefficient
C_x and C_y force reactions *felt* by the camshaft
D_h hydraulic diameter
D_R rotor diameter
D_c cylinder diameter
D_{cms} External diameter of the camshaft
E_{YD} annual energy yield in Wh
E_f wound excitation voltage
F_{IN} Transmitted force(to the camshaft) due to power compression of the hydraulic fluid
F_P force due to fluid compression
F_{fp} friction force between the piston's body and the cylinder sleeve
F_{fr} friction force between the piston ring and piston sleeve
F_{gp} weight force for the combined mass of piston-ring-rod-bearing assembly
F_{grc} weight force for all rotating parts
F_{sp} force absorbed by the return spring dependent on displacement r_{C1}
G_R Center of rotation of roller
G_{gpc} Center of mass of piston ring roller assembly
G_{grc} Center of mass of rotating parts
I_a stator current
J_{G_R} polar moment of inertia in the $\hat{k}$ axis
J_C polar moment of inertia of rotating parts
J_G generator moment of inertia
J_{RT} polar moment of inertia of the wind turbine rotor
K_{sp} spring stiffness constant
K_w friction coefficient for turbulent flow
L_p length of the pipes
M_{C1} mass contained inside the pressure chamber C1
N_{fp} associated normal force to friction force F_{fp}
N_{fr} associated normal force to friction force F_{fr}
P_D Discharge pressure
P_S Suction pressure
Q_{in} input volumetric flow
Q_{out} output volumetric flow
$R_{Artemis}$ rotor radius for the computer model
R_{BDC} minimum value for r_{Cn} at the bottom dead center
R_{DFIG3G} rotor radius of 45 m
R_{TDC} minimum value for r_{Cn} at the top dead center
R_{pr} radius of the camshaft's prime circle
R_{rlr} Roller radius
R_s synchronous resistance
S_l slip of the machine expressed in decimal value

$T_{F_{IN}}$	torque due to transmitted load to the piston at an effective lever arm
T_{IN}	prime's mover torque
T_{OUT}	net torque in the motor shaft
T_V	torque product of friction forces in the valve's disc
$T_{el,3\varphi}$	electrical torque
T_{eq}	equivalent time
T_{idl}	parasitic torque due to idling cylinders
T_{yr}	total number of hours in one year
U_a	wind speed at nacelle height
V_{C1}	variable volume comprehended between the upper part of the piston and the top of the cylinder chamber
V_{C1}	control volume given by pressure chamber C1
$V_{NET,C1}$	net fluid volume that fits into the pressure chamber when piston is at the BDC
V_{NET}	Net volume
$V_{ext,C1}$	volume comprehended between the upper most part of the pressure chamber cavity and the top of the piston at the TDC
V_t	voltage at the terminals
$W_{Cu,loss,3\varphi}$	Cupper losses in the generator
$W_{El,Out}$	three phase electrical power delivered by the generator
W_{El}	Electric power
W_{Hyd}	Hydraulic power
$W_{IN,C1}$	input power to drive cylinder C1
$W_{IN,C1}$	input power to drive cylinder C1
$W_{IN,Req}$	input shaft power
W_{Mech}	Mechanic power
$W_{R,Grid}$	rated power fed to the grid
W_{Rat}	Rated power
W_{aero}	aerodynamic power
$W_{loss,fr,q_u,P}$	power losses due to friction in piping
$W_{loss,fr,q_u,T}$	power losses due to turbulent flow
$W_{m,us}$	mechanical power effectively transferred to fluid
X_S	Synchronous reactance
a_{C1}	Effective lever arm
b_e	signed distance from point C to E in Figure 3.5
f_G	Scale down factor for generator
f_{OWT}	scale down factor based on weight
f_{lc}	frequency of the load cycle
l_e	distance between the center of the camshaft and the center of rotation
l_{fp}	distance from the roller axis to the concentrated force N_{fp}
l_{fr}	distance from the roller axis to the concentrated force N_{fr}
l_{grc}	distance between the center of rotation and the center of mass for rotating parts
l_{rp}	Combined length of piston and rod assembly
$m_{G,1MVA}$	Mass of 1MVA synchronous generator
m_{gp}	net mass of piston-ring-rod-roller assembly
m_{grc}	mass of all rotating parts
n_N	maximum number of cylinders operating at rated power
p_{C1}	pressure in chamber of cylinder C1
q_u	immediate flow through an orifice
r_{C1}	Reciprocating displacement of the upper part of the piston C1 respect the piston sleeve
$\dot{r_{C1}}$	translational speed of piston in cylinder C1
$\ddot{r}_{C1}$	second time derivative(acceleration) of r_{C1}

s_a	distance between the prime circle and the center of rotation of the roller bearing measured over the follower axis line
$v_{r_{C1},A}$	velocity of the follower
$v_{T,E}$	tangential speed of point E seen by a static observer at point C in Figure 3.5
v_{eff}	effective fluid speed
$\ddot{x}$	acceleration in the horizontal axis
β_o	Bulk modulus of fluid
γ_{sa}	Phase shift angle in radians
ε	angular displacement of the motor shaft
$\dot{\varepsilon}$	angular speed of the motor shaft
$\dot{\varepsilon}_s$	synchronous angular speed (1500 RPM)
$\ddot{\varepsilon}$	Angular acceleration of the motor shaft
η_{Cu}	partial efficiency due to copper loses
$\eta_{G,eff}$	overall efficiency of the generator
η_{Manuf}	upper limit of efficiency according with manufacturer in the generator
η_P	Pump efficiency
η_{Vol}	volumetric efficiency of the machine
η_{dv}	dynamic viscosity
η_m	mechanic efficiency
η_m	Motor efficiency
η_{mh}	Mechanic-hydraulic efficiency
θ_0	absolute starting position at t=0 of the camshaft angular displacement
θ	Angular displacement of monocylinder model
$\dot{\theta}$	angular speed of the camshaft
$\ddot{\theta}$	second time derivative of camshaft angular displacement
$\theta_{RT,0}$	Original angular position of the rotor
θ_{RT}	Angular displacement of rotor shaft
$\dot{\theta}_{RT}$	Angular rotor speed
$\ddot{\theta}_{RT}$	Angular rotor acceleration
μ_f	friction coefficient ($\dot{r}$ dependent)
ρ_{Mach}	Machine density
ρ_{Pow}	power density
ρ_{air}	air density
ρ_o	fluid density
χ_{Cu}	copper loss factor
ϵ_0	pretensioning of the spring
Δp	differential of pressure between reservoirs
$\Delta V_{C1,Rat}$	rated cubic displacement for cylinder C1
COE	Levelized cost of energy
N	Total number of cylinders in the machine
PF	power factor
$\Sigma F_{\hat{\imath}}$	force balance in $\hat{\imath}$ direction
$\Sigma F_{\vec{r}}$	force balance in the radial coordinate r
$\Sigma M_{\hat{k},G_R}$	moment balance respect to center of mass G_R
$\Sigma M_{\hat{k},C}$	moment balance respect to the point C
CF_o	compressibility factor for the used fluid (inverse of Bulk modulus)
Re	Reynolds number
cf	capacity factor
f	friction factor for laminar flow ($Re < 2500$)
δ	power angle
ϕ	pressure angle

Abbreviations

ADD	Artemis Digital Displacement
TDC	Top dead center
BDC	Bottom dead center
DFIG3G	doubly fed induction generator with three-stage gearbox
DDSG	direct drive synchronous generator
DDPMG	direct drive permanent magnet generator
PMG1G	permanent magnet generator with single-stage gearbox
DFIG1G	doubly fed induction generator with single-stage gearbox

Subscript

P	Pump
m	Motor
RT	Rotor
Rat, R	Rated

IMPORTANT:

In this document, **symbol W has been reserved to describe Power**. Although this is not conventional, it was done **to avoid confusion with pressure** related terms.

1. Introduction.

Hydraulic systems are widely used in the wind turbine industry. In most cases, their use is limited to auxiliary mechanisms (like pitch or yaw system) intended to implement active control in modern wind turbines. Although in the late 1970s and early 1980s hydraulics were considered for large power transfer as substantial part of the drivetrain system; until early 2000s they were barely used for such task. Still, hydraulics might start to make their comeback to the market of large power transfer in the past decade since wind energy market has evolved in a more selective and competitive one.

The Electrical Power Processing research group, part of the section of Sustainable Electrical Engineering in the faculty of Electrical Engineering, Mathematics and Computer Science at Delft University of Technology is involved in the study of drivetrain technologies in wind turbines. One of the main ongoing research branches deals with current and future technologies employed in wind turbine industry. The main target of such research is to help extending the use of wind energy by reducing energy production cost so renewables can spread over. In such combined effort, different technologies of drivetrains are quantitatively analyzed so new perspectives can be explored.

This thesis presents a quantitative approach to the use of hydraulic systems for large quantities of power transmission. Special focus is paid to hydrostatic transmissions, particularly to those piston based machines that can be integrated in a wind turbine. The subject is boarded by building a semi-dynamic model that can integrate the operation principle either digital systems or simply conventional piston based machines. Then a study case of digital hydraulics is analyzed so some performance indicators can be built. Such performance indicator will eventually help drawing conclusions about the use of hydraulics in wind turbine industry.

The two most important goals of this chapter are to show how the contribution of this thesis relates with wind turbine industry and to introduce the reader with some basic concepts that will serve as basis for the formulation of the main research question.

Within this section, generalities in terms of the current state of the wind turbine industry are initially presented. Then some very basic energy concepts are recalled to later being used in the discussion of common technologies in drivetrain systems. In there, components and their function will be introduced. Then some concepts about hydraulics and fluid power are introduced. Then the main research question is presented to later summarize the goals and contribution of this thesis.

1.1. Wind Energy Industry

A sustained increase in power demand, an ongoing depletion of fossil fuels and social awareness about carbon emissions had set the scheme for innovative solutions in the energy sector. Based on those alternatives, an entire new industry is today growing steady. This industry targets all sustainable energy technologies. These technologies aim to transform energy from natural, abundant and renewable energy sources like solar, geothermal and wind.

In the past few decades, wind energy industry has been placed as one of the most suitable solutions for large scale implementation. Although there are a wide variety of wind energy harvesters, this branch of renewables is today mainly represented by the horizontal axis wind turbine.

The current wind turbine industry went from being a niche to the mature market in less than half century. The success of this industry can be attributed to low generation cost, large efficiency levels and large product lifetime. Figure 1.1presents the global cumulative installed capacity from 2000 to 2010[*1*]. As it can be in the graph, there is a tenfold in installed capacity within the decade. This rapidly evolving market has called the attention of large number of manufacturers. The range of production goes from simple components borrowed from other industries (like brake pads, power electronics, etc) to full wind turbine manufacturers. Also, the use of new design and production techniques had leaded the way to cheaper and more efficient and durable wind turbines.

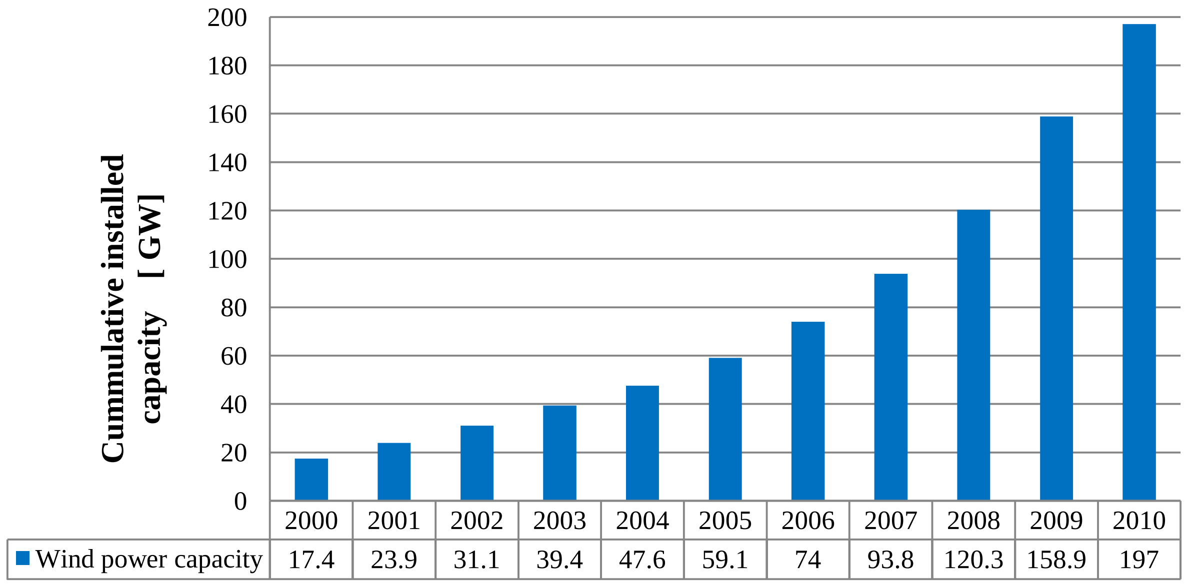

Figure 1.1 Global cumulative wind power capacity 2000-2010(GWEC 2011; EWEA 2011)

Current manufacturers are constantly exploring new alternatives to make wind turbines more attractive to investors. Therefore, continuous optimization is always encouraged. There are several areas where there is still room for optimization; one of them with a particular interest is reliability. Sometimes, reliability can be improved by reducing the number of components and having more robust systems. This is why there is a large room for optimization in the drivetrain system, where the larger number of components can be found. Although optimizations is encouraged, radical innovations are not always welcome by the industry. This is due to the fact that market and production techniques are more or less young to be entirely replaced by significantly different concepts. Before going in depth into wind turbines, lets make a small brake to recall some important energy concepts.

1.1.1. Energy conversion

Energy conversion is the process in which a particular energy source is transformed into another. There are three common means used to high power transfer: mechanic, electric and fluid power [*2*]. They are presented in Table 1.1.

Energy conversion processes normally occur in a particular machine (i.e. an electric motor transforms electric to mechanic power). On the other hand, power transmission makes reference to the way in which the energy is conducted into a conversion process (i.e. wires conducting current into the electric motor, or a rotating shaft as output for the motor). This is sketched in Figure 1.2.

Power transfer mechanism					
Electric		**Fluid**		**Mechanic**	
Concept	*Units*	*Concept*	*Units*	*Concept*	*Units*
Voltage (V)	$[V]$	Pressure (p)	$[Pa]$	Torque(T)	$[Nm]$
Current (I)	$[A]$	Vol. Flow (ϕ_v)	$[m^3/s]$	Angular speed(ω)	$[rad/s]$
$\boldsymbol{Power = VI}$	$[W]$	$\boldsymbol{Power = p\phi_v}$	$[W]$	$\boldsymbol{Power = T\omega}$	$[W]$

Table 1.1 Power transfer mechanisms

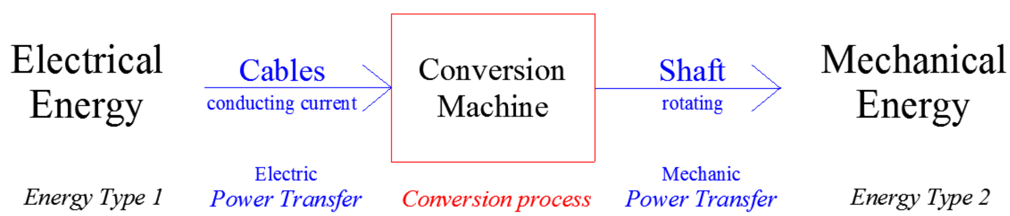

Figure 1.2 Energy conversion and power transfer

Bringing these concepts to the wind energy scheme, wind turbines are employed to convert aerodynamic energy into electrical energy. In such machinery, a primary energy conversion process occurs when aerodynamic energy is transformed into mechanical. This first process is achieved by the interaction of the rotor blades[1] with an air flow. Once mechanical energy is present in the main rotor shaft, this energy is transformed into electrical in a secondary energy conversion process. This last process occurs in the drivetrain system. A drivetrain system might use all the three different means of power transfer to convert the mechanical energy into electrical. This is illustrated on Figure 1.3, where the typical energy conversion process in wind turbines is presented.

[1] Aerodynamic shaped geometries capable to incorporate kinetic energy from a fluid into a rotating shaft.

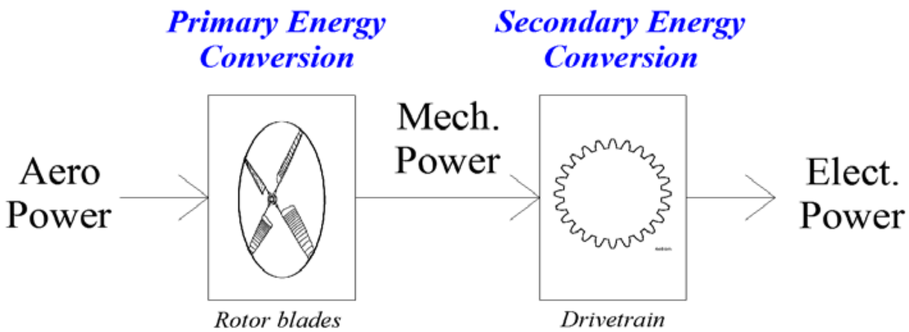

Figure 1.3 Energy Conversion Process in a wind turbine

1.1.2. Drivetrain Technologies

In this document, the ***drivetrain*** concept will be used to refer only the engaged machinery in the secondary energy conversion process in a wind turbine. This means: the one involved into transform the available mechanical energy into the desired format[2] of electrical energy. Since there is a direct relation between power and energy[3]; from now onwards, power related quantities are preferred over energetic quantities.

The main drivetrain's objective is to *manipulate* the available presentation of mechanical power[4] to be transformed into the desired presentation of electrical power. Losses minimization is always intended. In all existing systems, more than one component is required to achieve this task. Nevertheless, it is preferable to have as few as possible to increase efficiency and reliability levels.

In the most common cases, the drivetrain is often composed by a series of mechanic and electric machines transferring power among them. The configuration of such components varies widely from manufacturer to manufacturer. Among the most important reasons for this can be found: improve overall performance, cost reduction – both of them will eventually lead to a competitive advantage **-** , or just to overcome an existing regulation that bans that technology in a particular market. For instance, let's consider the drivetrain for the Vestas V80 2.0 MW wind turbine. This wind turbine is one of the today's most tested machinery in the industry having more than 4,000 specimens installed worldwide. In terms of drivetrain, on 2011 Vestas V80 2.0 MW, this turbine relies in: a 3-stage gearbox, an asynchronous generator, power electronics and a step up transformer [*3*], this is sketched in Figure 1.4.

When looking to Figure 1.4, a vague idea of the almost infinite possibilities for a drivetrain system might arise; and therefore the implicit question: What were the main reasons that drove the Vestas engineers to select this particular solution over all other possible arrangements? As was mentioned before, in some cases overcoming technology limitations is an important driver to select a particular drivetrain configuration. However, sometimes other environmental motives (like existing patents) can be as

[2] Electrical Energy presentation can vary according to the properties of the desired point of interconnection; so *format* is used to describe mostly the type and voltage level and number of phases in case of a AC current.
[3] Energy is the integral of power over a period of time, so this means that energy is normally expressed in the International System of Units as [Wh] while Power is expressed in terms of [W]
[4] Mechanical power, in a rotating shaft, is often described as the product of available torque and angular speed.

important as performance indicators (like efficiency).It is possible that this was the case for the current case of study. The Vestas V80 2.0 MW was especially designed to exploit the North American market (specifically U.S.A. market). It was introduced in 2003(year in which GE hold intellectual property according to patent US005083039[5]). Such patent holds intellectual property of the use of power electronic converters in variable speed wind turbines. The same patent already had been solid evidence in the banning process for the European company Enercon in the USA market[6]. The excuse was that Enercon employed electronic converters in similar fashion to GE in wind turbines. Having Enercon as an example, most wind turbines manufacturers that were aiming for the USA market were trying to stay safe away from tribunals. A clever solution from some companies was to use in a substantial different way electronic converters to those described in the patent. It is possible that Vestas might partially adopt the same idea in this wind turbine model at the cost of some reduced performance.

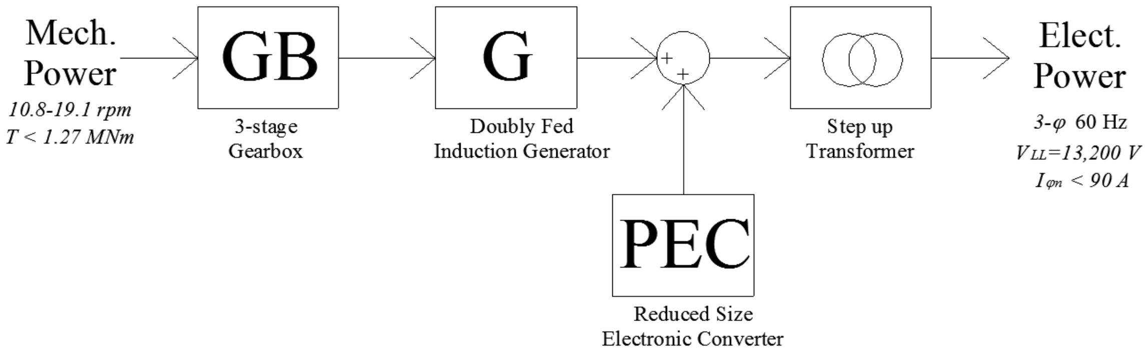

Figure 1.4 Drivetrain system from Vestas V80 2.0 MW

Whichever the drivers to select a particular configuration are, the main idea behind a drivetrain system is to transform power. The jump from mechanical to electrical energy will be normally done in an electrical machine called generator. This electrical machine is actually the only machine ideally desired. However, there are currently several types of generators and all of them might require different manipulation of input mechanic power. Sometimes this makes necessary to adapt the mechanical input –i.e. increase the angular speed – or the output electrical power –i.e. change the voltage level- to allow grid interconnection. Such power manipulation might insert up to two additional stages. Figure 1.5 represent this idea.

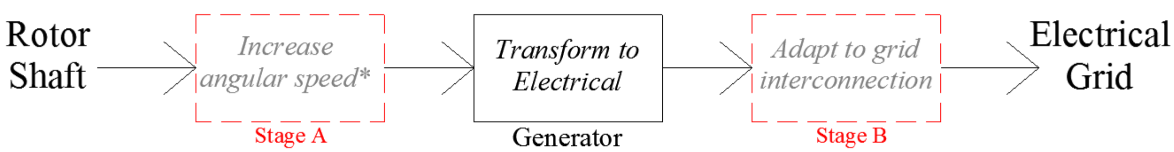

Figure 1.5 General idea behind a drivetrain

[5] This patent mostly talks about intellectual property of Power Electronic Converters used on variable speed wind turbines.

[6] After a series of painful trials it was determined to ban the European company in USA. until 2010 due to an infringement in the intellectual property related with the use of power electronic converter in variable speed wind turbines well documented in patent US005083039 [*40*].

As more stages are included the overall efficiency and reliability will drop. Nevertheless, there are solid motivations to have both stages. For instance, the main motivation to increase the angular speed of rotor shaft is to allow smaller sizes of generators. However, having a device that complies with Stage B in Figure 1.5 might allow working with standardized components. In both cases cost reduction is obtained at the cost of efficiency reduction. This concept can be easily observed in Figure 1.4 for Vestas V80 2.0 MW where both stages of Figure 1.5 are present (a gearbox and electronic converter plus step up transformer). In today's industry, there are some machines that get rid of one of these two stages – such is the case for the Direct Drive concept -. In any matter avoid both of them might be still too complicated.

As was mentioned before, there are three main ways to transfer large power quantities: mechanic, electric and fluid power. In today's wind turbine industry there are several drivetrain configurations that make use of at least of two different mechanisms: mechanic and electric. Since the final purpose of this document is to compare drivetrains configurations that make use of hydraulics (as power transfer mechanism) with those which does not use hydraulics, a clear separation between these two different arrangements is required. In this context, the ***hydraulic drivetrains*** will be defined as those configurations that incorporate *hydraulics* – at any point- for *significant* power transmission along the secondary energy conversion process referred to Figure 1.3. The reference point will be set by the so called ***non hydraulic drivetrains***. These non hydraulic systems will be defined as the ones that *do not incorporate* hydraulics for significant power transmission. This concept comprehends also those highly specialized drivetrains that avoids the use of gearbox (direct drive) or uses it in a specific arrange(differential arranges).

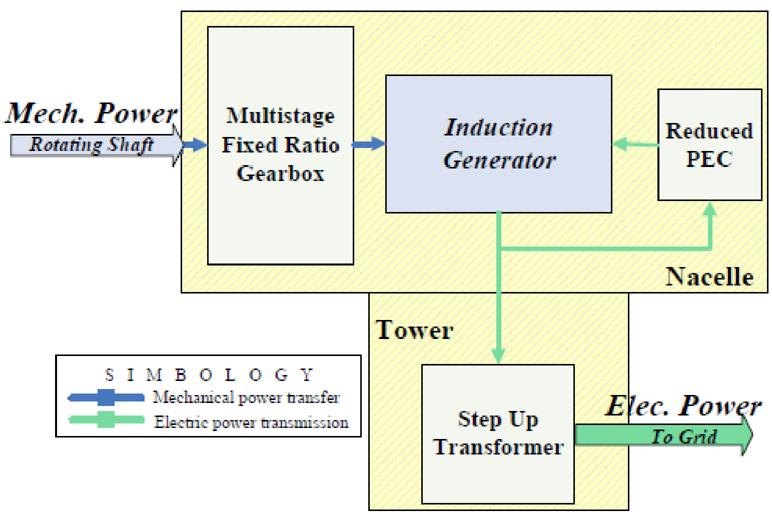

Figure 1.6 Example of non hydraulic drivetrain system

Figure 1.6 presents one of the multiple presentations of the non hydraulic drivetrains. Perhaps, this presentation is one of the most widely by popular wind turbine manufacturers like Vestas and Gamesa. This presentation consists in a multistage gearbox to increase the angular speed, a medium speed low voltage double fed induction generator, a reduced size power electronic converter and a step up transformer. As can be anticipated, the type of electrical generator sets the requirements for the rest of the drivetrain. Therefore, other common components that are often present in wind turbines' drivetrains are: gearboxes, power electronic converters and electrical transformers.

A gearbox is an assembly of gears that provides controlled angular speed change between a prime mover and a driven element. There are several gear configurations that can be used. Among the most common are planetary, helical or superimposed arrays. Each gearbox can have several stages and mixed styles (i.e. Vestas V80 2.0MW gearbox has one planetary stage followed by two helical stages). The function of a gearbox is increase the angular speed –therefore reduce the torque- of the rotor's shaft. In a wind turbine drivetrain, it can be located at stage A from Figure 1.5. If a gearbox is not desired, avoiding its use is possible either by using another high power transmission mechanism (i.e. hydrostatic transmission) or just having no device at all (direct drive). Any decision in here will directly impact the number of components in Stage B from Figure 1.5.

The most important component of the drivetrain is the electrical generator. Its task is to transform mechanical power into electrical. Today, electrical generators for wind turbine industry are normally custom-designed. This is due to the fact that fitting an off the shell machine sometimes requires too much components reducing considerably efficiency and reliability. Moreover, each particular drivetrain can make use of multiple machines in parallel, and there are several types of electrical machines that can work as generator. The most common types are: synchronous generator (SG), asynchronous or induction generator (IG), double fed induction generator (DFIG) and permanent magnet generator (PM) with all their different variations. All different types of generators have advantages and disadvantages over the others; therefore, some of them are preferred in particular situations. Also, in some cases, generators already deliver electrical power at the grid's properties (like a high voltage electrically exited synchronous generator). Nevertheless, for those which do not (asynchronous electric generators) some extra devices might be required. Among these complementary devices power electronic converter and step up transformers can be found.

A power electronic converter is located at Stage B of Figure 1.5. This is a device capable to receive a varying AC frequency current and varying voltage and transform it to a particular AC current at a specific voltage. There are multiple types and styles of electronic converters; but all of them are based on semiconductors (i.e. thyristors, IGBTs, diodes, etc). The discussion of the technology of such devices is out of the scope of this document. This is due to the fact that hydraulic drivetrains can override the use of electronic converters.

Also in stage B, a step up transformer can be found. Such device is capable to couple two AC circuits magnetically [*4*]. Such magnetic coupling allows to increase (or reduce) the tension of the output electrical AC power. The idea to step up the voltage is to reduce resistive losses due to current transmission through cables. To avoid the use of a step up transformer, a *high* tension at the output of the generator (or electronic converter must be used). *High* is in the order of standard distribution voltages (~6.3kV per phase, or other similar tension).

In addition to these commonly used components (related with electric and mechanical power transfer), it is possible to find also machines related with fluid power transfer. If any, these hydraulic components would be located on stage A from Figure 1.5. The reason for this is that hydraulic power in wind turbines is mostly oriented to manipulate mechanical power available in the rotor's shaft. To stress the large number of alternatives for drivetrain's component selection in wind turbines Figure 1.7 was built. In there, once again three main stages are found. They are referred to those in Figure 1.5. Inside each section some of the most commonly used components are presented. Regardless the extensive possibilities, some of them are impractical due to low performance or incompatibility to expected electrical properties. Therefore, the selected type of generator will necessarily affect options left for Stage A and Stage B selection. The order of selection is commutable and at much one stage can be suppressed (A or B) if the right components are selected. For instance, by considering Direct Drive for Stage A (suppression of component in stage A), Stage B will be limited to necessarily use a electronic converter (and very likely to have a step up transformer too) and those generators in which the use of this device can be justified. By the end, one mechanical component was replaced by one electronic component. This constant tradeoff between components selection is a direct consequence of fixing the format of output electrical power (i.e. line voltage of 11 kV at 50 Hz for some Dutch power transmission lines or 13.2 kV line voltage at 60 Hz for North American distribution grids).

Either by looking a competitive advantage or just to overcome existing market regulations, the drivetrain can also providse the manufacturer's brands signature too. All these together had caused the wide drivetrain variety of today's wind industry. This large variety explicitly confirms that there is nothing like conventional in this market, just partially similar solutions and all of them based in cost reduction.

Cost reduction has been the major trend in wind turbine industry since late 1970s. In early stages, where the priority for wind turbine industry was to survive, this trend forced to limit the power transfer options inside the *good deal*[7] range. This limited the use of fluid power transfer in wind turbines to experimental level where they proved to be inefficient outside of rated power[5], where wind turbine spends more of their time(65-75% of their lifetime working at below rated power). Because of non specialized machinery and the lack of motivation to build it, hydraulics proved to be very inefficient (60% overall efficiency when working below rated power). Since the main intention for wind turbines was to stay in the market, hydraulics turned unaffordable three decades ago. Then, two decades after, wind turbines hold into the market and actually started booming (past decade). Turbines started to grow in size and complexity and some critical endurance problems become evident (mostly related with geared components and PECs) the need to think outside the box again. At the same time, some revolutionary designs proved that the industry was ready to pay for performance and reliability. Among these new approaches direct drive and hydraulic drivetrains can be found.

[7] Well experimented machinery, good overall efficiency, manufacturing capability and that allows sharing standardized components with other industry.

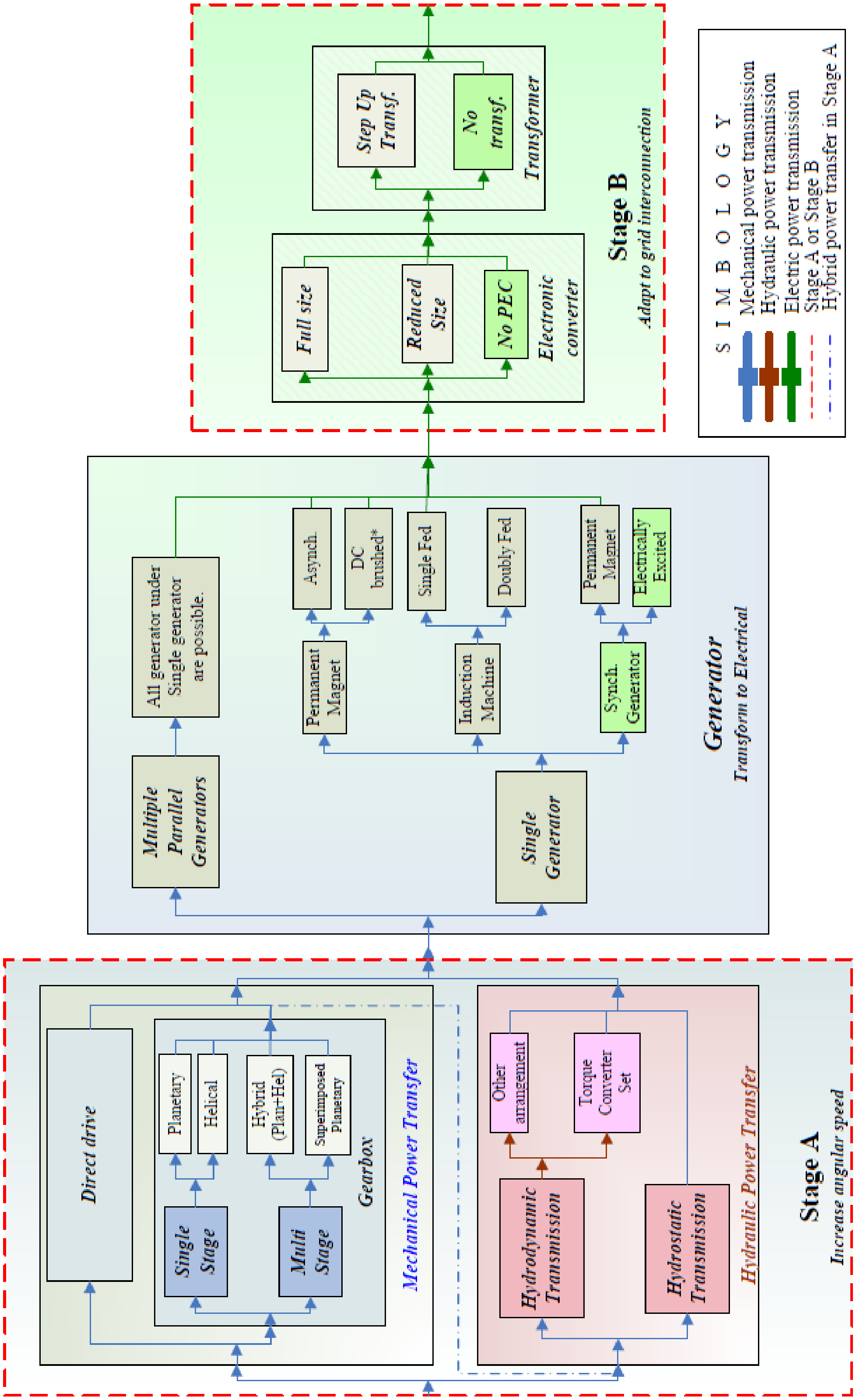

Figure 1.7 Drivetrain alternatives for wind turbines

1.1.3. Hydraulics in Wind Turbines

Frequent failure in critical components injured the impeccable image of wind turbines and made evident the need for more specialized machinery. In order to solve these problems, the industry first tried to get rid of the problematic components: gearbox and electronic converters. Such was the case for radical concepts like the direct drive concept, which gets rid of the gearbox by making use of a highly specialized generator and a full size converter. This direct drive concept set new references for drivetrain efficiencies and reliability. They were based mostly in component suppression. Regardless the advantages, some tradeoffs in terms of weight, cost and size become evident; but the market was willing to pay for them. After a successful introduction and some experience with these new turbines, two things were clear for the wind turbine industry: first, the time for highly specialized drivetrains had come; and secondly, although the efficiency levels were great, the electronic converter was still there as the weakest link in the chain. Although the electronic converter represented direct threat to the system reliability record, this was not exactly the most important problem at that time. The big issue was that the electronic converter, the star of this new drivetrain system, was keeping out this drivetrain outside the USA premium market because of existing regulations[8]. But still, the market had spoken: they were willing to bid for highly specialized systems.

In fact, the industry already had a solution for the PEC issue long time ago: use a synchronous generator directly connected to the grid. This synchronous generator might offer some other advantages like power factor control and higher energy quality production. Although highly tested solution was not exactly new, there was still one major issue to be solved: feed a constant angular speed to the generator over a wider range of wind speed. If the use of directly connected synchronous generators was intended, then the need for a new component in the wind turbine business became evident. The most important requirement of this component was to transform a variable angular speed-variable torque input shaft to a constant angular speed-variable torque output shaft to be fed to the generator. So they borrowed from other industries the concept of a variable ratio transmission.

Variable ratio transmissions had been present for long time. Normally, this machinery uses a different power transfer mechanism to partially (or entirely) decouple power from the main stream. This decoupled power is used to generate a variable ratio[9] over the output power flow. The decouple power mechanism can be any one of the three available ones. Very often, this kind of transmission prefers hydraulic coupling (fluid power transfer) over the other mechanisms to generate the variable ratio. Although some variable ratio transmissions based on fluid power transfer were proposed for wind turbines since the late 1970s, it was until thirty years after that the time for these transmissions would come with market acceptance. In modern machinery, variable ratio transmissions are very often found in heavy duty machinery. For the purpose of this document, variable ratio transmissions are grouped in three different branches: hydrostatic, hydrodynamic and hybrid. A *hydrostatic* transmission uses a combination of positive displacement machines to obtain the variable ratio. In same fashion, *hydrodynamic* transmission uses a combination of hydrodynamic machines. The *hybrid* transmission is used to refer any combination

[8] GE versus Enercon case commented in section 1.3

[9] The variable ratio term comes from increasing the content of a particular parameter in an output power flow. Parameters for every kind of power transfer mechanism were defined in Table 1.1 Power transfer mechanisms. For instance: in a mechanic system, the ratio between angular speed and torque; or in an electric system, the ratio between voltage and current.

of hydrostatic-hydrodynamic, mechanical-electrical, or mechanical-hydraulic (any kind). These concepts will be further explained in Chapter 2.

Today, fluid power transfer is synonymous of robustness and high power density. These two features are direct consequence of the large force density possible to transmit by means of a fluid. Although this large force density is still smaller than the potential limit of mechanical systems, in hydraulic systems the force is transferred over a wider area than in a mechanical system[10]. Because of this, hydraulic component design is often limited only by the maximum pressure that a pump can reach, and not by the material properties, which is the case for mechanic power transfer. This allows hydraulic systems to have small mechanical stress concentration eventually leading to lower maintenance levels[11] and more compact geometries. This means that relatively *small* machines can handle large force densities. Another important advantage of hydraulics is that the driving fluid can work as heat remover. This ensures temperature regulation and guarantees endurance under normal operating conditions. Finally, hydraulic systems can easily reach efficiencies as high as 96% at rated power. Table 1.2 summarizes important comparative numbers between the three most common power transfer mechanisms. Such table shows that while the electrical power transfer is limited by air gap saturation and mechanical systems are limited by the plastic deformation of material by itself, fluid power transmission is actually limited by the existing machinery dedicated to fluid compression. The direct consequence is to have larger implicit safety factors (in terms of machinery integrity) than those obtained in mechanic power transfer.

Although hydraulic systems can offer robustness for extra heavy duty machinery, very often they used to be controlled by flow regulating valves that severely decreases efficiency levels when not working at rated power (more deeply boarded in chapter 2.). This changed when digital hydraulics arrived few years ago. Basically, digital hydraulics are an optimized-software controllable version of common hydraulic machines. The arrival of this new kind of machines revolutionizes the reach of hydraulics in several industries (by solving the problem of low efficiencies plus control enhancement). Regardless the advantages of digital hydraulics, they still have common weakness with their predecessors. For instance, under abnormal operating conditions, the potential danger for a leak to occur is always present. This normally draws some extra attention due to potential environmental hazard. Also, system performance is very dependent on the fluid condition, so proper maintenance and continuous filtering is required to stretch the fluid's life as much as possible. In a few words, as any system they have some advantages, but for sure some other disadvantages. This is the starting point for this graduation project. In the following sections, the hypothesis and the more important research questions will be presented.

Concept	**Symbol**	**Power transfer mechanism**		
		Electric	Fluid	Mechanical
Main limitation		Air gap saturation	H. Pumps	Material
Force Density	$F_d\ [^N/_{m^2}]$	50×10^3	100×10^6	500×10^6
Factor	$1/F_A$	1/10000	1/5	1
Area factor	F_A	10000	5	1

Table 1.2 Power transfer mechanisms

[10] In a geared transmission, the force must be transmitted in the contact point between gears, which ideally must be infinitely small to avoid noise. In the case of a hydraulic rotary component, the force should be applied in a much larger area, which allows much smaller machines. See factor F_A on Table 1.2
[11] Except for the driving fluid, that eventually will require to be replaced.

1.2. Goals of this thesis

In the past sections, a preamble about wind turbine industry, technologies used, important definitions and some clues about hydraulics were presented. Based on that, the following hypothesis can be formulated:

Hydraulic drivetrains have a competitive advantage over non-hydraulic drivetrains.

As complementary part of the hypothesis, let's say that the use of hydraulics allows direct use of an off-the shell high speed-high voltage electrically excited synchronous generator. The use of this kind of generator makes unnecessary the use of highly specialized costly electrical machine, electronic converters and a step up transformers. Therefore, number of components is minimized and efficiency and reliability should increase. To asses such hypothesis, the main research question is:

How large are the advantages and tradeoffs that a hydraulic based drivetrain system has over a non hydraulic drivetrain system in a wind turbine?

To help answering this main research question, some other secondary questions to be answered are:

- From all different hydraulic drivetrains, which are the most suitable topologies that are worth to be researched?
- Is it possible to decrease the level of complexity of drivetrain components by using a hydraulic drivetrain?
- What would be the impact in final price per kWh generated with this new topology?
- Can the use of a hydrostatic transmission in a wind turbine drivetrain improve the overall performance and reliability of the system?

The main goal for this document is to answer the main research question and secondary research questions. This means evaluate the use of modern hydraulic drivetrains in wind turbines. To help answering this research question, performance and its impact in terms of economics should be quantified. Based on the time scope for this graduation project, the best tool to help quantifying was defined as a computer model. This computer model targets the steady state condition only. Experimental validation of this model is out of the scope of this document.

As secondary goals, can be found:

- The selected drivetrain to be modelled should be relatively recent.
- The constructed model should be capable to represent the physics behind the hydraulics in steady state conditions.
- Model dynamics should or be ready to be implemented as far as possible.
- Performance indicators should be useful to compare hydraulic drivetrains with non hydraulic ones. Such indicators aim to respond efficiency related matters but also economic considerations.
- Reliability, operability and maintenance should be assessed as far as possible

On next section, the contribution of this thesis will be presented.

1.3. Contribution of this thesis

This section presents the main contribution of this document. This contribution is mainly in the study field of hydraulic drivetrains for wind turbines. This thesis sets a solid starting point for a research based in hydrostatic transmissions that uses piston based pumps and motors. On next, the most important contributions and the chapter of appearance are highlighted:

1. I showed that hydraulic systems might be also used to transfer significant amount of power in wind turbines. To do so, I presented several possibilities of component selection in wind turbines' drivetrain (using or not using hydraulics). Then, the potential advantages of fluid power transfer were qualitatively presented followed by a small introduction about digital hydraulics.**– see introductory part of Chapter 1.**
2. I presented the wide variety and principles of operation on which variable ratio transmissions can work. Special interest was paid for those based on fluid power. I also showed that the use of hydraulics is not entirely new in the wind turbine industry by means of a literature study.**– see Chapter 2**
3. I showed that it is possible to model a multicylinder piston based hydraulic machine by means of several monocylinder systems in parallel. I also showed that this monocylinder machine model can be extended to several kinds of piston based hydraulic machines by making the proper set of considerations. This was proven by boarding two significantly different machines (ring cam digital pump and high speed digital motor) with the same monocylinder model. **–see Chapter 3 and 4.**
4. I showed the large software dependence of digital hydraulic machines by means of emulating this function in the computer model. I also showed that performance of computer model is as good as the software quality is. A similar scenario for the real systems is expected. **–see Chapter 4.**
5. I showed that it is possible to estimate numeric values in the range from the real system by using scarce factual information (1.6 MW Artemis drivetrain). Also, I showed that the results of computer simulations were in the range of some results published by the drivetrain manufacturer. **–see Chapter 4.**
6. I showed that hydraulic drivetrains are a competitive technology that can actually stand side to side with popular arrays in terms of energy production cost, machinery cost, and efficiency levels. However, I presented that for small nominal power capacities, the advantages of this drivetrains were scarce in terms of quantitative indicators.**– see Chapter 5.**

On next, the organization of this document is briefly presented.

1.4. Organization of this Thesis

This document tries to answer the research question in six chapters:

1. **Chapter One: Introduction.** This first chapter (this one) sets a preamble about the use and possible advantages of hydraulic drivetrains in wind turbines. General ideas and definitions are made. Also, three main power transfer mechanisms are presented: mechanic, electric and hydraulic. Later, some popular drivetrain configurations are discussed in terms of power transfer. Then, Figure 1.7 tries to give a general idea about the wide variety of possibilities for component

selection in a wind turbine drivetrain. Finally, the main and secondary research questions are presented.

2. **Chapter Two: Literature Review.** This second chapter formally introduces variable ratio transmissions. Then, after discussing principle of operation of hydraulic variable ratio transmissions, some drivetrains that make use of hydraulics for significant power transfer are discussed qualitatively. By the end of this chapter, conclusions are drawn and Artemis Drivetrain topology is selected for further study.
3. **Chapter Three. Modeling.** This chapter defines a methodology to study the Artemis drivetrain. To do so, a more general approach is selected (conventional radial piston pump) so the contribution of this document can be extended. As a product of this approach, a dynamic model for a monocylinder conventional machine is presented. Then digital machines are introduced as optimized conventional machines. Later, the monocylinder model is subjected to several considerations that will make it *suitable* to represent monocylinder models that integrates main machines' features used in the 1.6 MW Artemis drivetrain. Then, some complementary models are presented (intended to model the use of hydraulic drivetrains in wind turbines: rotor and synchronous generator). Finally, conclusions are drawn.
4. **Chapter Four. Computer Model.** In this chapter, the monocylinder models introduced in chapter 3 are used to assemble a multicylinder machine. Computer modeling is done by means of Matlab Simulink®. Then, some results are discussed and compared with values published by Artemis Ltd. Afterwards; computer model limitations are discussed to finally draw some conclusions about the computer model.
5. **Chapter Five. Indicators.** In this section, some commonly indicators are selected to allow comparison. Two kinds of indicators are presented: quantitative and qualitative. Each one will be discussed. Nevertheless only those with quantitative approach will be used to draw conclusions by the end of this chapter. Just before the conclusions, the built quantitative indicators will be used to compare the case of study (1.6 MW Artemis drivetrain) with some other commonly used topologies.
6. **Chapter Six. Conclusions.** This last chapter draws general conclusions about topics discussed in this document. First, conclusions about variable ratio transmissions and hydraulic power transfer are presented; then some other general conclusions about the monocylinder model are done to be followed by comments on the integration of this monocylinder model in the computer model. Finally, a preamble about the use of hydraulic drivetrain in wind turbines breach the way to the direct answer of the research question by the end of this chapter.
7. **Appendices.** This last section is reserved for all detailed explanations or parameters that were required at some point during this document. Whenever is necessary, any of the six chapter might make a quick reference to this section.

This concludes this chapter. In the next chapter variable ratio transmissions will be formally introduced and literature review about hydraulic drivetrain systems will be presented.

2. Literature Review

2.1. Introduction

The main target of this chapter is to inform the reader about the historic (and current) use of hydraulic drivetrains. To do so, first an introduction to fluid power based variable ratio transmissions and flow control is done. Then a relevant historic case of hydraulic drivetrain used in the late 1970s is presented (Bendix SWT-3). Afterwards, some currently market available hydraulic drivetrains are introduced (Wikov, WinDrive, ChapDrive, DOT and Artemis). Later, conclusions are presented and the motivation for the selected technology is summarized.

2.2. Variable Ratio Transmission

Variable ratio transmissions were introduced in section 1.1.3. As was mentioned before, variable ratio transmission links a mechanic power input with an output of the same kind but in different presentation (angular speed and torque). For those devices that uses fluid transfer to partially (or entirely) decouple power for the input power stream hydraulic pump and hydraulic motors are often required. Defining a *hydraulic pump* as a device that transforms mechanical power into a fluid flow, and a *hydraulic motor* as the one that uses the fluid flow to drive a mechanical load; then these devices can operate under two different principles: hydrostatic and hydrodynamic.

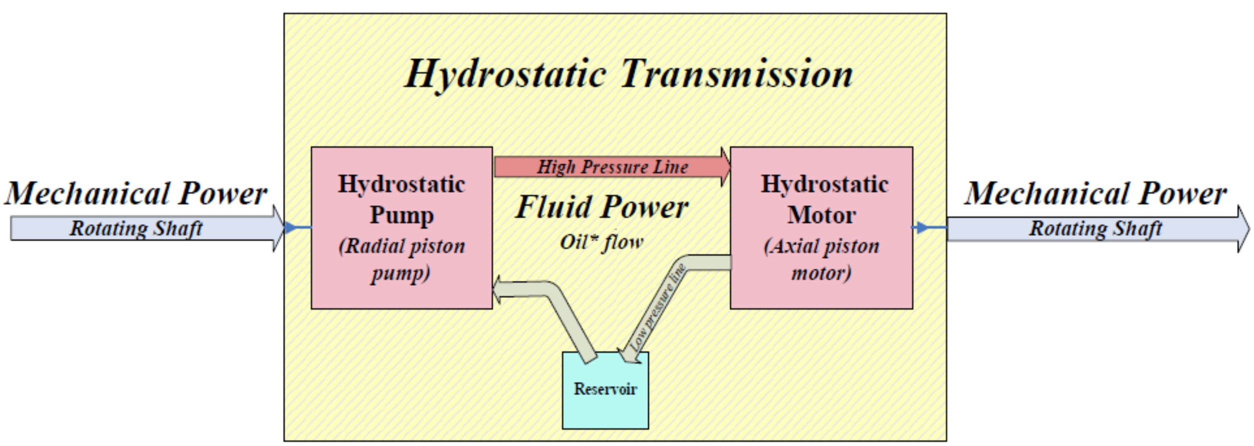

Figure 2.1 Hydrostatic Transmission

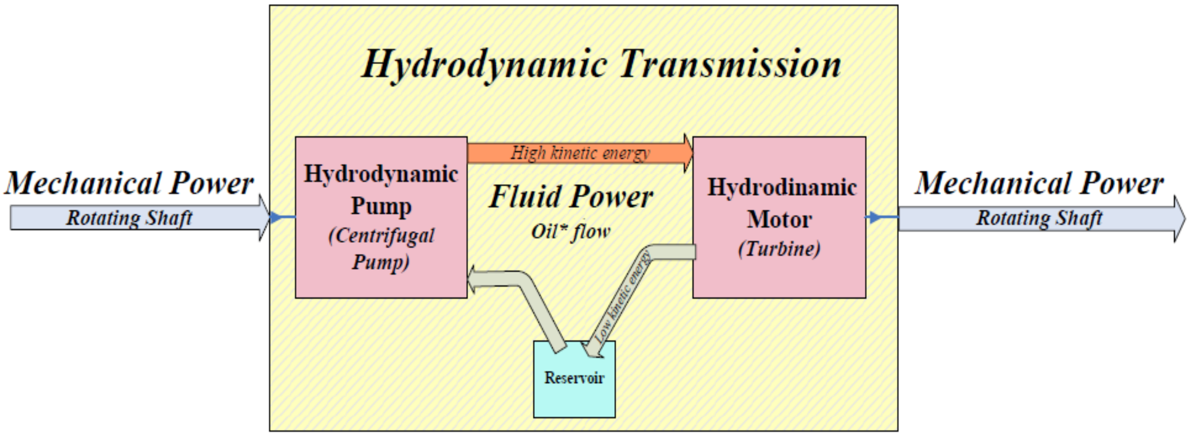

Figure 2.2 Hydrodynamic Transmission

2.2.1. Operating Principle

The hydrostatic principle is based in change of volume. Initially a chamber is connected to an inlet port . The chamber increases in volume pulling fluid into it, then the inlet is closed and an outlet is opened to allow the fluid expulsion while the chamber volume is reduced. This principle is also referred as *positive displacement* because the mechanism initially traps the fluid and then it forces to be displaced towards the discharge line.

The hydrodynamic principle makes use of a spinning body to transfer momentum to a fluid in the shape of tangential velocity[12]. While in the case of a positive displacement device the oil is forced to leave the chamber by decreasing the volume; in the case of hydrodynamics, fluid particles are tangentially accelerated in a rotating body. Eventually, the particle leaves the spinning body and because of flow continuity, each particle that leaves is replaced by another one with low kinetic content. When the particles leave the revolving body, they already have large kinetic energy content that is intended to be recovered in next stage (in the shape of potential energy or extracted by the use of an hydrodynamic motor). Because of this operating principle, large rotating speeds are required (about ~100 RPM and larger).

In any case, the motor operation is the opposite of pumping operation. When a hydraulic pump is driving a hydraulic motor a power transmission is formed. If the pump and motor works based on positive displacement principle (fluid flow), then the transmission is called hydrostatic transmission. If the components works based on momentum transfer, then the transmission is called hydrodynamic. Both transmissions are sketched in Figure 2.1 and Figure 2.2 respectively.

2.2.2. Fixed and variable displacement

Although there are only two basic operating principles, there is a wide variety of pump styles (and therefore motors). Some of them are presented in Figure 2.3 and Figure 2.4. In such figures, it can be observed that there are devices of *fixed displacement* and *variable displacement.* The fixed displacement

[12] In the case of hydrostatic pump, the fluid was displaced by the decrease in volume having all fluid displaced by the end of the cycle. For the case of hydrodynamic pump

devices makes reference to those that, in absence of any external flow control circuit, can provide a flow of fluid only dependent in the fluid properties and mechanical power input(for pumps). A fixed displacement machine might become a user controlled machine by means of an external flow control circuit. Still significant efficiency tradeoffs are present due to increased drag in the control circuit.

On the other hand, the variable displacement devices allow flow control through built in-user controlled mechanisms (no directly related with power input and fluid properties). This helps to vary the amount of power transfer. Most of the cases, conventional variable displacement machinery is basically fixed displacement machines with an optimized built in flow control circuits. Still increased losses are present.

In the past decade, developments on software control made possible the introduction to the market of *digital hydraulics*. These are an entire new kind of machinery based on hydrostatic fixed displacement piston based machines. They have the capability to behave as variable displacement machines by partially deactivating some pressure chambers so partial load conditions can be reached. These devices will be further discussed in chapter 0 Also, multiple pump/motor setups is also a possibility. Such arrangements can be done by locating multiple devices in parallel or series array.

Regardless the selected configuration, there are some devices capable to handle larger power densities than others. The systems that can handle the largest force densities are normally from hydrostatic type with radial or axial piston configuration. Radial piston pump/motor is more often used for rotating prime movers and it is sketched in Figure 2.5. In the following sections a deeper insight to flow control methods in variable ratio transmissions and the application for these devices in wind turbines will be discussed.

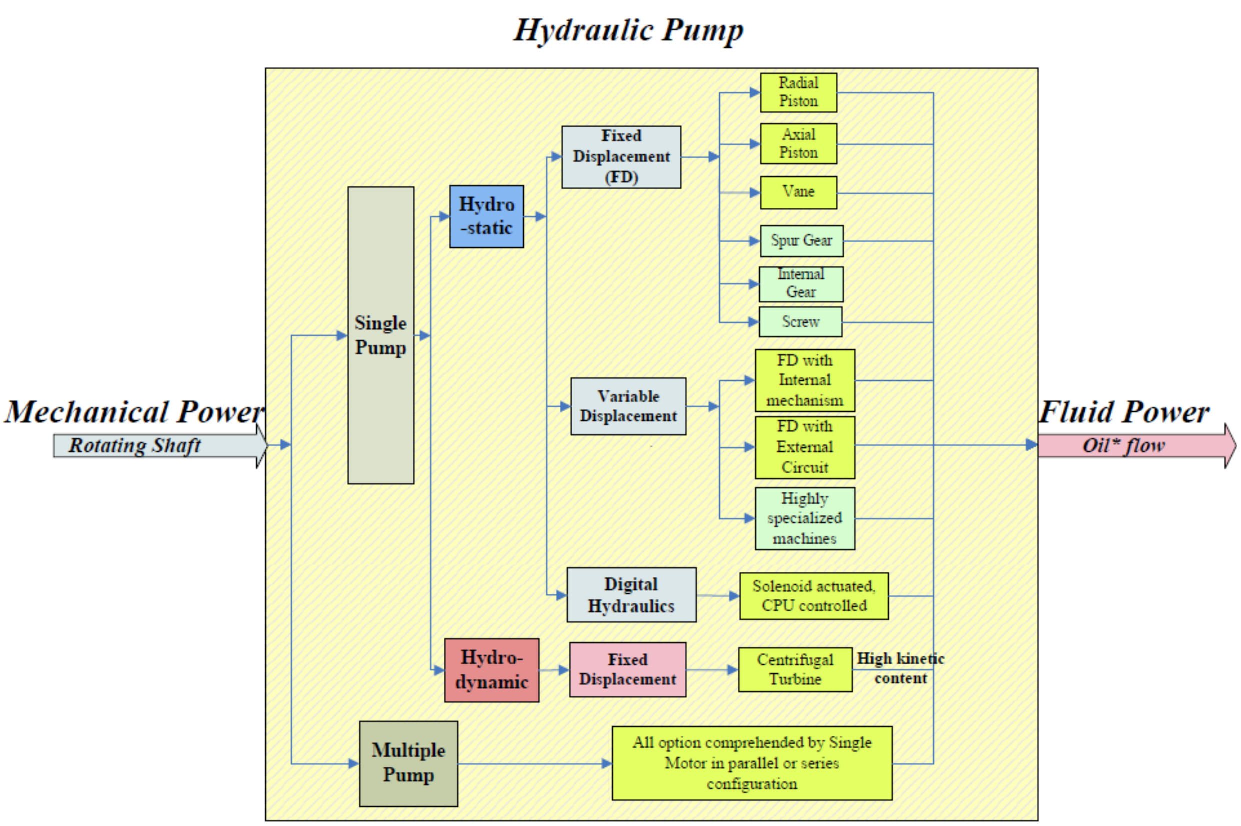

Figure 2.3 Common types of hydraulic pumps

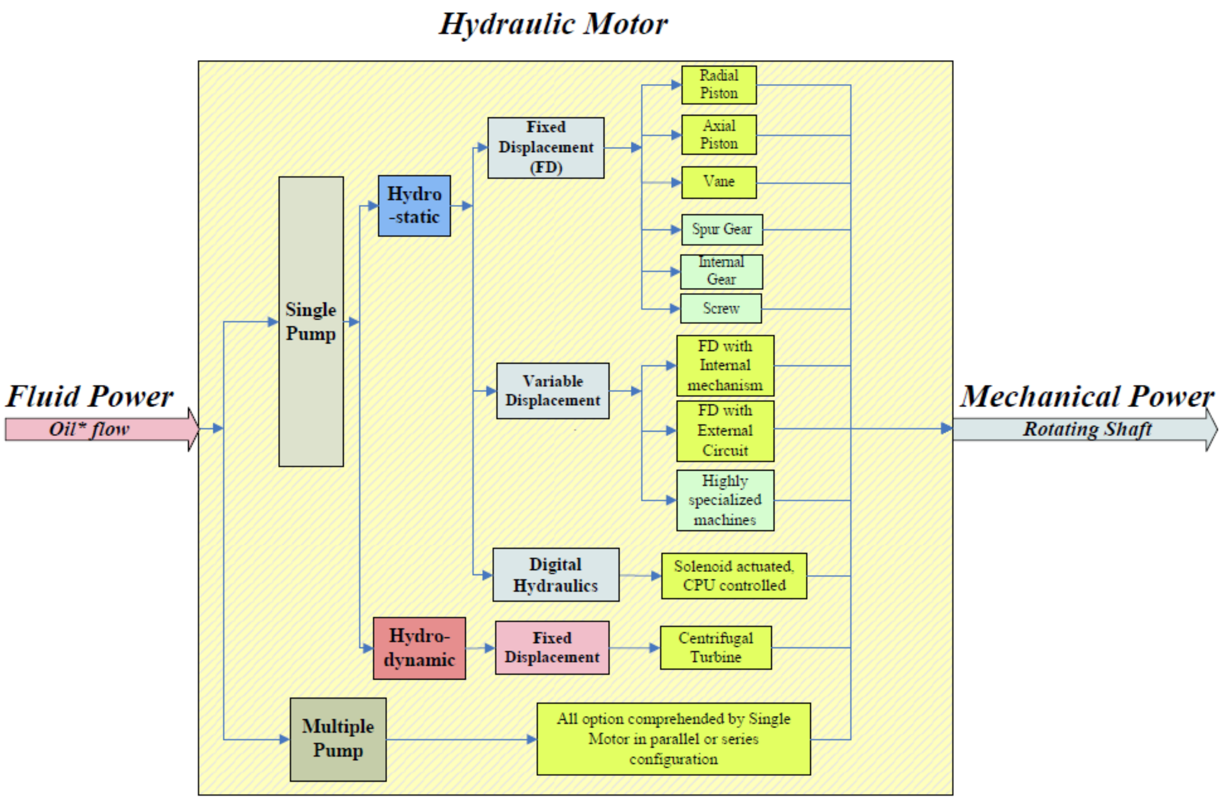

Figure 2.4 Common types of hydraulic motors.

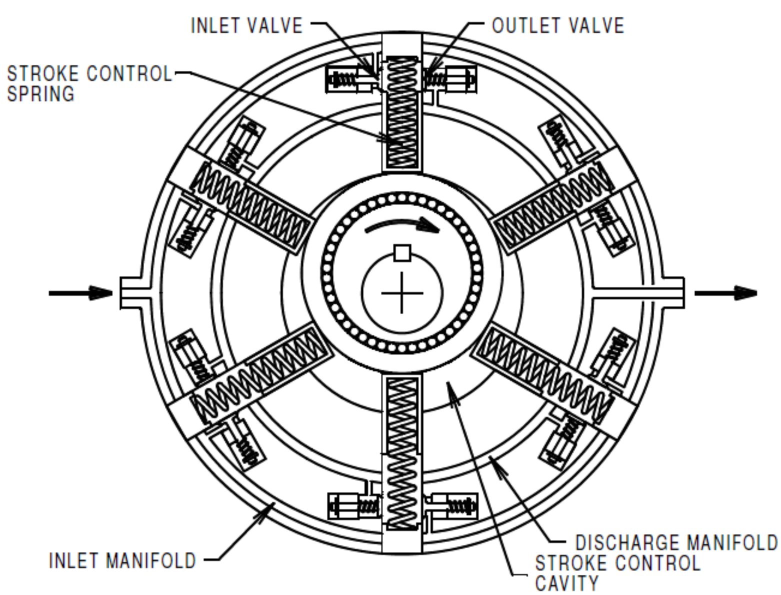

Figure 2.5 Radial piston pump

2.2.3. Flow control

As discussed before, variable ratio transmissions can work based on fluid power transfer. In such cases, power is transmitted from a higher to lower energy content through a flow of fluid. It was also mentioned that a hydraulic transmission[13] is normally composed by a pumping stage followed by a motoring one. The most common devices were introduced in the previous section. Among them, two large groups can be identified: fixed displacement and variable displacement. These devices differentiate each other by introducing the possibility of vary the magnitude of power transfer. Nevertheless, both styles can be controlled either by the input power, by the fluid properties, by built-in function in pumps and motors or by an external fluid control circuit.

In hydraulic systems, power is being transferred by a flow of fluid. Transferred power is directly proportional to the product of volumetric flow of fluid between stages and pressure difference (refer to Table 1.1). By controlling at least one of these parameters the amount of transferred power can be controlled too. Practical approaches to control power transfer typically involve reduction in the input power or redirection of power through an external flow circuit. In fact, there is another way to control power transfer: by altering fluid properties. However, this is not practical since it might endanger fluid's lifetime and system's integrity.

To clarify information contained in the past paragraph, let's consider a large power fixed displacement hydraulic component (like a radial piston fixed displacement pump). When no external fluid control circuit is available and the fluid properties remain uncontrolled, the only remaining control parameter is the input power. When the hydraulic component is working at power levels below its rated capability, it is said that the element is working at *partial load*. Partial load power control is the most commonly used method to control hydraulic devices. However, it had been discovered that working fixed displacement devices in this condition might lead to reduced efficiencies (about 60% or worse) [5]. Additionally, flow regulation by external flow circuits might lead to worse efficiency levels because of increased power dissipation due to drag in control circuit.

Overcome this power losses had been the main target of variable displacement devices. In the past, these machines used to only incorporate sliding surfaces as flow control mechanisms or even built in valves, which not always achieved power losses minimization. Then, with the arrival of new control techniques, digital hydraulics became feasible. This new components introduced new designs that incorporate built in valves in a much more efficient way, but best than all, user controlled. This allowed overcoming efficiency issues at partial loads. A clear example of the use of this type of machinery is Artemis drivetrain.

As mentioned before, the application of hydraulics to wind turbines is not exactly a novel idea. In fact, in the early1980s it was aborted because of low reported efficiencies. Nevertheless, today the future for hydraulics seems to be different because of the introduction of digital hydraulics and the evolution of the wind turbine market. On next, some hydraulic drivetrains will be presented. Most of them are currently available in the market. As a historic reference, one experimental hydraulic drivetrain used in the late 1970s is presented too.

[13] From now onwards, hydraulic transmission will be used as synonym of variable ratio transmission based on fluid power transfer.

2.3. Hydraulic drivetrains in Wind Turbines

In this section, the most relevant cases of wind turbines that incorporate fluid power transfer are presented. The Bendix SWT-3 is an important historic reference for the use of hydraulic drivetrains in wind turbines. Later some other currently available drivetrain systems will be presented: Wikov W2000-SPG, Voith WinDrive, ChapDrive, DOT and Artemis Digital Displacement.

2.3.1. Bendix SWT-3

In the late 1970s, some experiments were carried out and reported low performance levels. In those experiments, which were based on standardized hydraulic components, the need for highly specialized hydraulic machines was made evident. This experimental turbine was called SWT-3.

The SWT-3 was a private experimental venture between Bendix Corporation Energy and the Southern California Edison utility company. In general terms, the SWT-3 was a variable speed wind turbine with a rated electrical power of 3MW. Important remarks about the geometry are: a 51 m rotor diameter, hub height of 33 m, a rigid triangular truss configuration, yaw system in the base of metallic truss. The complex drivetrain concept incorporated a first gearbox that was driving a hydrostatic transmission (fixed displacement pumps in the nacelle and variable displacement motors at the tower base). The transmission regulates the angular speed through a second gearbox for a low voltage electrically excited synchronous generator. Then the generator was connected to a step up transformer that was directly connected to the grid. Generator, step up transformer and yaw system were located at the tower base. In terms of control, it had full blade pitch and yaw control. Controller was implemented in a microprocessor. Figure 2.6 sketches the geometry of SWT-3 wind turbine.

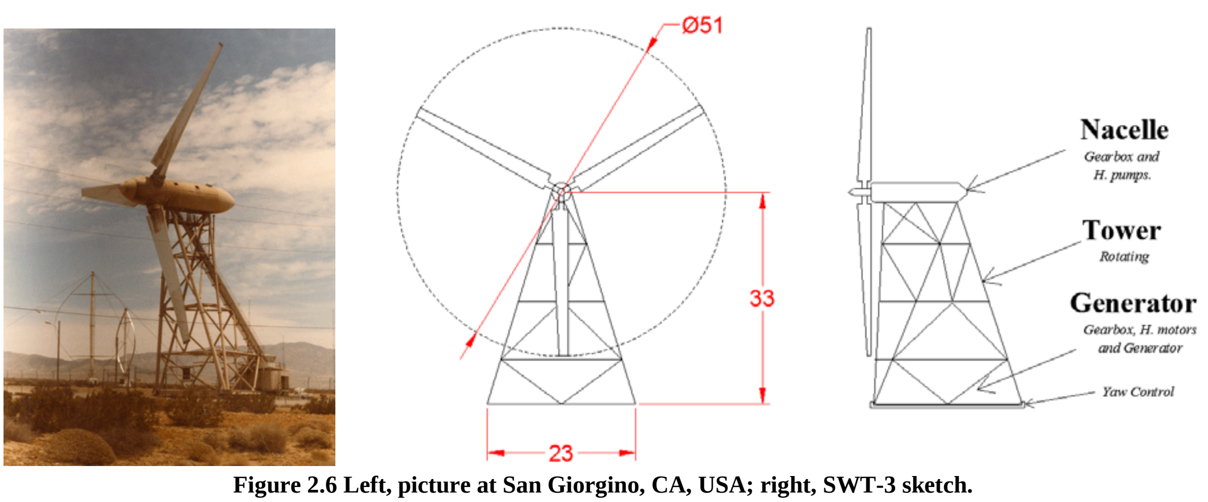

Figure 2.6 Left, picture at San Giorgino, CA, USA; right, SWT-3 sketch.

The idea was simple: drive a pump (s) with the aerodynamic power in the rotor; then send the oil to the tower base where some hydraulic motor (s) will keep a synchronous speed at variable torque. By the time that the SWT-3 turbine was being designed, it was already known that hydrostatic transmissions (based on fixed displacement devices) working below rated levels might have very low overall efficiency. At that time, all the available variable displacement devices were based on sliding surfaces (built-in flow control circuit) that would introduce larger dissipative losses. In a newborn formal industry and with uncertain future, the development from scratch for highly specialized machinery to be used for private experimental purposes was not affordable. It was preferred to proceed with standardized components just to have a first impression about the potential of this idea. Since one large pump would be too inefficient besides the fact that it would be scarce, it was selected to proceed with 14 standard fixed displacement pumps[14] connected to 18 standard variable displacement motors[15]. The fixed displacement pumps will be sequentially activated in such a way that only one out of fourteen will be working at partial load[16]. The variable displacement motors worked also based on sliding surfaces; however they were required to assure torque regulation at constant angular speed. Since standardized components (pumps and motors) were brought from other sectors from the industry, other extra *power manipulations* were required before and after the hydrostatic transmission. By the really end, the SWT-3 drivetrain had too many components; and therefore, it was neither simple nor efficient. Figure 2.7 presents a simplified sketch for the complex SWT-3 drivetrain.

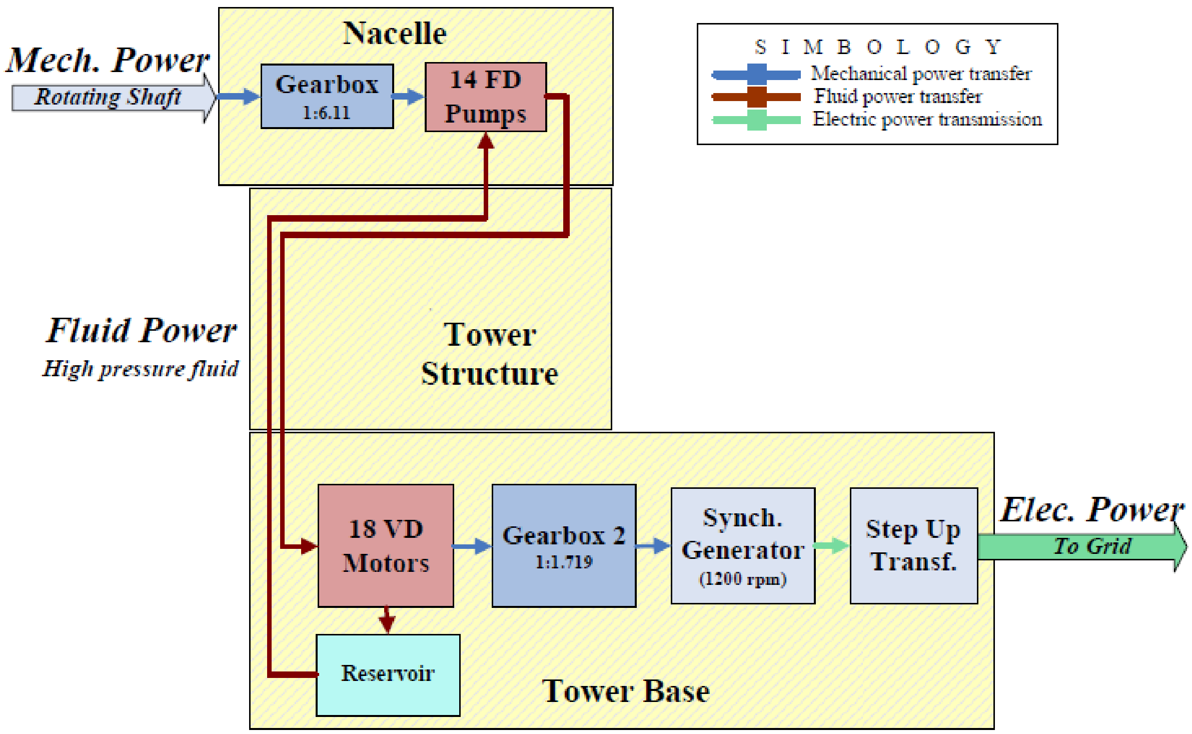

Figure 2.7 SWT-3 - 3MW wind turbine drivetrain

Although the complex drivetrain of the SWT-3 proved the feasibility and some of the advantages of fluid power transfer, it never jumped to the mass production. At the time that it was proposed (newborn wind turbine industry), it was just too complicated. By the middle 1980s, when the oil crisis was old news and environmental awareness was almost forgotten again, this project was abandoned and the turbine was demolished.

[14] Rated power about 300 HP (~220 kW), a common size for crane and boat propulsion.
[15] About 225 HP (~170 kW) rated power. Same case than selected pumps.
[16] The SWT-3 designer decided to divide the rated load in 14 partial loads, according the available aerodynamic power the microcontroller will decide how many partial loads were clutched into the main shaft in such a way that only one of the would be working at partial load.

Although the complex drivetrain always remained in the experimental level, it settled the reference point for some other developments that would come after.

2.3.2. Wikov W2000 SPG

This drivetrain was brought to the market in 2007 by Wikov Wind, a Czech company dedicated to wind turbine industry. The presentation was a 2 MW wind turbine with a rotor diameter about 93 m and hub height up to 100 m. This turbine introduced a variable ratio gearbox from Orbital2, a British firm, followed by a high voltage electrically excited synchronous generator (6.3 kV) that can be directly connected to the grid with no step up transformer required. Figure 2.8 presents the picture of the W2000 2MW SPG transmission and the sketch of the Wikov W2000 SPG power plant. The drivetrain system for the Wikov W2000 SPG wind turbine is presented in Figure 2.9.

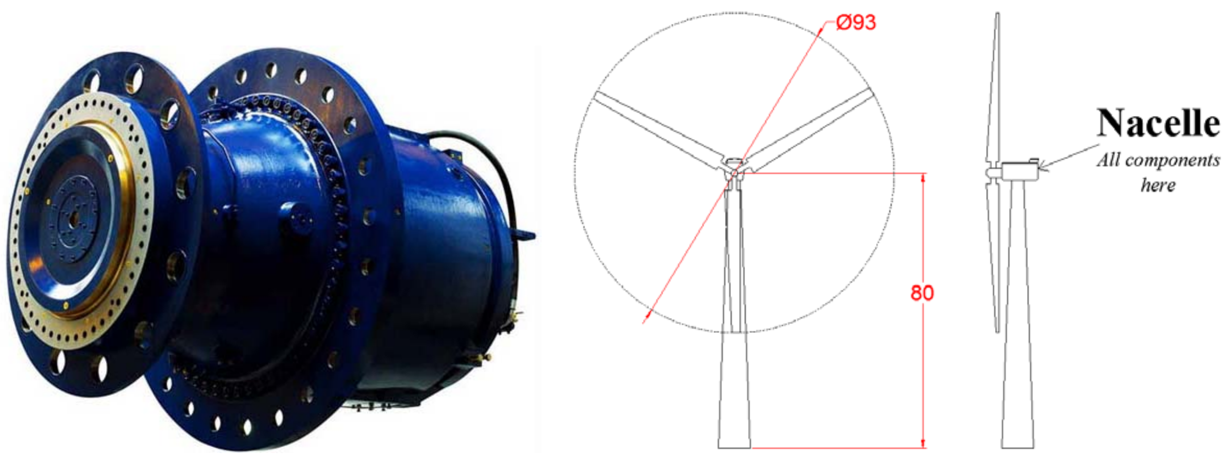

Figure 2.8 Left, W2000 2MW hybrid variable ratio transmission. Right, sketch of Wikov 2MW wind turbine.

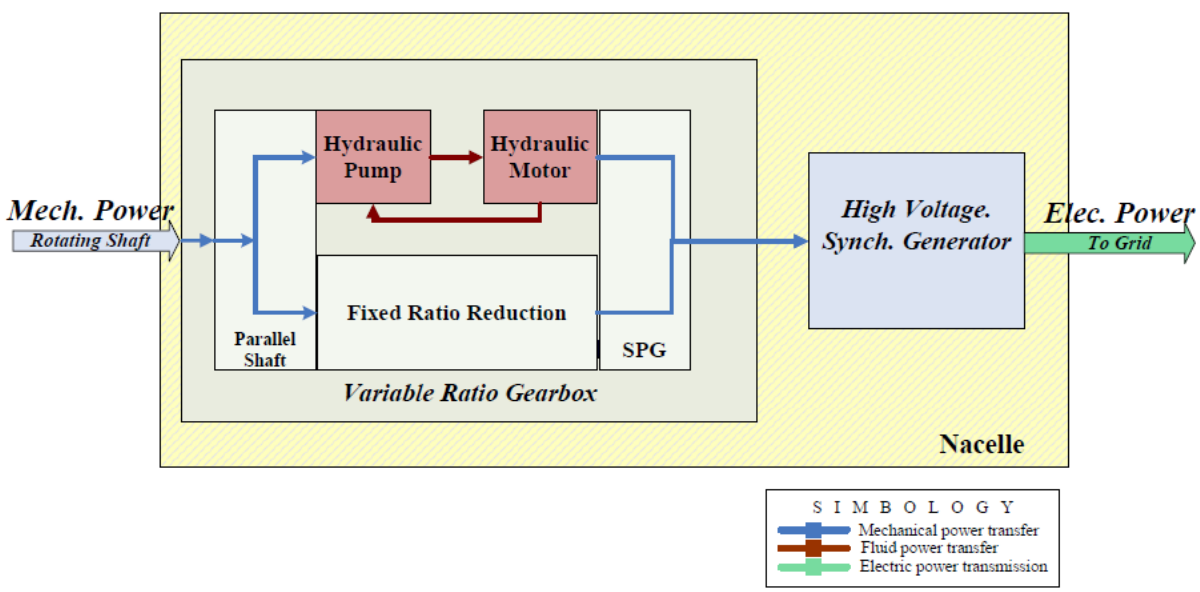

Figure 2.9 Wikov W2000 SPG drivetrain (2 MW wind turbine)

Besides the variable ratio transmission, the drivetrain for this 2 MW wind turbine is quite simple. In general, the variable ratio gearbox splits the input power in two parts, one larger than the other. The largest power is passed through a fixed ratio geared transmission (mechanical power transfer); while the small part is passed though a CPU controlled hydrostatic transmission. The hydrostatic transmission will drive a reaction superimposed gear (SPG) to achieve a variable ratio transmission. The variable ratio is directly proportional to the size of the auxiliary reaction machinery (the larger the unit the larger the variable ratio, but the more losses in auxiliary unit). As it can be inferred, this transmission belongs to the hybrid variable ratio transmissions category. This clever design was originally designed and produced by Orbital2. In 2006, Orbital2 licensed the component to Wikov, who used this transmission in the wind turbine industry.

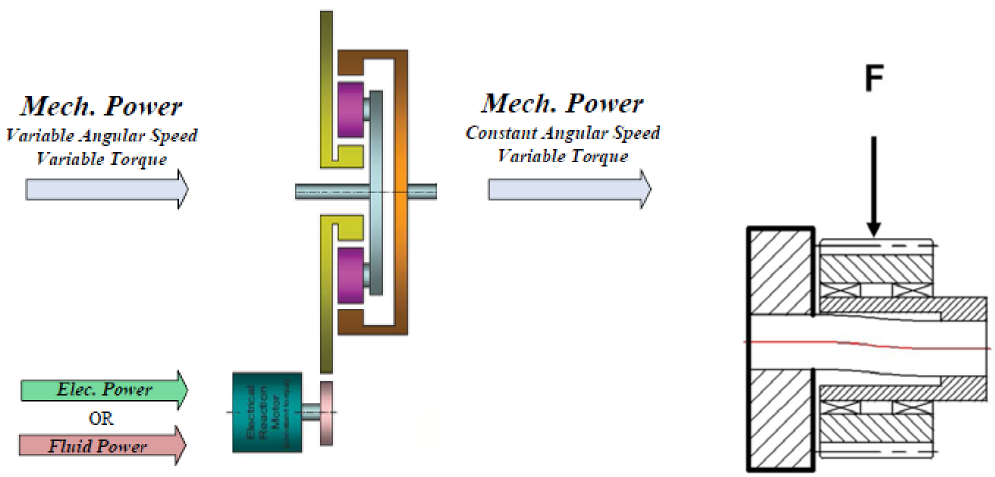

Figure 2.10 Left, SPG principle in LS1; right, flexible pin technology

This variable ratio transmission works based on the patented Super Positioned Gear (SPG) principle, but also incorporates the flexible pin technology. The SPG system consists in including a reaction gear - controlled either by a hydraulic or electric drive - in combination with a planetary gear to allow an effective variable ratio. For the case of Wikov, a hydrostatic transmission is preferred over electrical actuation. In terms of the flexible pin technology, it consists in allowing certain elastic deformation in the sun gear's shaft to guarantee an equal loading over all satellite gears in planetary gear sets. The equal loading allows using the optimum number of satellite gears and therefore more compact geometries are accomplished [*6*]. These two innovative principles are sketched in Figure 2.10.

Although the configuration is radical and the applied principles might look new for the wind industry, they had been present almost since the beginning of formal existence of this industry. Actually, the variable ratio gearbox today used in the Wikov W2000 SPG wind turbine has its origins in the experimental turbine Orkney LS1.

The LS1 was a 2 bladed, 70 m rotor diameter, pitch controlled wind turbine that incorporated variable ratio gearbox (in the nacelle) followed by a 3 MW synchronous generator (located at tower base) and a step up transformer (at the tower base). The LS1 was born as a product of oil crisis in the late 1970s. In those times, worldwide governments got concerned about renewables and Britain was not the exception. By early 1980s several wind energy experiments were started in the Orkney Islands, among them the LS1 wind turbine, which was erected in 1982. This turbine included very innovative concepts like the SPG, which in this case was implemented by means of a electric motor and was responsible for the variable ratio gearbox, and the flexible pin technology patented by Mr. Ray J. Hicks, who later will become the Orbital2 company founder. The LS1 wind turbine is sketched in Figure 2.11.

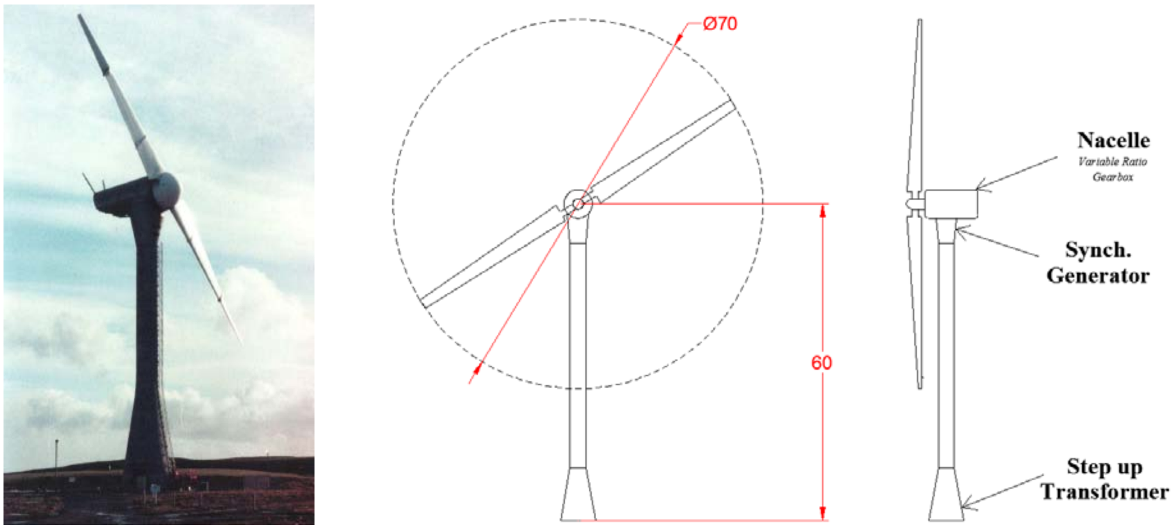

Figure 2.11 LS1 wind turbine

The drivetrain for the LS1 wind turbine is represented in Figure 2.12. The LS1 wind turbine had a similar fate than the SWT-3; so it never overcame experimental stage. Nevertheless, flexible pin technology and the SPG principle will revive in the W2000 SPG wind turbine (shown in Figure 2.9) with slight modifications jumping into mass production. Although the wind turbine structure of the LS1 and the Wikov W2000 are significantly different (i.e. concrete tower and 2 blades in LS1versus 3 blades on metallic, etc.), only two main differences can be pinpointed in the drivetrain system: in the W2000 SPG a high voltage synchronous generator so no step up transformer is required anymore; and, in the W2000 SPG the electrical reaction motor is replaced by a hydrostatic transmission connected directly to the rotor and intended to drive the reaction gear.

In the variable ratio SPG gearbox, speed regulation is achieved by adjusting the angular speed of the reaction gear, which is propelled by the CPU controlled hydrostatic transmission. As mentioned before, in this gearbox the input power is divided in two shafts. One of them will be fed to the hydrostatic transmission which eventually will drive the reaction gear in the SPG system; while the other is passed through a fixed ratio reduction to be delivered as the prime mover for the SPG system. The geared fixed ratio reduction will be referred as train A. When the angular speed of train A is lower than the required to synchronize the generator, the auxiliary hydrostatic transmission directs the power to drive the reaction gear in direction opposite to train A rotation (reduced torque condition but increased angular speed). On the other hand, when the angular speed driven by train A is larger than the required; then, the reaction gear is driven in the same direction than rotating train A to create the opposite reaction (increased torque with angular speed reduction). The angular speed regulation range directly depends on the rated power of the hydrostatic transmission [*7*]. In the case for the Wikov W2000 SPG wind turbine; according to manufacturer data the drivetrain is capable to deliver electrical power at synchronous speed for wind speeds between 3 - 20 m/s (after synchronization) for Specification 93 TCIIIB [*8*].

In the W2000 SPG fluid power is only used to control the output angular speed. Although the largest part of power is being transmitted mechanically by the geared transmission; important weight savings are product of a slender gearbox design. This drivetrain also gets rid of components like electronic power converters and step up transformers through to the use of high voltage electrically excited synchronous generator . Despite the increased reliability with the use of flexible pin technology [9], the fact is that the W2000 SPG is still a geared transmission that makes use of a hydrostatic transmission to control a secondary set of gears (the reaction gear from the SPG system). So advantages within this drivetrain are more related with the use of planetary gears and flexible pin technology rather than fluid power transfer; therefore this drivetrain system can be accurately described as a high evolved gearbox rather than a hydraulic transmission.

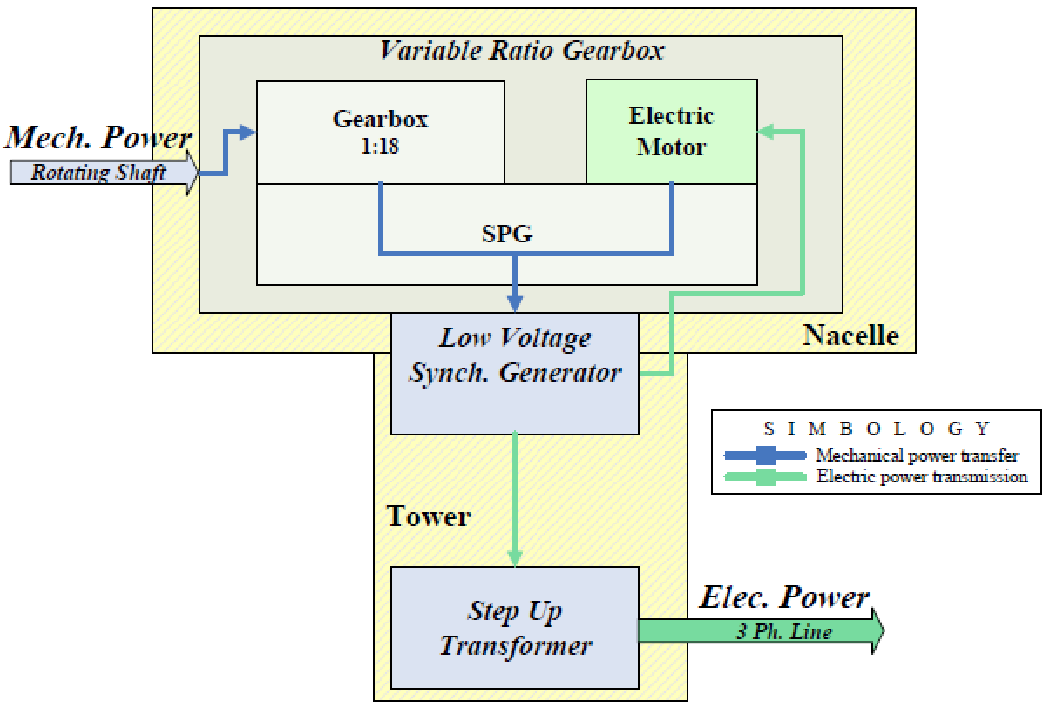

Figure 2.12 Orkney LS1 drivetrain(3 MW wind turbine).

2.3.3. DeWind 2 MW WinDrive®

The WinDrive technology was conceived in early 2003 by Voith, a German large power transmission producer. WinDrive technology has its origins in the wind industry's need to avoid the use of power electronic components. Voith already have the Voith Vorecom transmission: a well proven large power transmission with a variable speed planetary gear set. This system was designed for constant speed - variable torque input and variable speed – variable torque output. Since Vorecom's design parameters were the mirrored ones that wind industry needed, the starting idea was to mirror the Vorecom system to create the WinDrive system. The concept proved functional by late 2003, and by 2005 DeWind, an originally German wind turbine manufacturer, jumped into the train with a 2 MW wind turbine platform. By 2007 a prototype was already operating in Cuxhaven, Germany. One year later 2 more prototypes in a well designed marketing campaign were erected in Texas, USA and Argentina. In 2009 WinDrive was granted by the Hermes Award (a German technology prize) and by 2010 DeWind was bought by Daewoo Shipbuilding and Marine Engineering Co., Ltd (DSME).

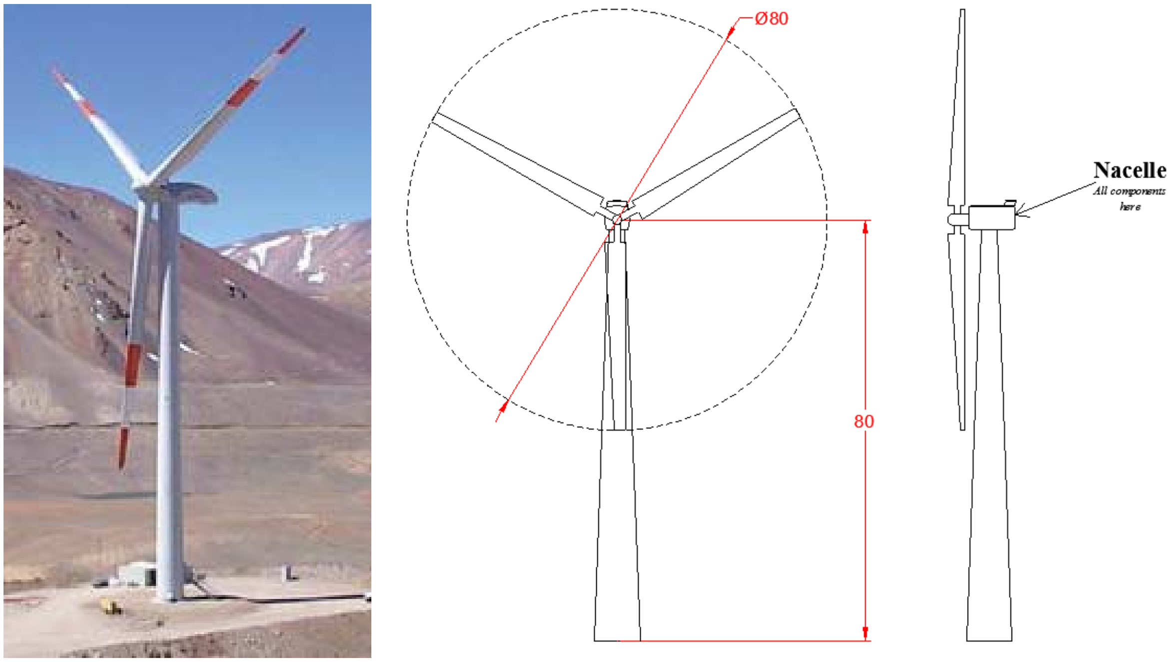

Figure 2.13 DeWind D8 2MW wind turbine

The Voith WinDrive system was originally mounted on a DeWind D8 2000 kW specially modified to fit the new system. This was a 3 bladed-80 m diameter rotor and 80 m hub height wind turbine. This wind turbine is sketched in Figure 2.13. Originally, the DeWind D8 2 MW, had a fixed ratio gearbox followed by a DFIG, a reduced size electronic converter and a step up transformer. After the WinDrive system was fitted, the use of a high voltage electrically excited synchronous generator was possible and therefore neither PEC nor step up transformer were any longer required. This new configuration was called DeWind D8.2 2000 kW. The drivetrain for the DeWind D8 2000kW and the new version DeWind D8.2 2000 kW are sketched in Figure 2.14.

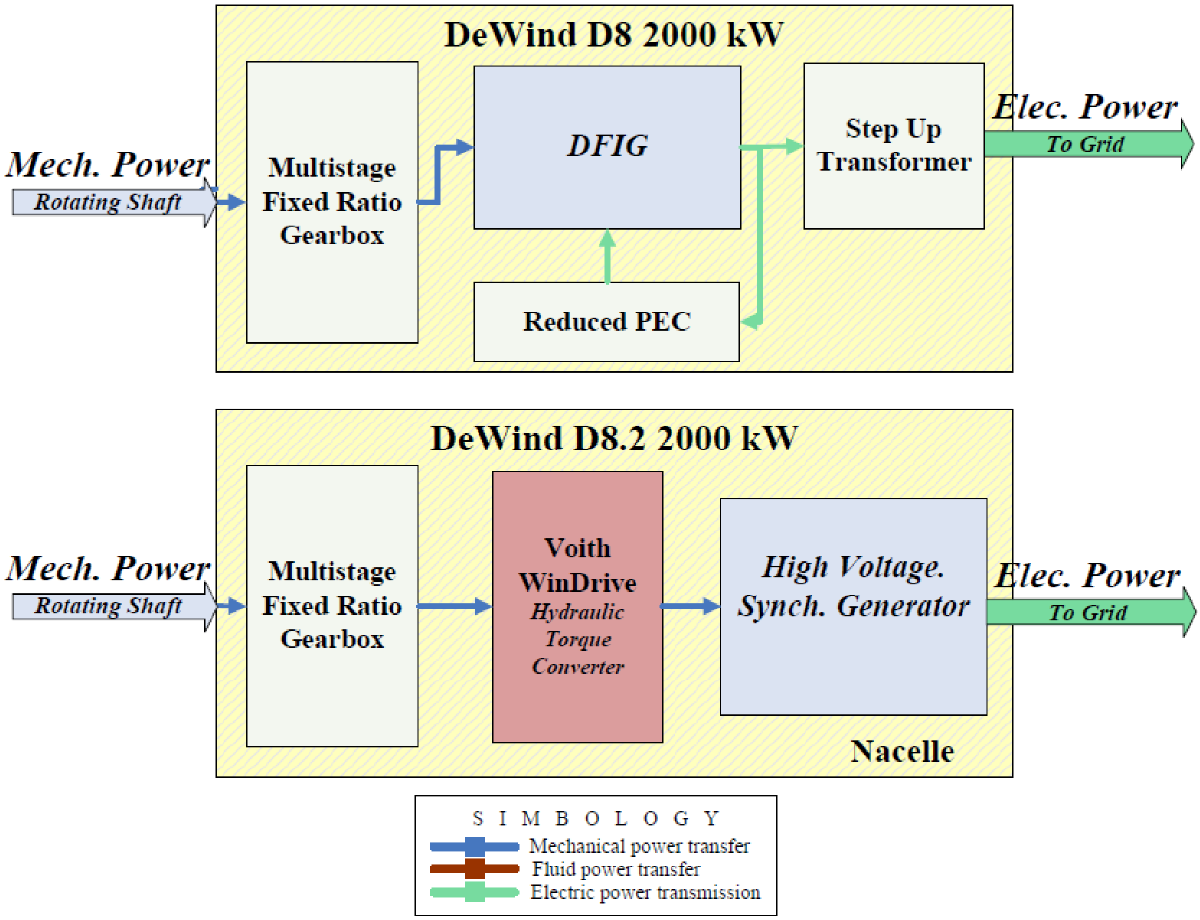

Figure 2.14 Top, DeWind D8 drivetrain; bottom, DeWind D8.2 drivetrain with Voith WinDrive

The more important reasons that made a success the introduction of the Voith WinDrive system to the market was its high adaptability and modular nature. Such was the case that after being a few years in the experimental market several manufacturers started to consider including this system in their drivetrain (i.e. BARD[17]). The WinDrive system can be considered as an extra mechanical component that is located between the gearbox and the electrical generator. It replaces the power electronic converter and step up transformer functions by making possible to fit a high voltage electrically excited synchronous generator. The WinDrive system can be considered as a high performance part for a conventional fixed ratio gearbox. WinDrive makes possible to upgrade a conventional gearbox into a variable ratio one. To do so, the WinDrive system uses a series of planetary gear sets to split the power input in two sections. One of these sections drives power directly through a fixed ratio rotating shaft while the other uses fluid power transfer (hydrodynamic principle) to increase the effective torque of the same output shaft. In order to do this, a torque converter set (a particular array of hydrodynamic transmission) is used.

A torque converter set block diagram is illustrated in Figure 2.15. Although operating principles are similar to those in a hydrodynamic transmission (shown in Figure 2.2); it can be differentiated by the presence of a stator as an intermediate stage among the centrifugal pump and the turbine. The function of

[17] Since late 2009 Voith had been working in scale up this system to sizes about 5.0 - 6.5 MW in partnerships with BARD, a german wind turbine producer specialized in offshore facilities.

this component is to produce an extra torque when a high slippage condition is present between pump and turbine. This high slippage condition is achieved when the angular speed of the turbine is significantly different to the angular speed of the pump. The stator is a kind of small turbine that requires smaller flow (compared with the turbine) to be driven. The stator is designed to extract power from remaining fluid's kinetic energy (after passing through the turbine) and incorporate it as additional torque to the same shaft driven by the turbine. The stator has mechanical connection to the turbine by means a rotational spring. Under low slipping condition the relative angular displacement between stator and turbine is near to zero and the stator function is only to provide an effective path for the turbine's outcoming fluid. Now, under a high slipping condition, the stator receives an oil flow with high kinetic content; this makes it to increase its relative angular displacement respect to the turbine storing energy in the rotational spring. The elongation in the rotational spring generates an effective torque directly applied over the turbine. This additional torque plus the one product of fluid coupling will eventually accelerate the turbine (or to have a steady increased torque condition if deformation is held) until relative angular displacement between these parts are near to zero, where the low slipping condition will be achieved. Based on this, it can be said that the torque converter is basically a hydrodynamic transmission with assisted turbine start. This operating principle gives the torque converter the characteristic feature to increase effective torque over output shaft. If the output shaft is kept at a constant speed by means of another device (i.e. a synchronous generator) then the power variations can be absorbed in terms of torque variations at constant speed.

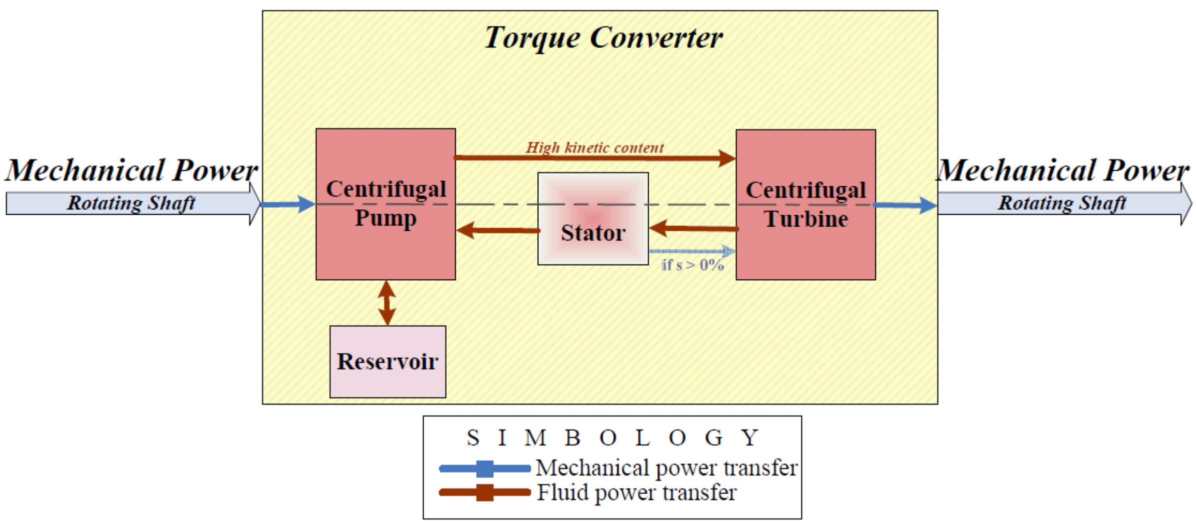

Figure 2.15 Torque Converter Set. *s* means slip.

The way in which this concept is applied to the WinDrive system is by initially splitting the power input in two parts. One of them, as was mentioned before, is directly driven by a fixed ratio transmission and passed through the WinDrive system as mechanical energy in a rotating shaft (for convenience, this shaft will be called Shaft A). The remaining mechanical power is originally increased in kinetic content by several epicyclic stages to later be transferred through fluid power inside the torque converter set. Consider that the entire torque converter set is coaxially located to Shaft A, but only the turbine is mechanically linked to Shaft A. The fluid power transfer will transform any additional power available at the input into torque variations at constant angular speed (given by Shaft A). To do so, the mechanical power with large kinetic content drives a hydrodynamic pump. Therefore, high kinetic content fluid is driven from pump to turbine inducing torque variations over the turbine. Because of the shape of the turbine, the fluid leaves this component still with kinetic content, which is directly proportional to the present slipping condition (the larger the slippage the larger the kinetic content). After leaving the turbine, the fluid reaches the stator. The stator is designed to incorporate outgoing fluid as increased torque to the turbine and had mechanical linkage to the turbine by means of a rotational spring. Because of the kinetic content, the stator presents a relative angular displacement respect to the turbine. This displacement is displayed as torque increase applied over the turbine. Since the angular speed of Shaft A remains fixed, then the synchronous generator must absorb this input torque availability by generating more electrical power. Since the turbine is rotating at the same angular speed than Shaft A, the pump angular speed would normally be higher than the Shaft A; therefore torque converter set will be subject of a high slipping condition. This condition will lead to a steady condition where the stator would have relative displacement with respect to the turbine position. This condition will eventually lead to a steady torque increase due to turbine plus stator action. This torque increase will try to change the angular speed of A. Since this speed must remain fixed, the torque demanded by the electrical generator must be increased in order to keep an equilibrium condition. This operating condition is kept all along power variations once the synchronous angular speed for Shaft A is achieved. Figure 2.16 sketch this operating principle.

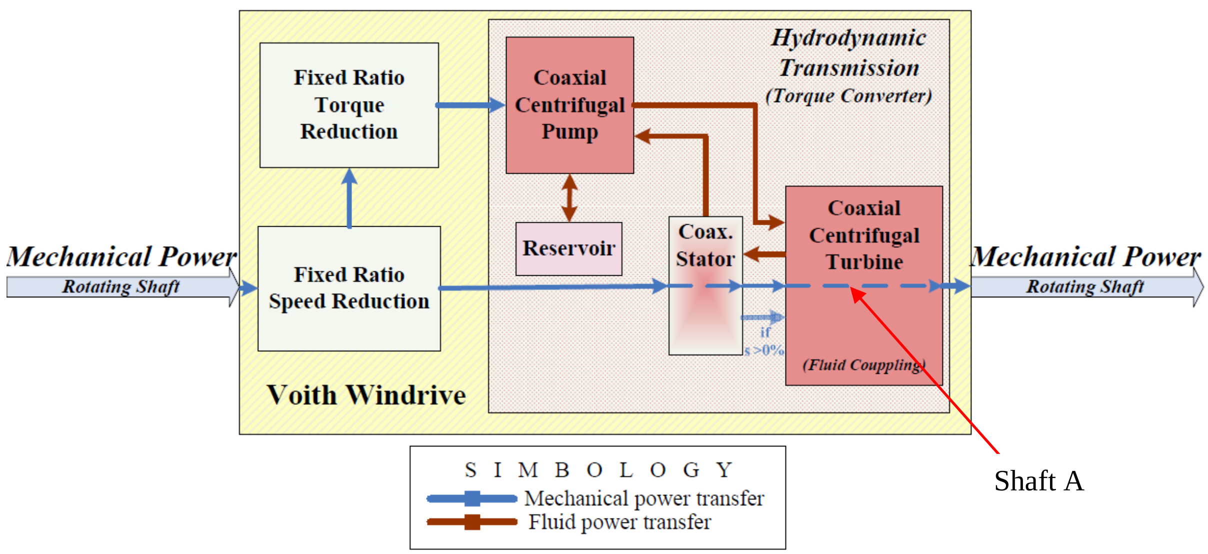

Figure 2.16 Voith WinDrive functional block diagram

The conception of the WinDrive system as an external component opened its market range to even be used as an upgrade for conventional drivetrain systems. The WinDrive system not only minimizes the use of extra components; but also reduces mechanical stresses in the gearbox by splitting power flow into two different mechanisms (fluid and mechanical power); one of them providing implicit stress damping. Also, this system allows saving weight by two means: it allows keeping the gearbox[18] and taking out two components by adding one extra. Since the WinDrive system just upgrades a conventional gearbox into a variable ratio one; this solution might not be considered to be slender design since the number of components is not being entirely optimized. However this system had proven to be innovative and commercially successful in wind turbine industry.

[18] Which eventually lead to more compact electric machines due to increased angular speed.

2.3.4. ChapDrive and DOT drivetrain concepts

The wind energy industry is mostly based in low scale generation (up to a few MW per plant). Due to this, the number of required generating plants must be large enough to cope with power demand. Another important fact is that the market had showed a sustained preference for green energy. But, it also exhibited that it is preferable to have the energy harvesters as far as possible. This constant tradeoff between benefits and sacrifices made the wind turbine industry go offshore. Going offshore implies more expensive and risky operation than onshore. In the past few years, a couple of radical offshore oriented concepts were developed. Some of them incorporate fluid power transfer as predominant mechanism claiming that it is possible to abate energy prize up to 20% compared with conventional offshore technologies. Among these concepts, the ChapDrive drivetrain concept and Delft Offshore Turbine (DOT) drivetrain concept can be found.

The ChapDrive is an innovative drivetrain concept that proposes to replace the entire drivetrain by a hydrostatic transmission and a synchronous generator. It was originated in late 2004 as a proposition for floating offshore structures at the Norwegian University of Science and Technology. In 2005 received funding from Statoil to build a 50 kW first prototype, eventually this lead to a 300 kW second prototype built in 2006. The prototype built in 2006 was implemented in a 225 kW wind turbine (Vestas V27 225 kW) and it was subjected to extensive studies and several overhauling processes. Based on 300 kW prototype results, in 2008 a new 900 kW prototype was erected and tested in a Danish wind turbine (Neg Micon NG52 – 900 kW). The results for the last prototype were presented in 2010, which served as basis for the conceptual design for a 5MW turbine intended to employ the ChapDrive concept. Figure 2.17 sketches the dimension of the wind turbines employed to test the ChapDrive.

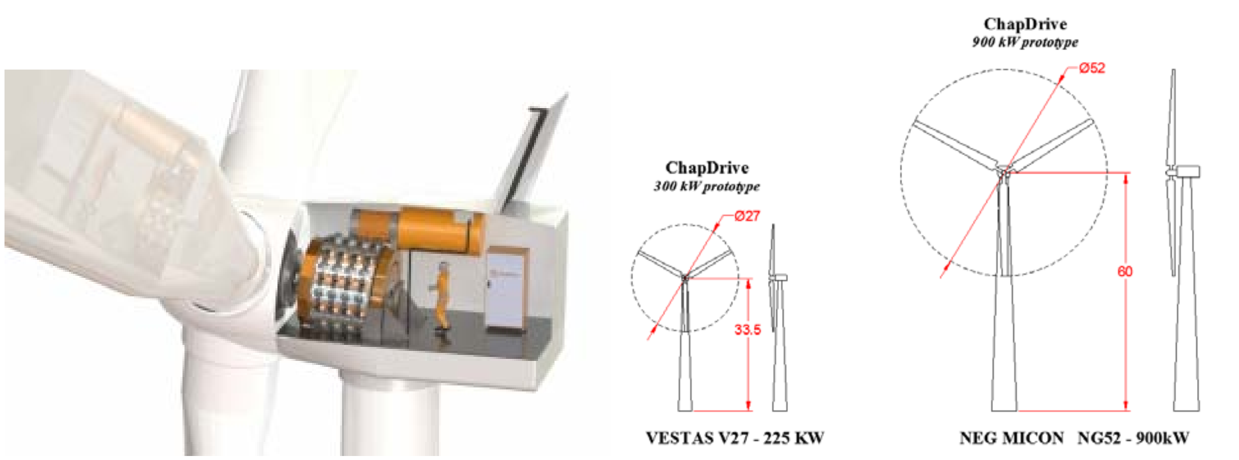

Figure 2.17 Left and middle, 300 and 900 kW ChapDrive prototypes; right, solid foundation ChapDrive Concept

The drivetrain proposed by a the ChapDrive concept is implemented by connecting a low speed fixed displacement hydraulic pump that takes oil from the reservoir and send it to a high speed variable displacement hydraulic motor. The hydraulic motor is intended to maintain a constant angular speed – variable torque directed to an electrically excited synchronous generator. The interaction between elements is directed by the ChapDrive Control system. With the targeted intention to take wind farms offshore, the ChapDrive concept proposes two different topologies according to the foundation of the wind turbine. For solid foundation (on shore and low depth offshore) they propose to have the hydrostatic transmission and the electrical generator inside the nacelle. In this configuration, only electrical power will be evacuated from the nacelle (presented in the right image of Figure 2.17). The other array is oriented for floating structures (high depth offshore). In this case, they propose to have only the hydraulic pump in the nacelle; reservoir, hydraulic motor and electrical generator will be located at the seal level inside the tower structure (intended to offer a lower center of mass). In this configuration, fluid power is being transmitted from nacelle to tower base, where it will be eventually transformed to electric power. These two drivetrain arrays are presented in Figure 2.18.

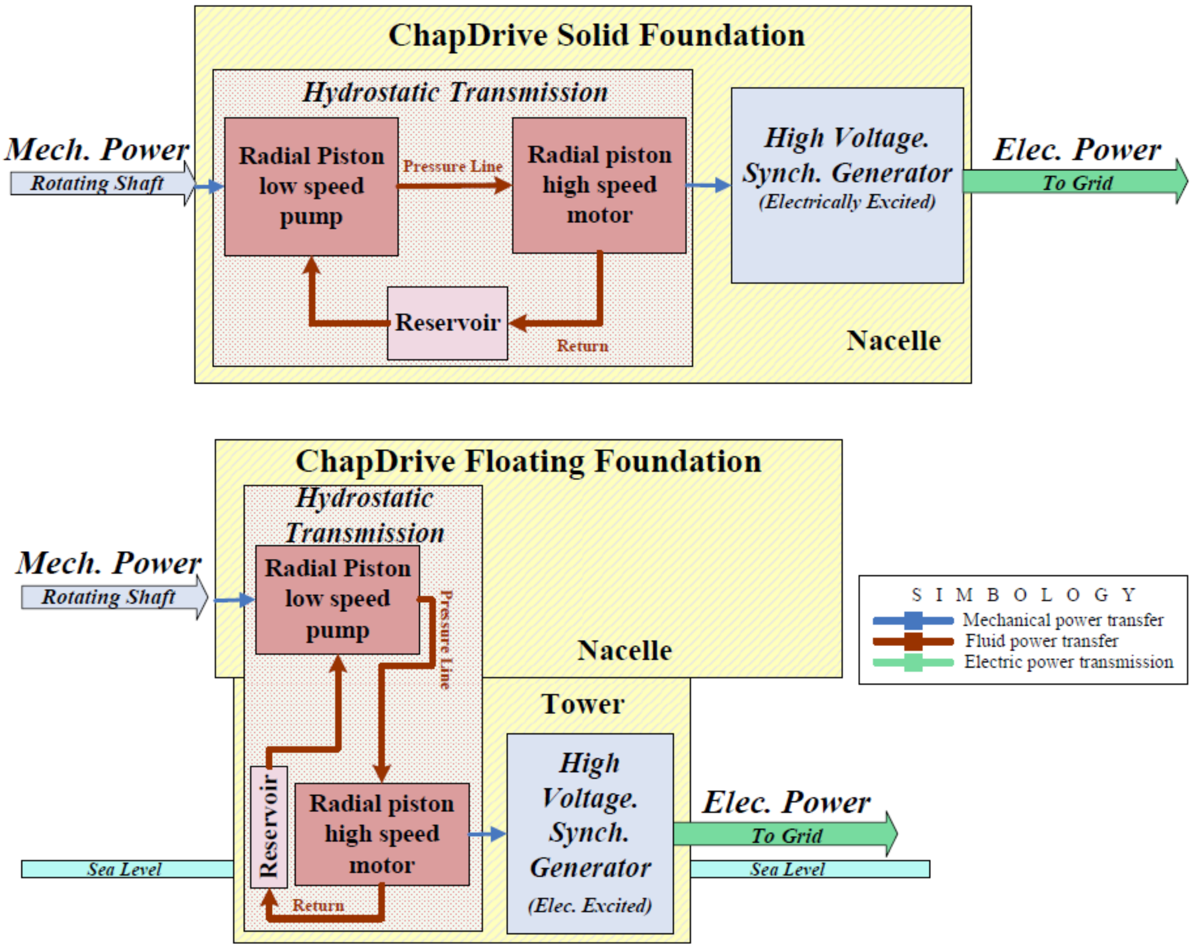

Figure 2.18 ChapDrive drivetrain.

On the other hand, the DOT concept was originated in the Delft University of Technology and proposes an innovative concept for large wind turbines (5-10 MW). This wind turbine concept asserts the use of a 2 bladed rotor geometry driving a hydraulic pump in the nacelle driving oil towards a hydraulic motor at the tower base (hydrostatic transmission)[*10*]. The mechanical energy in the tower base is used to drive a second hydraulic pump (fixed displacement) that will drive sea water to a large Pelton turbine (hydrodynamic turbine). The last turbine would receive the incoming fluid power from one or several wind turbines and transform it to mechanic power. The mechanical power will be later transformed to mechanical in a large electrical generator. Since 2010 exhaustive drivetrain testing had been carried out in a small scale laboratory set up. Based on results, in 2011 the proposal for a small scale prototype was approved. Such prototype is currently under construction and it is expected to be tested along 2012. The DOT drivetrain concept is sketched in Figure 2.19.

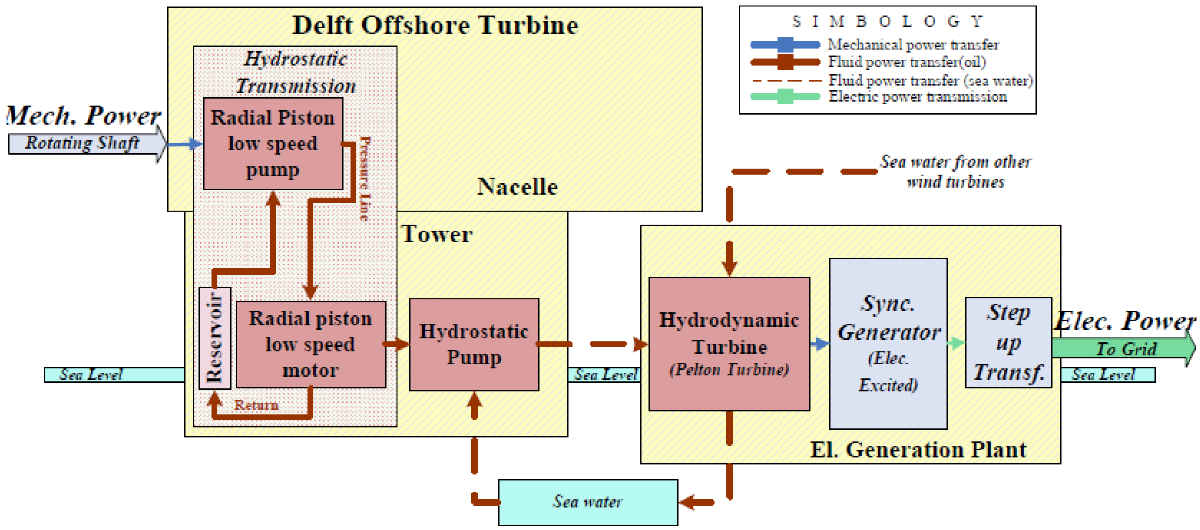

Figure 2.19 DOT concept

2.3.5. Artemis Digital Displacement

Artemis Digital Displacement system materializes the concept presented so far as digital hydraulics. Digital hydraulics overcome current issues with low efficiency levels at partial load condition(in motors and pumps) by proposing software controllable[19] radial piston pumps and motors. Their main feature is to provide high efficiency levels at any load condition. This is achieved by adjusting the actuator's behavior for all operating points based on *preprogrammed* functions. Artemis Ltd. (Scottish company incubated at the University of Edinburgh) had already a working test bench of an automotive transmission by 2005. This prototype incorporated an Artemis Digital Displacement hydrostatic transmission driven by an internal combustion engine[20]. This technology reported fuel saving of about 30-50%. Artemis' products formally jumped to the wind industry sector on late 2006, where a publication related to the use of Artemis products as drivetrain for wind turbines was presented by Dr. William Rampen (chairman and founder of Artemis Ltd.) in Bremen, Germany. At that time, Rampen reported results of simulations and test for their products compared with others available in the hydraulics market [5]. By 2007 they obtained patents for their products used in similar applications to those for wind turbine industry. Then, in 2009 they presented laboratory results for their 1.6 MW working prototype (shown later in Figure 2.20) for a wind turbine drivetrain. Since then, Artemis' products had been gaining terrain and reputation in the market. For late 2010, Mitsubishi bought Artemis Ltd. and started working in a 5 MW wind turbine based on Artemis Digital Displacement machines. Figure 2.20 present the a 1.6 MW low speed hydraulic pump (about 1.50 m in diameter) and a 0.8 MW high speed hydraulic motor (~0.50 m diameter) subjected to laboratory tests whose results were presented in 2009.

[19] The Digital Displacement system relies entirely in software to implement pump/motoring function or even braking.
[20] The internal combustion engine drives a Digital Displacement pump, the pump drives oil to a Digital Displacement motor, which propels a medium size sedan (a BMW serie 5).

Figure 2.20 Artemis Digital Displacement 1.6 MW low speed pump (left) and 0.8 MW high speed hydraulic motor(right)

The Artemis Digital Displacement drivetrain system minimizes the use of other components by integrating a hydrostatic transmission based on digital hydraulics. The variable ratio transmission takes care of angular speed regulation making possible to fit a high speed-high voltage electrically excited synchronous generator, which can be connected directly to the grid. The hydrostatic transmission integrates a Digital Displacement radial piston pump (rated power 1.6 MW). The output fluid power drives 2 hydraulic motors (rated power 0.8 MW) that can work independently. Then, the hydraulic motors drives independently two high speed generators (rated power 0.8 MW at 1500 RPM). The fact that two off the shell generators can be operated separately helps minimizing parasitic losses in the generators. This is presented in Figure 2.21.

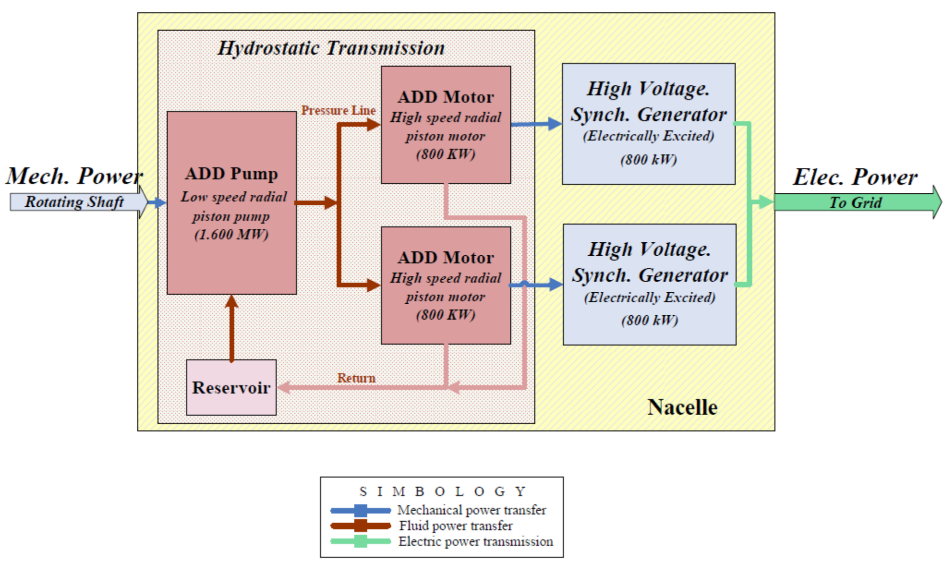

Figure 2.21 Artemis drivetrain

The Digital Displacement pump works based on the same principle that drives oil in a fixed displacement radial piston pump (presented in Figure 2.5). The operation principle of such device will be studied in more detail in the following chapter. For now, let’s consider that in a radial piston pump, the input mechanical power (contained in a rotating shaft) is used to drive a moving piston that is coaxially located inside a spatially fixed cylinder. It is possible to have several of these piston-cylinder sets located inside the same pump in a radial array. These cylinder-piston sets are each one equipped with at least two valves (admission or low pressure valve and expulsion of high pressure valve). The cylinder-piston set has the capability to vary cyclically its volume depending on the angular position of the rotating shaft (θ). The varying volume (volume A) is comprehended between a moving piston and the top of the cylinder. This idea is presented in Figure 2.22.

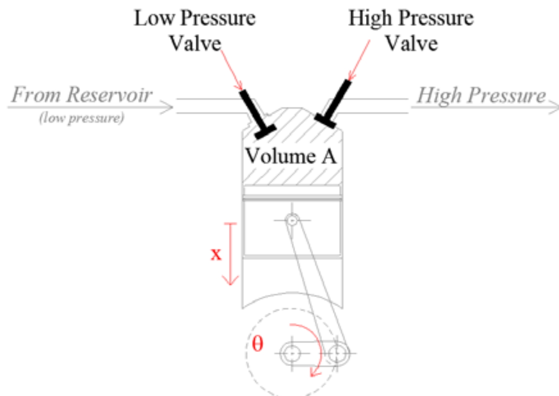

Figure 2.22 Cylinder Piston set.

In a normal fixed displacement radial piston pump the low and high pressure valves are mechanically controlled by a camshaft that is normally geared to the crankshaft (pump's input shaft) implying that the valves only open (or close) at an specific crankshaft's position (θ). So, there is no way to control the outgoing flow from the pump besides the input power, properties of the fluid or an external control circuit. In all cases, power losses are increased. The Digital hydraulics overcomes the flow control issue by electrically triggering the low and high pressure valves by means of software controlled solenoids. Also, low and high pressure valves in Artemis Digital Displacement products claim to incorporate a particular design that minimizes drag in all implementable functions. Software control makes possible to command any valve in any cylinder at any crankshaft position (θ). Therefore it is possible to implement several functions (i.e. idling, braking and full or partial flow) in the same machinery by just changing the software code. In terms of the Artemis Digital Displacement hydraulic motor, its operation is exactly the opposite than the pump described here. By the end, electrical triggered valves increase controllability of the system. This allows working some piston-cylinder sets at full load while the rest are idled in the same radial piston pump. This is equivalent to have several mono-cylinder radial piston pumps that can be clutched at will. So, any power availability can be split over the selected number of cylinders working them close to its rated power (analogous to the 14 pumps in the SWT-3).

Regardless all advantages, there is one important disadvantage: digital hydraulics and the use of hydraulics are *quite new* in the market of wind turbines. The wind turbine industry, in the past, had shown reluctant tendencies to very large changes in conventional systems. Since these systems imply a defiant evolution, it is possible that not all major players are willing to risk their old proven concepts for this new technology. Therefore they might struggle to keep reach the mass production levels in the industry.

On next, conclusions about this chapter will be presented. In there, one specific path of research will be selected to be studied in depth, built a computer model and eventually evaluate quantitatively advantages of hydraulic drivetrains versus non hydraulic ones.

2.4. Conclusion

In this chapter, a brief introduction to fluid power based variable ratio transmissions was presented. Then some current available hydraulic drivetrain systems were qualitatively described. On next, the general conclusions of this chapter will be presented.

A variable ratio transmission based on fluid power uses a hydraulic pump driving a hydraulic motor to create a variable ratio. There are two main operating principles: hydrostatic and hydrodynamic. Also, variable ratio transmissions can be classified in three main branches (based on operating principle): hydrostatic, hydrodynamic and hybrid. Because of the wide variety of hydraulic machines, combinations for variable ratio transmissions are almost endless. Regardless the base operating principle or the selected machines, flow can be controlled by three means: built-in mechanism, external control circuit and fluid properties.

Conventional hydrostatic transmissions perform badly when working below rated operating condition (efficiency ~60%). Since a wind turbine spends about ~65% of its life in this condition [*5*], it proved to be very inefficient the use of conventional hydraulics in the early 1980s with the Bendix SWT-3. This was not affordable for a new born industry.

Today, more advanced control techniques (Wikov, Artemis, etc.) or highly specialized machinery (WinDrive) made possible a wiser use of hydraulics that might overcome low efficiency issues. One clear example is digital hydraulics, which address this issue by partially *shutting down* the machine to minimize parasitic losses. As a result, better efficiencies can be obtained. Some manufacturers like Artemis claims to be able reaching drivetrain efficiencies as high as 91% in partial load condition. These improvements are based on valves controllability. This also allows changing by software the machine behavior.

Among the advantages of using hydraulics in wind turbines' drivetrains can be found: weight reduction, lack of geared machinery, compatibility with synchronous generators, and a highly experienced industry around cylinder based hydrostatic transmission components. Such advantages allow a slender design minimizing the net number of components.

All presented drivetrains, all of them present unique advantages over the others; for instance, while Artemis minimized the number of components, WinDrive can easily upgrade old drivetrain systems. Nevertheless, the particular selection for hydraulic drivetrain to be study in the upcoming chapters is Artemis Digital Displacement. The main reason for this is that the study of a hydrostatic variable ratio transmission using piston based machinery can easily extend the contribution of this document since most of the presented hydraulic drivetrains are (or can be) implemented with piston based hydraulic machinery: Artemis, DOT, ChapDrive and even Wikov. This will allow the reuse of the built computer model for further research. To guarantee such recyclability, the research approach will target the physics behind conventional hydraulic piston based machines so Artemis Digital Displacement can be approached as a particular case of study. Then the model, with slight modifications, would be capable to represent some other machines if required. The fundamentals for such computer model will be introduced in the following chapter.

3. Modeling

3.1. Introduction

The past chapter summarized some existing hydraulic drivetrains. From all different topologies, special interest will be paid to Artemis Digital Displacement drivetrain. However, instead of modeling exclusively this hydraulic drivetrain, a more general approach is preferred. This more general approach intends to extend the contribution of this document by facilitating the modeling of some other piston based hydraulic drivetrains with minimal effort. Therefore, this chapter will discuss the fundamentals of the computer model presented later in Chapter 4.

Then, the main goal of this chapter is to discuss the physics and operating principle of a piston based hydrostatic transmission. In general, the transmission will be formed by a pump, lines and a motor. Both machines belong to the radial piston fixed displacement characterization. The physics of the system will be approached by first modeling a conventional fixed displacement monocylinder radial piston pump. Then, the machines' optimization will be integrated based on the Artemis Digital Displacement machines operation. Bear in mind that the particular geometry of Artemis 1.6 MW system is dealt as a particular case of study intended to exemplify the applicability of this model. Also, some complementary models (rotor and generator) will be described within this chapter. These models are intended to complement the hydrostatic transmission in a wind turbine drivetrain system.

3.2. Conventional radial piston pump

In order to have a deeper understanding of modern piston-based hydraulic drivetrains used in wind turbines, a model for a conventional radial piston pump will be derived. This first model is aimed to understand the physics behind the operating principle, current deficiencies and their cause, and how do they affect the system performance. This knowledge will serve as foundation to later discuss the claimed advantages of a particular case of study: Artemis Digital Displacement. For now, let's focus in a conventional radial piston pump.

3.2.1. Geometry and reciprocating motion

The power transfer process inside a hydrostatic transmission is done by a flow of fluid between stages (pump and motor) at a particular build up pressure. The build up pressure is product of the combination of physics behind the motor and the mechanical load driven by the motor. To understand this power flow process in hydraulic machines, it is required to take a look into the physics of radial piston machines. The main objectives of this section are: introduce a generic geometry of a radial piston hydraulic machine, study the basic displacement equations for the moving pistons inside this machine, and define a variable volume in the cylinder chamber. Later on, this knowledge will be used to study the flow of fluid into (and from) the chamber.

Speaking about geometry, Figure 3.1 illustrates a single stage- six cylinder radial piston pump. In there, the isometric view sketches the general geometry of such machine while the Section A-A view represents the inner part of the pump. Inside each cylinder there is a piston connected to the camshaft by a rod. The piston presents a reciprocating motion pushed outwards by the camshaft, and inwards by the return spring placed between the rod and the piston sleeve. In Figure 3.1 the return springs had been suppressed to avoid confusion; nevertheless, the spring is depicted on Figure 3.3, where a parts description of each cylinder set is done.

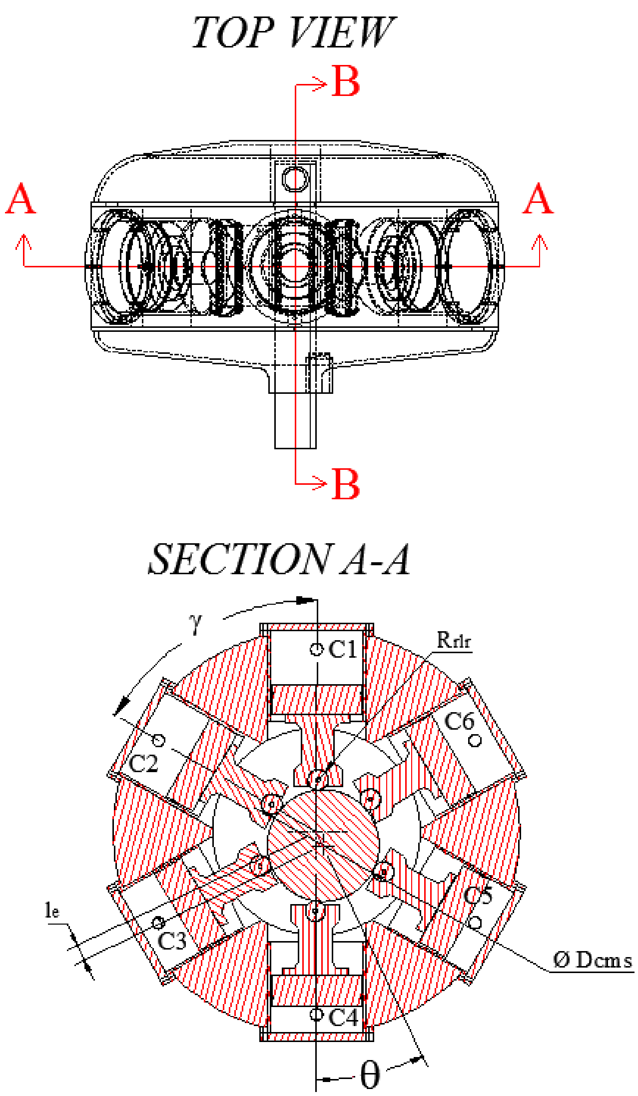

Figure 3.1 Six cylinder radial piston pump.

Notice that in Figure 3.3 both valve's disks are attached to the camshaft. Since there is physical connection between valve's disk and camshaft, they are moving at the same angular speed. This means that there is only one possible configuration for the low and high pressure valve for any angular position (θ). Ideally, this configuration is such that only one valve is open simultaneously (i.e. for C1, high pressure valve open for $0 < \theta < \pi$, low pressure valve open for $\pi < \theta < 2\pi$); however, this is not practically implementable because of *incompressibility of fluids* property (commented later on section 3.2.4).

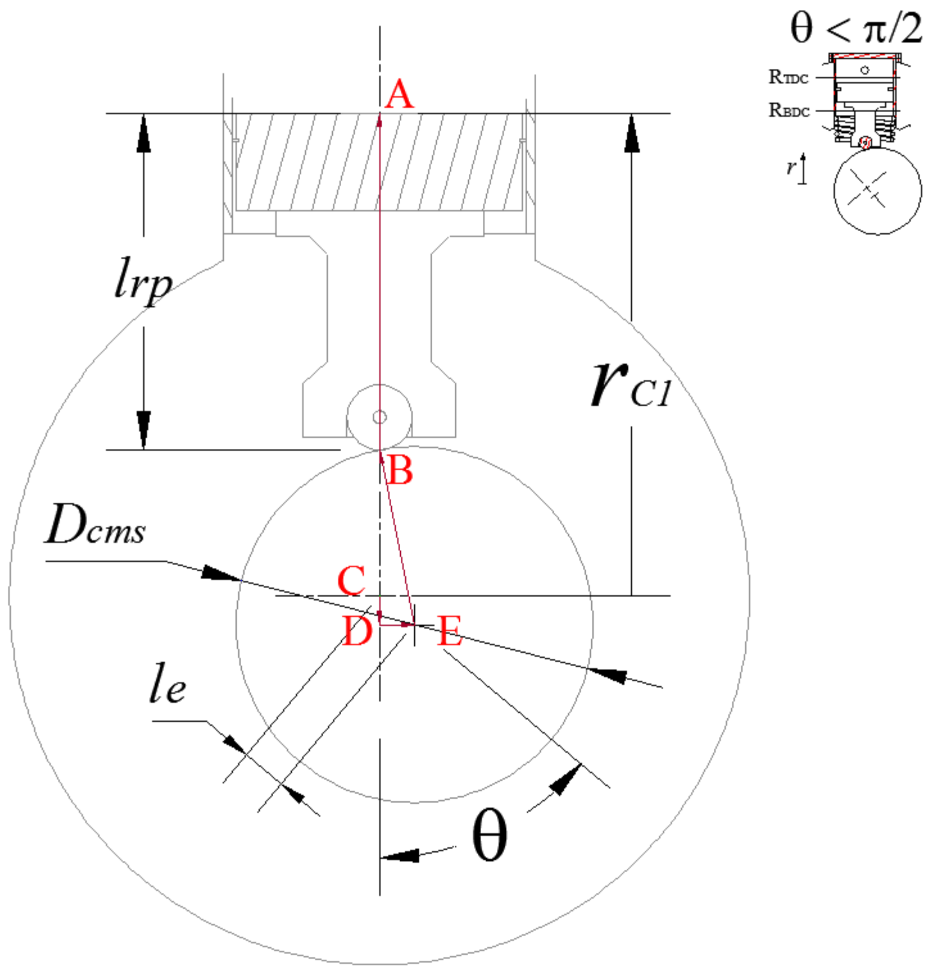

Figure 3.2 Sketch for radial coordinate

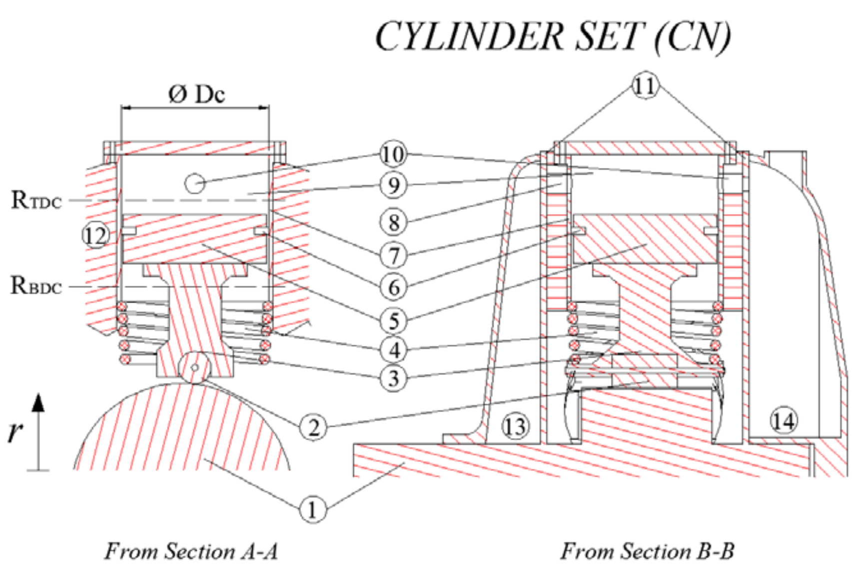

PARTS	
1.	Camshaft
2.	Roller(Bearing)
3.	Rod
4.	Return Spring
5.	Piston
6.	Piston Ring
7.	Cylinder Sleeve
8.	Low Press valve
9.	Pressure chamber
10.	High Press valve
11.	Valve's disk
12.	Housing
13.	Suction Manifold
14.	Discharge Manif.

Figure 3.3 One single cylinder set parts

In Figure 3.1, a N cylinder radial piston pump contains N assemblies of very similar dimensions and geometry but shifted $\frac{2\pi}{N}\ rad$ from each one. Therefore, it is possible to describe physics in all cylinders and their related forces as a function of angular position in the housing. For this objective, phase shift angle γ has been defined as:

$$\gamma_{sa} = \frac{2\pi}{N} \qquad \textbf{Eq. 3.1}$$

Where:
N is the total number of cylinders
γ_{sa} is the phase shift angle in radians ($\frac{\pi}{3}\ rad$ for N=6)

The phase shift angle describes the angular separation between cylinders in the pump housing. It is defined arbitrary as zero for cylinder denoted as C1 and increases in the same direction than DOF θ. Based on this, cylinders can be numbered as presented in Figure 3.1.

It is very convenient to relate the reciprocating displacement of the pistons with the angular displacement θ in radial coordinates. The radial coordinate *r* (Figure 3.3) can be aligned to any cylinder set axis and is defined positive in any direction outwards the center of rotation. In general, *r* will be studied from the bottom dead center (R_{BDC}), which is the smallest value of radial coordinate *r*, to the top dead center (R_{TDC}), which is the maximum value for *r*. This is valid for all cylinders and is lustrated in Figure 3.3. In the other hand, θ (Figure 3.1) ***is used to represent the angular displacement of the camshaft defined as zero when piston C1 is at*** $\boldsymbol{R_{BDC}}$ (Eq. 3.1). Based on this preamble, the ***reciprocating displacement of the upper part of piston for cylinder C1 (***$\boldsymbol{r_{C1}}$***)*** in radial coordinates can be expressed as (see Figure 3.2):

$$r_{C1} = l_{rp} + \sqrt{\frac{D_{cms}^2}{4} - (l_e \sin(\theta))^2} - l_e \cos(\theta) \qquad \textbf{Eq. 3.2}$$

Where: (all referred to Figure 3.1)
r_{C1} is the reciprocating displacement of the upper part of the piston C1 respect the piston sleeve.
l_{rp} is the combined length of piston and rod assembly
D_{cms} is the external diameter of the camshaft
l_e is the distance between the center of the camshaft and the center of rotation
θ is the angular displacement of the camshaft (defined as zero where C1 is at R_{BDC})

Figure 3.2 can be used for better understanding of Eq. 3.2. In there, also a vector approach ($\overrightarrow{CD} + \overrightarrow{DE} + \overrightarrow{EB} + \overrightarrow{BA} = \overrightarrow{r_{C1}}$) can be used. Although the results are the same, approach in Eq. 3.2 was selected because of simplicity.

The main advantage of working in radial coordinates is to facilitate future reproduction of similar approach than the one presented in Eq. 3.2 for any other cylinder in the machine. To do so, the phase angle ϕ will be defined. The phase angle describes the absolute position of any cylinder in a hydraulic machine. Having said this, the Eq. 3.2 can be extrapolated to cover, for instance, cylinder C2 (in Figure 3.1) or a generic cylinder Cn in any possible position. This is summarized in Eq. 3.3:

$$r_{C2} = l_{rp} + \sqrt{\frac{D_{cms}^2}{4} - (l_e \sin(\theta + \gamma))^2} - l_e \cos(\theta + \gamma)$$

$$\dots \qquad \textbf{Eq. 3.3}$$

$$\mathrm{r_{Cn}} = l_{rp} + \sqrt{\frac{\mathrm{D_{cms}^2}}{4} - (l_e \sin(\theta + (\mathrm{n}-1)\gamma))^2} - l_e \cos(\theta + (\mathrm{n}-1\,)\gamma)$$

Where:
γ is the absolute phase angle in radians
r_{C2} is the reciprocating displacement of the upper part of the piston C2 respect the piston sleeve
r_{Cn} is the reciprocating displacement of the upper part of a generic piston located at any radial position defined in terms of ϕ and γ

Finally, values for R_{BDC} and R_{TDC} can be obtained either by looking at the first derivative of r_{C1} respect to θ or just by simple analysis in the geometry. These values are presented in Eq. 3.4.

$$R_{BDC} = l_{rp} + \frac{D_{cms}}{2} - l_e \quad @ \quad \theta = 0, 2\pi, 4\pi \dots$$

$$R_{TDC} = l_{rp} + \frac{D_{cms}}{2} + l_e \quad @ \quad \theta = \pi, 3\pi, 5\pi \dots \qquad \textbf{Eq. 3.4}$$

Where:
R_{BDC} is the minimum value for r_{Cn} at the bottom dead center (BDC)
R_{TDC} is the minimum value for r_{Cn} at the top dead center (TDC)

Since geometries for N cylinders can be considered very similar, a first approach will be done by considering only cylinder C1. Then this analysis will be extended to N cylinders by using a similar approach to the one depicted for Eq. 3.4. This will be used to estimate the entire system performance[21].

Before that, let's introduce a varying volume between the upper part of the piston and the top of the cylinder chamber denoted V_{C1}, and the rated cubic displacement called $\Delta V_{C1,Rat}$. The volume V_{C1} is the space comprehended between the reciprocating motion of piston C1 and the upper most part of the chamber.[22] The rated cubic displacement is a commonly used measure to describe piston based machines. Both parameters are presented in Eq. 3.5.

In such expression, the cross sectional area of the cylinder of diameter D_c is related with the linear motion of the piston r_{C1}. Also, the rated cylinder displacement ($\Delta V_{C1,Rat}$) can be estimated by recalling R_{BDC}. The pressure chamber volume for cylinder C_n can be estimated in similar fashion to those for C1.

$$V_{C1} = A_p(R_{TDC} - r_{C1}) = \frac{\pi}{4} D_c^2 (R_{TDC} - r_{C1})$$

$$\Delta V_{C1,Rat} = \frac{\pi}{4} D_c^2 (R_{TDC} - R_{BDC}) \qquad \textbf{Eq. 3.5}$$

[21] Although there is no evidence to suggest that this system is linear so the superposition principle can be applied; there is also no evidence to said that the system is NOT linear, therefore this first approach is will be considered because of simplicity.
[22] Beware that there is a complementary volume comprehended between the TDC and the upper part of the pressure chamber. Its function is to allow operability of valves and manufacturability of components. Very often this volume is from 1-3 times ΔV_{C1}.

Where:
V_{C1} is a the variable volume comprehended between the upper part of the piston and the top of the cylinder chamber
$\Delta V_{C1,Rat}$ is the rated cubic displacement for cylinder C1 (or Cn)
A_p is the cross section of the moving piston (for practical purposes, equal to the cylinder)
D_c is the cylinder diameter

In the next section, further discussion in the interaction of piston-rod assembly and camshaft will be presented.

3.2.2. Camshaft geometry

In a radial piston hydraulic pump, power is transmitted from the camshaft to the pistons. Power transferred to pistons is used to compress the fluid. Because of the geometric complexity and reciprocating pistons' motion, the orientation of the transmission line for internal forces' (between camshaft and pistons) varies as a function on θ. This section will discuss the interaction between the camshaft and the piston rod assembly. The main target of this section is to achieve one expression for the pressure angle (ϕ), which can be used to describe the orientation of the transmitted force from the camshaft to the piston. This expression will be accomplished by using an interesting relationship (described in Eq. 3.9) proper from circular plane motion. Before get there, some important remarks about cam geometries will be presented. The intention of these remarks is to provide the reader with some richer background about commonly used terms from now onwards.

So far, the term camshaft had been used to make reference to the input shaft of a radial piston pump. It also had been said that the piston-rod assembly is activated by the interaction with the camshaft. The main reason to refer the camshaft as is (and not only as an input shaft), is due to the specific geometry that this component must have to transfer reciprocating motion to the pistons. Norton [*11*] defines a cam as *a specially shaped piece of metal or other material arranged to move the follower in a controlled fashion*. For the case of study, the cam is the part of the input shaft that is in contact with the bearings driving the pistons' motion in a controlled reciprocating motion. In this scheme, the input shaft with a cam surface can be referred as *camshaft*; while the piston-rod-bearing assembly can also be called *follower.*

There are infinite arrangements that can work for a cam-follower mechanism. Each different configuration will transfer different characteristics of motion to the follower (acceleration, velocity, force, direction, etc.). In conventional radial piston pumps, the use of radial followers (or aligned followers) is a common practice. The arrangement denoted as *aligned followers* is a particular case of the general cam-follower geometry in which the eccentricity[23] is equal to zero [*11*] (followers aligned to the center of rotation C in Figure 3.4). Furthermore, a *radial cam* is one particular case of cam geometry with constant curvature (circular cross section). Also, the cam has a circular cross section. This geometric configuration was selected to model the present system because of simplicity. Nevertheless, a large radial piston pump can also use a non radial cam and unaligned followers (and all possible combinations). For the purposes of this document (evaluate performance of hydraulic drivetrain systems in wind turbines) it is considered

[23] Eccentricity is the shortest distance between the follower's axis of motion (perpendicular) and the center of rotation of the cam.

that a radial cam in combination with radial followers is adequate to offer an insight of the system's physics.

Figure 3.4 presents a simplified diagram for a radial cam-radial follower mechanism with one single translational follower. This sketch is similar to the case of study that will be used to model a monocylinder radial piston pump. In there, it can be observed that the line denoted as follower axis is aligned with the center of rotation C. The cam shape presented in Figure 3.4 had a constant immediate center at point B[24] (circular cross section). The load line (force transmission line) between curved geometries is formed between the centers of curvature for the surfaces in contact (between point B and point A). Between the follower axis and the load line, the pressure angle ϕ is formed (triangle CAD). The pressure angle is dependent on θ. Furthermore, the line for effective lever arm is formed perpendicular to the load line and the intersection with the center of rotation C (formed from point C to D). Therefore the angle between the center line and the effective lever arm line is also ϕ (angle BCD).

There are some other important geometric definitions to be considered: The base circle of radius R_{bs} and the prime circle of radius R_{pr} are centered in the center of rotation C. The base circle is *the smallest circle which can be drawn tangent to the physical cam surface* [*11*] and the prime circle *is the smallest circle which can be drawn tangent to the pitch curve*. The pitch curve is *the locus of the centerline of the follower(s).*This pitch curve is defined by the interaction of the cam surface and the center of the roller (point A) of radius R_{rlr}. Now, b_e is signed distance over the perpendicular line to follower axis from the center of rotation C to the intersection with the load line (from point C to E in Figure 3.5 and from point C to B in Figure 3.4). Notice that b_e is dependent on θ. Then, for the depicted condition in Figure 3.4 $(\theta = \pi/2)$, b_e is maximum equal to the constant distance from C to B (l_e in Figure 3.1 or Figure 3.5). For the case $\theta = -\pi/2$, then b_e is minimum ($b_e = -l_e$). Nevertheless, when θ is outside those values, b_e aquires a value within the range $-l_e < b_e < l_e$. For instance, when $\theta = \pi/4$ (as depicted in Figure 3.5) b_e is some other distance within that range.

Remember that the final goal for this section is to determine the pressure angle (ϕ). In order to do this, a trigonometric relation can be used in the triangle ACE. For those purposes sides AC and CE must be known. To know b_e(or side CE) let's consider **instant centers** of rotation. An instant center of rotation, by definition, is defined as *a point, common to two rigid bodies (links) in plane motion that has the same instantaneous velocity in each body*. Furthermore, point E is the instant center of rotation for links CE and EA. Therefore, point C must have the same instantaneous velocity than point A. Since point C is fixed (center of camshaft rotation); instant center E becomes a rotating reference. Then a static observer in point C will see that E varies its position at rate of:

$$v_{T,E} = b_e\dot{\theta} = \dot{r_{C1}} \qquad \textbf{Eq. 3.6}$$

Where:
$v_{T,E}$ is the tangential speed of point E seen by a static observer at point C. Units are length per second (m/s).
b_e is the signed distance from point C to E in Figure 3.5. Units are length (m).
$\dot{\theta}$ is the angular speed of the camshaft in units radians per second (rad/s).
$\dot{r_{C1}}$ is the translational speed of piston in cylinder C1 in length per second (m/s)

[24] This is a special case for cam geometry known as radial cam

Now, because of E is common instant center for link CE as well as for link EA; then, instantaneous velocity of point E ($v_{T,E}$) must be the same than instantaneous velocity of point A. This was also expressed in Eq. 3.6.

Then, by applying the chain rule to Eq. 3.7, it is possible to say that:

$$\dot{r_{C1}} = \frac{dr_{C1}}{dt}$$
$$\frac{dr_{C1}}{dt}\left(\frac{d\theta}{d\theta}\right) = \frac{dr_{C1}}{d\theta}\left(\frac{d\theta}{dt}\right) \qquad \textbf{Eq. 3.7}$$
$$\dot{r_{C1}} = \frac{dr_{C1}}{d\theta}\dot{\theta}$$

Then, by defining:

$$v_{r_{C1},A} = \frac{dr_{C1}}{d\theta} \qquad \textbf{Eq. 3.8}$$

It is possible to say that:

$$b_e = v_{r_{C1},A} \qquad \textbf{Eq. 3.9}$$

Where:
$v_{r_{C1},A}$ is velocity of the follower (piston) in units of length per radian (m/rad)

Beware that in Eq. 3.9 there is units mismatch (length versus length per radian). The fact is that this expression does not relate units. What it says is that **the distance b_e in length units is numerically equal to the velocity of the follower $v_{r_{C1},A}$ in units length per radian** [*11*]. This expression (Eq. 3.9) is independent of angular speed $\dot{\theta}$ and can be used to know the pressure angle ϕ.

To do so, as mentioned before, a trigonometric relation can be set for the triangle ACE. Then, side AC can be expressed as $R_{pr} + s_a$ in Figure 3.4 or $r_{C1} - l_{rp}$. Then the following trigonometric expression can be set:

$$b_e = \left(R_{pr} + s_a\right)\tan\phi$$
$$\tan\phi = \frac{b_e}{\left(R_{pr} + s_a\right)} = \frac{v_{r_{C1},A}}{\left(R_{pr} + \left(r_{C1} - l_{rp} - R_{pr}\right)\right)} \qquad \textbf{Eq. 3.10}$$
$$\phi = \tan^{-1}\left(\frac{v_{r_{C1},A}}{r_{C1} - l_{rp}}\right)$$

Where:
ϕ is the pressure angle in radians
R_{pr} is the radius of the camshaft's prime circle
s_a is the distance between the prime circle and the center of rotation of the roller bearing measured over the follower axis line.

By knowing ϕ, the estimation of forces and moments felt by the camshaft becomes feasible. Therefore, mechanical torque and flow of fluid can be also estimated. This will be estimated in the next section.

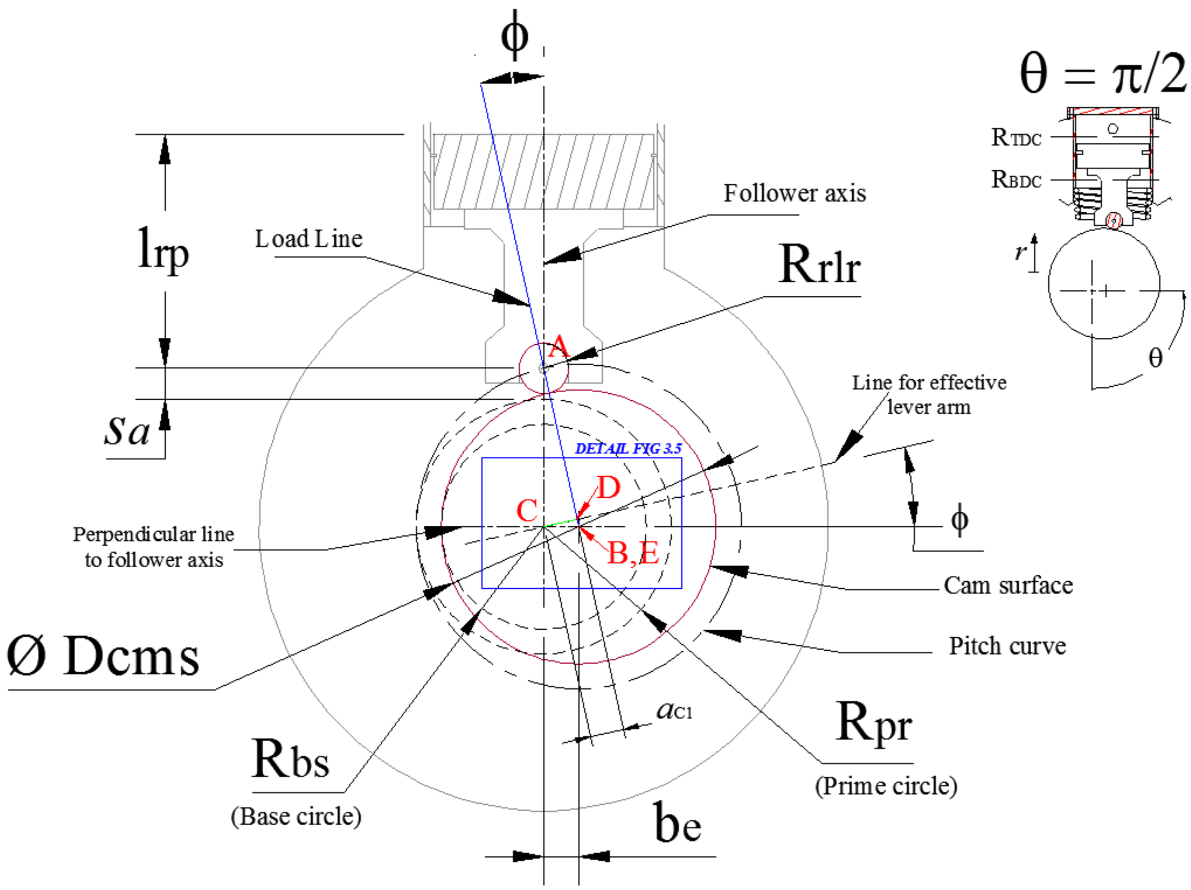

Figure 3.4 Camshaft geometry (see detail on blue box in Figure 3.5)

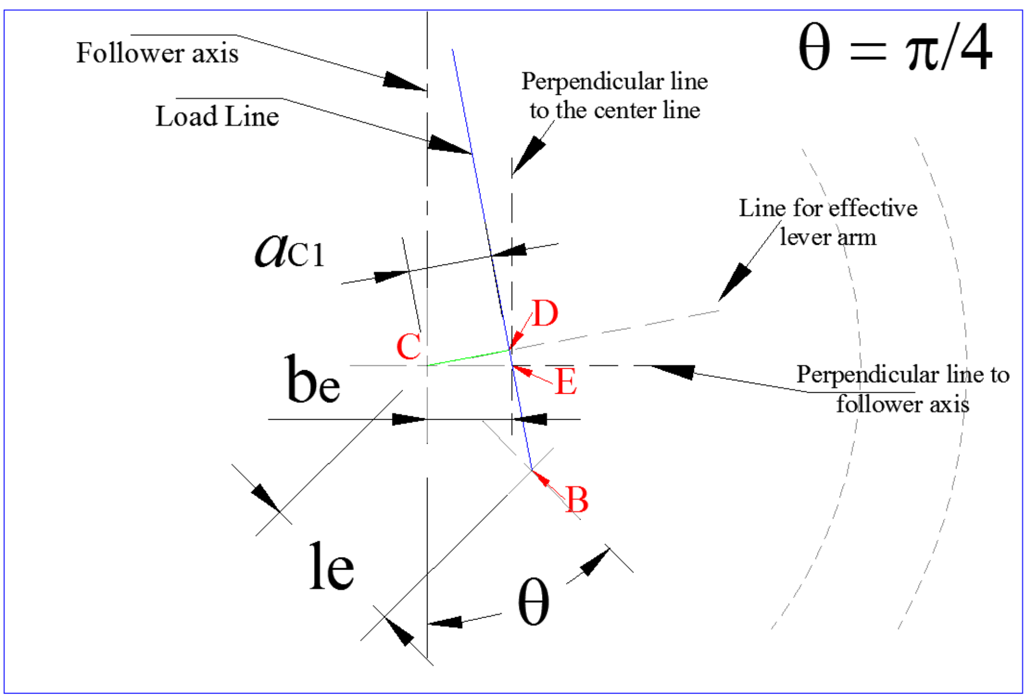

Figure 3.5 Detail in blue box of Figure 3.4

3.2.3. Force and moment balances

The past section introduced an expression for the pressure angle ϕ. Now, in this section force and moment balances will be derived based in geometric considerations presented in 3.2.1 and 3.2.2. The intention to derive force and moment balances is to introduce a dynamic model for the monocylinder machine described in Figure 3.4. Later on, this monocylinder machine will be used to represent a multicylinder machine (section 4.2). For now, consider Figure 3.6. In there, a simplified 2D free body diagram for the piston and camshaft of cylinder C1 is presented. Three different colors are used: black, blue and red. Black is used to represent conservative forces mostly related with inertial considerations. Red is used for dissipative loads like friction and its associated forces. And blue denotes external excitations.

Following this reasoning and diagrams sketched in Figure 3.6, the direction of the transmitted load force F_{IN} (to the camshaft) can be related with ϕ as:

$$\overrightarrow{F_{IN}} = \begin{pmatrix} F_{IN}\cos\left(\frac{3\pi}{2}+\phi\right) \\ F_{IN}\sin\left(\frac{3\pi}{2}+\phi\right) \\ 0 \end{pmatrix} (\hat{\imath} \quad \hat{\jmath} \quad \hat{k}) \qquad \textbf{Eq. 3.11}$$

Where:
$(\hat{\imath} \quad \hat{\jmath} \quad \hat{k})$ is the matrix of standard unity vectors for rectangular coordinates (defined in Figure 3.6).
F_{IN} is the transmitted force(to the camshaft) due to power compression of the hydraulic fluid
$\overrightarrow{F_{IN}}$ is the force vector defined in unity vectors

The purpose of using unity vectors $(\hat{\imath} \quad \hat{\jmath} \quad \hat{k})$ is to aware the reader that while the forces are interacting in the same plane, the resultant moments are normal to that plane. Then, it is possible to vectorize the transmitted load F_{IN} with the effective lever arm a_{C1} (θ dependent) to estimate the resultant torque due to compression (or suction) of the fluid as presented on next:

$$\overrightarrow{a_{C1}} = \begin{pmatrix} b_e\cos(\theta_0+\theta) \\ b_e\sin(\theta_0+\theta) \\ 0 \end{pmatrix} (\hat{\imath} \quad \hat{\jmath} \quad \hat{k})$$

$$T_{F_{IN}} = \overrightarrow{a_{C1}} \times \overrightarrow{F_{IN}} \qquad \textbf{Eq. 3.12}$$

$$T_{F_{IN}} = F_{IN} l_e(\sin\theta\cos\phi - \cos\theta\, sin\phi) \quad (\hat{k})$$

Where:
$\overrightarrow{a_{C1}}$ is the effective lever arm in 3D unity vectors
θ_0 is the absolute starting position at t=0 of the camshaft angular displacement($\theta_0 = 0$ for t=0)
$T_{F_{IN}}$ is the torque due to transmitted load to the piston at an effective lever arm. Its direction is normal to the plane of interaction of forces.

Based on this approach, the second motion law (2^{nd} Newton's law) can be written for two bodies: the piston-ring-rod-roller assembly and the camshaft. This law is applied for the piston-ring-rod-roller assembly as follows:

$$\sum F_{\vec{r}} = m_{gp}\ddot{r}$$
$$m_{gp}\ddot{r} = F_{IN}\cos\phi - F_{gp} - F_{sp} - F_{fr} - F_{fp} - F_P \qquad \textbf{Eq. 3.13}$$

$$\sum F_{\hat{\imath}} = m_{gp}\ddot{x} = 0$$
$$0 = N_{fp} - F_{IN}\sin\phi - N_{fr} \qquad \textbf{Eq. 3.14}$$

$$\sum M_{\hat{k},G_R} = J_{G_R}\ddot{\theta} = 0$$
$$0 = \frac{1}{2}D_c \cdot F_{fp} - \frac{1}{2}D_c \cdot F_{fr} + l_{fr} \cdot N_{fr} - l_{fp} \cdot N_{fp} \qquad \textbf{Eq. 3.15}$$

Where:
$\Sigma F_{\vec{r}}$ is the force balance in the radial coordinate r (aligned with follower axis of C1)
m_{gp} is the net mass of piston-ring-rod-roller assembly
$\ddot{r}$ is the second time derivative of r_{C1}
F_{gp} is the weight force for the combined mass of piston-ring-rod-bearing assembly
F_{sp} represents the conservative force absorbed by the return spring dependent on displacement r_{C1}
F_{fr} is the friction force between the piston ring and piston sleeve F_{fr} in the surface of contact
F_{fp} is the friction force between the piston's body and the cylinder sleeve (present over the lubricated external piston surface).
F_P is the force due to fluid compression
$\Sigma F_{\hat{\imath}}$ is the force balance in $\hat{\imath}$ direction(horizontal axis for Figure 3.6).
$\ddot{x}$ is the acceleration in the horizontal axis
N_{fp} and N_{fr} are the associated normal force to friction force F_{fp} and F_{fr} respectively
$\Sigma M_{\hat{k},G_R}$ is the moment balance respect to center of mass G_R
J_{G_R} is polar moment of inertia in the $\hat{k}$ axis
$\ddot{\theta}$ is the second time derivative of angular displacement
l_{fr} and l_{fp} are the distances from the roller axis to the concentrated forces N_{fr} and N_{fp} respectively

Then, a similar forces and moment balances can be considered for the camshaft free body diagram presented on Figure 3.6 right:

$$\sum F_{\hat{\imath}} = m_{gp}\ddot{x} = 0$$
$$0 = C_x + F_{IN}\sin\phi \qquad \textbf{Eq. 3.16}$$

$$\sum F_{\hat{\jmath}} = m_{grc}\ddot{y} = 0$$
$$0 = C_y - F_{grc} - F_{IN}\cos\phi \qquad \textbf{Eq. 3.17}$$

$$\sum M_{\hat{k},C} = J_C\ddot{\theta}$$
$$J_C\ddot{\theta} = T_{IN} - T_V + T_{F_{IN}} - l_{grc}\sin\theta \cdot F_{grc} \qquad \textbf{Eq. 3.18}$$

Where:
m_{grc} is the mass of all rotating parts
F_{grc} is the weight force for all rotating parts (input shaft, valve's discs, camshaft) located at its particular center of mass (point G_{grc}).

C_x and C_y are the force reactions *felt* by the camshaft in $\hat{\imath}$ and $\hat{\jmath}$ respectively.
$\Sigma M_{\hat{k},C}$ is the moment balance respect to the point C
J_C is the polar moment of inertia of rotating parts in $\hat{k}$
T_V is the parasitic torque product of friction forces in the valve's disc
T_{IN} is the prime's mover torque
l_{grc} is the distance between the center of rotation and the center of mass for rotating parts
F_{IN} is the transmitted force (to the camshaft) due to power compression of the hydraulic fluid

In general, some important remarks are:

A. In Eq. 3.14,Eq. 3.16 and Eq. 3.17, no displacement is expected, therefore force balances are equal to zero (in equilibrium).
B. Friction forces F_{fr} and F_{fp} and their associated normal forces (N_{fr}, N_{fp}) are present along the entire cylindrical surface. However, according with Eq. 3.14 and Eq. 3.15 they might have an uneven distribution. Awareness about this load imbalance is important for component's design where wear considerations are important. Nevertheless, for the purposes of this document, this representation is considered enough.
C. Eq. 3.16 and Eq. 3.17 offers information about the loads in the main bearings of the pump

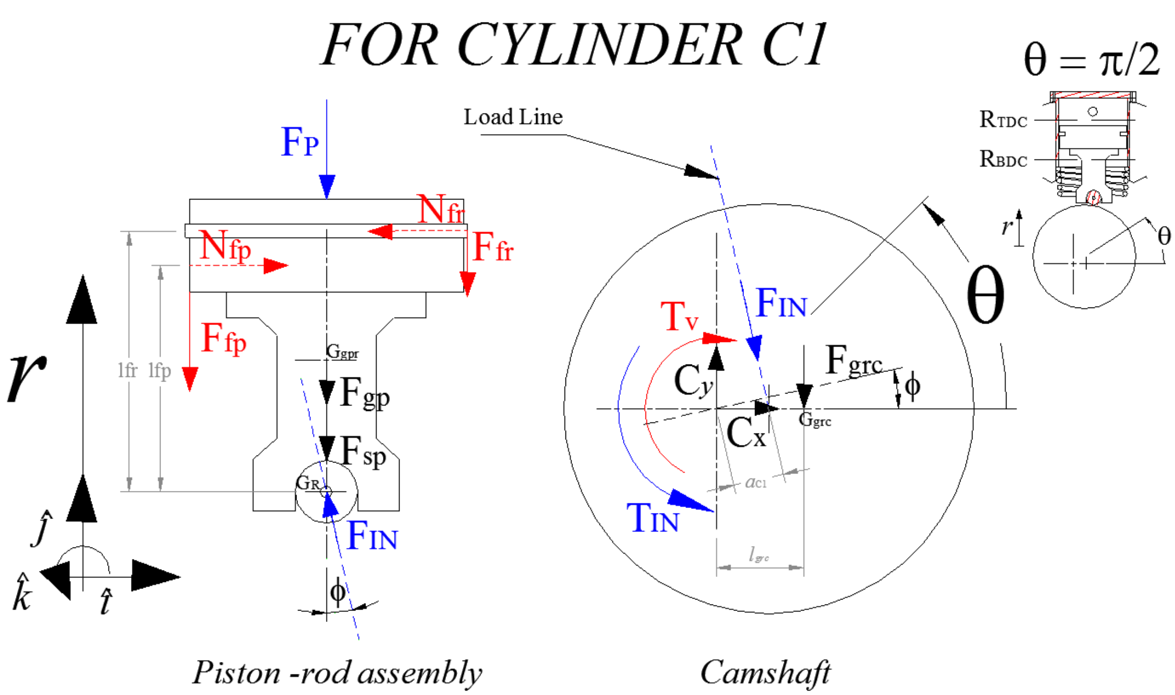

Figure 3.6 Free body diagram for one cylinder radial piston pump for 0 < θ < π.

It is important to remember that positive displacement pumps (like radial piston pumps) are devices oriented to supply flow of fluid (not pressure). Although pumps are not oriented to create pressure, pressure is build up as response of the hydraulic circuit to this flow of fluid [*12*].

For better understanding, a straight analogy to electrical systems can be made by considering current flowing through an electrical resistance. This case is analogous to a flow of fluid through a hydraulic circuit (pipelines). In the electric circuit, the flow of current creates a difference of potential between resistance terminals; in same fashion, the flow of fluid through a pipe generates a pressure drop. In both systems, the combination of the build up pressure (or voltage) and the flow of fluid (or current) are in charge of power transmission. This is the reason for which hydraulic components must be designed not only to handle flow, but also significant pressures. Very often, radial piston pumps are one of the devices that can handle larger power densities (operating pressures about 500-700 bar commercially available) still being relatively compact.

Before going on, please notice that in this entire document **symbol W is reserved to describe Power.** Although this symbol is not commonly used for this purpose; **it was selected to avoid confusion** with pressure (p_{C1}, P_D, P_S). Therefore, please be aware of this notation along the rest of this document.

On Appendix A, a detailed description of the operating principle of the radial axis pump side to side with a detailed explanation of the forces and moments are included. Based on that, the resultant force of mechanic power transfer to the fluid (F_P) can be modeled as:

$$F_P = \frac{\cos\phi}{l_e(\sin\theta\cos\phi - \cos\theta\, sin\phi)}\left(J_C\ddot{\theta} - \frac{W_{IN,C1}}{\dot{\theta}} - T_V - l_{grc}\sin\theta\, F_{grc}\right) - m_{gp}(\ddot{r} + g) - K_{sp}(\epsilon_0 + r) - \mu_f\left(N_{fr} + N_{fp}\right) \qquad \textbf{Eq. 3.19}$$

Where:
F_P is the force due to fluid compression (resultant force of mechanic power transfer)
$W_{IN,C1}$ is the input power to drive cylinder C1
K_{sp} the spring stiffness constant
ϵ_0 pretensioning of the spring
μ_f is the friction coefficient ($\dot{r}$ dependent - Eq. 7.5),

Eq. 3.19 classify the forces by color according with their nature (black for conservative, blue for external and red for non conservative). Also, new variables are used. These are explained in detail on Appendix A. In similar fashion, F_P can also be estimated as:

$$F_P = \frac{\pi D_c^2}{4} p_{C1} \qquad \textbf{Eq. 3.20}$$

Where:
p_{C1} is the pressure in chamber of cylinder C1 (function of θ).

Relations presented from Eq. 3.13 to Eq. 3.21 will be used to describe a dynamic model for the moving piston C1 in later sections.

3.2.4. Mechanic to hydraulic power conversion

In the past sections geometry, basic displacement equations and forces balances have been discussed. Now, it is time to take a look into power transformation process from mechanic to hydraulic. This process occurs in a volume changing chamber that *compresses* some fluid at the expense of some torque input in the camshaft. This process will be discussed in this section.

As mentioned last section, the force F_P is the resultant force of the power conversion process. In the hydraulic side, force F_P depends on geometry and chamber's pressure as presented by Eq. 3.19. Pressure in the cylinder chamber (p_{C1}) is a direct function of r_{C1} displacement and the net mass flow from the chamber to the outside world. This can be expressed by relating the continuity equation and the Bulk modulus equation. The continuity equation says that the rate of change of mass in a control volume C1 is directly proportional to the net flow; so, everything that goes in must eventually leave. This can be expressed as:

$$\frac{dM_{C1}}{dt} = \rho_o(Q_{in} - Q_{out})$$
$$\frac{dM_{C1}}{dt} = \frac{d(V_{C1}\rho_o)}{dt} = \rho_o\frac{dV_{C1}}{dt} + V_{C1}\frac{d\rho_o}{dt} \quad \textbf{Eq. 3.21}$$

Where:
M_{C1} is the mass contained inside the pressure chamber C1
V_{C1} is the control volume given by pressure chamber C1
ρ_o is the fluid density
Q_{in} and Q_{out} are the input and output volumetric flows respectively

On the other hand, the Bulk modulus equation relates changes in liquid pressure to the change of volume. This can be expressed as:

$$\beta_o = -\frac{dp_{C1}}{dV_{C1}/V_{C1}} \quad or$$
$$\frac{d\rho_o}{dt} = \frac{\rho_o}{\beta_o}\frac{dp_{C1}}{dt} \quad \textbf{Eq. 3.22}$$

Where
β_o is the fluid's Bulk modulus

On section 3.2.1, it was introduced the so called *incompressibility of fluids* property. Compressibility is defined as "*the ability of liquid to change its volume when its pressure varies*" [*13*].There is no such thing like incompressible liquids. In fact, most liquids present some degree of compressibility, but often very small. Because of this, in several occasions is accurate enough to assume incompressible liquids to allow a more simple reasoning; but when performance is being evaluated, pressure change is required. For our purposes (compare performance of hydraulic drivetrains in a wind turbine with non hydraulic drivetrains) is required to consider that liquid is subjected to compression and therefore a pressure is built up.

Now, Eq. 3.21 and Eq. 3.22 can be combined relating both principles. This is done in Eq. 3.23:

$$\frac{dp_{C1}}{dt} = \frac{\beta_{oil}}{V_{C1}}\left(-\frac{dV_{C1}}{dt} + Q_{in} - Q_{out}\right) \quad \textbf{Eq. 3.23}$$

This last equation (Eq. 3.23) will be related with Eq. 3.19 and Eq. 3.20 to represent the dynamic model of a monocylinder radial piston pump. Still, some complementary comprehension about the valves' action is required. Valves operation in conventional radial piston pumps is discussed in the next section.

3.2.5. Valves' operation

In this section, some complementary comprehension about valves' action in conventional radial piston machines is presented. This knowledge is necessary to later understand how digital hydraulics overcome some of the disadvantages of conventional machines.

In terms of valve's operation, it would be desirable to operate independently one single valve at any time in piston based machines (as mentioned in section 3.2.1). Nevertheless, having such discrete valves' operation is not feasible in practice because disk's valves are dependent on camshaft position θ (Figure 3.3). Discrete operation in system depicted in Figure 3.3 would cause step changes in pressure, and consequently impact loads and noise [*14*]. To guarantee endurance, sudden changes in loads must be avoided. To do so, the disc's plates incorporate relief notches to allow successive changes in pressure. These relief notches are pyramidal shaped ditches located at the start of the suction and discharge port. Figure 3.7 presents a detailed view of valve's disc geometry. In there, the front view (a) presents important geometric characteristics and introduces three angles ($\alpha_{V1} - \alpha_{V3}$) to describe the section A-A view (c). Also the way in which those valve's discs are assembled into the radial piston pump are presented in (b) describing important parts (use Figure 3.1 and Figure 3.3 for better appreciation). Be aware that high pressure valve's disc and low pressure valve's disc are very similar in geometry; but when assembly, they are normally positioned shifted about 180 degrees each other. This shift allows the operation presented in Figure 3.8. In there, the same section line (Section A-A) employed in Figure 3.7 is used to describe one single cylinder and its interaction with the both valve's discs. This interaction leads to 6 different regions where the net volumetric flow ($Q_{in} - Q_{out}$) is different.

Each possible combination of valve's disc with the cylinder port corresponds to a unique value of θ. Then, every region corresponds to a particular range of θ. To have a better understanding, consider a static cylinder C1 port presented at the top of Figure 3.7a. This port sees how θ varies (both valve's disc are rotating at the same speed and follows displacement θ). Since there is a unique combination (designed to avoid shock loads) the static C1 port sees 6 different regions described in Figure 3.8 (related with $\alpha_{V1} - \alpha_{V6}$ in Figure 3.7) in one revolution. The *unrolled* representation respect to θ displacement for cross section A-A is presented in Figure 3.7c. In there, a static cylinder C1 observes how θ varies as well as the changing geometry of the relief notches. Finally, Figure 3.7b gives an idea in a 3D plane of the current location of the discussed components.

Region	**θ Range**	$\boldsymbol{\theta_{ac\_RX}}$	$\boldsymbol{p_{C1}}$
1	$\theta_{ac_{R1}} < \theta \leq \theta_{ac_{R1}} + \alpha_{V1}$	$\theta_{ac_{R6}} + \alpha_{V6}$	P_S
2~BDC	$\theta_{ac_{R2}} < \theta \leq \theta_{ac_{R2}} + \alpha_{V2}$	$\theta_{ac_{R1}} + \alpha_{V1}$	p_{C1}(Eq. 3.23)
3	$\theta_{ac_{R3}} < \theta \leq \theta_{ac_{R3}} + \alpha_{V3}$	$\theta_{ac_{R2}} + \alpha_{V2}$	p_{C1}(Eq. 3.23)
4	$\theta_{ac_{R4}} < \theta \leq \theta_{ac_{R4}} + \alpha_{V4}$	$\theta_{ac_{R3}} + \alpha_{V3}$	P_D
5~TDC	$\theta_{ac_{R5}} < \theta \leq \theta_{ac_{R5}} + \alpha_{V5}$	$\theta_{ac_{R4}} + \alpha_{V4}$	p_{C1}(Eq. 3.23)
6	$\theta_{ac_{R6}} < \theta \leq \theta_{ac_{R6}} + \alpha_{V6}$	$\theta_{ac_{R5}} + \alpha_{V5}$	p_{C1}(Eq. 3.23)

Table 3.1 Regions related to θ

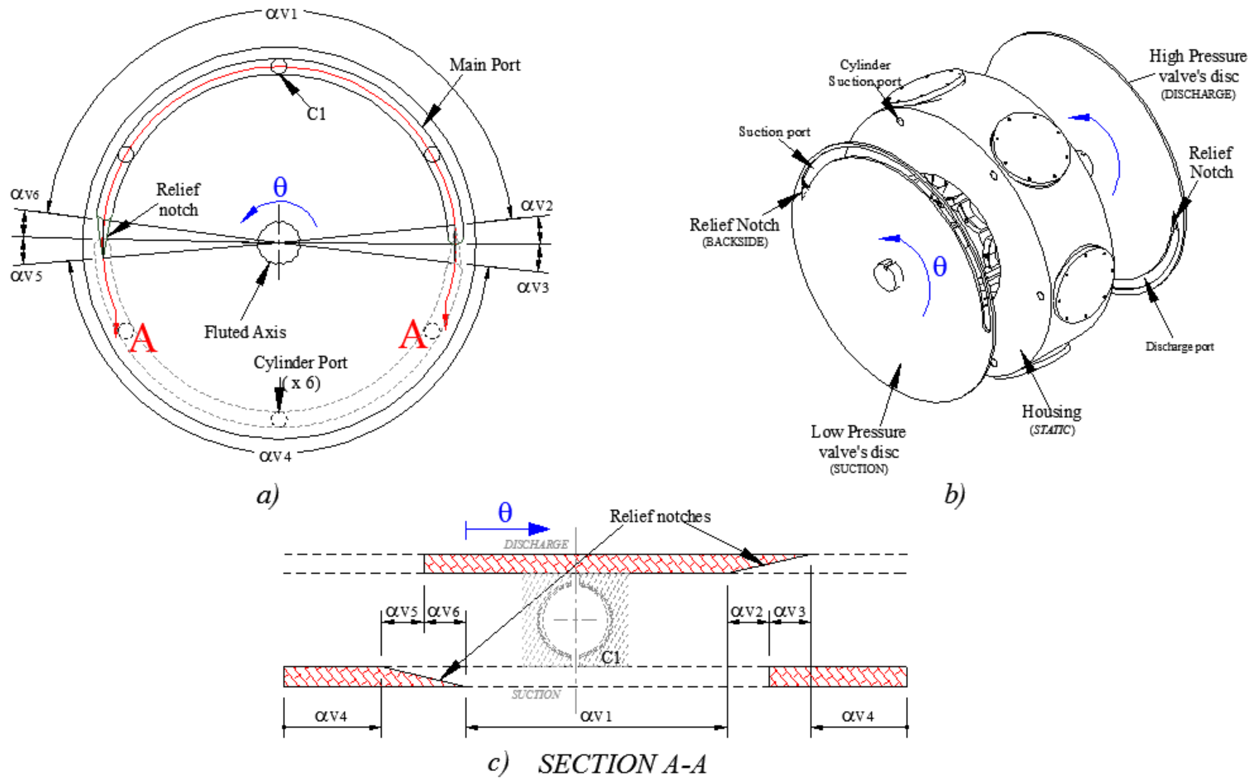

Figure 3.7 Valve's Disc geometry. a) front view of valve's discs, b) isometric view for assembly, and c) cross section of valve's disc

Because of these particular regions, pressure inside cylinder C1 (p_{c1}) changes depending on θ. In some cases, p_{c1} is equal either to the pressure present in the suction manifold (P_S) - Region 1- or to the pressure in the discharge manifold (P_D) – region 4. In the rest of the cases, p_{c1} is function of the immediate net flow into the chamber ($q_{in} - q_{out}$). The ranges of θ for which the regions are valid can be summarized in Table 3.1. In there, cumulative variable $\theta_{ac_{RX}}$ that represents the absolute value of θ for region X is introduced. Notice that during Region 2 and 5, the BDC and TDC are respectively reached by the piston. Therefore, regions 3 and 6 represents those ranges of θ in which the piston is *very* close to the BDC and TDC but net flow into the chamber C1 is still related with the relief notches.

On next, a couple of equations will be presented. Their main target is to assess the parameters that might be involved in the quantification of volumetric flow rates during a changing condition. To estimate the immediate net flow at those particular regions, the orifice flow equation (Eq. 3.24) can be used [*15*]:

$$q_u = A_u C_{d,u} \sqrt{\frac{2(\Delta p)}{\rho_o}} \qquad \textbf{Eq. 3.24}$$

Where:
q_u is the immediate flow through an orifice
A_u is the area of the orifice through which the fluid is passing
$C_{d,u}$ is the discharge coefficient (depending on the geometry)
Δp is the differential of pressure between reservoirs

Notice that for a conventional radial piston pump, A_u is only constant for Region 1 and 4; and a function of angular displacement for Region 2,3,5 and 6. Also, C_d coefficients (often estimated by empirical models) are function of Reynolds number (Re). The Reynolds number equation is presented on next:

$$Re = \frac{\rho_o v_{eff} D_h}{\eta_{dv}} \qquad \textbf{Eq. 3.25}$$

Where:
Re is the Reynolds number
v_{eff} is the effective fluid speed
D_h is the hydraulic diameter
η_{dv} is the dynamic viscosity

Notice that Re is used only to estimate the values C_d; nevertheless, because the changing geometry(because the disc is rotating) both values are θ dependent.

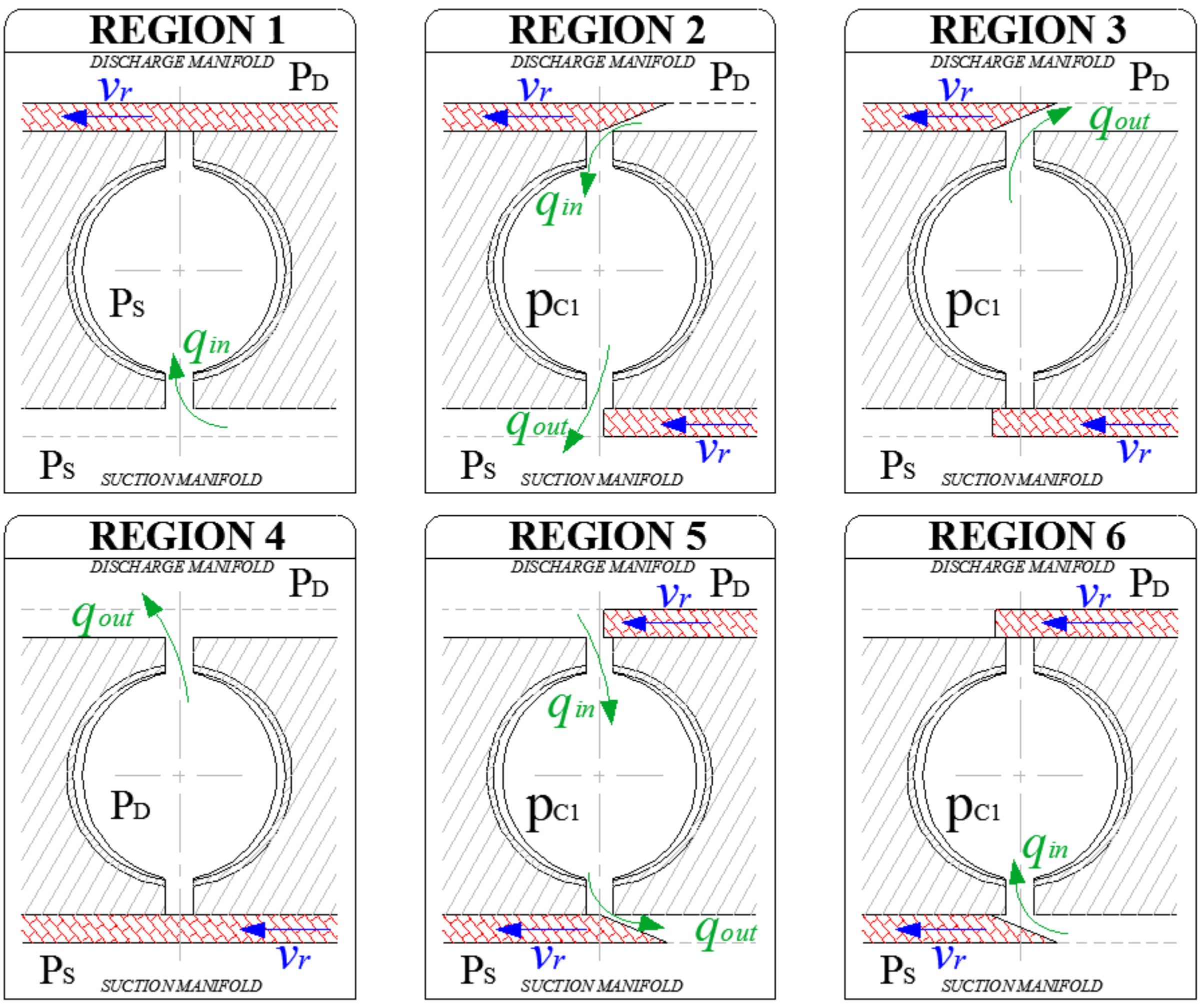

Figure 3.8 Six regions for flow into and from the control volume C1 (top view for cylinder C1)

Also, realize that from the all six possible regions described in Figure 3.8, the only *required* regions are Region 1 and Region 4, which are valid almost for all the range of θ related with suction and discharge respectively. Be aware that discrete operation of such regions is not possible since the flow control mechanism and pressure inside the chamber are both θ dependent. Therefore the other 4 regions are introduced as *transition regions*. These transition regions are required to avoid shock loads due to sudden changes in pressure. Preventing impact loads will lead to fatigue and wear prevention increasing machine endurance. The price to pay for this load reduction is traduced in terms of energy losses: due to flow friction in regions 2, 3, 5 and 6 (variable effective fluid speed v_{eff} and port area A_u) and due to negative volumetric flow during region 2 and region 5 (explained on next).

The negative mass flow present in region 2 and 5 can be considered as a non recoverable power leak that can be explained as following: Fluid power transfer can be expressed in terms of mass flow (Eq. 3.21). A conventional radial piston pump is intended to drive oil from suction port to discharge port. During region 2 and 5, there is a negative flow. This means that fluid flows from discharge to suction manifold. In this process, the fluid is subjected to two main losses: friction losses going through discharge port, cylinder chamber and suction port; and power dissipation in low pressure port. The last is larger than the first one, but both of them are non recoverable.

Power dissipation in the suction manifold is further explained in Appendix C. For now, let's say that energy is a function of time:

$$E_X = \int_{t_{1,X}}^{t_{2,X}} W_X \, dt \qquad \textbf{Eq. 3.26}$$

Where:
E_X is the energy of event X
W_X is the instantaneous power involved in event X
$t_{1,X}$ and $t_{2,X}$ is the time of the start and end of event X respectively

The larger time the condition of Region 2 and 5 is held, the larger the energy leaks the system has. The amount of time that transient conditions are held is determined by the angular speed $\dot{\theta}$ at which the machine is operated. The lower the speed, the larger the time that transient conditions are hold. Therefore, the faster the machine is operated, the smaller the leaks due to Region 2 and 5 are. Nevertheless, larger values of $\dot{\theta}$ lead to larger dissipative forces, mechanical stresses and thermal expansion (halting condition). Then, the optimal point of operation for conventional radial piston pumps is given at rated speed; where the best deal for this tradeoff between power leaks, losses and endurance is obtained. Operating these machines above rated speed cannot be hold for long times (excessive wear); but operate them below rated speeds turns out to be very inefficient [*5*].

Even though transition regions might be an important cause of losses in conventional machines, they are out of the scope of this document. The reason for this is that modern digital hydraulics machines allow the discrete operation of valves. This minimizes the effects of such transition regions in the overall system performance. For a more comprehensive discussion about the effect of transition regions in conventional radial piston machines the reader is referred to Kavanagh [*14*]. In there, a detailed modeling for an axial piston pump with swash plate flow control is done. The modeled system in [*14*] is different from the conventional radial piston pump studied in here; but, the fluid flow into the chamber is controlled in similar fashion so similar conclusions can be obtained. Also, this literature offers model validation for a particular geometry and stresses the importance of the detailed knowledge of dimensions and the particularity of any numerical solution.

In the next section, other important energy considerations applicable for conventional machines as well as for digital hydraulics are presented. These simple energy considerations are intended to provide a light overview of the important parameters that defines machine efficiency.

3.2.6. Energy considerations

In the past section, valves' operation and their deficiencies were presented. Now is time to present the most relevant causes of power loses. Within this section, losses estimation will be carried out. Among them: power losses due to friction, leakage losses due to geometric tolerances, and mechanic energy.

To start, let's stress that energy and power losses are strongly geometry dependent. Therefore, a good knowledge of geometric ratios and tolerances is required for an accurate analytical estimation. Still, if no specific geometry information is available, some estimation can be done by using very simple definitions applicable for any piston based machine. Elementary definitions are considered enough for the purposes of this document (hydraulic drivetrains in wind turbines).

In the representation of a hydrostatic transmission (Figure 2.1) there is a hydraulic pump driving a hydraulic motor through hydraulic lines. Every part of the hydrostatic transmission accounts for different types of losses. For instance; while lines mostly accounts for drag losses, pump and motors accounts for mechanic, hydraulic and drag losses.

For the case of hydraulic lines, let's say that a flow of fluid through lines is subjected to friction losses. Reynolds number determines how these losses can be modeled: turbulent or laminar. Is of common practice, in hydraulic circuits, to keep $v_{eff} < 1.5$ [m/s] for suction lines (reduce possibility of cavitation at the pump) and $v_{eff} < 4.5$ [m/s] for discharge lines (excessive shock loads) [*15*]. In both cases, friction losses in lines should be modeled as laminar flow (Re<2500) using d'Arcy formula:

$$W_{loss,fr,q_u,P} = \frac{1}{2} f \frac{L_p}{D_h} \rho_o v_{eff}^2 \qquad \textbf{Eq. 3.27}$$
$$f = \frac{64}{Re}$$

Where:
$W_{loss,fr,q_u,P}$ are the power losses due to friction in piping
f is the friction factor for laminar flow ($Re < 2500$)
L_p is the length of the pipes

Before the fluid can be put into (or removed from) lines, it normally must go through a valve port, bend or manifold. In this case, it is common practice to model the oil flow as turbulent according with:

$$W_{loss,fr,q_u,T} = \frac{1}{2} q_u \rho_{oil} K_w v_{eff}^2 \qquad \textbf{Eq. 3.28}$$

Where:
$W_{loss,fr,q_u,T}$ is the power losses due to turbulent flow
K_w is the friction coefficient for the particular port.

While Eq. 3.28 accounts for drag losses inside hydraulic machines, piston based hydraulic machines are also subjected to other important losses. Such losses are assessed by means of the volumetric and mechanical efficiency. While ***volumetric efficiency*** accounts for losses related to leaks and unrecoverable power during compression, ***mechanical efficiency*** describes rotational losses.

Explaining further the concept of volumetric efficiency, let's recall that linear displacement of the piston will cause a changing volume in the pressure chamber. Since the piston have a relative displacement respect to the cylinder, some degree of lubrication is required to guarantee endurance and minimize friction (refer to Appendix A for detailed description). Furthermore, the piston is moving in and outwards. In that motion, it only performs significant work in half cycle (outwards if pump operation and inwards if motor operation). Due to machine design and manufacturing tolerances, the required lubrication is provided by allowing some degree of leakages in the significant work half cycle. This means that, while the piston is pushing oil out of the pressure chamber (in a pump), some leakages are intended to occur (between the piston ring and the cylinder sleeve) to lubricate the system. Oil leaks do not perform effective work since they do not leave the chamber in the desired way (continuity equation principle). This is known as *slip* (S_l) and can be considered as losses. Slip must be experimentally determined and very often is in the range of 1% to 3% of ΔV_{C1} [*16*]. Nevertheless, when there is no experimental data is a common practice [*17*] to use $S_l = 0.02$.

On the other hand, there is an *additional* volume ($V_{ext,C1}$) in the pressure chamber comprehended between TDC and the upper most part of the pressure chamber on net volume $V_{NET,C1}$. The reason for this additional space is mainly to allow valves' operability. However, the fluid contained in there requires power to be compressed. Such power barely is recovered; then, this must be considered as a loss too. Both leakages and losses due to compression in $V_{ext,C1}$ are assessed by volumetric efficiency and can be estimated as:

$$\eta_{Vol} = \frac{1 - (\Delta p\, CF_o)\left(1 + V_{ext,C1}/\Delta V_{C1}\right)}{1 - (\Delta p\, CF)} - S_l$$
$$V_{ext,C1} = V_{NET,C1} - \Delta V_{C1}$$
$$CF_o = \frac{1}{\beta_o}$$
Eq. 3.29

Where:
η_{Vol} is the volumetric efficiency of the machine
CF_o is the compressibility factor for the used fluid (inverse of Bulk modulus)
$V_{NET,C1}$ is the net fluid volume that fits into the pressure chamber when piston is at the BDC
$V_{ext,C1}$ is the volume comprehended between the upper most part of the pressure chamber cavity and the top of the piston at the TDC.
S_l is the slip of the machine expressed in decimal value ($S_l \sim 0.02$)

Furthermore, η_{Vol} is sensitive to aging (normal wear) and, most important, to manufacturing and design tolerances. Therefore particular values can be expected for very similar machines.

Now, in terms of mechanic efficiency (η_m), this accounts for losses due to non conservative forces inside the machine. This efficiency can be estimated as follows:

$$\eta_m = \frac{W_{m,us}}{W_{IN,Req}} = \frac{W_{m,us}}{\dot{\theta} T_{IN,Req}} \qquad \textbf{Eq. 3.30}$$

Where:
η_m is the mechanic efficiency
$W_{m,us}$ is the mechanical power effectively transferred to fluid (only power to displace the oil)
$W_{IN,Req}$ is the input shaft power (includes losses due to mechanical friction in bearing and sliding interfaces)

Very often, mechanic efficiency in radial piston machines is very high. Typical values for η_m are in the order of 0.99.

The combination of volumetric and mechanic efficiency provides the overall efficiency of the system. This efficiency is called ***mechanic-hydraulic efficiency*** (η_{mh}) and is presented in Eq. 3.31.

$$\eta_{mh} = \eta_m \eta_{Vol} \qquad \textbf{Eq. 3.31}$$

The reader is referred to Henshaw [*16*], Miller [*17*] and Catania & Ferrari [*18*] for a more comprehensive explanation of correlation between η_{Vol}, η_m and η_{mh}.

3.2.7. Thermodynamics

This last section is intended awaking awareness in the reader that some other losses can exist in a radial piston pump. A clear example of this can be found with the thermodynamic losses. Such losses appear in the shape of warming up of the fluid due to compression and decompression. These kinds of losses are not considered in any model presented in this document because the current approach was considered as accurate enough. Nevertheless, such losses are present in the system and should be considered for a more detailed approximation than the one presented in this document.

The working cycle for a single cylinder pump is presented in Figure 3.9. It is possible to explain the same operating principle for a single cylinder pump previously introduced with words (or with regions in section 3.2.4). The history goes as follows: In point 1 the piston is at the BDC position (region 2), then in point 2 the suction valve closes entirely (region 3); from that point until point 3 (line AB) a isentropic process can be assumed while the fluid is being *pressurized* up to the load pressure (start of region 4, because of compression a change of temperature can be expected); then the oil is discharged at constant pressure P_D (end of Region 4) in an isothermal process (line BC) until it reaches the TDC (point 4 or region 5); afterwards the discharge valve is entirely closed (point 5) followed for an isentropic process (line CD) were a negative pressurization is established when the piston starts moving downwards (point 6) concluding with the suction of the oil from the reservoir (isothermal line DA). The effect of such working cycle over the system efficiency is mostly given in oil temperature increase. As it can be expected, energy invested in such temperature increase cannot be easily recovered; therefore, constitute losses to the system. Also, the fact that oil is warming up, and given that oil properties vary respect to temperature, might endanger the affect the mechanical and volumetric efficiency of the system. For a more detailed explanation of the thermodynamic losses involved in the compression of oil, the reader is referred to Catania & Ferrari [*18*] and to Henshaw [*16*] where a deeper study is presented.

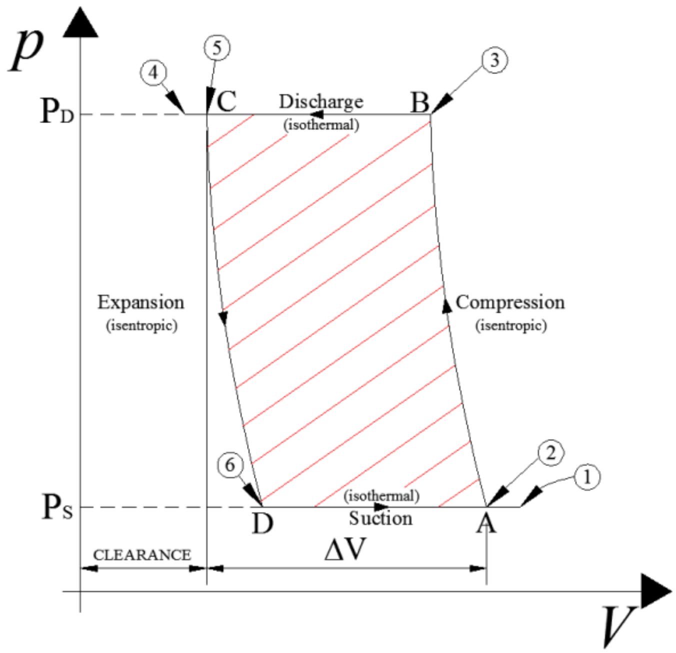

Figure 3.9 Work cycle for a single cylinder pump

Based on the work cycle, it is possible to estimate the thermal efficiency. The thermal efficiency relates the dashed area in Figure 3.9 (output work) with the input power invested into the system. The thermal effects in the oil are not intended to be modeled in this document. It is considered that they are out of the scope of this document. If thermal considerations are desired, the reader is referred to Catania [*18*], Henshaw [*16*] and Miller [*17*].

3.2.8. Power Flow in a conventional radial piston pump

This section summarizes the topics discussed in section 3.2.6 and 3.2.7. For this purpose, the power flow for a conventional radial piston pump is presented in Figure 3.10. In there, the most important efficiencies in the hydraulic machine can be observed.

To estimate rotational losses, mechanical efficiency (Eq. 3.30) must be considered. Then, thermodynamic losses should be estimated by means of a thermodynamic efficiency (not presented in this document). Afterwards, volumetric losses are estimated by means of the volumetric efficiency (Eq. 3.29). Finally drag losses in the machine ports and manifold are estimated using turbulent flow estimation (Eq. 3.28). The power flow diagram for the motor is the inverse than the pump. Beware that loses in piping (Eq. 3.27) does not belong neither to pump nor motor; so they should be considered separately.

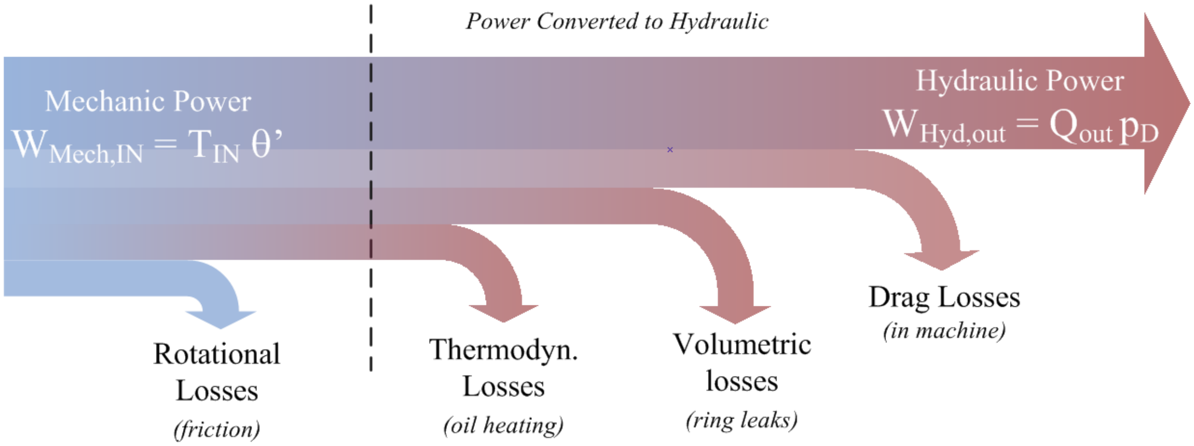

Figure 3.10 Power flow in a conventional radial piston pump

Later on, similar power flow diagrams will be presented for digital hydraulic machines. In those diagrams, thermodynamic losses will be suppressed since they are neglected in this document. For now, this concludes the discussion of conventional radial piston machines. In the next section, digital hydraulics and the way of how they overcome some disadvantages are discussed in section 3.3.

3.3. Digital Hydraulics

The target of this section is to recall some important facts of digital hydraulics at the time that significant differences with conventional machines are pointed out. Therefore, this section is an introduction for the specific case of study presented in the following section.

Digital hydraulic machines are very similar machines to those introduced as *conventional* in the past section. The main difference is that digital machines allow controlling independently flow through valves (8 and 10 in Figure 3.3) by means of an electrical signal. The electrical signal is intended to drive a solenoid driven valve. Also, this electrical signal might come from a software based controller so performance can be enhanced for a particular load condition by allowing disabling individual cylinders.

Because of hydraulic machines normally imply large power densities, the use of very robust valves is required; therefore, transient in digital valves might turn to be more or less sluggish (in terms of tens of milliseconds). Appendix C presents some typical response times for currently commercially available solenoid-operated digital-hydraulic valves. Due to this sluggish operation and depending on the angular speed requirements, digital valves can be operated only once or multiple times per load cycle (stroke in the case of a cylinder-based machine).

If the frequency of the load cycle (f_{lc}) of a particular hydraulic system is low enough (for instance, f_{lc} << 1 Hz), it is possible to think about some kind of pulse width modulation (PWM). Nevertheless, if the frequency is larger, then the valves can be barely acted once per load cycle. For instance, a 6 cylinder radial piston motor driving the output shaft at 1500 RPM (like the one presented in Figure 3.1) has $f_{lc} = 25$ Hz, therefore digital valves can only afford to operate once per load cycle with a careful timing tuning.

Further explanation about the interaction between digital valves and pump mechanism (to conform a digital hydraulic machine) will be provided by the study case of Artemis Digital Displacement machine in section 3.4. In there, a simple model for such system and complementary components required in a wind turbine will be suggested.

3.4. Case of study: Artemis Digital Displacement

This section introduces a set of equations intended to build a computer model that represents the Artemis Digital Displacement (ADD) drivetrain. The model will be boarded as a specific case that makes use of the equations presented in sections 3.2 and 3.3. Although some equations might represent a dynamic model (like those of the monocylinder machine presented in section 3.2); they are used only for steady state in this document. Dynamic modeling and experimental validation of computer models and results presented within this graduation project are left for later research stages.

In the next subsection a brief recapitulation of Artemis drivetrain is presented. Then a set of assumptions applicable to the dynamic model of the monocylinder machine (presented at the end of section 3.2.4) are introduced. Such assumptions are aimed to obtain a rather simple monocylinder machine representation for pumping and motoring operation under the constraints that Artemis hydraulic machines uses in their 1.6 MW system. The final products of this section are two monocylinder machine models (one for Artemis ring cam pump and another for Artemis motor). These will be presented by the end of section 3.4.2 and 3.4.4 respectively.

3.4.1. Description of Artemis Digital Displacement drivetrain

Artemis drivetrain is formed by a hydrostatic transmission followed by two parallel synchronous generators as presented in Figure 3.11. The hydrostatic transmission is given by a high efficiency - low speed ring cam radial piston pump driving a high speed radial piston motor. Although operation principle remains the same, dimensions, number of cylinders and configuration might be different between pump and motor. In general, the Artemis Digital Displacement machines can be considered as an optimized radial piston machines. The optimization consist in reducing slipping surfaces; but most important, by making the valve’s operation independent of the angular displacement of rotor shaft. This unconstrained dependence allows individual operation of each cylinder. Discrete operation of cylinders helps to dramatically reduce leakage losses in preselected cylinders (those cylinders that are not required to fit the current load condition, are just idled). Also, effects due to transition regions (regions 2, 3, 5 and 6) are minimized by means of careful software tuning. By the end of the day, optimization is reduced to intelligent control of suction and discharge valves, which are triggered by electric solenoids.

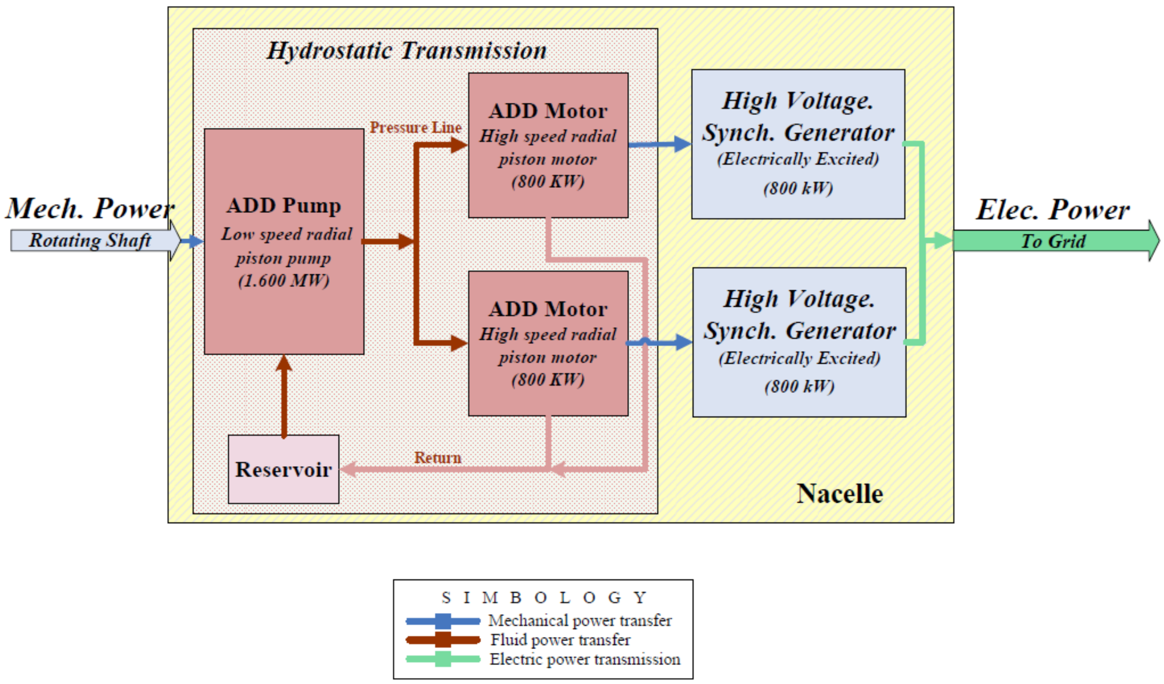

Figure 3.11 Artemis 1.6 MW drivetrain system

Software control makes possible to implement, and tune up, any kind of machine behavior (idling, braking, pumping or motoring) within the same hardware. For instance, it is possible to idle some cylinders (aimed to reduce leakage losses on those cylinders) while the rest works at rated power, making possible to fit any partial load condition with the minimum number of cylinders working at rated power.

In general, operating principle for Artemis machines is very similar to the one presented in Figure 3.1. As it will be proven in the subsequent sections, radial piston **hydraulic machines should be designed with a considerable small piston stroke so the ripple in the flow can be minimized** [*16*] [*17*]. Reduced piston stroke means only one thing: large number of cylinders. This means that distance l_e should be relatively small compared with the camshaft (or ring cam) dimensions since several cylinders must be fit radially [*18*]. This principle is widely used in the industry by several manufacturers and designers, including Artemis.

Artemis drivetrain uses a low rotating pump driving a high speed hydraulic motor (s). For the 1.6 MW system (rated power), one low speed pump drives two 800 kW hydraulic motors. The hydraulic motors drive one electrically excited high voltage synchronous generator each one. The model built in this document focus in this system. This is presented in Figure 3.11.

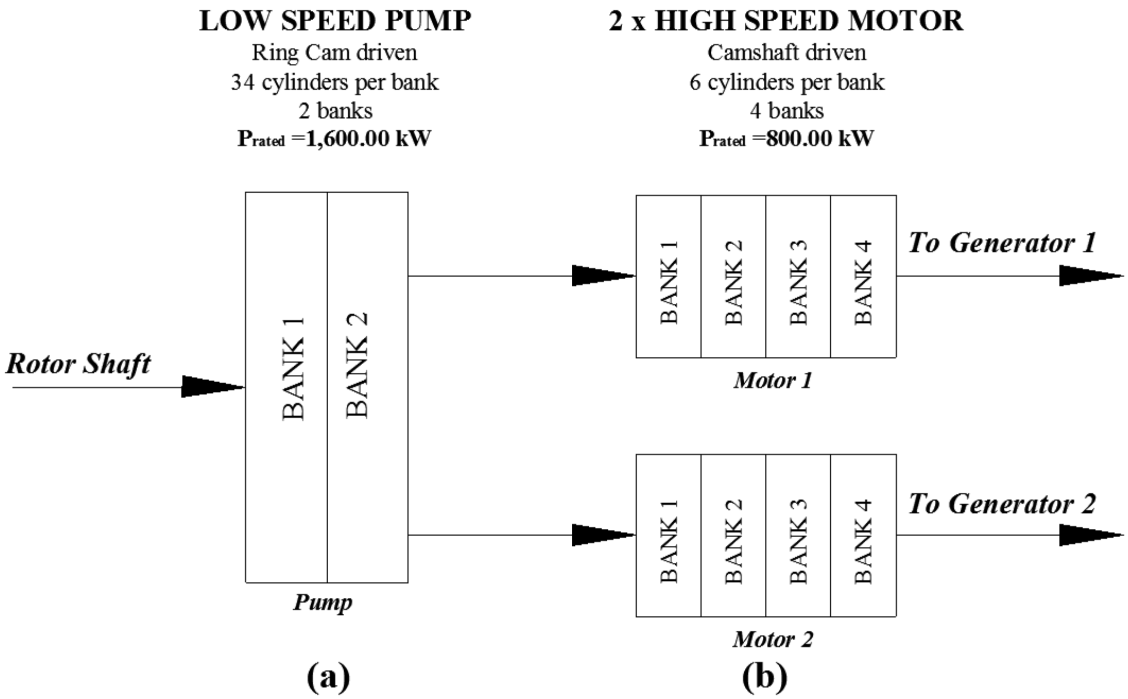

Figure 3.12 Schematic representation of the ADD pump(a) and ADD motor(b).

Artemis Digital Displacement motor has in total 24 cylinders of same geometry. They are distributed in 4 banks. Each bank contains 6 cylinders equally radially distributed. The banks are stacked over each other. One single camshaft drives the 24 cylinders so each cylinder had one full stroke any single revolution. The cross section of the ADD high speed motor looks very similar to that presented in Figure 3.1. A schematic view of the motor is presented in Figure 3.12b. On the other hand, the ADD low speed pump has a total of 68 cylinders contained in two parallel banks. Although the principle of operation is similar to the motor, the ADD pump uses a different mechanism to drive the cylinders up and down: a ring cam. A ring cam is a large rotating piece concentric to the main axis of rotation. It does not have any kind of eccentricity. Instead, a ring cam had a sequence of specially shaped lobes over the all external cylindrical surface. The combination between lobes and rotation of the ring cam makes possible to drive the cylinder stroke. In the case of the ADD 1.6 MW pump, the 24 lobes drive up and down all cylinders 24 times per single revolution of the ring cam. The shape of the lobe determines the motion characteristics of radial coordinate $\boldsymbol{r}$. Figure 3.13 presents a simplified cross section of the ADD low speed radial piston pump. In there, the springs were removed to allow a clearer perspective. For a detailed view of the employed components for each cylinder, refer to Figure 3.14, where the cross section of a cylinder for a motor is presented. The components employed for piston and cylinder only differ in dimensions.

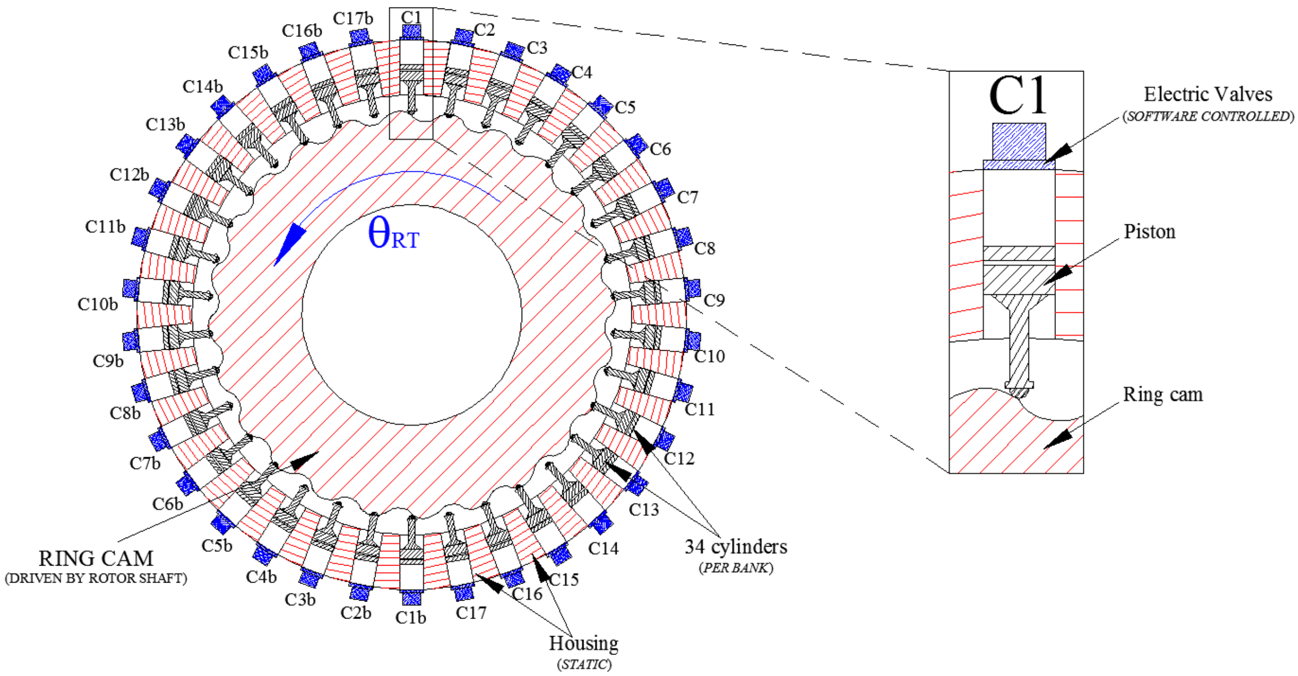

Figure 3.13 Simplified cross section for one bank of low speed ADD pump

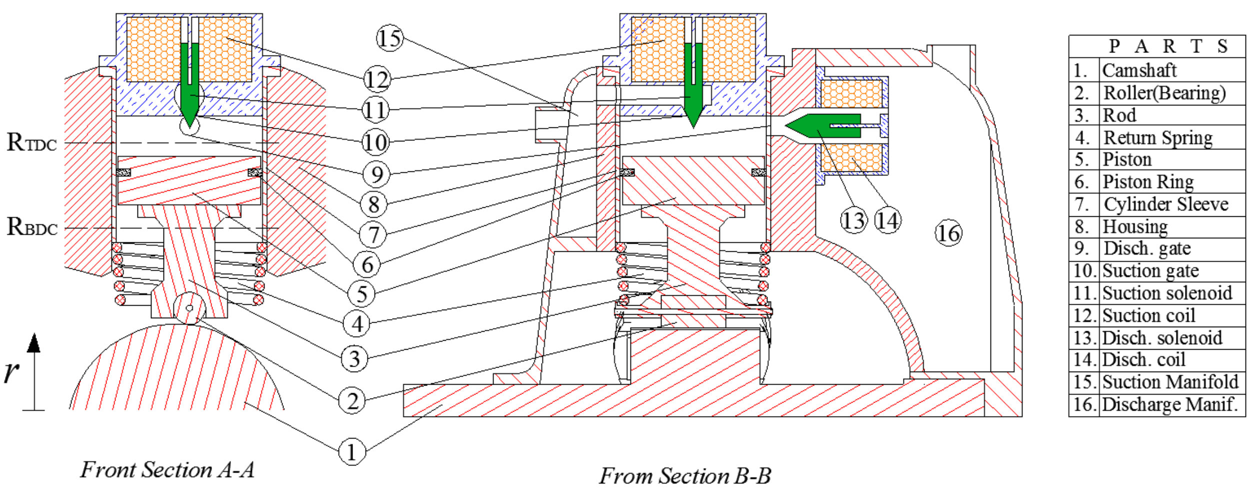

Figure 3.14 One single cylinder set with electric valves

The cross sections depicted in Figure 3.13 and Figure 3.14 were elaborated based on the described operating principle by Rampen [*19*] (compare with Figure 3.14 with Figure 3.3). Figure 3.14 describes the most important parts that make possible the operation of each cylinder. Notice that in Figure 3.14 the valve’s discs are not present any longer for ADD machine; also, the net flow into the chamber is controlled by the configuration of the suction and discharge gates (10 and 9 respectively) and the solenoids (11 and 13), which allow oil fed into the cylinder. Solenoids are driven by electric coils (12 and 14) that are controlled by software. Figure 3.14 presents an idea about what could be used as suction and discharge valves based in the claim made by the manufacturer (use of *high performance valves* [*5*] to minimize losses due to drag -low K_W in Eq. 3.28-).

The use of software controlled valves and the valves by themselves are the most distinctive components of ADD machines. As mentioned before, electric control releases the dependence on angular displacement θ for valves' operation; so valves can be controlled at will.

In Appendix B wind turbines' drivetrains are introduced along with some specific ranges of rotor's angular speed ($\dot{\theta_{RT}}$). Then, in Appendix C, some commercially available electric valves are presented along with typical response times and basic operation principle. Based on those values, it can be observed that at rated values, the difference between the response times of the valves and the transient stages (region 2,3,5 and 6 in a conventional radial piston pump) are not significantly different (ratio of about 3-1:1-3). However, for electric valves, the response time is not function of θ_{RT}, but from the electromagnetic coupling of the solenoid, which can be commanded at will by means of an electrical signal. This means that in a more or less steady condition (minimal variation in rotor angular speed and load pressure established in discharge port), the response time is more or less constant and independent of $\dot{\theta}_{RT}$. Independent response times in combination with careful tuning might eventually lead to minimize effects of unwanted regions (2, 3, 5 and 6) and therefore power losses.

Also, the capability to command valves at will, allows the possibility to *idle* some cylinders (as much as demanded for the partial power operating condition) minimizing effects of volumetric efficiency in those cylinders that are not strictly required. For instance, in the low speed pump, if the partial load condition is about 50% (~800 kW) of rated power and assuming a linear relation between the number of cylinders and rated power, 34 cylinders (1 bank) can be worked at rated power, while the other bank is left idle minimizing it losses to just parasitic drag. For the same partial operating condition, one single hydraulic motor can drive one single 800 kW synchronous generator minimizing parasitic losses of dragging a full size motor (1.6 MW) and generator. Added to this, software controlled valves allows the possibility to have even wear in all components. Consider the case in which due to oil impurities, one random cylinder wears prematurely. After sensing that premature wear, it is possible to take particular load circumstances with that particular cylinder by means of the software control. It is possible to allow an *easy ride* in that particular cylinder while some other cylinder takes its place in the power transmission process. Therefore, the time down of the machine can be minimized or even prevented until maintenance is available.

In the next sections, assumptions for representing a monocylinder machine in pump and motoring operation are presented. Such assumptions profit from particular constrains given by the 1.6MW Artemis drivetrain trying to use (for pump and motor) the same monocylinder machine presented in section 3.2.4.

3.4.2. Model of hydraulic pump

In this section, the dynamic model from monocylinder machine introduced in section 3.2 will be used to represent a monocylinder machine that represents one single cylinder of the Artemis low speed ring cam pump. This will be achieved by making some assumptions that will simplify the original dynamic model. Since a camshaft monocylinder model will be used to represent a ring cam multicylinder machine, a very important remark (valid only for the ring cam pump) must be done: The angular displacement of the rotor shaft and ring cam (θ_{RT}), and its time derivatives**, is not the same** degree of freedom than angular displacement in the monocylinder machine model depicted in section 3.2.4 (θ). In fact, they are related by:

$$\theta = 24\,\theta_{RT}$$
$$\dot{\theta} = 24\,\dot{\theta}_{RT} \qquad \textbf{Eq. 3.32}$$
$$\ddot{\theta} = 24\,\ddot{\theta}_{RT}$$

Where:
θ_{RT} is the angular displacement of the rotor shaft(or ring cam)
$\dot{\theta}_{RT}$ and $\ddot{\theta}_{RT}$ are the first and second time derivatives of θ_{RT}
θ is the angular displacement of the camshaft based monocylinder machine presented in section 3.2
$\dot{\theta}$ and $\ddot{\theta}$ are the first and second time derivatives of θ

Now, the pumping operation of hydraulic machines consists in transferring power from a rotating shaft to a flow of fluid. In one twenty fourth (1/24 th) of revolution from the rotor shaft, the cylinder sucks oil from the reservoir (in 1/48th of revolution) and delivers it to the discharge ports (in another 1/48th of revolution). In the pump, the discharge event is the one that involves the largest energy content and therefore larger loads are present in components later introduced in Figure 3.14. Such components must be designed to stand work and inertial loads derived from normal operation condition.

In order to target the final goal of this document (model a hydraulic drivetrain in a wind turbine) based on the limited information available about detailed machine geometry, the following premises will be considered onwards for the Artemis pump. These considerations are intended to be applied in the model for a conventional radial piston monocylinder machine given by Eq. 3.19, Eq. 3.20 and Eq. 3.23:

A. **The lobe profile can be represented as a cam profile.** The lobes (located in the ring cam) provide a cyclic profile to the static follower (piston-rod assembly). This cyclic profile drives the follower up and down. Because of cyclic characteristics and continuous curvature within each lobe; a lobe can be represented by the effect of a camshaft profile [*11*]. The camshaft profile is preferred because it directly allows the estimation of physics according with models applicable for motor geometry (section 3.2).
B. **The ring cam profile can be represented by a transmission ratio and a camshaft profile.** The ring cam in the ADD pump has 24 symmetric lobes. The lobes are symmetrically distributed along the entire ring cam circumference. The follower motion path described by each lobe in the ring cam can be represented with a camshaft profile that has the similar motion path. Then, this motion path (or camshaft profile) accurately represents one stroke of the piston. There are 24 strokes of the piston per rotor shaft revolution. This 24 strokes per revolution can be represented by the use of a lossless transmission (ratio 1:24) before the monocylinder machine camshaft. Then, each 1/24th of rotor angular displacement will represent one full stroke of the piston in the monocylinder model. Therefore, according with Eq. 3.32, this holds true:
$$\left(\theta_{RT,0} < \theta_{RT} < \theta_{RT,0} + 2\pi/24\right) \leftrightarrow (\theta_0 < \theta < \theta_0 + 2\pi)$$
C. **Friction in the piston neglectable.** Attending to a first impression in a lossless system; but more important, by neglecting friction forces, all geometric parameters expressed in Eq. 3.20 are no longer required, so the model simplifies considerably. The losses due to friction are intended to be considered in the shape of a gain for the overall system. This gain will be determined according with common values for efficiencies depicted in section 3.2.6.
D. **Inertial forces neglectable.** The magnitude of the inertial forces (mass times linear acceleration or moment of inertia times angular acceleration) are very small compared with force F_P. The main reason for this is that the pump is rotating *very* slow (few tens of RPM); and even with the

24 lobes acting per revolution, the magnitude of inertial forces is still very small. Also, the fact that the upper surface of the cylinder is interacting with a liquid fluid implies some degree of viscous damping that makes even smaller the impact of these forces in the overall performance of the system.

E. **Spring force neglectable**. The main purpose of the return spring (4 in Figure 3.14) is to assure the contact (avoid jumps) between the camshaft (1) surface and the bearing surface (2) when inertial forces are present. Since inertial forces are expected to be very small (see last assumption), the spring force required would be of the same magnitude, which compared with force F_P will be very small. Therefore is neglected too.

F. **Angular acceleration very small ($\ddot{\boldsymbol{\theta}}_{\boldsymbol{RT}}\sim\mathbf{0}$)**. In a wind turbine, the large size and weight of the rotor gives a very large moment of inertia (J_{RT}) to the input shaft of the pump. In Eq. 3.19, the term $J_C\ddot{\theta}$ accounts for a torque input present during transients (change of angular speed of the rotor) that eventually disappears when the new equilibrium condition is achieved (~constant speed implies $\ddot{\theta}_{RT}\sim 0$ and therefore $\ddot{\theta}\sim 0$) . Under these steady conditions, this term disappears.

Based on these assumptions, the dynamic model can be presented as:

$$T_{ReqC1} = \left(\frac{\pi D_{c,P}^2}{4} p_{C1,P}\right)\left(\frac{\sin\theta\cos\phi - \cos\theta\, sin\phi}{\cos\phi}\right) l_e = J_{RT}\ddot{\theta} - \frac{W_{IN,C1}}{\dot{\theta}}$$
$$p_{C1} = P_{D,P} \quad (0 < \theta \leq \pi)$$
$$p_{C1} = P_{S,P} \quad (\pi < \theta \leq 2\pi)$$

Eq. 3.33

Where:
T_{ReqC1} is the required torque to drive piston C1
J_{RT} is the polar moment of inertia of the wind turbine rotor plus the rotating parts of the machine
$D_{c,P}$ is the diameter of the pump cylinder
$p_{C1,P}$ is the pressure inside the pump cylinder
θ is the angular displacement of the camshaft in the monocylinder machine ($\theta = 24\,\theta_{RT}$)
$\dot{\theta}$ and $\ddot{\theta}$ are the first and second time derivatives of θ according with Eq. 3.32
ϕ is the pressure angle between the lobe and the roller for cylinder C1
$P_{D,P}$ is the discharge pressure in the pump
$P_{S,P}$ is the suction pressure in the pump
$W_{IN,C1}$ is the input power to drive cylinder C1

In this last expression, the values for p_{C1} as function of θ are intended to represent the operation during regions 1 and 4. Notice that the operation exclusively in region 1 and 4 is an idealized scenario. In fact, during the time that solenoid valves open or close, very similar regions to those presented in regions 3 and 6 are induced. For the current model this transient stage is just neglected due to simplicity.

Now, in terms of the continuity equation (Eq. 3.23), this can be simplified as follows:

$$\frac{dV_{C1}}{dt} = Q_{in,P} - Q_{out,P}$$
$$Q_{in,P} = 0 \qquad (0 < \theta \leq \pi)$$
$$Q_{out,P} = 0 \qquad (\pi < \theta \leq 2\pi)$$

Eq. 3.34

Where:
$Q_{in,P}$ is the input volumetric flow into cylinder C1 at the pump

$Q_{out,P}$ is the outgoing volumetric flow from cylinder C1 at the pump

Beware that $Q_{in,P} = 0$ in the range where the piston is *pushing* fluid out of the chamber (piston going outwards in the range $0 < \theta \leq \pi$ while having suction valve closed and discharge valve opened). Now, for the rest of the revolution ($\pi < \theta \leq 2\pi$), the valves' position is toggled to allow the fluid suction into the chamber while the piston is going inwards ($Q_{out,P} = 0$). Then, T_{ReqC1} in Eq. 3.33 can be related with the input torque T_{IN} by:

$$T_{IN} = \frac{W_{IN}}{\dot{\theta}_{RT}} \qquad \textbf{Eq. 3.35}$$

$$T_{avail} = T_{IN} - n_N T_{ReqC1} - T_{idl} = J_{RT}\ddot{\theta}_{RT} \qquad \textbf{Eq. 3.36}$$

Where:
T_{IN} is the input torque in the rotor shaft
W_{IN} is the input mechanical power in the rotor shaft(is the aerodynamic power if friction in main bearings are neglected).
T_{avail} is the net torque available in the rotor shaft(should be zero for steady state condition)
n_N is the maximum number of cylinders operating at rated power
T_{idl} is the parasitic torque due to idling cylinders

If T_{avail} is larger than zero, then this torque will be directed to the $n_N + 1$ cylinder that would be working at partial power. In this way, angular acceleration in the rotor shaft is avoided in a steady state condition. In case of increase of aerodynamic power available (therefore increase in T_{IN} and T_{avail}) and if $T_{avail} > T_{ReqC1}$, then cylinder $n_N + 1$ will be operated at rated power and the left torque (if any) sent another cylinder working at partial load. Viceversa operation applies for a reduction in aerodynamic power in the rotor. This paragraph constitutes the conceptual modeling of the software control logic applied to the Artemis machine, where any partial load condition is achieved by the combination of n_N cylinders working at rated power, plus one extra cylinder working below rated power. All remaining cylinders are being idled ($N - (n_N + 1)$). Idling operation for Artemis machine induce losses of the range of 7 W/(l/min) [5].

In the described scheme, Eq. 3.33 and Eq. 3.34 represent the mechanics behind one single cylinder of the Artemis Digital Displacement pump. On the other hand, Eq. 3.36 incorporates the torque control logic into the machine, which will command the flow control logic. These models can be extended to N cylinder by using the phase angle γ, which will imply a phase shift between flows depending on the number and the location of the operating cylinders.

In the following sections, considerations for hydraulic lines and monocylinder machine in motoring mode are presented.

3.4.3. Model of lines

The lines would be modeled as ideal for this moment. Eventually some losses in steady state, and therefore pressure drop, can be considered according with Eq. 3.27 and Eq. 3.28.

3.4.4. Model of hydraulic motor

In section 3.4.2 the monocylinder model was adapted to represent one single cylinder in the 1.6MW Artemis ring cam pump. Now, in this section, the monocylinder dynamic model will be once again manipulated so it can be used to represent one single cylinder in the 800 kW Artemis high speed motor. To do so, some assumptions will be considered as it was done for the Artemis low speed pump. However, unlike the ring cam pump, the motor allows the direct application of the dynamic monocylinder model introduced in section 3.2 since geometry is camshaft based.

Let's start saying that the motoring operation of hydraulic machines is the opposite of pumping operation: a flow of fluid is used to drive an output shaft. This means that for motoring purposes, the high energy content occurs in during the suction event (different from pumping operation). In general, very similar machine components to the ones used for the pump machine can be used here (use Figure 3.14 as geometry reference). However, if machines are highly optimized, then component sizing might differ even for same rated power and speed.

In terms of a hydraulic motor model, a correct approach would represent that the rotation of the shaft follows the flow of fluid entering the machine. Modeling this for a conventional radial piston motor (where all pistons are working simultaneously) is only matter of rearranging equations Eq. 3.19 and Eq. 3.23. Then some simplifications should be made (like those presented on section 3.4.2) and eventually obtain a set of equations similar to Eq. 3.33 and Eq. 3.34. In such model and aimed to control a constant angular speed, a variable flow control representation would be required within the hydraulic circuit (lines between pump and motor). Although the described model might satisfy the requirements for a conventional radial piston motor, this is not the case for an Artemis machine.

Artemis machine integrates the flow control within the machine, and the logic is directed by software (similar to the one described at the end of section 3.4.2). Therefore, it is required either to integrate a model of valve's control within the machine (intended to guarantee a constant speed at the output shaft) or make some assumptions that already represents the optimal software control into the machine. The first option might represent more accurately what is actually implemented in the Artemis machine. However, it might become too complicated because of implementation (and tuning) of several functions by software. The second option will lose some accuracy since it would consider only the optimal working operating condition (hardly achieved after careful tuning and in steady operation in the real machine); but would be simpler. The simpler design implies that no tuning is possible, and it would be implicitly consider that the motor reaches a steady operation *immediately*, eliminating the possibility to have a clear picture during transients. For the purposes of this document, although its deficiencies, it is believed that the second option is accurate enough. Before going through the assumptions for the hydraulic motor, let's name the degree of freedom that describes the angular displacement for the output shaft in the hydraulic motor as ε. In same fashion its time derivatives can be defined: $\dot{\varepsilon}$ as angular speed and $\ddot{\varepsilon}$ as the angular acceleration in the output shaft. Based on this, the following assumptions will be made:

A. **Constant angular speed at the output shaft.** Two main remarks. First, the target of the Artemis control is to maintain a constant angular speed at the output; therefore, by making this assumption the *optimal* software logic is being implemented implicitly. Second, constant angular speed means no angular acceleration ($\ddot{\varepsilon} = 0$); in the real machine, and because only an approximation to the optimal operating point is possible, there will be values of $\ddot{\varepsilon}$ very small, so it is for sure possible to say $\ddot{\varepsilon}\sim 0$.

B. **Friction in pistons neglectable.** Consideration aimed to simplify the model and very similar to those presented in section 3.4.

C. **Camshaft inertial force neglectable.** The magnitude of the forces is very small compared with F_P at any time.

D. **Piston Inertial forces balanced with spring forces.** In this case, the camshaft is rotating at constant speed of 1500 RPM. This frequency induces large accelerations in the piston's motion (magnitudes ~$450\ m/s^2$ for the modeled geometry[25]) that combined with the small estimated mass[26] generates inertial forces ~3 times the required force to evacuate the oil from the chamber. This means, that the return spring must be stiff enough to store this energy during discharge (small stresses in components, but larger risk of surface separation between camshaft and roller bearing), and release it during suction (larger stresses in components, but no risk to surface separation). On the other hand, the upper surface of the piston is in contact with oil, which provides some kind of controlled (by electric valves) viscous damping. If both effects are considered, then it should be safe to consider that the inertial loads had minimal effect in the energy recovering process (suction), where the force due to pressure in the motor ($F_{P,m}$) is very large compared with inertial and spring loads.

Based on these remarks, then it is possible to model the Artemis motor as a machine that is running at constant speed of 1500 RPM for all times that oil flow is available. The magnitude of the flow will set the number of operating cylinders, and therefore, the output power. The recovered torque in the motor shaft due to the action of cylinder C1 can be estimated by:

$$\begin{aligned} T_{outC1,m} &= F_{P,m}\left(\frac{\sin\varepsilon\cos\phi_m - \cos\varepsilon\, sin\phi_m}{\cos\phi_m}\right) \\ &= \frac{\pi D_{c,m}^2}{4} p_{C1,m}\left(\frac{\sin\varepsilon\cos\phi_m - \cos\varepsilon\, sin\phi_m}{\cos\phi_m}\right) \\ &= \frac{W_{OUT,C1}}{\dot{\varepsilon}} \end{aligned} \qquad \textbf{Eq. 3.37}$$

$$\begin{aligned} p_{C1,m} &= P_{S,m} \qquad (0 < \varepsilon \leq \pi) \\ p_{C1,m} &= P_{D,m} \qquad (\pi < \varepsilon \leq 2\pi) \\ \dot{\varepsilon} &= 1500\ RPM \approx 157\ [rad/s] \\ \ddot{\varepsilon} &= 0\ [rad/s^2] \end{aligned}$$

Where:

$T_{outC1,m}$ is the recovered torque in the motor shaft due to cylinder C1
$F_{P,m}$ is the force felt by the piston because of the pressurized fluid in the cylinder chamber
$D_{c,m}$ is the motor cylinder diameter
ε is the angular displacement of the motor shaft
$\dot{\varepsilon}$ and $\ddot{\varepsilon}$ are the angular speed and acceleration respectively
$p_{C1,m}$ is the pressure in the motor cylinder chamber

[25] The modeled geometries for the pump and motor were done based on visual inspection of available illustrations for the 1.5 MW system. Therefore geometries and motion displacements values must be considered for illustrative purposes.

[26] Based on cast iron density and volumes according with geometry ($\sim$ 1 kg per cylinder-rod assembly).

$P_{S,m}$ is the suction pressure in the motor manifold
$P_{D,m}$ is the discharge pressure in the motor manifold
$W_{OUT,C1}$ is the recovered mechanical power due to cylinder C1 in the motor

Then, the continuity equation for the motor operation can be rewritten as:

$$\frac{dV_{C1,m}}{dt} = Q_{in,m} - Q_{out,m}$$

Eq. 3.38

$$Q_{in,m} = 0 \qquad (0 < \varepsilon \leq \pi)$$
$$Q_{out,m} = 0 \qquad (\pi < \varepsilon \leq 2\pi)$$

Where:
$V_{C1,m}$ is the control volume of cylinder C1 in the motor
$Q_{in,m}$ is the input volumetric flow to the control volume $V_{C1,m}$
$Q_{out,m}$ is the outgoing volumetric flow from the control volume $V_{C1,m}$

Once again, $Q_{in,m}$ is zero for the first half of camshaft revolution since the fluid is being driven out form the cylinder chamber. Then, for the other half of revolution valves are toggled, power is being extracted from the fluid by allowing input flow while $Q_{out,m} = 0$ (closed output valve).

Finally, Eq. 3.37 and Eq. 3.38 constitute the model for one single cylinder motor (analogous to Eq. 3.33 and Eq. 3.34). Be aware than expression Eq. 3.38 is practically the same than Eq. 3.34 (including boundary conditions). This is due to the fact that the operation of the machine is exactly the same; but the motor extracts power according with Eq. 3.37 at the boundary conditions denoted in there.

Since $T_{outC1,m}$ only considers recovered power from one single cylinder; it is required to relate this quantity with the net output torque (T_{OUT}) by means of the motor phase shift angle ($\gamma_{sa,m}$). By using $\gamma_{sa,m}$ similar torques will be harvested for all other cylinders. However, such harvested torques will be shifted according with the cylinder phase angle ($\gamma_{m,n}$) degrees along every revolution. This idea can be expressed as:

$$T_{OUT} = \sum_{n=1}^{N} \vec{\boldsymbol{T}}_{\boldsymbol{outXn}} - T_{idl,m} = \sum_{n=1}^{N} (T_{outC1,m} < \gamma_{m,n}) - T_{idl,m}$$ **Eq. 3.39**

Where:
T_{OUT} is the net torque in the motor shaft
$\vec{\boldsymbol{T}}_{\boldsymbol{outXn}}$ is a generic recovered torque vector in the motor
$T_{outC1,m}$ is the magnitude of any generic recovered torque vector
$\gamma_{m,n}$ is the phase angle for cylinder n
$T_{idl,m}$ is the parasitic torque due to idling cylinders

Eq. 3.39 summarizes the idea of represent 24 cylinders (in the motor) with one single cylinder shifted according with the phase shift angle.

This concludes the modeling of the hydrostatic transmission of the Artemis 1.6 MW drivetrain system. In the following section, some other complementary models will be introduced.

3.5. Complementary models

Because the main target of this document is to model the use of hydraulic drivetrains in wind turbines, it can be expected that the main input and output be in terms of wind power (wind speed) and electric power (current and voltage). Therefore, some other complementary models are required to complement the hydrostatic transmission subassembly (check Figure 3.11). This section is dedicated to present simple models for the conversion of wind power to mechanical energy (in the rotor) and from mechanical energy to electrical energy (in the generator). On next, such models will be presented.

3.5.1. Rotor

A wind turbine is complex machinery that harvest energy from a moving mass of air and transform it into electrical power. The harvested energy is incorporated to a rotating shaft. This rotating shaft will be the input for the drivetrain system; therefore, the way in which power is delivered should be understood correctly.

A rotor can harvest power according with [*20*]:

$$\begin{gathered} W_{aero} = \frac{1}{2}\rho_{air} A_R C_p U_a^3 \\ A_R = \frac{\pi}{4} D_R^2 \end{gathered} \qquad \textbf{Eq. 3.40}$$

Where:
W_{aero} is the aerodynamic power
ρ_{air} is the air density
A_R is the swept rotor area
C_p is the power coefficient
U_a is the wind speed at nacelle height
D_R is the rotor diameter

The power coefficient gives an idea about how efficient the wind power is being adhered to the rotor shaft. Normally, C_p varies in the range $0 < C_p < 0.50$ depending in the aerodynamic configuration of the blade at the particular wind speed (effective C_p can be influenced by the chord distribution, twist angle distribution and active pitch control among others).

If losses in the rotor shaft bearings are neglected, then it can be said that:

$$\begin{gathered} W_{aero} = W_{IN} \\ \frac{1}{2}\rho_{air} A_R C_p U_a^3 = T_{IN}\dot{\theta} \end{gathered} \qquad \textbf{Eq. 3.41}$$

The detailed modeling of rotor geometry is out of the scope of this document. Instead, a commercially available geometry (ENERCON E82 [*21*]) was scaled down to fit the required input power (~1.6 MW) to drive the modeled drivetrain system. The most important characteristics of rotor for E82 and the one used for the model are presented in Table 3.2. In there, the most important change is given by the rotor diameter that was scaled down to fit the rated power of the Artemis drivetrain.

Beware that from data presented in Table 3.2, the values from the scaled down rotor model are more or less *unusual* (smaller rotational speed and tip speed ratio). Normally, smaller rotor diameter implies larger angular speed since tip speed ratio is tried to be maximized to improve aerodynamic performance [*20*]. This is not the case for the presented case. The present case was estimated by assuming that power coefficient of E82 will not be affected by a decrease in blade length. Although this is unusual, the optimization of this rotor model will be left for future work. For now, this model is used to provide a input vector of angular displacement (and its time derivatives) in a steady state. Therefore, this model is considered as accurate enough to evaluate performance of hydraulic drivetrains in wind turbines in steady state.

	E82	Model
Rated Power [kW]	2,000	1,600
Rotor diameter [m]	82	72
Swept Area [m^2]	5,281	4,072
Number of blades	3	3
Rated wind speed [m/s]	13	14
Cut in wind speed [m/s]	3.5	3.5
Cut out wind speed [m/s]	28	28
Rotational speed [RPM]	6 to 18	5 to 17
Rated tip speed ratio [-]	5.9	4.6

Table 3.2 Rotor parameters for E82 and computer model.

3.5.2. High voltage - high speed electrically excited synchronous generator

In a wind turbine, the task for the electric generator is to transform the harvested aerodynamic power into usable electric power. Moreover, wind turbines are located inside wind farms, which posses a very often a medium voltage interconnection grid, or directly connected to the general distribution grid. Whichever is the case, the electrical power presents particular constraints (grid voltage, frequency, phase sequence and phase angle) that must be complied by electric system of the wind turbine if interconnection is desired. As was presented in section 1.1.2, wind turbine industry uses several layouts to comply with these constraints. For instance, one layout could be a double fed induction generators followed by an electronic converter and a step up transformers. In the case of the analyzed drivetrains, since speed regulation is being done at the hydrostatic transmission, the use of a directly connected electrically excited synchronous generator is possible. This array gets rid of the PEC (the generator is synchronously connected to the grid), and the use of a step up transformer can be avoided if a *high voltage* electrically excited synchronous generator is selected. This is the current case since it minimizes the number of components in the drivetrain increasing efficiency levels.

3 Phase Synchronous Generator			
Apparent Power		1 MVA	
Nominal Voltage (V_t)		11 kV	
Angular Speed ($\dot{\varepsilon}$)		1500 RPM	
PF		0.85	
Configuration		Δ	
Poles		4*	
Base values (PU system)			
Base voltage	V_b	6351	V/phase
Base Current	I_b	52.49	A
Base Imped.	Z_b	121	Ohm
Synchronous machine parameters			
	Per Unit	Net Value	Units
R	0.010 -0.005	1.21	Ohm
Xs	1.000-1.500	121	Ohm

Table 3.3 Synchronous Machine parameters (* for nominal speed of 1500 RPM)

For this section, the model for a high voltage electrically excited synchronous generator will be done. The model presented on next targets steady state conditions. Some important assumptions that are made are:

A. **The synchronous generator has a cylindrical rotor, 3 phases, 4 poles, apparent and real power of 1 MVA and 0.85 MW respectively, power factor of 0.85 lagging and delta configuration. The machine is connected to a grid with line voltage of 11 kV.** Based on technical information from common manufacturers [*22*].
B. **The angular speed of the input shaft is regulated at 1500 RPM.** It is assumed that the hydrostatic transmission has the capability to keep the input shaft of the synchronous generator at rated angular speed. This is the basis so the steady state model can be valid.
C. **The synchronous generator is connected to an infinite strong bus.** It is assumed that the frequency, phase angle and sequence are the same to those in the generator. Also, the infinite bus is stable and the contribution of the generator does not affect the performance of the grid.
D. **The generator is a balanced system.** All three phases have similar values of synchronous impedance, therefore the analysis for one phase can be extended for all other phases.

Based on the past assumptions, the equivalent circuit and the phasor diagram for an electrically excited synchronous generator can be observed in Figure 3.15a and 3.15b respectively.

The condition for a steady state in the generator is given by:

$$\begin{gathered} J_G \ddot{\varepsilon} = T_{OUT} - T_{el,3\varphi} = 0 \\ T_{el,3\varphi} = T_{OUT} \end{gathered} \qquad \textbf{Eq. 3.42}$$

Where:
J_G is the generator moment of inertia
$\ddot{\varepsilon}$ is the angular acceleration of the generator shaft (connected to hydraulic motor shaft by *rigid* coupling)
T_{OUT} is the net output torque fed by the hydraulic motor to the generator
$T_{el,3\varphi}$ is the electrical torque due to energy transformation

The electrical torque can be related with electric power by:

$$T_{el,3\varphi} = \frac{3|V_t||E_f|}{\dot{\varepsilon}_s X_s} \sin\delta \qquad \textbf{Eq. 3.43}$$

Where:
V_t is the voltage at the terminals (grid line to line voltage)
E_f is the wound excitation voltage
X_s is the synchronous reactance (~1.0-1.5 p.u. [*23*])
$\dot{\varepsilon}_s$ is the synchronous angular speed (1500 RPM)
δ is the power angle

The excitation voltage can be estimated by:

$$\begin{gathered} \hat{E}_f = \hat{V}_t + \hat{I}_a \cdot (R_s + j X_s) \\ \hat{V}_t = (V_t \angle 0°) \\ \hat{I}_a = (I_a \angle \phi) \\ \hat{E}_f = (E_f \angle \delta) \end{gathered} \qquad \textbf{Eq. 3.44}$$

Where:
I_a is the stator current (denoted in Figure 3.15)
R_s is the synchronous resistance (~0.01-0.005 p.u[*23*])

The magnitude of the stator current can be estimated as:

$$|I_a| = \frac{T_{OUT}\dot{\varepsilon_s}}{3\,V_t\,PF} \qquad \textbf{Eq. 3.45}$$

Where:
$|I_a|$ is the magnitude of the stator current
PF is the power factor

So this steady state model could be useful, some numeric values were required. Such values are summarized in Table 3.3

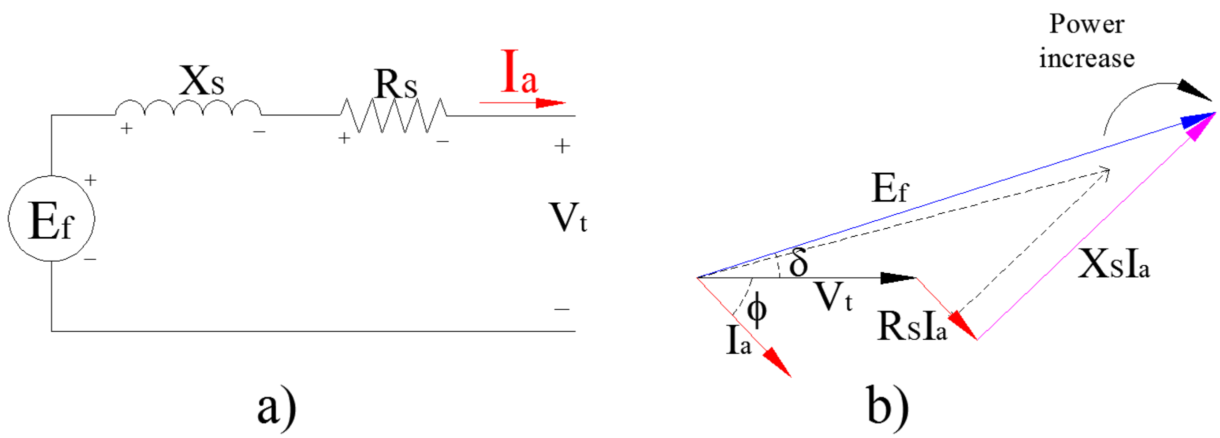

Figure 3.15 Synchronous generator equivalent circuit (a) and phasor diagram(b)

Now, in terms of losses, there are several types of losses involved in the power conversion in a synchronous generator: Stray, friction, windage, core and copper losses [*24*]. Such losses are presented in Figure 3.16 in the shape of a power flow for a synchronous generator.

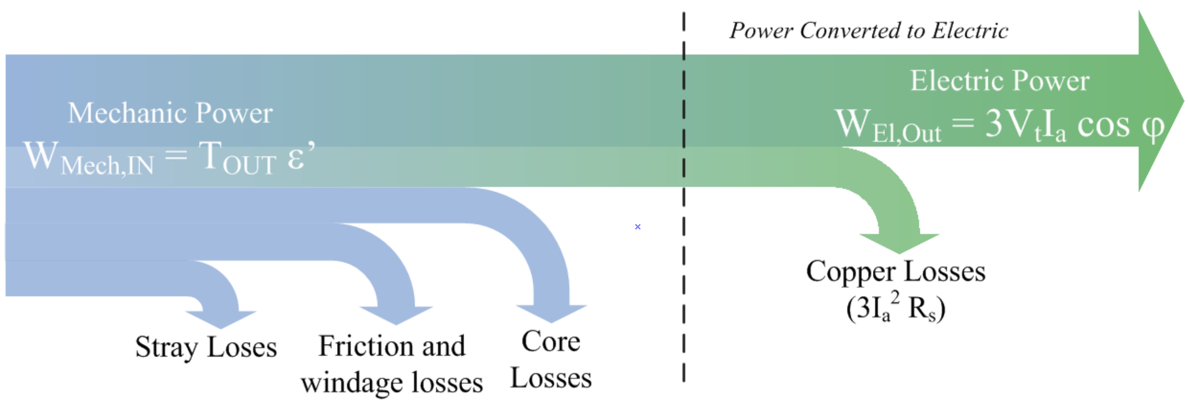

Figure 3.16 Power flow in an electrically excited synchronous generator

On the other hand, copper losses in the three stator windings ($W_{Cu,loss,3\varphi}$) can be estimated by:

$$W_{Cu,loss,3\varphi} = 3I_aR_s \qquad \textbf{Eq. 3.46}$$

Because of large nominal power (1MVA) and angular speed (1500 RPM), it is expected that overall efficiency will be quite high. On the other hand, there is no information available about stray, friction, windage and core losses for the particular machine. Therefore, a simpler approach was selected to estimate losses in generator: work with technical figures of efficiency. To do so, it will be considered that combined losses due to stray, friction, windage, core and wound excitation accounts for 2% of the total power. To this quantity, copper losses will be subtracted so the overall efficiency of the generator is less than 98% (more or less complying with manufacturer's technical information for high speed high voltage synchronous generator type 1DU). This is expressed on next:

$$
\begin{gathered}
W_{El,Out} = (\eta_{Manuf}\,\eta_{Cu})W_{IN} \\
\eta_{G,eff} = \eta_{Manuf}\,(1-\chi_{Cu}) < 98\% \\
\chi_{Cu} = \frac{3I_a^2R_s}{3V_tI_a\cos\phi + 3I_a^2R_s}
\end{gathered}
\qquad \textbf{Eq. 3.47}
$$

Where:
$W_{El,Out}$ is the three phase electrical power delivered by the generator
η_{Manuf} is the upper limit of efficiency according with manufacturer [*22*] (η_{Manuf}~98%)
η_{Cu} is the partial efficiency due to copper loses
$\eta_{G,eff}$ is the overall efficiency of the generator
χ_{Cu} is the cupper loss factor

Based on these figures, a steady state model for a generator can be computed. Furthermore, this concludes the complementary models required for the representation of a wind turbine that uses a hydraulic drivetrain.

3.6. Conclusion

In this section, the physics behind a conventional fixed displacement radial piston pump were presented. Then, this knowledge was used to approach a specific drivetrain layout. This study case corresponds to the 1.6 MW Artemis drivetrain. This drivetrain is formed by a hydrostatic transmission (based on Artemis Digital Displacement machines), and two high voltage-high speed electrically excited synchronous generator. Therefore, come complementary models (rotor and generators) were introduced too. Equations here presented will serve as basis for subsequent sections, where a computer model will be presented.

In general terms, conventional piston based machines have two important sources of losses: volumetric leaks and transition regions. Abate losses due to volumetric efficiency (in one single cylinder) is very hard since endurance of the system relies in lubrication. On the other hand, transition regions are dependent of angular displacement due to valves mechanism, and therefore very hard to eradicate.

By using electrically triggered valves the θ dependence is removed. Also individual cylinder control is possible. Therefore, overall volumetric efficiency (all pump) can be effectively raised by idling cylinders that are not required to transfer power. Nevertheless, software dependence is increased (the dynamic response of the machine is as good as the software control commands). Software control on digital hydraulic machines is out of the scope of this document; therefore some assumptions were made.

Finally, loses in complementary models (pipe lines, rotor and generator) will be estimated in the steady state. There is still some room for improvement in there as well in the detail of the proposed models. Nevertheless, for the purposes of this document (model hydraulic drivetrains in wind turbines) the proposed equations are considered as accurate enough.

4. Computer Model

4.1. Introduction

The past chapter introduced the physics behind a conventional monocylinder radial piston machine. Also, that general monocylinder machine was adapted to represent monocylinder machines according with Artemis Digital Displacement machines. Now, for this chapter, those monocylinder machines will be integrated in a computer model to eventually represent the Artemis drivetrain system. Therefore, the main objective of this chapter is to discuss a computer model that assembles the use of a hydrostatic transmission in a wind turbine. Such hydrostatic transmission is formed by digital hydraulic machines from the type radial piston. Modeled machinery is based on the 1.6 MW Artemis drivetrain. Also, this chapter presents simulation results and scope of limitations of such model. All computer models presented in this section will be built using MatLab Simulink.

To do so, first a monocylinder machine computer model will be presented. Then this model will be used to integrate the multicylinder machines that eventually will form the hydrostatic transmission. Afterwards, some complementary computer models (aimed to integrate the hydrostatic transmission in a wind turbine according with Artemis drivetrain) will be presented for a synchronous generator and a wind turbine rotor. All models will be assembled together and simulations will be run. Then, the results of steady state simulations will be compared with analytical verifications under similar load conditions. Later, model limitations will be discussed to finally draw some conclusions by the end of this chapter.

4.2. Model built in MATLAB Simulink®

The main target of this document is to find out how large are the advantages of using hydraulic drivetrains in wind turbines respect with non hydraulic drivetrains. For this purpose, a computer model was built. This computer model aims to model the interaction between a hydrostatic transmission and a high speed synchronous generator in a ~2 MW wind turbine. To narrow down the possibilities of the model, a particular case of study was selected: Artemis drivetrain system.

Artemis drivetrain system was introduced in section 2.3.5. Technical specifications of this drivetrain system were summarized in Figure 3.12. Also, physics behind the operating principle for conventional and digital piston based hydraulic machines were presented in chapter 3 Based on that, this section introduces some computer models: first a mono-cylinder system is presented; then, this monocylinder model is used to represent the two different multi-cylinder machines for 1.6 MW Artemis drivetrain. Afterwards, complementary models (for steady state conditions) for the rotor and the synchronous generator are introduced.

In all cases, models require numeric entry of some data (i.e. diameter of pistons in hydraulic machines, synchronous reactance, etc). Such data will be introduced section 4.3.

4.2.1. Monocylinder digital machine

This section presents a computer model for a monocylinder machine based on equations and assumptions presented in section 3.4. Such dynamics were modeled in Matlab Simulink. The model for pumping operation is presented in Figure 4.1. The computer model used to exemplify the pumping operation was slightly modified to represent the motoring mode. Nevertheless, models and physics behind them are very similar for both cases.

The monocylinder model is capable to model physical properties as: piston displacement and its time derivatives($r, \dot{r}$ and $\ddot{r}$), effective pressure in the chamber (p_{cyl}), transmitted force and torque from camshaft to follower (F_P and T_{ReqC1}), effective mechanical and hydraulic power ($W_{Mech,C1}$ and $W_{Hyd,C1}$) and volumetric flow into (and from) the pressure chamber(Q_{in} and Q_{out} respectively). These parameters will be used to model the entire machines (pump and motor).

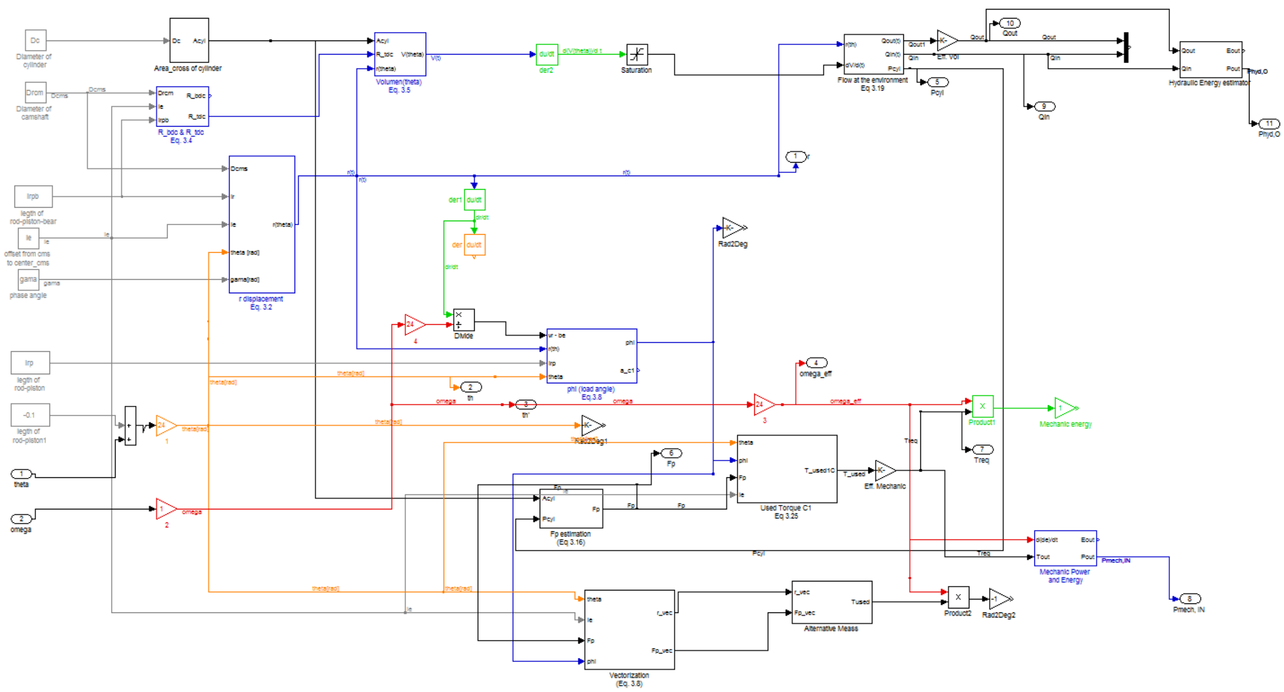

Figure 4.1 Monocylinder system in pumping mode (motoring is the reverse of pumping operation)

4.2.2. Multi-cylinder digital machines

In this section, the monocylinder model presented in 4.2.1 is used to *assembly* both Artemis machines (motor and pump). For the particular case of study, motor and pump have a significantly different layout (recall Figure 3.12). Therefore assumptions (presented in sections 3.4.2 for pump and 3.4.4 for motor) were integrated in the assembly model so the basic construction block (monocylinder model) can be used in both machines by adjusting geometric ratios respectively.

In general, for both machines, the large number of cylinders (68 for pump and 24 for motor) were classified according with DOF for piston displacement and its time derivatives ($r, \dot{r}$ and $\ddot{r}$). This classification showed that the operation of the Artemis machines can be approached by a few *characteristic cylinders*. A characteristic cylinder (for this document) is defined as a piston-cylinders set with a particular initial condition for DOF. Based on this, 17 characteristic cylinders were identified for the digital pump, and 6 for the Artemis motor. Since all characteristic cylinders operates based on the same principle (monocylinder machine), only a diphase between each characteristic cylinder was required to set the 17 different boundary conditions for the pump (6 for the motor). This is presented in Figure 4.2 for the Artemis pump. In there, the 24 lobe -ring cam implementation is presented by means of a direct 1:24 ratio. In terms of the Artemis motor, similar implementation was done. However, the ring cam implementation was not required since the motor stage works directly with camshaft. This is presented in Figure 4.3. An important remark is that the basic building block (monocylinder machines) works in similar fashion in motor and pump model; but, the input numerical values that describes the machines' geometry are significantly different. This is the main reason for which one model for a monocylinder machine could be used for two entirely different machines.

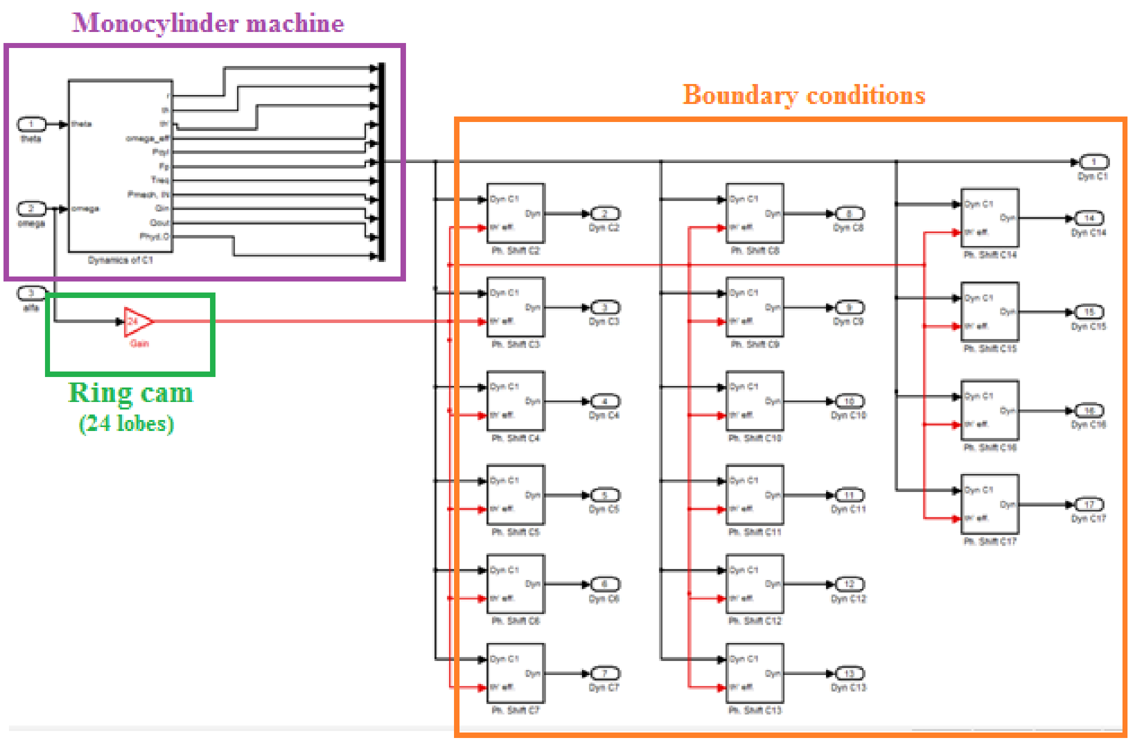

Figure 4.2 Boundary conditions and Ring cam implementation for Artemis pump.

Discrete activation of each cylinder is the main feature of digital hydraulic machines. Furthermore, net machine loads (net required torque, net outgoing oil flow, etc.) are directly related with boundary conditions due to physical position (characteristic cylinders) and the number of operating cylinders. Therefore, an idling (or active) cylinder will directly influence the amount of power transfer. To implement this in the current model, a load-dependent activation sequence should be defined. The main target of such sequence is to determine which cylinder is brought to operation, as discrete unit, during a particular load condition. This sequence does not directly represent the timing for the opening of the inlet and outlet valves. Actually, the cylinder is dealt as a unit that already assumes the *perfect* operation of flow valves (minimize transition region, avoids pressure builds up, and their action are perfectly synchronized to deliver power in the piston's way up for pumping operation). Then, what activating sequence says is how many of any characteristic cylinder type (17 for pump and 6 for motor) must be working under a particular load so the ripple in hydraulic (or mechanic) power can be minimized.

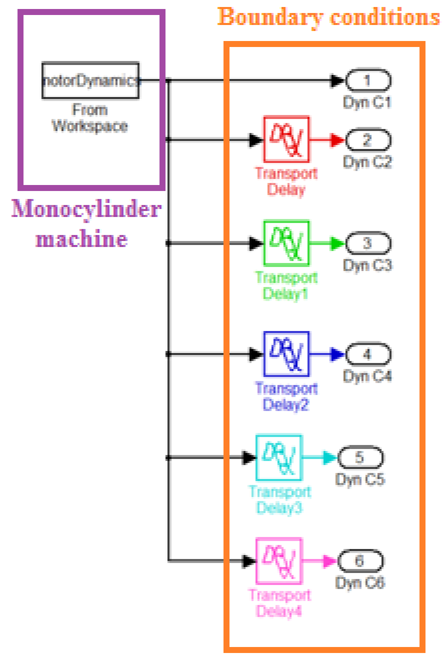

Figure 4.3 Boundary conditions implementation for motor.

Since fatigue is directly related with load fluctuations; then, by minimizing torque ripple (for input at the pump, or output shaft in the motor), it is possible to attenuate fatigue effects (especially important for long endurance machines like wind turbines). This stresses the fact that digital hydraulic machines are *extremely* software dependent. Therefore the entire performance of the machine is as good as the software quality is. The design of a high quality software control is out of the scope of this document. Nevertheless, some firing order sequences were built for illustrative purposes. One non optimal activation sequence for the pump and two versions (one better than the other, none optimal) for the motor are presented on Appendix E. In there, the criterion used to determine such firing orders is mentioned.

Bear in mind that activation sequences presented in Table 7.3-Table 7.5 **are just three possibilities** out of a large number of options: in the model ~17! for pump and 6! for motor; in real system ~68! for pump and 24! for motor. Therefore, the presented permutations might not be the optimal ones. The optimal permutation for activation sequence is out of the scope of this document as well as the valve timing. To further explain the effect on firing sequences, in section 4.4.2 two different sequences are used in the motor (simplest case) to exemplify the extent of software quality. But for now; the multicylinder model for the Artemis Digital Displacement pump is presented in Figure 4.4. Then Figure 4.5 presents the computer model for the Artemis Digital Displacement motor.

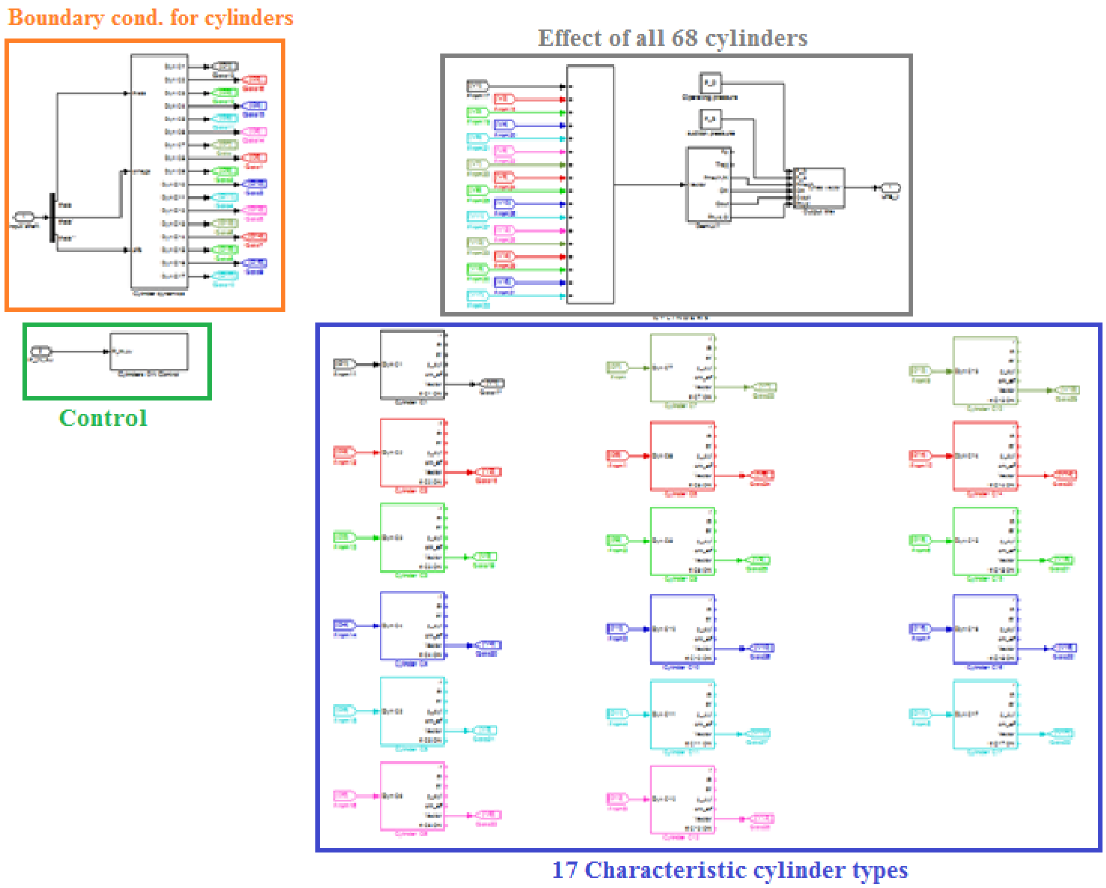

Figure 4.4 1.6 MW Artemis Digital Displacement pump (68 cylinder digital radial piston ring cam pump)

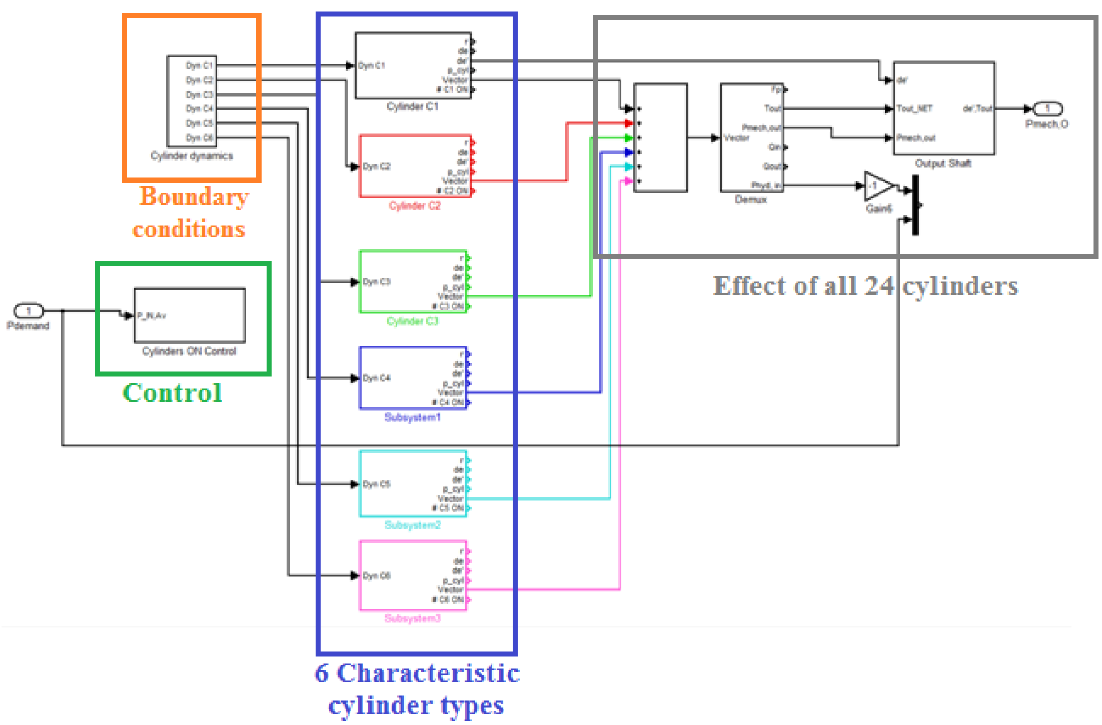

Figure 4.5 800 kW Artemis Digital Displacement motor computer model(24 cylinder digital radial piston motor)

Computer model for pump (Figure 4.4) receives a set of numeric values containing available torque, rotor angular displacement and its two time derivatives ($T_{IN}, \theta_{RT}, \dot{\theta}_{RT}$ and $\ddot{\theta}_{RT}$ respectively). Then, this model is capable to deliver all same outputs than monocylinder machine but for each one of the 17 characteristic cylinder types ($r, \dot{r}, \ddot{r}$, p_{cyl} , F_P , $T_{Req,C1-17}$, $W_{Mech,C1-17}$, $W_{Hyd,C1-17}$, $Q_{in,C1-17}$ and $Q_{out,C1-17}$) and important net quantities: net required torque for all active cylinders and idled ones ($T_{Req,NET}$); net mechanical (used) and hydraulic (output) power ($W_{Mech,NET}$ and $W_{Hyd,NET}$); and net input (output) flow ($Q_{in,NET}$ and $Q_{out,NET}$). In similar fashion, the motor model is capable to present the same signals for the 6 characteristic types of cylinders and net important quantities.

Before going to the next section, let's stress that inlet and outlet valves can operate *up to* once per cylinder stroke. This is due to heavy required mechanisms to control large amounts of hydraulic power (refer to Appendix C for common response times of hydraulic valves). Therefore, with current technology, is not possible to implement control techniques for inertial systems like the similar in hydraulics of what is pulse width modulation for electric devices. The valves are still too slow for the cylinder stroke frequency (~6 Hz for pump and ~25 Hz for motor).

4.2.3. Synchronous generator

Now, is time to present the computer model for 800 kW high speed- high voltage electrically excited synchronous generator. This model is valid only for steady state conditions and can provide an idea about the most important performance parameters: stator current magnitude, excitation voltage required, power angle and efficiency. Also, a representation for the grid voltage and stator line current feed by the generator is integrated. Assumptions and steady state models were introduced in section 3.5.2. The computer model is model is presented in Figure 4.6.

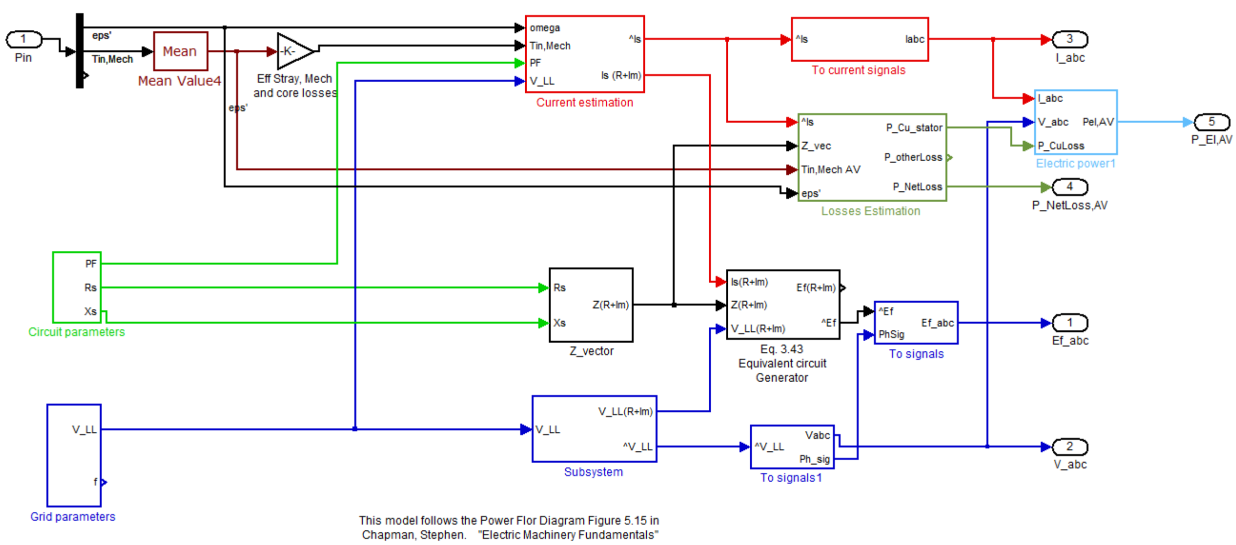

Figure 4.6 Steady state model for a synchronous generator.

4.2.4. Artemis drivetrain system

Once that all components required for the Artemis drivetrain (Figure 3.11) were presented, is time to introduce the full drivetrain impression. This is shown in Figure 4.7. In there, a very similar arrangement to the one exhibited in Figure 3.11 is visible. The drivetrain is formed by one 1.6 MW Artemis pump (68 cylinder 24-lobe ring cam digital pump), piping, two 800 kW Artemis motors (24 cylinder radial piston digital motor) and two 800 kW high voltage-high speed electrically excited synchronous generators.

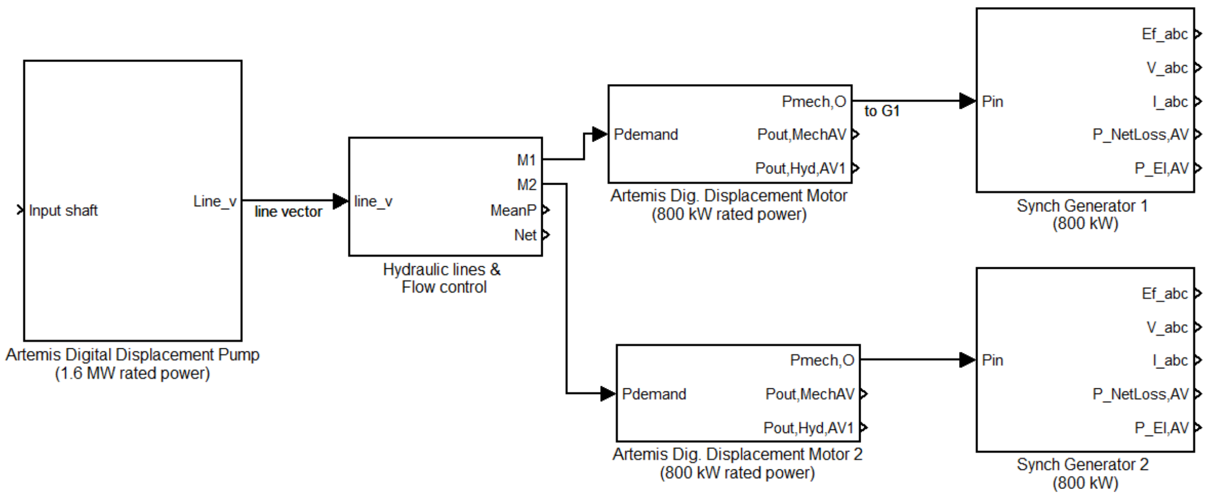

Figure 4.7 Artemis drivetrain computer model.

This drivetrain system is fed by a vector ("Input shaft" on left of Figure 4.7) that contains rotor shaft angular displacement and its time derivatives ($\theta_{RT}, \dot{\theta}_{RT}$ and $\ddot{\theta}_{RT}$) and mechanical torque(T_{IN}). Based on this vector, the model can estimate any of the variables of the monocylinder, pump, motors and generators' model. The input parameters are estimated with the complementary model of the rotor (section 4.2.5). The resulting parameters are estimated used the models presented so far.

4.2.5. Rotor model

The rotor is the prime mover for the drivetrain system. It provides the mechanic input power (in a rotating shaft) that the drivetrain will convert in electric power. This mechanical power comes in the shape of mechanical torque (T_{IN}) and angular speed ($\dot{\theta}_{RT}$). Since our drivetrain system models the physics behind the digital hydrostatic transmission is advisable to know θ_{RT} and $\ddot{\theta}_{RT}$ too. Therefore, the computer model for the background (discussed in section 3.5.1) is now presented in Figure 4.8.

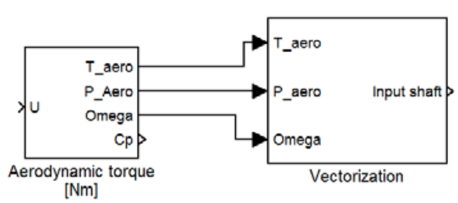

Figure 4.8 Rotor model

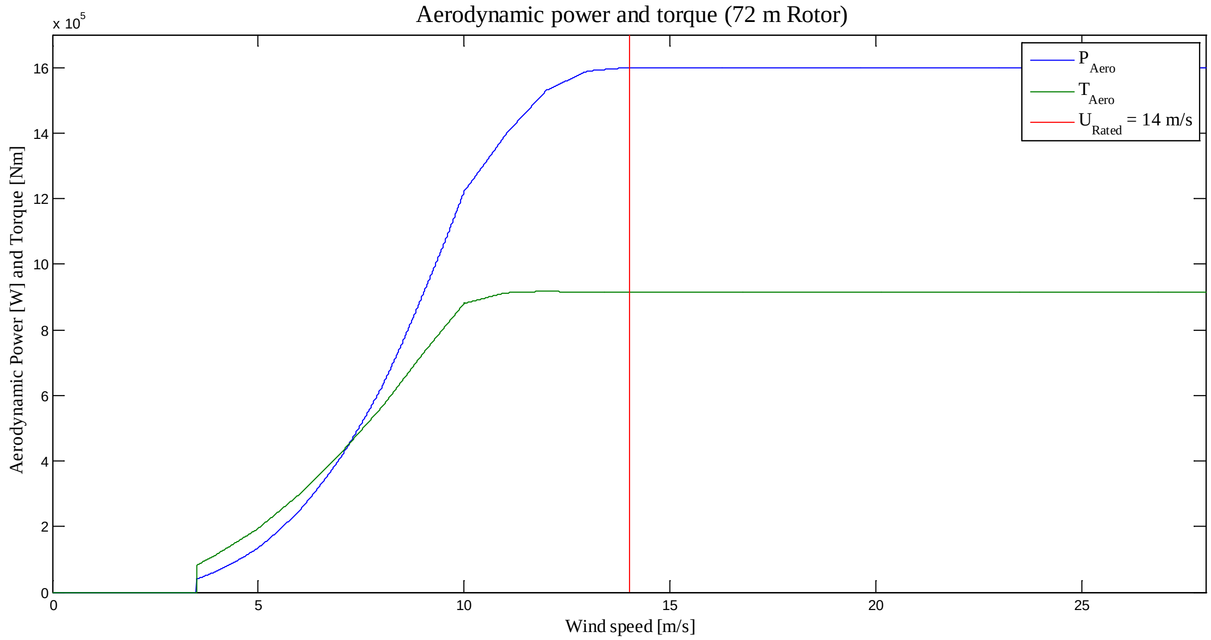

Figure 4.9 Aerodynamic power and torque for rotor model.

To fit the requirements set by the drivetrain, the rotor diameter for Enercon E82 was scaled down from 82 m to 72 m (assuming that aerodynamic parameters were not affected although tip speed ratio for the new computer model had a low value). By the end, the rated performance of the rotor was similar to the rated capacity of the drivetrain (1.6 MW). Since this document focus in quantifying advantages of hydraulic drivetrains in the steady state; this model was considered as accurate enough.

4.3. Steady state simulation

The last section presented a computer model intended to represent the 1.6 MW Artemis drivetrain. Now, this section present some estimated numeric values and the results of simulations using those values for the computer model introduced before.

One of the largest weaknesses of computer models is that results are as good as the quality of input information. The models presented in this document are not exception. To have an accurate representation of the system, models need factual information about some important geometric aspects (piston diameter, lobe height, camshaft diameter, etc.). If this information is available, the presented models will represent the physics behind the system. This was not the case for the 1.6MW Artemis drivetrain since no detailed information was available.

For the specific case of using this model to represent the Artemis drivetrain system, some important issues must be considered:

A. Artemis machines are a *new* technology subjected to intellectual property. This currently makes very hard to find specific information.
B. Limited specific information increases the model proneness to present non accurate results. In a few words, results are as good as the input parameters.

To overcome these important challenges, a blend of available information, careful visual inspection of pictures' [*25*] and assumptions were made. All together, allowed to estimate some numeric values that are believed to be close enough to those in the real system.

In this section, the numerical estimation of such required parameters will be presented side to side with the results of a steady state simulation. The main goal is to *verify* that model's simulation results are more or less in the range of values that one would expect in a hydrostatic transmission under similar conditions. Also, results will be compared with the scarce information published by manufacturers. Especial attention will be paid to the hydrostatic transmission.

Bear in mind that none of the estimated parameters in this section was verified with the manufacturer. However, numeric values were considered as accurate enough for the purposes of this document (quantify advantages of hydraulic drivetrains over non hydraulic drivetrains). Also, beware that this computer model is extendable to any kind of fixed displacement radial piston hydraulic machine, so Artemis drivetrain can be approached as one particular case of study on the application of such model to a particular geometry.

4.3.1. 1.6 MW 68-cylinder Artemis Digital Displacement pump

In this section, the numeric values used in the pump computer model are presented. Such values were used to estimate how power and efficiency changes depending on the load condition. For this purpose, three main load conditions (100%, 66% and 20% rated power) are used to observe efficiency and power estimation results. Such results were considered adequate after comparing with literature references. Finally an efficiency plot for the Artemis 1.6 MW pump was built.

Artemis Digital Displacement Pump	
Rated Power [MW] ($W_{Rat,P}$)	1.600
Rated angular speed [RPM][27] ($\theta_{Rat,P}$)	~16.7
Total number of cylinders (N_P)	68
Cylinders per bank	34
Number of banks	2
Type of mechanism	Ring cam
Number of lobes (Lo_P)	24
Machine External Radius [m] ($R_{P,ext}$)	~1.500
Geometrical ratio 1 (G_1)	~0.800
Geometrical ratio 2 (G_2)	~0.760
Geometrical ratio 3 (G_3)	~0.580
Geometrical ratio 4 (G_4)	~0.020
Geometrical ratio 5 (G_5)	~0.033
Geometrical ratio 6 (G_6)	~0.133
Geometrical ratio 7 (G_7)	~0.033

Table 4.1 Geometric information for the pump.

To achieve such coherent results, numeric values were estimated based on geometry and appearance (visual inspection of figures presented in [*25*]). Numeric values product of this assessment are presented in Table 4.1. Such parameters make reference to very general parameters (like number of cylinders per bank and number of banks, etc) and to believed geometric ratios (like external diameter and geometric ratios). Meaning of geometric ratio and their estimation are presented in Appendix F on Table 7.6.

Artemis Digital Displacement Pump	
Cylinder diameter ($D_{C,P}$) [m]	~0.075
Radial displacement (Δr_P) [m]	0.030
Rated cubic displacement ($\Delta V_{C1,P}$) [cc]	~132.50
Height of piston ($l_{p,P}$) [m]	0.100
Roller diameter ($2R_{rlr,P}$) [m]	0.050
Inner diameter of ring cam[m]	0.870
Outer diameter of ring cam[m]	0.900
Suction Pressure ($P_{S,P}$)	~1 bar
Discharge Pressure ($P_{D,P}$)	~300 bar
Volumetric Efficiency (η_{Vol})	~96%
Mechanical Efficiency (η_m)[28]	~99%
Hydraulic-Mechanic Efficiency(η_{hm})	~95%

Table 4.2 Estimated numeric values for pump

Based on values presented in Table 4.1, some other values were deduced. Such estimated parameters are presented in Table 4.2. The reasoning followed to asses such values is available on Appendix F.

The computer model was assembled using these numeric values and simulations were executed. The results of such simulation are presented in Figure 4.10 for $U > U_{Rat}(100\,\%\, W_{Rat} = 1.60\ MW)$; Figure 4.11 for $U{\sim}10\ m/s$ ($66\,\%\, W_{Rat}$) and Figure 4.12 for $U{\sim}6\ m/s$ ($20\%\, W_R$).

Note that in Figure 4.10, the average pump efficiency (η_P) is equal to the rated value (η_{hm}). As more cylinders are being shut down, efficiency will drops proportionally (Figure 4.11 and Figure 4.12). Still, efficiency levels per stage are better than those for conventional systems [*5*]. Also, beware that there is a power ripple (better appreciated in Figure 4.10) at the output hydraulic power. Such ripple represent less than 1% of rated power and is due to the combined action of all active cylinders pushing fluid (at a given operating pressure) out of the pressure chamber.

[27] Deducted from data on Enercon E82 rotor (later adapted to 72 m diameter to deliver $P_{Aero}{\sim}1.60$ MW).
[28] Assumed value based on literature in Henshaw[*16*].

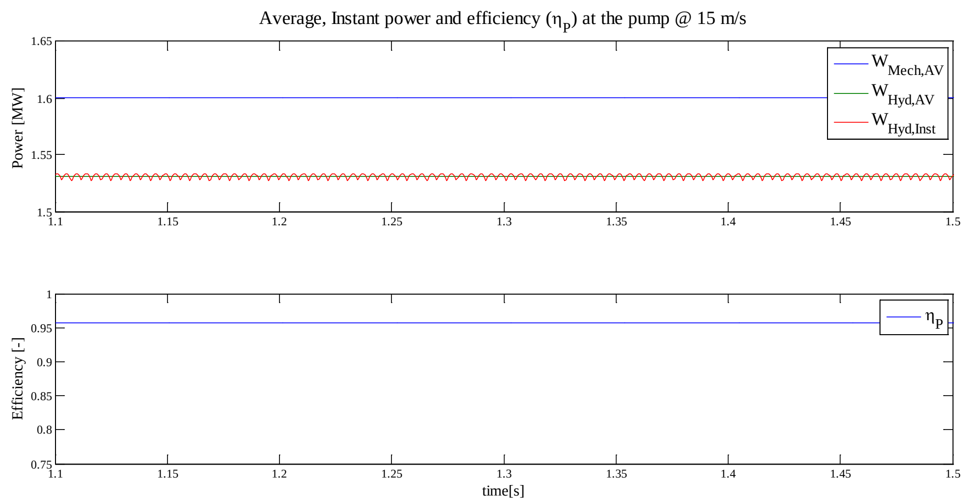

Figure 4.10 Efficiency, average and instantaneous power for pump at U=15m/s

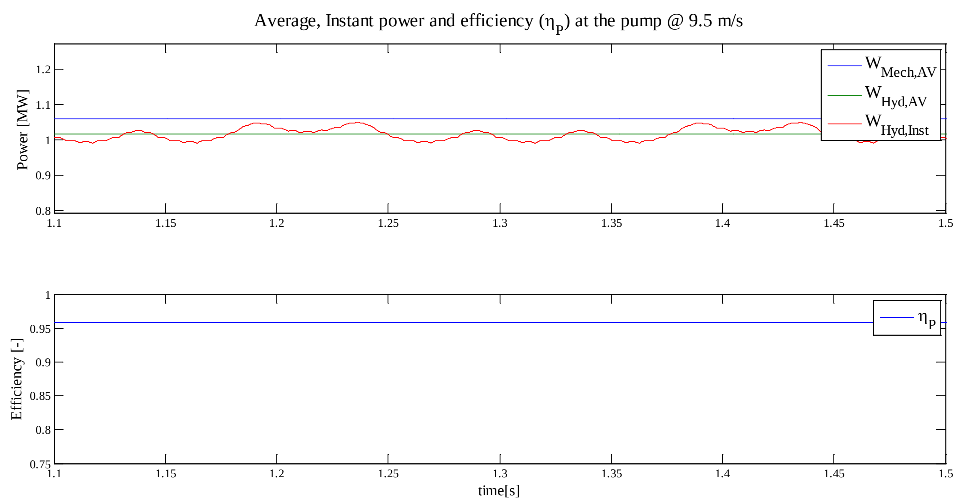

Figure 4.11 Efficiency, average and instantaneous power for pump at U=9.5 m/s

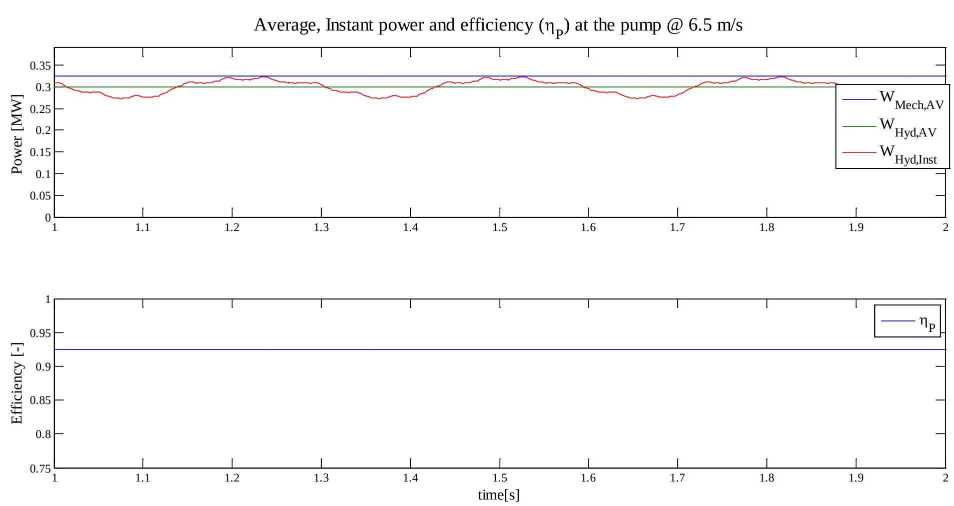

Figure 4.12 Efficiency, average and instantaneous power for pump at U=6.5 m/s

On the other hand, Figure 4.11 and Figure 4.12 presents and oscillating behavior (low frequency) in the instantaneous power. This unsteady lecture is due to some model deficiencies (mostly related with firing sequence or with non modeled effects as convergence of fluid in the output manifold, pressure drop due to friction losses, etc.). However, for the purposes of this document, the obtained results for average values of hydraulic power and pump efficiency were considered accurate enough.

Based on the same approach, a pump efficiency plot versus wind speed was built. This is presented on next:

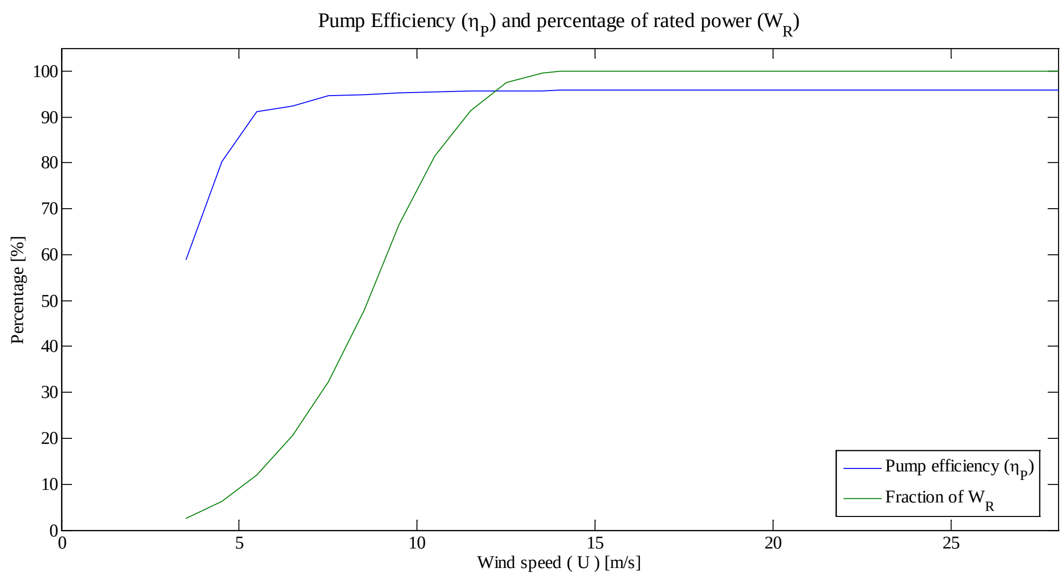

Figure 4.13 Pump efficiency and percentage of rated power versus wind speed

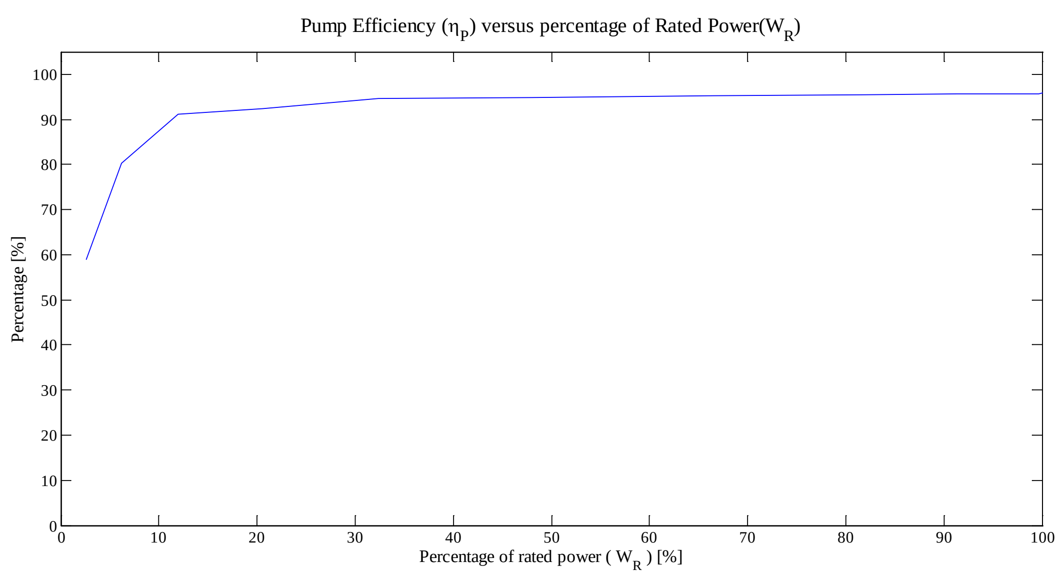

Figure 4.14 Pump Efficiency versus percentage of rated power

Figure 4.13 and Figure 4.14 shows very similar results to those presented in Rampen [5] [*26*]. Based on these results, it was possible to illustrate a power flow that facilitates the understanding of the efficiency concept in a digital radial piston pump. This power flow is presented in Figure 4.15. The main difference of this power flow with the one presented in section 3.2.8 is the fact that digital pumps introduces idling losses. Although the present flow diagram seems more complex, the fact is that while in conventional pumps all cylinders (or its flow) are subjected to all conventional losses (rotational, thermodynamic, volumetric and drag), in digital pumps only active cylinders are subjected to all conventional losses while the non active ones are only subjected to idling losses. By the end of the day, efficiencies achieved by digital machines at partial load are much larger than those in conventional pumps.

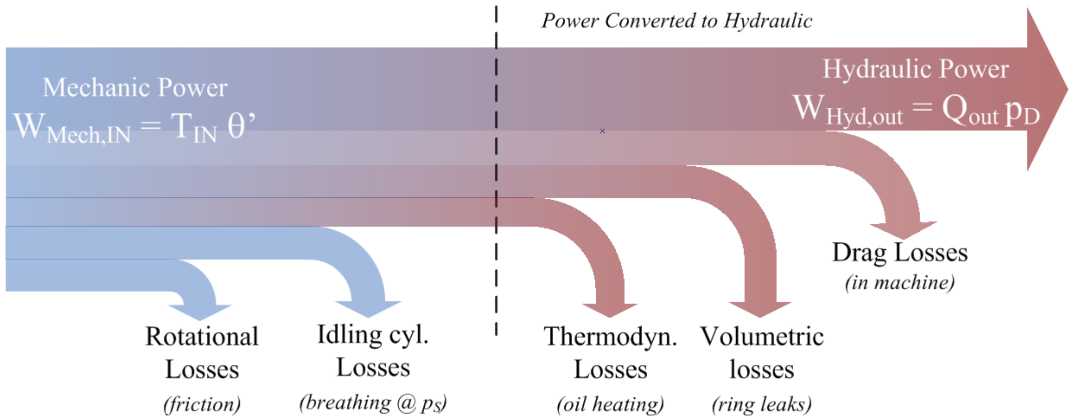

Figure 4.15 Power flow for digital radial piston pump

Beware that in the computer model presented in here, only rotational, idling and volumetric losses are considered. The other two kinds of losses are left for future work. In the next section, very similar considerations than the ones presented in here were done for the Artemis motor computer model.

4.3.2. 800 kW 24 cylinder Artemis Digital Displacement motor

In this section, numeric values used for the digital hydraulic motor are presented. Such values were organized in very similar fashion to those already presented for the pump. In here, three similar load conditions (100%, ~61% and ~22% or motor rated power) will be used to exemplify the case of the motor. Also, a motor efficiency plot as a function of wind speed was build. Once again after comparing the model results with available literature references, the results were considered accurate enough.

Once again, general information about geometry is presented but for the motor this time (Table 4.3). Beware that although geometric values were estimated in exactly the same way that those on Table 4.1; values are not the same since motor and pump geometry are different (discussed in 4.2.2). Later on, Table 4.4 summarizes the important numerical values determined for the motor. The estimation of such values was also similar to that presented in Appendix F.

Then, from Figure 4.17 to Figure 4.19 efficiency, instant and average power for the hydraulic digital motor for 100%, 61% and 22% of rated power are presented. Then, in Figure 4.20 the efficiency is plotted as a function of fraction of rated power. In there, the motor efficiency shows a very similar performance than the pump presented in the past section. Once again, similar results to those presented in Rampen [*5*] [*26*] are achieved. Later, in section 5.2.3, estimated computer model efficiency will be compared with the efficiency illustrated in the literature of Rampen [*5*].

Artemis Digital Displacement Motor	
Rated Power [MW] ($W_{Rat,P}$)	800
Rated angular speed [RPM][29] ($\theta_{Rat,P}$)	~1500
Total number of cylinders (N_P)	24
Cylinders per bank	6
Number of banks	4
Type of mechanism	Camshaft
Number of motors per drivetrain	2
Machine External Radius [m] ($R_{P,ext}$)	~0.500
Geometrical ratio 1 (G_1)	~0.480
Geometrical ratio 2 (G_2)	~0.420
Geometrical ratio 3 (G_3)	~0.170
Geometrical ratio 4 (G_4)	~0.030
Geometrical ratio 5 (G_5)	~0.120
Geometrical ratio 6 (G_6)	~0.120
Geometrical ratio 7 (G_7)	~0.040

Table 4.3 Geometric information for the motor.

Artemis Digital Displacement Motor	
Cylinder diameter ($D_{C,M}$) [m]	~0.060
Radial displacement (Δr_M) [m](delta r)	0.015
Rated cubic displacement ($\Delta V_{C1,M}$) [cc]	~45
Height of piston ($l_{p,M}$) [m]	0.030
Roller diameter($2R_{rlr,M}$) [m]	0.020
Inner diameter of machine block[m]	0.145
Outer diameter of camshaft	0.085
P_S ($P_{S,M}$)	~300 bar
P_D ($P_{D,M}$)	~1 bar
Volumetric Efficiency (η_{Vol})	~96%
Mechanical Efficiency (η_m)	~99%
Hydraulic-Mechanic Efficiency(η_{hm})	~95%

Table 4.4 Estimated numerical values for the motor.

Then, the flow diagram for the digital hydraulic motor is presented in Figure 4.16. Once again, only active cylinders are subjected to all conventional losses while non active cylinders are exclusively subjected to Idling cylinder losses. Bear in mind that the current model does not account for drag or thermodynamic losses. Once again, results presented on next are very similar to those used by the manufacturer [5] [26] .

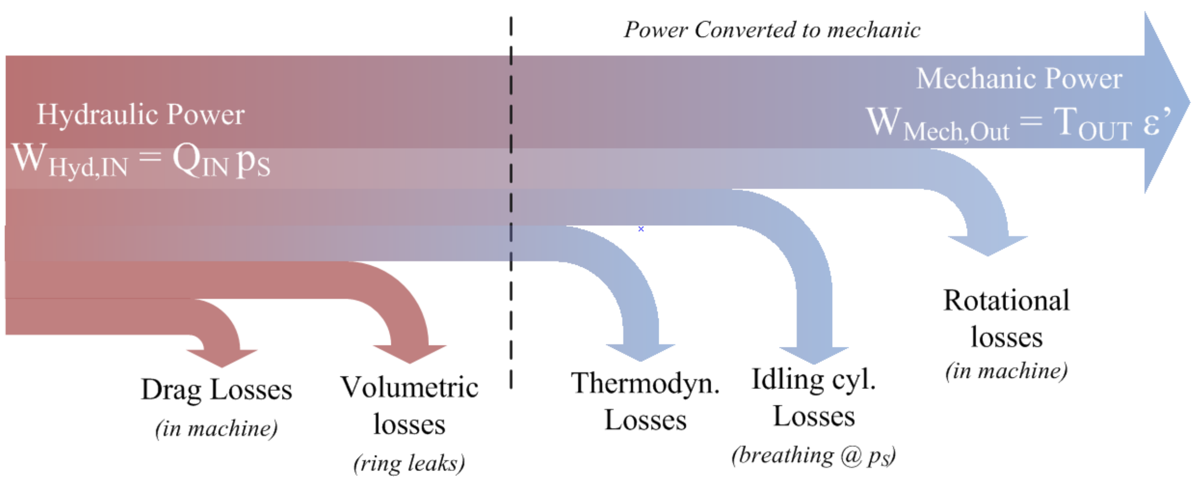

Figure 4.16 Flow diagram for digital motor.

In the next section, the most important limitations for the computer model are discussed.

[29] Deducted from data on Enercon E82 rotor (later adapted to 72 m diameter to deliver P_{Aero}~1.60 MW).

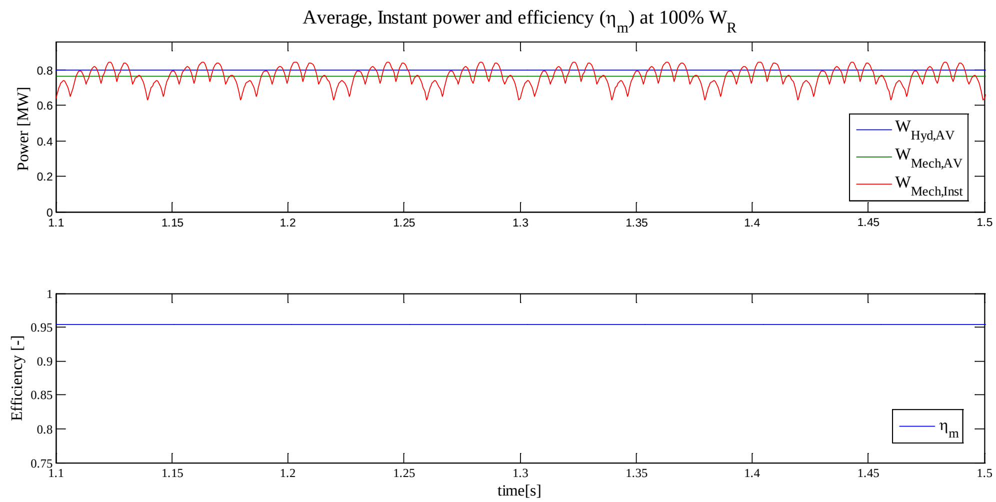

Figure 4.17 Power and motor efficiency for 100% of rated power.

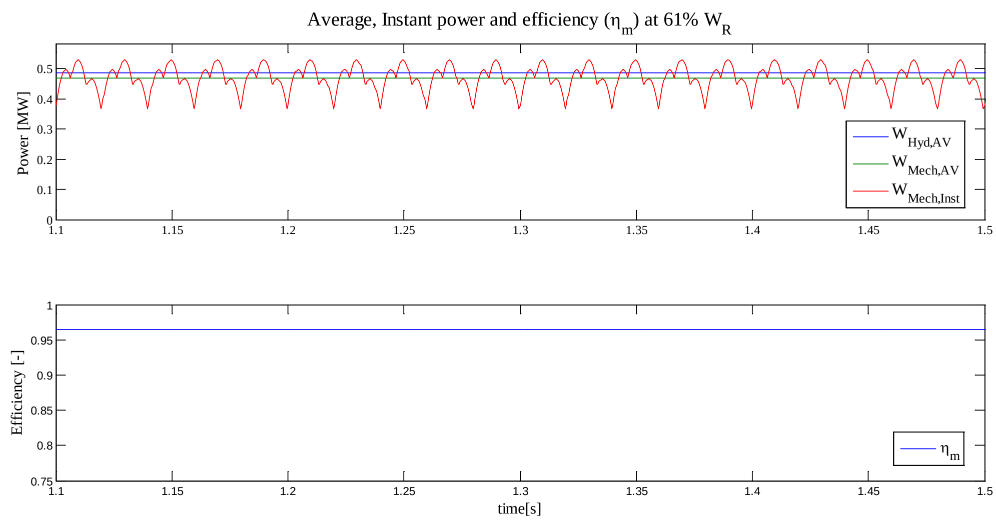

Figure 4.18 Power and motor efficiency for 61% of rated power.

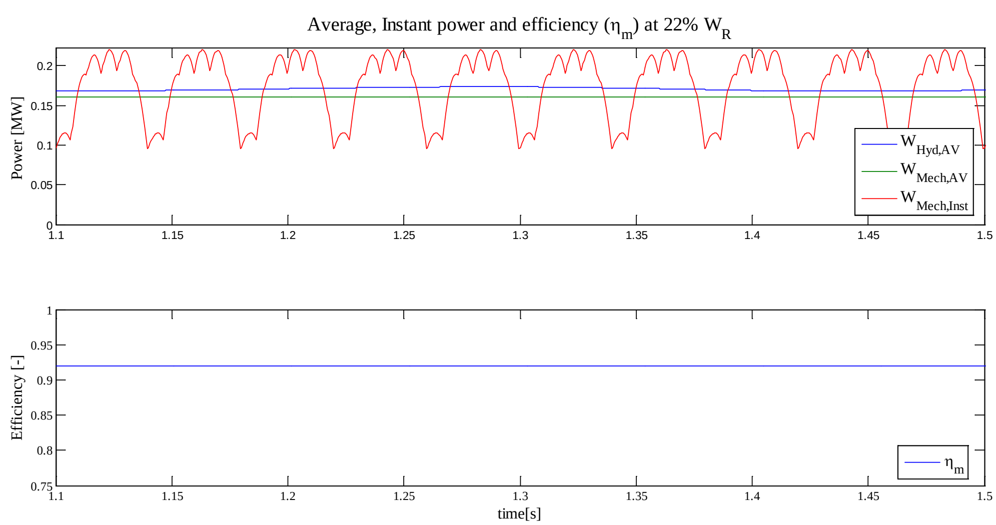

Figure 4.19 Power and motor efficiency for 21% of rated power.

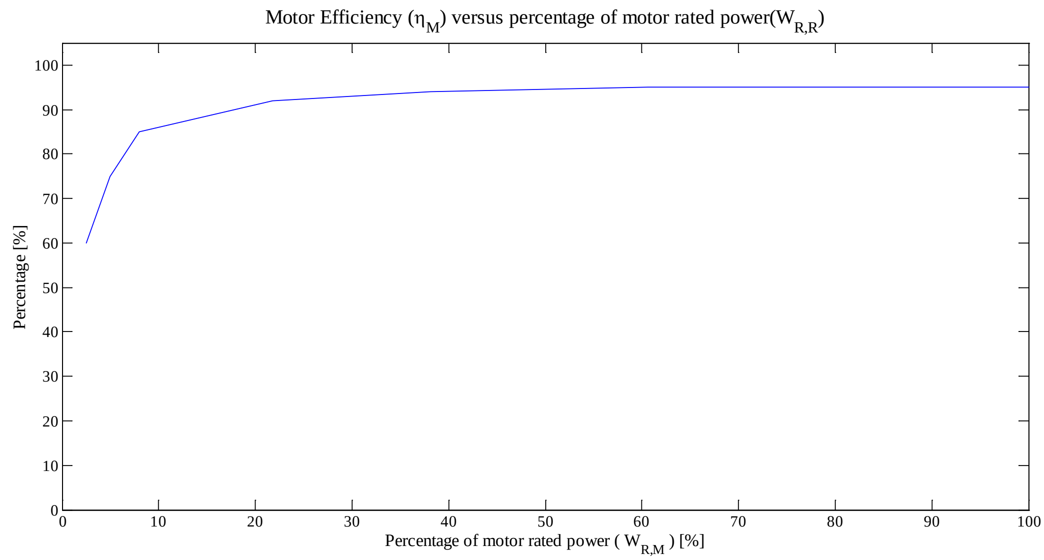

Figure 4.20 Motor Efficiency versus percentage of rated power

4.4. Model Limitations

In this section, some remarks about computer model limitations are done. Among those limitations can be found strictly use for steady state conditions, software sensibility and adaptability to represent analogous systems. On next, such limitations will be further commented.

Before discussing the specific limitations let's start saying that the results for the specific case of study (Artemis drivetrain) are product of a computer model. This means that the output is as good as the input numeric values. Although there is a strong confidence about the magnitude of numeric values presented in section 4.3, such ciphers were not confirmed by the drivetrain manufacturer. Therefore the results presented in here, are just a well founded estimation of about how does a modern hydraulic drivetrain (based on digital radial piston machines) should perform in a wind turbine. For the purposes of this document, this is considered enough.

On next, the three main limitations are briefly commented.

4.4.1. Steady state model and dynamics

The computer model presented in this document is intended to represent the Artemis drivetrain system in a steady state condition. The steady state point of operation can be selected from all possible load conditions along the wind speed range for the modeled turbine (3.5-28 m/s representing up to ~1.4MW electric). Beware that this is not a dynamic model. Although some precautions had been taken to make this model ready for implementation of dynamics, still some work is required. This pending works comes in the area of component interconnection. To explain further this, let's take a look specifically to Eq. 3.19, Eq. 3.33, Eq. 3.36 and Eq. 3.37. In the first mentioned equation (Eq. 3.19) the entire dynamics of the one single cylinder are included. Also, when this equation is brought to represent the Artemis pump system (Eq. 3.33) it still contains the angular acceleration of the rotor shaft but some other internal parameters had been neglected (piston mass, spring force, etc.). Later on, all angular acceleration will be neglected assuming a constant speed in the motor (Eq. 3.37). In both cases, the way in which the steady state condition are being handled for the hydraulic machine is by making the acceleration term ($\ddot{\theta}$ or $\ddot{\varepsilon}$) equal to zero. Then, the model is ready to implement a variable angular acceleration for the hydraulic machines without much trouble. However, the interconnection between components (i.e. rotor shaft with hydraulic pump, pump with motors, or motors with generators) does not account for dynamics since system inertia (moment of inertia for rotating systems and hydraulic capacitance for hydraulic lines) is not being considered yet. Consequently, in the current state, this model is not ready to represent transient conditions, so its use should be limited only for the steady state.

Although its limitations, the implemented model control system already allows following any load condition. But as you might find in Figure 4.21, dynamics are not implemented (output immediately follows the load) but the control system fitted effectively any load condition; therefore this steady state model is ready for implementation of dynamics.

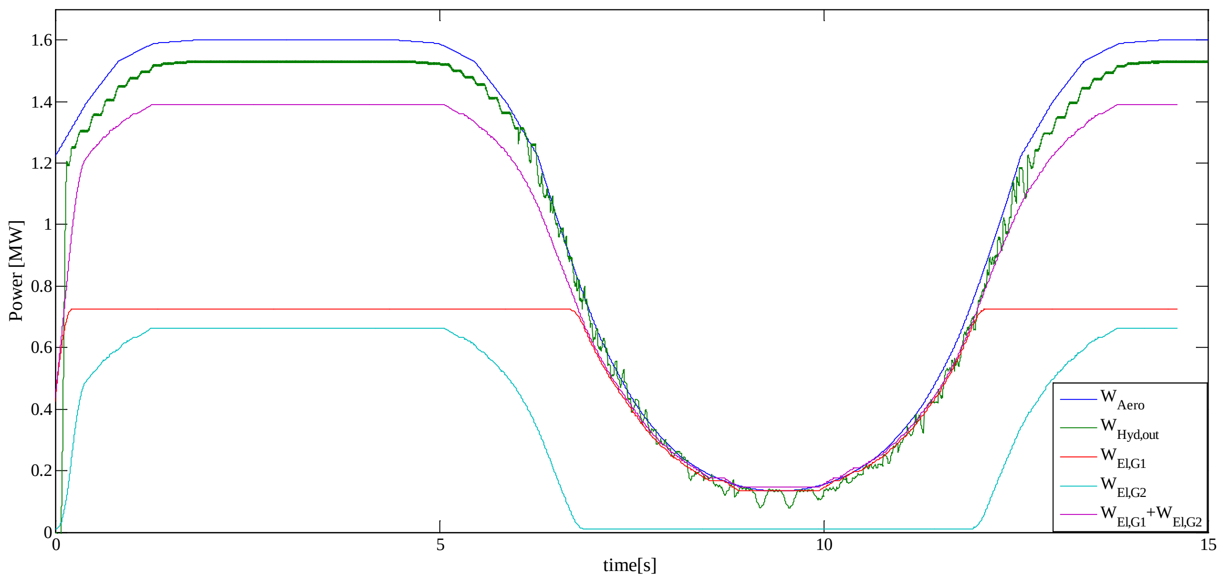

Figure 4.21 Control system fitting any load condition (immediate mechanical power at motors were omitted for visualization purposes).

4.4.2. Software quality

Another important limitation is the large software dependence. In the present document, software makes reference to the cylinder activation sequence presented in section 4.2 and Appendix E. Because this system has the capability to operate individually any cylinder, a set of control commands is required to define which cylinder will operate under which conditions. This makes this model highly sensitive to software quality. For instance, a bad selection of activation sequence could affect the torque or volumetric flow ripple (for motor or pump respectively). Actually, this large software dependence reassembles the real Artemis Digital Displacement machines, which also require careful tuning to operate efficiently. To explain further this idea, two scenarios for the hydraulic motor output torque are presented in Figure 4.22 under the exact same load conditions. However, in both scenarios two different activation sequences were employed. In the top one, the activating sequence presented in Table 7.4 on Appendix E was used. As is visible, large torque pulsations are the direct consequence of poor software quality. Then, in the bottom of same figure better results can be appreciated. Such results are product of a more careful software tuning presented in Table 7.5. Such sequence was designed to minimize torque ripple with a simple algorithm. Bear in mind that the hydraulic motor has 4 banks of 6 cylinders each; therefore ripple balance is not a big issue. For the case of the 68 cylinder pump, software tuning becomes more complicated. As mentioned before, software tuning is not the main purpose of this document, but the importance of such software quality (not achieved in here) needs to be stressed.

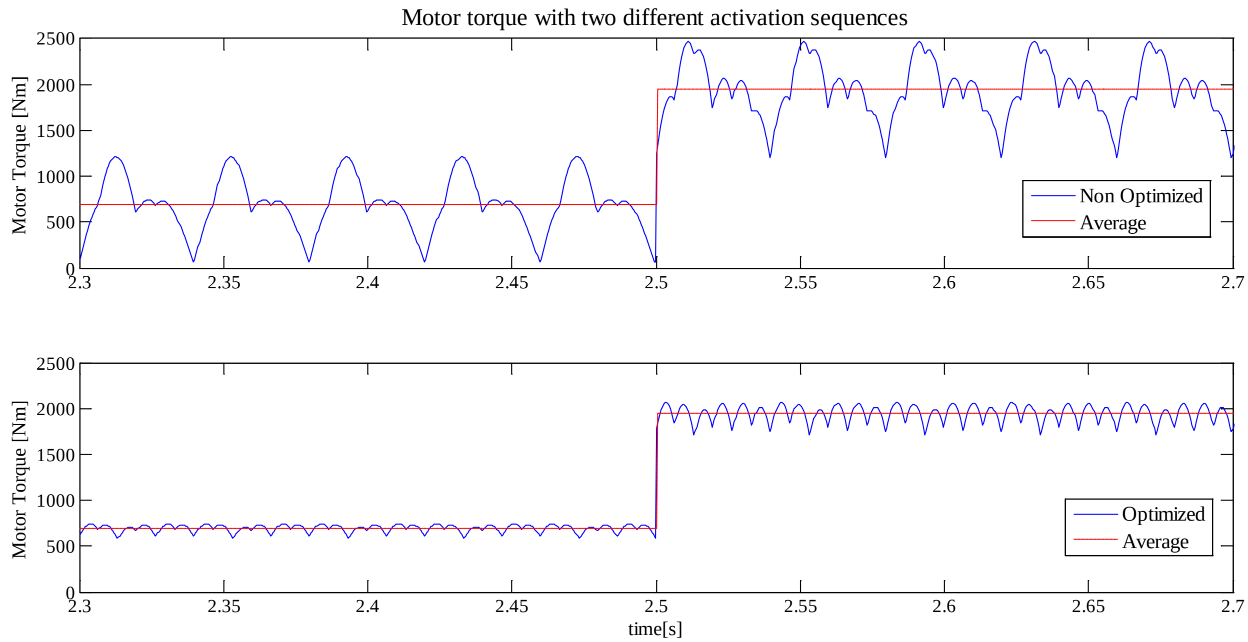

Figure 4.22 Motor torque with Non Optimized(top) and Optimized(bottom) activation sequences

4.4.3. Model adaptability

Another important model limitation is the use of this computer model to represent other analogous systems. Although this is feasible, the future user should better focus in building the new system based on the monocylinder machine model (discussed in section 4.2.1) rather than Artemis study case, which already employees some assumptions (sections 3.4.2 and 3.4.4) that might not be valid for the new system. However, if this study case is taken as starting point, then the future user should always question the veracity and applicability of assumptions done for the Artemis machines in the new system.

Bear in mind that the monocylinder machine was introduced as a general case to increase the contribution of this graduation project so other hydraulic systems can be presented. In general, a solid foundation for the one single cylinder (in chapter 3) should guarantee the recyclability of the monocylinder machine model. But the integration of such model into multicylinder machines is still pending work. The two different machines discussed for the Artemis drivetrain are intended to exemplify the use of the same one single cylinder model for two different geometries. In this way, the use of this single cylinder model can be extended to *any* other piston based hydraulic machine (radial and axial configuration); but similar assumptions to those in sections 3.4.2 and 3.4.4 should be done. For instance, if a conventional(no digital control) ring cam hydraulic pump is intended to be modeled, then a mixture between the Artemis pump modeled in here plus some specific non variable activation sequence must be used. Once again becomes evident that the better knowledge about the real system operation and geometry, the better the results that can be achieved.

In the next sections, partial conclusions for this chapter are described.

4.5. Conclusion

This chapter's objective was to present and discuss a computer model that assembles the use of 1.6MW Artemis drivetrain in a wind turbine. To do so, some idea about the model construction in Matlab Simulink®, geometric parameter estimation and some simulation's result were presented. Then, based on model behavior and obtained results, some model limitations were stressed. Now, this section will present some partial conclusions about this section.

The presented computer model is intended to represent the 1.6 MW Artemis drivetrain in the steady state. This model is not ready to represent transient conditions; to do so, further work is required. Still, the results achieved with this simple approach were considered accurate enough to respond the main research question presented in section 1.2.

Then, let's say that it is possible to estimate the performance of a multicylinder hydraulic machine by means of several one single cylinder models in a specific geometric configuration. This configuration must reflect the arrangement in the real system. This approach is especially useful when modeling digital machines, where discrete cylinder operation should be represented. Nevertheless, the use of this scheme will require the design of an activation sequence to control which cylinder is enabled when. Still, any model of digital machine based in single cylinder model can be transformed into a conventional hydraulic machine under a particular activation sequence (all active for any load condition).

The fact of some kind of control algorithm is required to set an activation sequence makes the one single cylinder approach very sensitive to software quality. This is also valid for real digital hydraulic machines. Although algorithms in real systems might be much more complicated than the ones presented in this document, the implementation of such control sequences are useful to alive awareness about the importance (and degree of complexity) of software in real systems.

Still with these limitations, very similar results to those published by the manufacturer [*25*] , [*27*] were obtained in the computer model simulations. Since these results were obtained based on a set of geometric parameters, it was considered that those values are in the range (or close enough) to the ones in the real system.

Finally, let's say that computer models are valuable tools that can offer an *idea* about the performance of a system. The quality of such solution is directly related with detailed knowledge about principle of operation and geometry of the real system. Then, these two concepts become an important factor for accurate results. Although detailed knowledge about geometry in the real system was not accessible, the results presented in this section are considered accurate enough for the purposes of this document.

5. Indicators

5.1. Introduction

In the past chapter a computer model and simulation results for the specific case of study were presented. The results of steady state simulations for Artemis drivetrain were considered as accurate enough after comparing model efficiency with values published by the manufacturer. Now, in this section some indicators will be presented. The main target of such indicators is to quantify the advantages of hydraulic drivetrains over non hydraulic ones. Eventually, they will allow serve as reference to compare the special case of study with non hydraulic drivetrains.

In this section, *quantitative* and *qualitative* indicators will be presented trying to stress some particular advantages for the particular case of study. The quantitative indicators are presented in section 5.2 and they are five: system size, weight, efficiency, cost estimation and energy yield. These indicators were selected because they are often used to compare among non hydraulic drivetrains. Also, because of their nature, these indicators will be used to draw conclusions by the end of this chapter.

On the other hand, qualitative indicators are important remarks rather than indicators. Such observation has none or very fragile quantitative background. However, they are intended to discuss some possible (dis)advantages that hydraulic drivetrains might have over non hydraulic ones. They will be presented on section 5.3. Unlike quantitative indicators, qualitative indicators cannot be used to draw conclusions.

Then, based on quantitative indicators, some comments will be drawn in section 5.4 to final make some conclusion by the end of this chapter.

5.2. Quantitative indicators' construction

In today's wind turbine industry there is anything like conventional. A highly competitive market had led to a large number of drivetrain systems with a wide variety of specialized components. Most of them provide a particular advantage over their competitors varying from high efficiency to well proven technologies. Such subjective qualitative perception plus the wide variety of configurations had made necessary the use of some particular indicators to compare between different technologies. There are several indicators that can be used in evaluating advantages of a particular drivetrain; but, by the end of the day all of them try assessing the net energy cost.

In this section, five indicators were selected to quantify the advantages of the particular case of study. The selected indicators are: dimensions and volume, weight, efficiency, cost estimation and energy yield. The reason of selecting these particular indicators is that they are often used when comparing wind turbines of different technology.

On next, the description of the indicators will be presented. Bear in mind that all indicators built in this document are estimations based on other machinery (except for the synchronous generator) since factual information is still very scarce.

5.2.1. System size

This section will estimate physical dimensions for the particular case of study. To this purpose, a simplified 3D model was built. Due to intellectual property concerns, not enough factual information was available. Still a simple representation was achieved by means of three different sources: manufacturer information in old papers, images' visual inspection and numeric values determined in section 4.3. Although the dimensions presented in here might not be the factual value, they should be close enough to real ranges. Dimension estimation will allow forming more reliable indicators in upcoming sections. Then, the 3D model is presented in Figure 5.1. In there, the digital pump (blue), motors (orange) and synchronous generators (dark red) are presented. Also, a sketch of a 1.75 height person is included (in green) for better appreciation. Later on, estimated dimensions are presented in Figure 5.2.

Artemis Digital Displacement pump	
Estimated as	cylinder
External diameter[m]	1.50
Length [m]	0.50
Body Volume [m^3] ($V_{body,P}$)	~0.60
Artemis Digital Displacement Motor	
Estimated as	cylinder
External diameter[m]	0.50
Length [m]	0.60
Body Volume [m^3] ($V_{body,M}$)	~0.25
Synchronous Generator	
Estimated as (covers)	Prism
Width[m]	0.80
Height[m]	0.80
Length [m]	1.50
Body Volume [m^3] ($V_{body,G}$)	~1.00
Rotor Diameter[m]	~0.70

Table 5.1 Relevant dimensions and Volume of 2.6 MW Artemis drivetrain system

Now, volumes were estimated approximating the shape of components to standard solid figures (cubes, cylinders, etc). The most relevant information about geometry is summarized in Table 5.1.

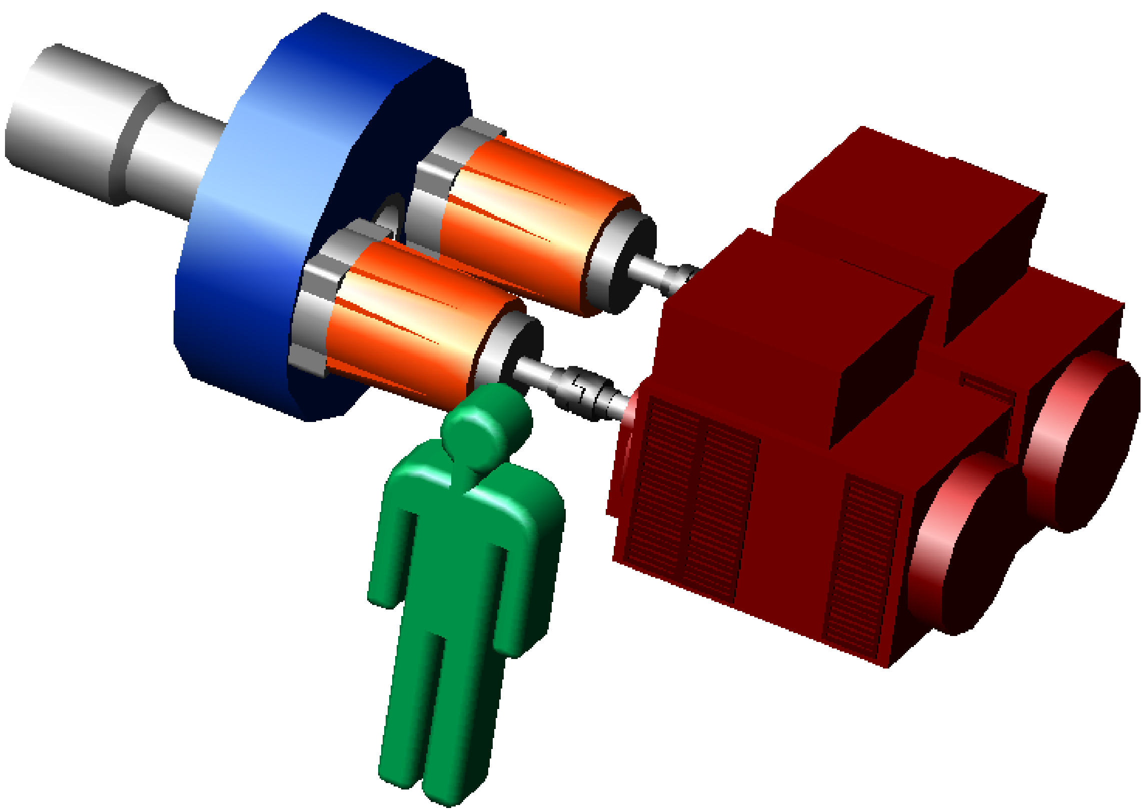

Figure 5.1 Simplified 3D model for 1.6 MW Artemis drivetrain (Blue - 68 cyl. pump, Orange - 24 cyl. Motor, Dark red - 800 KW Synch. generator)

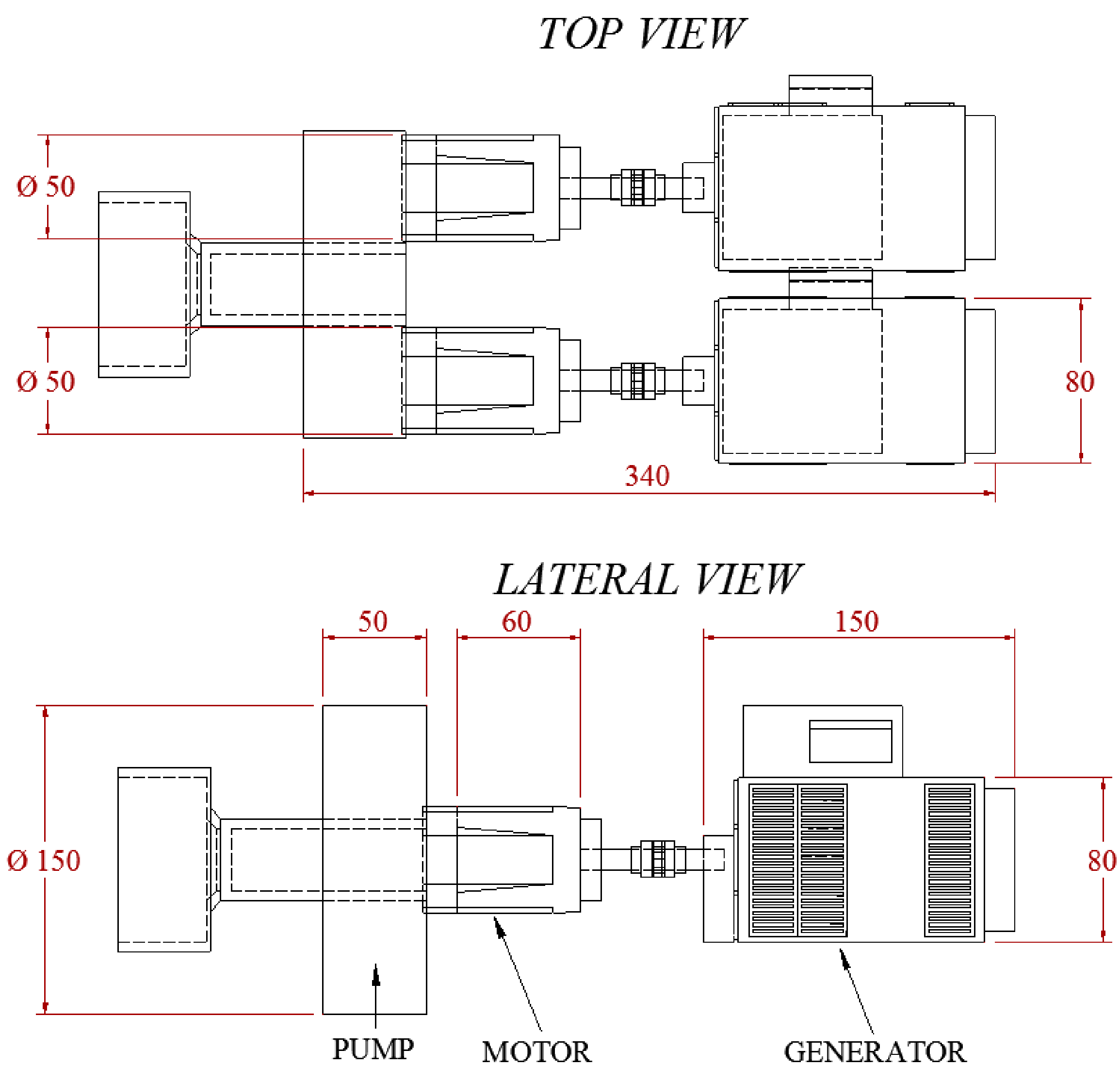

Figure 5.2 Estimated Dimensions for 1.6 MW Artemis drivetrain system

5.2.2. Weight estimation

This section is dedicated to estimate mass for the drivetrain components. Among the components, the synchronous generator counts with factual information provided by the manufacturer. However, there is no factual information for Artemis pump and motor. Then these values will be estimated in some different way.

For now, let's talk about the synchronous generator. A range for the mass of this component ($m_{G,1MVA}$) is already provided in the manufacturer specifications (synch. generator type 1DB [*22*]). Based on that, a first order interpolation can be applied to estimate the mass value for $m_{G,1MVA}$. This is presented in Eq. 5.1.

$$\frac{2{,}800\ kVA - 380\ kVA}{12\ ton - 1.8\ ton} = \frac{2{,}800\ kVA - 1{,}000\ kVA}{12\ ton - m_{G,1MVA}} \qquad \textbf{Eq. 5.1}$$

$$m_{G,1MVA} \sim 4.41\ ton$$

Now, for the hydrostatic transmission, as mentioned before, there is hardly any factual information about the net weight of the system. Therefore, the estimation of representative values was done as follows: First, using dimensions denoted in sections 4.3.1, 4.3.2 and 5.2.1 and were used to estimate a weight assuming carbon steel composition. Then, this approach was compared with two more methods using constant ratios (obtained from small machinery of similar technology). In all cases, similar values were found. Based on this, it was possible to narrow the range of drivetrain components mass ($m_{X,est}$). All approaches are further explained on next.

A steel alloy composition for the first approach was selected. It might be the case that not only steel is used in the real system. Nevertheless, this material was selected because its relatively high density (ρ_{Steel}~$7850\ kg/m^3$). Although there are some other *commonly* used metallic materials (i.e. stainless steel, cast iron, aluminum T6, etc.) for manufacture piston based machines, most of them show a smaller (or very similar for stainless steel $\rho_{StlssSteel}$~$8010\ kg/m^3$) weight to volume ratio than carbon steel. Therefore, steel can safely represent the upper limit for weight

Artemis Digital Displacement pump	
Solid Volume [m^3]	0.590
68 cyl of 133cc [m^3]	-0.009
Space between ring cam and block[m^3]	-0.075
Inner shaft [m^3]	-0.182
Net Volume[m^3] ($V_{NET,P}$)	0.325
Mass (steel) [ton]($m_{P,est,1}$)	~2.5
Artemis Digital Displacement Motor	
Solid Volume [m^3]	0.118
24 cyl of 50cc [m^3]	-0.001
Space between camshaft and block[m^3]	-0.007
Net Volume[m^3] ($V_{NET,M}$)	0.110
Mass (steel) [ton] ($m_{M,est,1}$)	~0.9

Table 5.2 Estimated weight based on carbon steel.

To do so, the known volumes of *empty* spaces (i.e. cylinder displacement, empty space between ring cam and cylinder block, and inner shaft mainly in section 3.4.1) were subtracted to the *entire machine* volume (section 5.2.1). These results reassemble one of the heaviest system versions and they are presented for pump and motor in Table 5.2.

For the second method and third method (weight estimation by constant ratios), similar radial piston fixed displacement machines were considered. All considered machines are currently commercially available; but, rated powers are relatively smaller than Artemis machines. Nevertheless, components' geometry and principle of operations is very similar (in geometry, camshaft configuration, designed for high speed 1200-1800 RPM). Analysis of technical information for all considered machines is presented in Appendix C. Based on such information, Figure 5.3 and Figure 5.4were built. In there, the so called *Power Density* (in units of kg/kW) and *Machine* Density (in units of kg/m^3) are presented. These ratios are estimated for each type of machine according with Eq. 5.2. The idea of introducing such parameters is to estimate a relation between rated power and mass.

$$Power\ Density = \frac{mass\ of machine}{rated\ power\ of\ machine}$$
$$Machine\ Density = \frac{mass\ of machine}{volume\ of\ machine} \qquad \textbf{Eq. 5.2}$$

For instance, in terms of power density, Figure 5.3 clearly shows a decreasing ratio as rated power increases. It also clearly shows a leap frog in technology with two of their basic machinery (Bosch Rexroth are slender and more modern machineries than Bosch Series C, this means that Rexroth machines are lighter than its predecessor Series C). Since Artemis machines are modern designs, with very similar configuration and geometry to those of Rexroth line; then this series (dashed blue line) is preferred over other technologies (Series 20,80, C or Model EO55) . Now, although there is clearly a decreasing tendency in Figure 5.3; a constant value is preferred since the rated power of samples (presented in plot) are just too far away from target values(1,600 and 800 kW). This constant value is the average of Rexroth series. Because of this constant *power density* and the decreasing tendency shown in plot, the result will be also an estimative of the heaviest mass in machines ($m_{P,est,2}$), which is considered accurate enough. The operations using constant power density for the pump are presented in Eq. 5.3.

$$\rho_{Pow} = \frac{average\ mass\ of\ Rexroth}{average\ rated\ power} \sim 1.3\,\frac{kg}{kW}$$
$$m_{P,est,2} = \rho_{Pow} W_{Rat,P} \sim 2.0\ ton$$
$$m_{M,est,2} = \rho_{Pow} W_{Rat,P} \sim 1.0\ ton$$

Eq. 5.3

Where:
ρ_{Pow} is the power density based on commercial values for similar technologies
$m_{P,est,2}$ is the estimated mass for the pump based in method 2 (power density)
$m_{M,est,2}$ is the estimated mass for the motor based in method 2 (power density)
$W_{Rat,P}$ is the rated power for the Artemis digital displacement pump in kW
$W_{Rat,M}$ is the rated power for the Artemis digital displacement motor in kW

As a third and last method, machine density was used. This method is very similar to power density. The machine density is the ratio of machine's mass over an estimated external volume of the machine (presented in section 5.2.1). Nevertheless, notice that Figure 5.4 now presents an almost constant trend. This trend is very similar to steel density (for small machines like series 20, 80 or model EO55) and some more different for larger machines (Rexroth and Series C). It is believed that the main reason for this is the integration of lighter materials than steel (i.e. aluminum) in the manufacture. This almost constant machine density (and net volumes in Table 5.2) will be used to estimate the components' mass ($m_{P,est,3}$). This is summarized in Eq. 5.4.

$$\rho_{Mach} = k_{LargeMach} \sim 5500\,\frac{kg}{m^3}$$
$$m_{P,est,3} = \rho_{Mach} V_{NET,P} \sim 1.7\ ton$$

Eq. 5.4

Where:
ρ_{Mach} is the power density based on commercial values for similar technologies
$k_{LargeMach}$ is the assumed value as constant for large hydraulic machines of similar tech (see Figure 5.4)
$m_{P,est,3}$ is the estimated mass for the pump based in method 3 (machine density)
$m_{M,est,3}$ is the estimated mass for the motor based in method 3 (machine density)
$V_{NET,P}$ is the net volume for the pump (see Table 5.2)
$V_{NET,M}$ is the net volume for the motor (see Table 5.2)

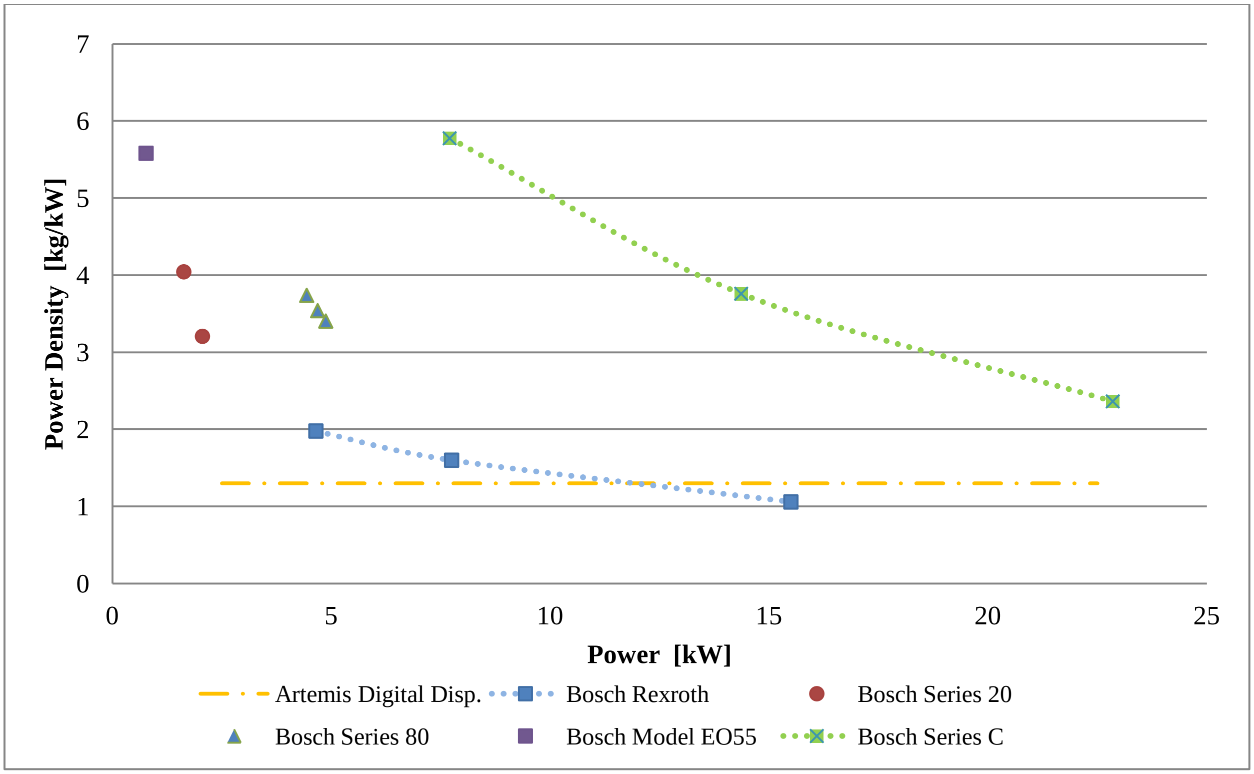

Figure 5.3 Power density versus rated power for high speed (1200-1800 RPM) commercial hydraulic machines.

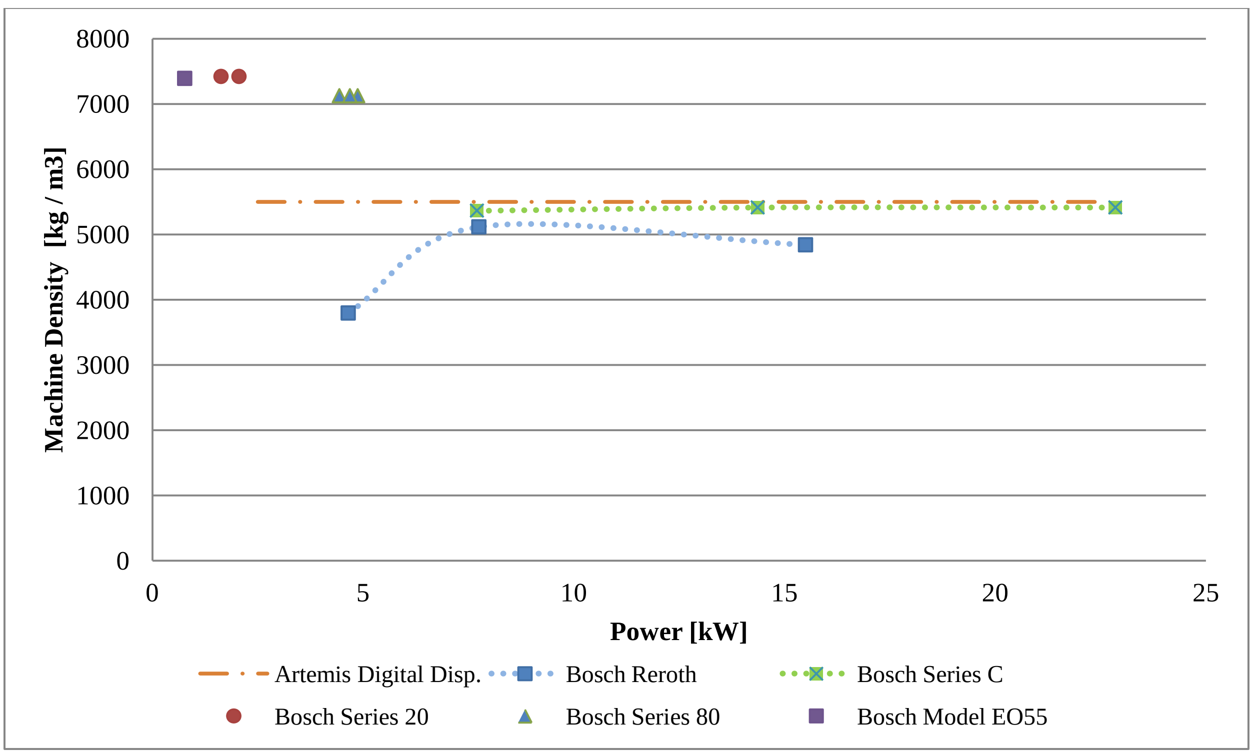

Figure 5.4 Machine density vs rated power in commercial high speed hydraulic machines

Finally, the average value of all three methods is presented in Table 5.3.

Artemis Digital Displacement pump	
Mass (steel) [ton]($\boldsymbol{m_{P,est,1}}$)	~2.5
Mass (Power density) [ton] ($\boldsymbol{m_{P,est,2}}$)	~2.0
Mass (Machine density) [ton] ($\boldsymbol{m_{P,est,3}}$)	~1.7
Average pump mass[ton] ($\boldsymbol{m_{P,Av}}$)	~2 ton
Effective density[ton] ($\boldsymbol{m_{P,Av}/V_{NET,P}}$)	~6150 kg/m^3
Artemis Digital Displacement Motor	
Mass (steel) [ton] ($\boldsymbol{m_{M,est,1}}$)	~0.9
Mass (Power density) [ton] ($\boldsymbol{m_{M,est,2}}$)	~1.0
Mass (Machine density) [ton] ($\boldsymbol{m_{M,est,3}}$)	~0.6
Average motor mass [ton] ($\boldsymbol{m_{M,Av}}$)	~0.8 ton
Effective density[ton] ($\boldsymbol{m_{M,Av}/V_{NET,P}}$)	~7000 kg/m^3
Synchronous generator	
Mass of generator	~4.4 ton

Table 5.3 Wight estimation for components

5.2.3. Efficiency

This section is intended to present efficiency of the overall drivetrain system. Then, figures in this section integrate the combined performance of hydraulic machines in section 4.3 with the synchronous generator and for the hydrostatic transmission by itself.

Figure 5.5 presents efficiency levels for the hydrostatic transmission alone (digital ring cam pump with high speed digital motor). In that figure, computer model results are presented side to side with values published by the manufacturer in [*25*] for their Digital Displacement system and a conventional radial piston pump. Such values are related with an average operating range (25% to 35% of rated power), where wind turbines operates most of the time [*5*], [*26*]. Inside that average operating area, there is a slight disagreement between the results provided by the computer model and values published by the manufacturer (~1% to 3% of net efficiency). Although this disagreement is considered as acceptable (due to very scarce information about detailed geometric tolerances), it is believed that smaller values in model simulation are mostly related with Artemis volumetric efficiency ($\eta_{Vol,ADD}$) that should be larger than the one used in here for both machines (η_{Vol}~96%). The results published by the manufacturer imply a $\eta_{Vol,ADD}$~97 %, which still sounds feasible with modern manufacturing techniques[30].

Still, results from computer model are considered as more conservative and without commercial interest. On the other hand, computer model results more or less reflect the idea presented by the manufacturer in [*26*] about that modern digital machines are much more efficient than conventional technologies that inside the Average Operating Area are already sacrificing ~30% of the power just in the hydrostatic transmission.

[30] Since 1980s volumetric efficiencies of 96% were achieved[*16*] without using computer aided design (CAD) nor computer aided manufacture (CAM). It makes sense to believe that the widely use of CAD and CAM processes make this optimization feasible today.

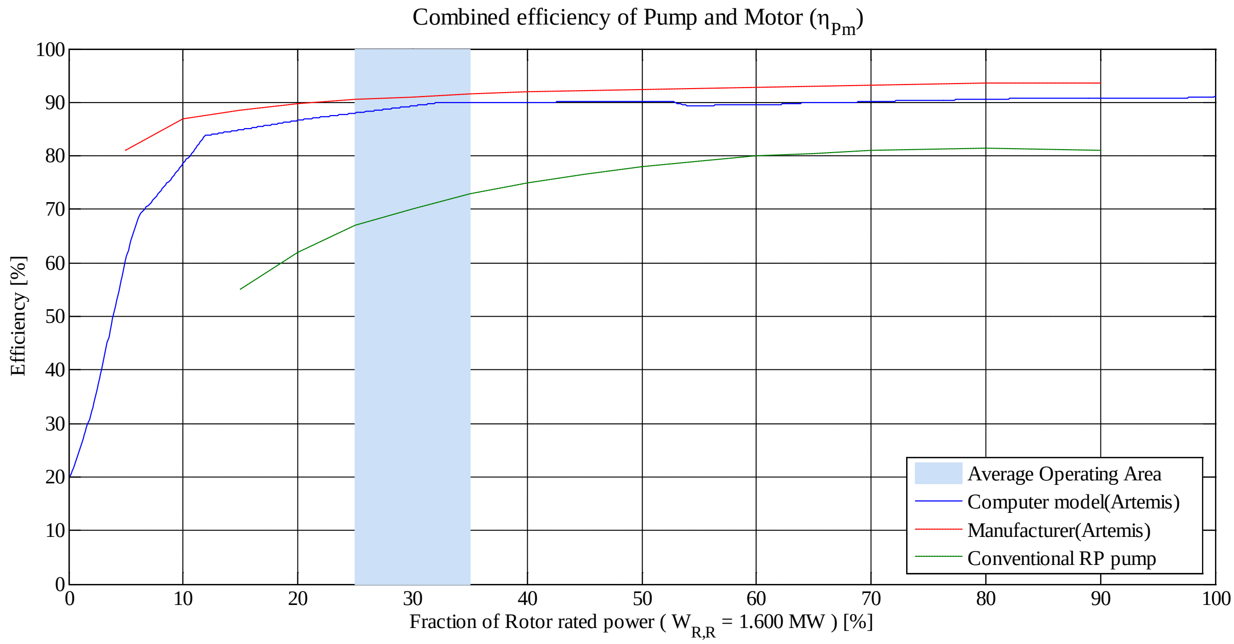

Figure 5.5 Efficiency for digital hydrostatic transmission.

Then, in same fashion, the efficiency for the entire drivetrain system (hydrostatic transmission plus synchronous generator) can be estimated with the computer model. This is presented in Figure 5.6. In there, an average drivetrain efficiency about ~88% for the Average operating Area is visible and about ~89% for the rated power. Notice that there is a small discontinuity in efficiency curve about 50% of rotor rated power ($W_{R,RT}$) in Figure 5.5 and Figure 5.6. This is the effect of start using the second motor-generator set (when available hydraulic power leaving the pump is higher than 800 kW, then, the second motor-generator set can start operating). This discontinuity is also visible in Figure 5.7, where efficiency is related with wind speed for the introduced turbine in section 3.5.1.

Figure 5.7 shows a small disagreement (~3%) between the computer model and values published by the manufacturer. This discordance is very similar to the one discussed for Figure 5.6; therefore this divergence is once again attributed to the volumetric efficiency used in this model. Once again, results from the computer model look more conservative. Still the real value should be determined empirically. This document does not count with empirical validation. Therefore this is reserved for future research.

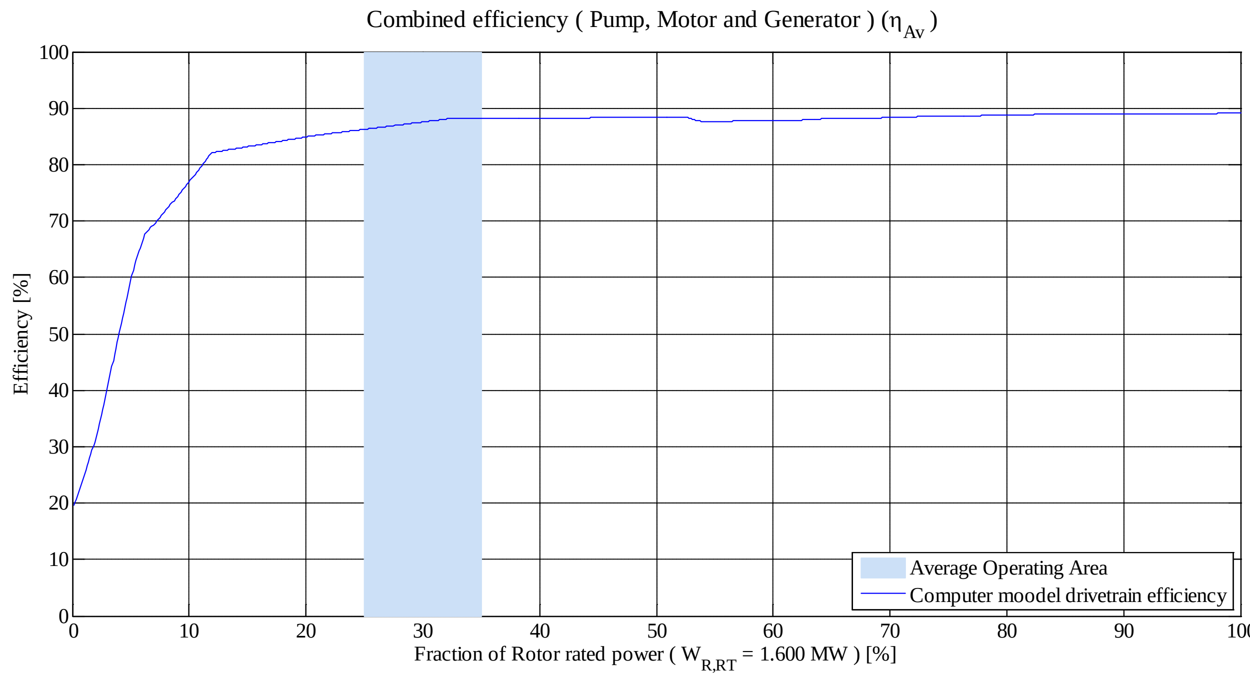

Figure 5.6 Artemis drivetrain efficiency from computer model

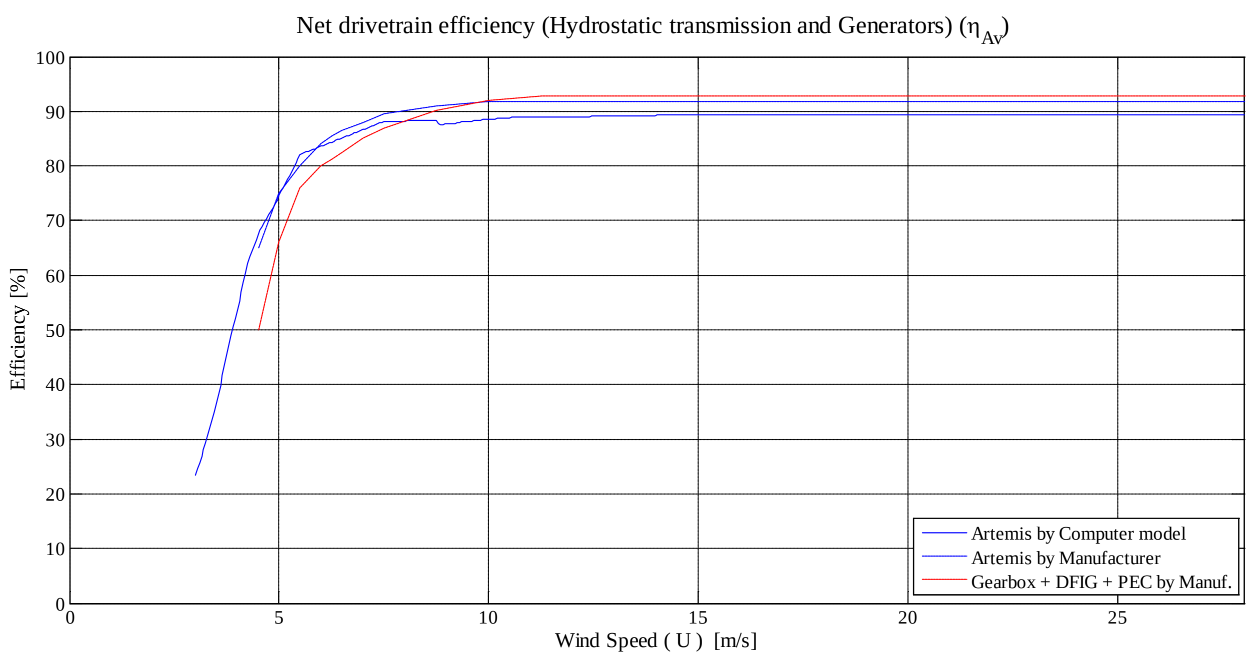

Figure 5.7 Drivetrain efficiency

In the next section, some cost estimation will be done. The target of such calculation is to approximate the final cost of energy production.

5.2.4. Cost

In this section, the cost of a wind turbine with a modern hydraulic drivetrain (Artemis) will be estimated. Once again, because of lack of factual information about Artemis drivetrain (or any similar), several assumptions will be made intended to allow the elaboration of some values. Also, some complementary information will be borrowed from some other sources ([*28*] , [*29*] , [*30*]) to obtain some numeric figures.

With the main intention to provide logic to numeric estimations, the following assumptions were considered:

A. **The raw material employed for a hydraulic machine is at least twice the net volume ($\boldsymbol{V_{NET}}$).** The body volume was presented on Table 5.2. It accounts for the external total machine volume. In order to manufacture a hydraulic machine, several machining processes are required. Most of these processes involve material removal (milling, lathing, grinding, finishing, etc.). The material to be removed accounts at least for another portion of the body volume.

B. **Hydraulic machines are done by using standard machining techniques.**

C. **The material matrix of the full component is made from stainless steel 304 (40%), aluminum 6061 T4 (35%) and steel alloy 4140 (25%).** This combined density is more or less the same than the estimated as Effective density in Table 5.3.

D. **The amount of material to be removed is more or less equal to $\boldsymbol{V_{body} - V_{NET}}$.** It is assumed that is possible to from the machine components by starting from a several pieces of standardized metallic bars. The net volume of raw material (according with material matrix expressed above) adds together the same amount than V_{body}. The solid raw material pieces will be cut to shape the components. The net volume of shaped components adds together a quantity similar to V_{NET}.

E. **The tools used for machining has at least 4 cutting edges.** Although very often cutting tools has 2 cutting edges, it is assumed that 4 cutting edges tools will be used to decrease machining time.

F. **The cutting speed for materials is assumed to be: steel alloy 4140 – 65 SFM (~20 MPM); stainless steel 304 – 75 SFM (~23 MPM) and aluminum 6061 – 250 SFM (~75 MPM).** SFM stands for surface feet per minute. MPM is meters per minute. These cutting speeds are considered intended to maximize life of cutting tools [*31*].

G. **The cost per machining hour is about ~ 25 euros.** This price is valid for CNC machinery [*29*].

H. **Net price of the machine is equal to the net sum of: used raw material, machining cost and some other complementary expenses.** To estimate the cost of raw material, prices and other important figures are included in Table 5.4. To estimate machining cost, estimation by Lovejoy [*29*] was used. Complementary expenses are estimated as 50% extra of the sum of raw material plus machining costs. Such complementary expenses includes extra material to assemble(bolts, nuts, etc.), intellectual property and commercial profit.

Material	Density $[kg/m^3]$	Cutting speed [SFM]	Rate of mat. rem. $[m^3/hr]$	Cost [€/kg]	Pump composition [%]	Motor Composition [%]
Steel Alloy 4140	7850	65	0.00038	€ 1.16	40%	40%
Aluminum 6061 T4	2700	250	0.00147	€ 2.56	35%	20%
Stainless Steel 303	8020	75	0.00044	€ 3.87	25%	40%

Table 5.4 Machines composition and important figures

Table 5.5 presents the estimated cost for the most important components in the hydrostatic transmission. According with such information, the cost of the full hydrostatic transmission should be about 130 k€ (150 k€ if some other intermediate components like hoses, shafts and manifolds).

Now, for the synchronous generator, it will be assumed that its cost is similar to the one presented in Polinder & et.al. [*28*] as DFIG3G because of similar rated parameters (rated speed 1200 RPM and rated power 3MW) and more or less similar technology. Nevertheless, the cost depicted in [*28*] will be scaled down to fit the specifications of the current case (rated speed 1500 RPM and 1MVA rated complex power). This scale down will be done through mass considerations. The scale down factor (f_G) is defined as:

$$f_G = \frac{m_{G,1MVA}}{m_{DFIG3G}} \sim 0.781 \quad \textbf{Eq. 5.5}$$

Where:
f_G is the scale down factor for the cost of the generator
$m_{G,1MVA}$ is the mass of the generator used for this model
m_{DFIG3G} is the mass for the generator presented as DFIG3G in [*27*]- TABLE II (5.25 ton)

By using this factor and estimated cost from [*28*], the generator cost estimation presented in Table 5.6 can be deduced.

1.6 MW Artemis Digital Displacement pump							
Material	**Mass of row material [kg]**	**Volume of raw material $[m^3]$**	**Volu me to cut $[m^3]$**	**Mach. time [hrs]**	**Cost of raw material [€]**	**Cost of machining (50€/hr) [€]**	**Comp. expenses 50 % [€]**
Steel Alloy 4140	1853	0.236	0.106	276	€ 2,148.32	€ 13,821.62	€ 7,984.97
Aluminum 6061 T4	558	0.207	0.093	63	€ 1,428.57	€ 3,144.42	€ 2,286.49
Stainless Steel 303	1183	0.148	0.066	150	€ 4,572.60	€ 7,486.71	€ 6,029.65
Net values	3593	0.590	0.265	489	€ 8,149.49	€ 24,452.74	€ 16,301.12
TOTAL EST. COST	**~50 k€**					***Estimated cost***	***€ 48,903.35***
800 kW Artemis Digital displacement motor							
Steel Alloy 4140	1853	0.100	0.056	146	€ 2,148.32	€ 7,301.99	€ 4,725.15
Aluminum 6061 T4	319	0.050	0.028	19	€ 816.32	€ 949.26	€ 882.79
Stainless Steel 303	1893	0.100	0.056	127	€ 7,316.16	€ 6,328.39	€ 6,822.27
Net values	4063.92	0.250	0.140		€ 10,280.80	€ 14,579.63	€ 12,430.22
TOTAL EST. COST	**~40 k€**					***Estimated cost***	***€ 37,290.66***

Table 5.5 Hydraulic machines estimated costs.

Concept	3MW DFIG3G [*27*]	1MVA Synch Gen.
Generator mass [ton]	5.25	4.4
Cost Generator active material [k€]	30	23.43
Cost Generator construction [k€]	30	23.43
	TOTAL EST. COST	**~47 K**

Table 5.6 1MVA Generator cost estimation

Finally, based in all estimated information, the cost estimation of the drivetrain system is presented in Table 5.7. This table reassembles parameters used in [*28*]. Once again, weight was used to determine a scale down factor (f_{OWT}) based on scaling law in [*20*]. The computation of f_{OWT} is presented in Eq. 5.6. The same factor was used for fields *"Other wind turbine parts appr."* and *"Margin for company profit"* .

$$f_{OWT} = \left(\frac{R_{Artemis}}{R_{DFIG3G}}\right)^3 = \left(\frac{36}{45}\right)^3 \sim 0.512 \qquad \textbf{Eq. 5.6}$$

Where:

f_{OWT} is the scale down factor based on weight
$R_{Artemis}$ is the rotor radius for the computer model
R_{DFIG3G} is the rotor radius used in [*27*]

Description	Qty	U. Cost [k€]	Import [k€]
1.6 MW Artemis Digital Pump	1	50	50
800 kW Artemis Digital Motor	2	40	80
1MVA Synch Generator	2	47	94
Drivetrain system		~224 k€	
Other Wind turbine parts[kE]		~667 k€	
Margin for company costs [kE]		~128 k€	
TOTAL EST. COST(C_{NET})		***~1000 k€***	

Table 5.7 1.6 MW wind turbine with hydraulic drivetrain estimated cost

In the next section, the annual energy production and the cost of energy production will be estimated.

5.2.5. Annual Energy Yield and Cost of energy

By the end of the day, all advantages or disadvantages of a wind turbine are tried to be assessed in terms of cost of energy. To estimate this parameter, annual energy yield and cost estimation are required. Cost estimation was done in the past section. Then, this section is dedicated to develop an educated guess about annual energy yield and cost of energy. Later on (section 5.4), these parameters will be used to compare Artemis drivetrain with some other different technologies.

Because of lack of detailed information about Artemis drivetrain plus the nature of other estimated indicators, a very simple approach for energy yield estimation is preferred over other options. The selected approach is called *levelized cost of energy* [*32*]. Based on that, the annual energy yield (E_{YD}) can be estimated as:

$$\begin{gathered} E_{YD} = T_{eq} W_{R,Grid} \\ T_{eq} = cf\ T_{yr} \end{gathered} \qquad \textbf{Eq. 5.7}$$

Where:
E_{YD} is the annual energy yield in Wh
T_{eq} is the equivalent time (in hours)
cf is the capacity factor
T_{yr} is the total number of hours in one year (8760 hours)
$W_{R,Grid}$ is the rated power fed to the grid (~1.40 MW for Artemis computer model)

The cf is the ratio of the equivalent time over the total time of the year. The T_{eq} accounts for the number of hours (running at full power) that the turbine should work to generate the same amount of energy that generates in one year. A reasonable capacity factor range for onshore modern wind turbines is $0.25 < cf < 0.40$ [*32*]. Based on this, the annual energy yield can be estimated inside the range of $3.07\ GWh < E_{YD} < 4.90\ GWh$. Then, the levelized cost of energy can be estimated as follows:

$$COE = \frac{E_{YD}}{C_{NET}} \qquad \textbf{Eq. 5.8}$$

Where:
COE is the levelized cost of energy
C_{NET} is the net cost of turbine determined in section 5.2.4.

Based on this, the cost of energy is in the range of $3.02\ kWh/€ < COE < 4.83\ kWh/€$. Then, by considering a more or less average value for future comparison it can be said that $COE \sim 3.63\ kWh/€$ with $cf \sim 0.30$. (or $COE \sim 4.00\ kWh/€$ with $cf \sim 0.33$)

In the next section, some other complementary remarks about particular (dis)advantages of a hydraulic drivetrain of this kind over non hydraulic drivetrains are stressed

5.3. Qualitative indicators and remarks

This section is dedicated to stress some other (dis)advantages than a hydraulic system might have over non hydraulic one. Beware that within this section, no formal conclusions are made since this document didn't offer solid evidence about these topics; however, these affairs represent important aspects or advantages that might require further research.

5.3.1. Reliability and Minimization of down time

This section will discuss the possibility of minimizing down time by reconfiguring the activation sequence of the digital hydrostatic transmission. To do so, let's start saying that a hydraulic machines very often has smaller mechanical stress concentration in their components, which makes them less prone to mechanical wear and failure (refer to chapter 1.1.3). Furthermore, hydrostatic transmissions are comprehended in Stage A in Figure 1.7, which main function is to increase angular speed, with the extra advantage of incorporate the angular speed regulation. Additionally, digital machines offer a discrete operation of any piston-cylinder set. Having that wind turbines spend more of their life time working below rated power [*5*], it is possible to think that discrete operation has several advantages over non discrete operation. Among them, increase of machine reliability and decrease of down time hours.

Discrete cylinder operation makes possible to consider any piston-cylinder set as an independent *monocylinder* machine connected to the same shaft. This also allows the implementation of the three main functions at any time: pumping, motoring and idling. Therefore, the performance of the machine can be enhanced by proper control algorithms and sensors. For instance, let's consider an uneven wear of some cylinders in a multicylinder digital machine, like the 1.6MW Artemis pump. If the monitoring system detects low performance on those particular cylinders, then the control system can decide to change its activation sequence to give an *easy* ride to those damaged cylinders. Some causes of low performance in any monocylinder machine might be: excessive leakages through ring, damaged roller, one discharge valve damaged, etc. All of them, might require the visit from a technician so it can be properly repaired. Nevertheless, if the activation sequence is modified (i.e. avoid the use of that particular cylinder by idling it or halting it in its TDC position) a minimization of down time can be achieved by sacrificing some rated power ($1/68^{th}$ per each cylinder damaged in the pump). This will give some room for maintenance planning without having to stop the turbine immediately. Therefore, the turbine can be kept operational until one technician is available to repair one or more cylinders at once in the same machine. This might have a direct impact in the minimization of down time hours [*33*].

Now, in terms of reliability, very often larger number of components leads to lower values on reliability. A digital hydrostatic transmission has larger number of components than a gearbox. Although in a gearbox, reliability is severely affected by increasing the number of components; in a digital hydrostatic transmission this might not the case. A particular geometric configuration and smart software control might actually provide a reliability increase in a digital hydrostatic machine. Since any single cylinder can be controlled independently, a digital hydrostatic transmission can be approached as several independent monocylinder machines connected to the same shaft. Based on this, the number of common critical parts is reduced (those that are shared by all monocylinder machines and, in case of failure, might require the immediate stop of the machine to avoid more damage). Also, these parts are commonly very robust (i.e. ring cam, camshaft, housing, manifolds, etc.). Then, the impact of more *frequent* failures in other parts (i.e. rings, piston, rod, spring, valves, etc.) will only affect their own monocylinder machine. In this way, the damage can be confined into monocylinder units that can be simply shut down until maintenance is available. It is worth to mention that this is not the case for a gearbox, where critical components (all gears for instance) often has a larger stress concentration and failure normally tends to spread very easily leading to the entire failure of the entire assembly. Stress concentration is normally worsened with small misalignments into the shafts due to manufacture tolerances, leading to prone to failure of the entire assembly.

This last sentence breach the way to the next section:

5.3.2. Reparability

In this section, the discrete nature of digital hydraulic machines will be used to introduce the idea than discrete systems in a hydrostatic machine are easier to repair than other kind of devices oriented for Stage A in Figure 1.7. Then, based on ideas presented on past section, let's start saying that in a digital hydrostatic transmission is possible to contain *frequent* failures within parallel and independent monocylinder machines.

As mentioned before in a digital hydrostatic machine, only few but very robust parts are commonly used by the independent monocylinder machines. These parts are either related with the power input or output from the entire assembly (ring cam, shaft, ring cam bearings, seals, manifolds, and housing). If one of these parts fails, then onsite reparation is very complicated because of the dimensions of the components (very similar scenario to the one in a gearbox). Nevertheless, parts that are more prone to failure are those contained in the monocylinder machine (rings, piston, rods, springs, rod bearing, etc). These parts are relatively small (see section 4.3) and their reparation on site is still feasible.

Because of the independent nature of the monocylinder machines, it is possible to stretch the maintenance as far as becomes cost effective. This means, that the digital machine can be reconfigured remotely to keep working until becomes affordable to send a technician to execute multiple reparations at one time.

Be aware that this is neither the case for a gearbox nor power electronic converter (both systems should be considered since the digital hydrostatic transmission increases and regulates angular speed at synchronous speed). When a failure in gearbox or PEC, there is no possibility of stretching operation time to make room for a maintenance service since the machine is already off. This issue is related with the array of components in both systems (they are mostly oriented to transfer power in series rather than in parallel). For instance, when there is excessive wear in a gear set inside a gearbox, at least two gears (each one in different shaft) are severely affected. Then a major a repair in situ becomes very complicated because of the size of the components and assembly complexity. In the case of the PEC, a simple resistor or transistor in the control circuit for the components might drive it out of service (in this case, reparation in situ is possible). In both cases, failures are uncontainable and require immediate action because machinery is already stopped.

Still, there are some other concerns related with environmental pollution commonly associated with hydraulic systems. These will be covered in the next section.

5.3.3. Potential leak

A hydraulic system, under the public opinion will be always related to *possible* leaks. This section deals with some arguments related with those potential leaks. To start, let’s say that in a normal operating condition, a leak should not occur. Leaks are very often product of misadjusted connections or misplaced seals. Very few times leaks are developed because lack of maintenance or normal wear [*13*]. Still, if a leak occurs in a wind turbine that used digital hydrostatic machines, the leak can be easily containable by redesigning the nacelle for that purpose.

To further explain fluid contention in the nacelle, consider than the 1.6 MW Artemis system should be capable of working with less than 800 liters of hydraulic fluid (including oil in reservoir, cylinders, manifolds and lines). Consider the worst case in which the leakage is not detected and the system keep running until it entirely empties the machines, lines and reservoir. In that case, in a nacelle of about 4.0 x 2.0 x 2.0 m (L x W x H based on dimensions depicted in Figure 5.2) 800 liters is 10 cm fluid height spread all over the nacelle floor. As it might be inferred, this is very little oil compared with the size of the system; therefore it should be possible to contain it inside the nacelle until technicians are available for maintenance. If some small modifications are made to the nacelle base (i.e. sealed and equipped with a small drainage at the lowest part), the oil can be safely recoverable without harming the environment.

5.3.4. Lifetime expectancy

This section presents some arguments about life expectancy on hydrostatic transmissions. Beware that the use of digital hydrostatic transmission in wind turbine industry is relatively new, so there is no substantial evidence about the numbers presented in here. Such numbers correspond to other industries that use similar technologies in different applications.

Although wind turbines spends more of their lifetime working below rated power [*5*]; they are currently being designed to last 25-30 years (>200,000 hrs). Furthermore, life expectancy of products is normally estimated at rated power and under normal operating conditions. For instance, gearboxes used for electric power generation at utilities often show a lifetime expectancy of 100,000 hrs at rated power [*34*]. When comparing these values with common values for piston based hydraulic machines, numbers might look amazingly low: ~15,000[31] hrs at rated power (these numbers are set for industry standards using cheap materials and are often dominated by wear in piston rings) [*35*].

By the end of the hydraulic machines lifetime, a replacement of piston rings is required to restore performance. Other parts apart from rings (like bearings) have very low wear and can easily stand the wind turbine lifetime. Although rated lifetime for hydraulic machines might look low, it is possible to be increased if manufacturing process is enhanced (i.e. thermal treatment or high tech materials in wearable parts). If this is done, then the life expectancy can be stretched 3 to 4 times [*35*]. Furthermore, discrete operation of monocylinder machines allows reeling active cylinders to achieve a more or less even wear in all pistons (implemented by software). Since a wind turbine spends more of its time working below rated power, then rated lifetime can effectively means twice or three times the same value. Still, no matter which arguments are presented, there is no evidence in the wind turbine field about these numbers. So, in the most conservative thinking, it becomes evident that at least one overhaul for the hydrostatic transmission will be required in the wind turbine life time. Although the overhauling process is more or less simple (roughly <0.5 hrs per cylinder); replacement parts cost (rings) is not as significant as downtime, decreased performance and labor. Furthermore, the cost of those concepts comprehended or derived from overhauling processes (man hours and parts cost) were not considered in section 5.2.4. Therefore, more research is required in terms of estimating lifetime expectancy and its impact in levelized cost of energy.

5.3.5. Quality of energy

This section makes some comments in terms of quality of energy. One might think that because the specific case of study for Artemis drivetrain avoids the use of power electronic converters, the content of time harmonics will be minimized. In fact, this holds true when the wind turbine is seen as an individual entity and high quality of energy (with low time harmonics content) can be found in the immediate electrical output of the wind turbine. Nevertheless, the importance of such time harmonics and their influence in grid stability needs to be reconsidered when thinking about wind farms connected to the main grid. This last scenario is actually the most common.

[31] These numbers are for very conventional solutions using cheap materials.

For grid connected systems, the grid by itself offers some kind of filtering (combined effect of power lines, transformers, switching equipment, etc.). Therefore, the harmonic content emission might become less relevant since time harmonics might be filtered by the grid. Furthermore, the wind turbine industry had develop some international standards (i.e. IEC 61400-21) intended to guarantee grid stability [*36*].

Still, standard IEC 61400-21 does not consider harmonic emission. Lately, harmonic emission had awakened interest of some leading countries in the wind turbine industry (Germany and Denmark), where *strict* national regulations had been implemented targeting to complement those loopholes in current international regulations. Such complementary regulations try to limit harmonic content in current and voltage [*36*]. Only in those scenarios, where harmonic emission is considered as relevant, hydraulic drivetrains might offer an extra advantage over non hydraulic drivetrains (those that incorporate PECs in their topologies). Still, this document did not cover this topic in detail; therefore, more research is encouraged.

5.4. Comments on comparison indicators

In the past sections, indicators and possible (dis)advantages were briefly discussed for a modern hydraulic drivetrain. To increase indicator's *accuracy*, a specific case of study was boarded: 1.6 MW Artemis drivetrain. Now, the estimative figures obtained in section 5.2 will be used to compare present case of study with a main reference (Polinder & et.al. [*28*]) that presents a rather similar estimation for different machines.

Beware that substantially different machines (rated power, drivetrain style, dimensions, etc.) are being compared with the main product of this document: a hydraulic drivetrain. Therefore, there are some indicators that had to be manipulated to show more coherent comparisons while other has to be simply eliminated (weight).

In Polinder & et.al. [*28*], five different drivetrain topologies are approached: doubly fed induction generator with three-stage gearbox (DFIG3G), direct drive synchronous generator (DDSG), direct drive permanent magnet generator (DDPMG), permanent magnet generator with single-stage gearbox (PMG1G) and doubly fed induction generator with single-stage gearbox (DFIG1G).

For all studied drivetrains, the levelized cost of energy (COE) and the drivetrain efficiency are the only indicators that can be directly used. These indicators are presented in Figure 5.8 and Figure 5.11 respectively for all six different technologies. In both cases, the hydraulic drivetrain appears as a feasible option within the range of current available drivetrains.

Based on comparison presented in Figure 5.8 and considering the limited specific information about 1.6 MW Artemis drivetrain plus none historic data about this array; for now, it is only possible to say that this drivetrain should be more or less a competitive technology in terms of levelized cost of energy.

Since the cases of study from [*28*] were based in a 3 MW wind turbine, while the hydraulic drivetrain presented in this document was based on a 1.6 MW wind turbine; it was decided to present cost information in the shape of a ration of the estimated drivetrain and machinery cost over the nominal power of the machine. In this way, the information will be given in k€ per MW of rated power. Then, Figure 5.9 presents a comparison of the entire wind turbine price compared with other turbines that uses different drivetrain systems, while Figure 5.10 present a comparison about the drivetrain cost. In Figure 5.9, it can be appreciated that hydraulic drivetrains might be the lowest cost solution per megawatt of installed capacity. Then, Figure 5.10 stress the reason for this: a quite *inexpensive* drivetrain solution because of the use of common materials and common manufacturing techniques.

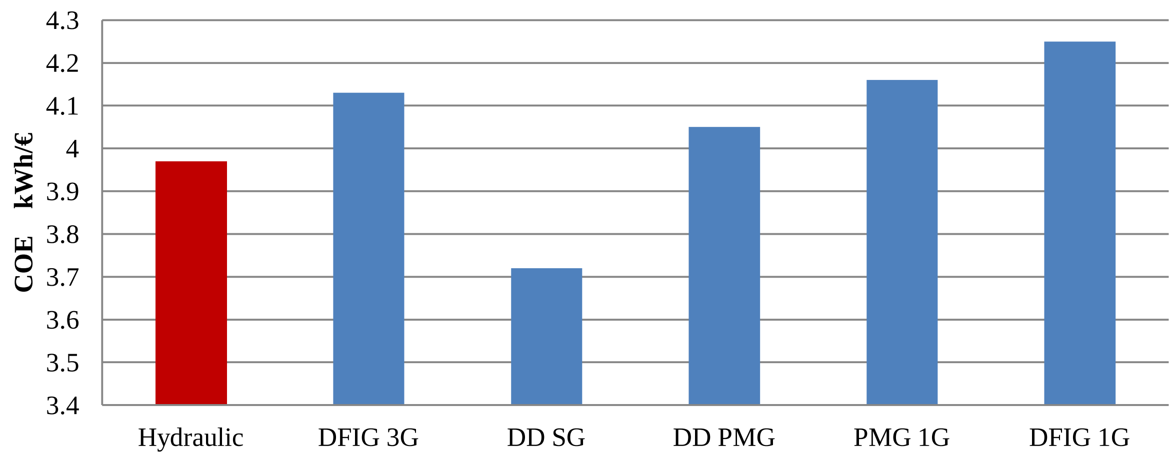

Figure 5.8 Levelized cost of energy for different drivetrains

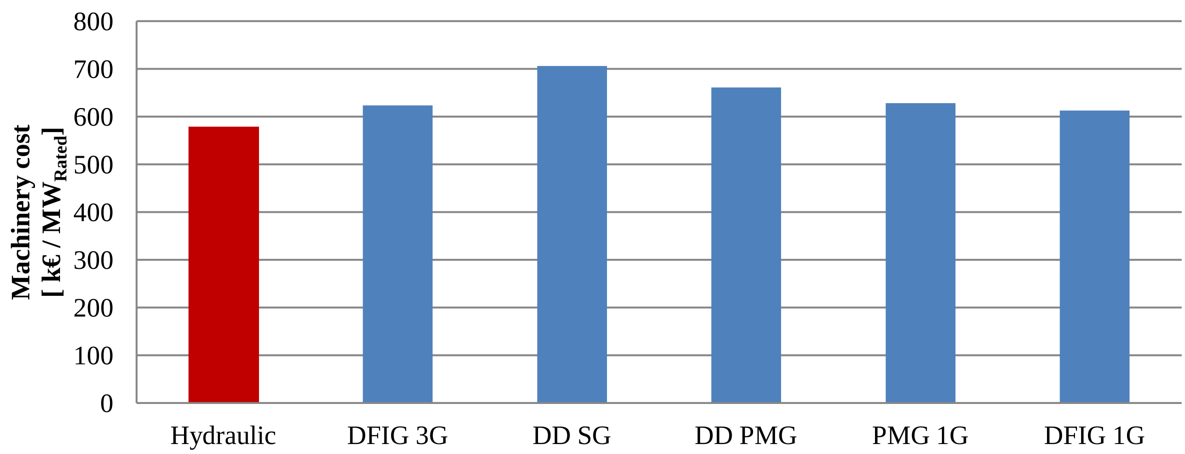

Figure 5.9 Machinery cost per MW rated power for different drivetrains

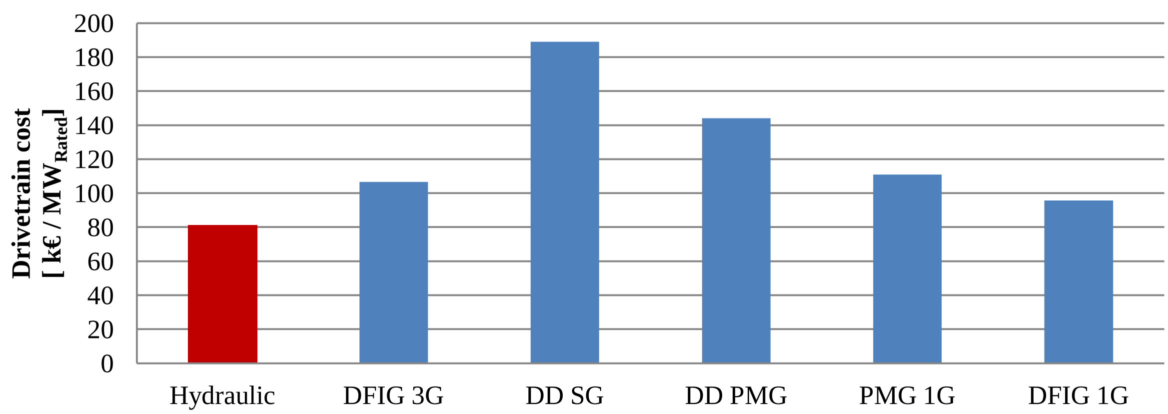

Figure 5.10 Drivetrain cost per MW of rated power for different drivetrains

After looking closely from Figure 5.8 to Figure 5.10, the reader might start wondering about the main reason for which a relatively cheap machine (hydraulic drivetrain) has an average levelized cost of energy. The answer to this inquiry is related with efficiency. As visible in Figure 5.11, hydraulic drivetrain has a low value for rated efficiency (just about ~88 %), which directly impacts the annual energy yield, eventually increasing the cost of energy. Although this efficiency is still low compared with other solutions, the cheap machinery cost allows hydraulic drivetrain today being competitive, which was not the case in the 1980s when they where aborted.

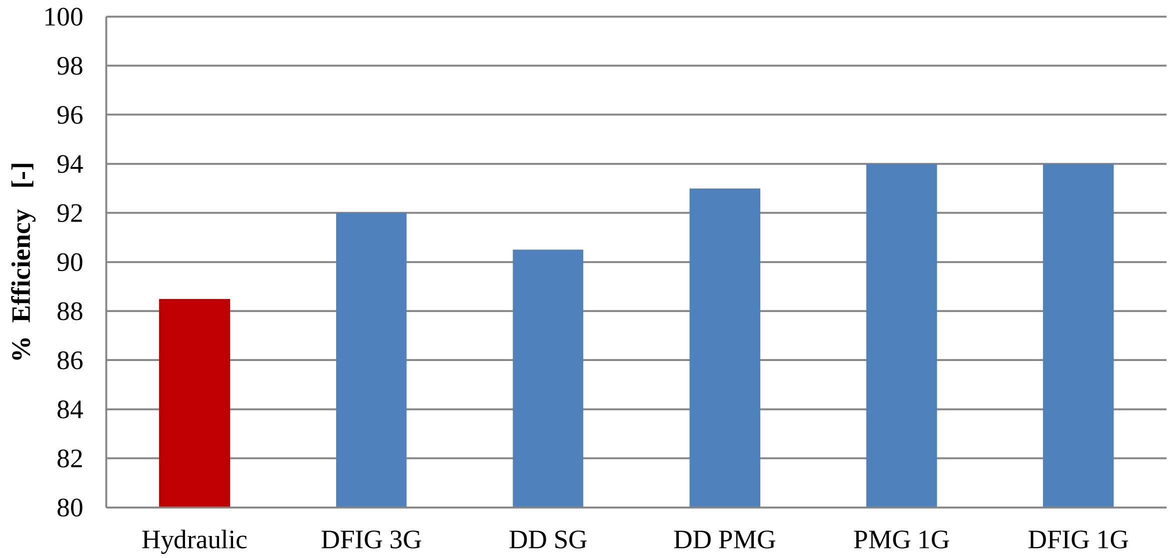

Figure 5.11 Drivetrain rated efficiency for different drivetrains.

Now, in terms of qualitative comments presented in section 5.3, there is a lack of quantitative proof. Furthermore, there is no historic evidence in the wind turbine industry that can support ideas expressed in that section. Then, no conclusions or comparisons can be made regarding those topics.

In the next section, conclusions will be drawn for this chapter.

5.5. Conclusions

Within this chapter, some indicators were built and presented: volume, dimensions, weight, efficiency and levelized cost of energy. Those indicators were described in section 5.2 and are aimed to facilitate quantitative comparison between hydraulic and non hydraulic drivetrains. Then, in section 5.3 some other important remarks were done in qualitative basis trying to describe some potential (dis)advantages of hydraulic drivetrains over non hydraulic. Later on, quantitative indicators were presented side to side with some other quantitative indicators presented by Polinder & et.al. [*27*]. Based on that comparison, this section will draw some partial conclusions about this chapter.

In a highly competitive wind turbine industry, where there is no such thing as conventional drivetrains, the use of quantitative indicators is required to provide an objective perspective about different drivetrains. There are a wide variety of indicators that can be used. Still, by the end of the day most of them try to asses cost of energy production.

Furthermore, 1.60 MW Artemis drivetrain was selected as a specific case of study representing modern hydraulic drivetrains based on hydrostatic transmission. Although there are much more possibilities, this drivetrain is considered as representative state of the art in hydrostatic transmissions. In that scheme, the Artemis drivetrain is a competitive technology in terms of levelized cost of energy. However, more specific information is required to narrow down the results.

Although the Artemis drivetrain machinery promises to be relatively low cost per megawatt of nominal power, relative low efficiencies are also something to be concerned. Still, there are some other parallel advantages (low drivetrain weight, compactness, reduced cost, use of conventional materials and manufacturing processes, modular configuration, discrete operation, etc.) that might become more relevant when dealing with some larger wind turbines, but for the 1.6 MW size, advantages are still scarce and makes this drivetrain just competitive.

Now, in section 5.3 some important remarks were considered. Since those remarks lack of scientific proof, no further comments are done at this time.

6. Conclusions

The wind energy industry has grown significantly in the past decades. It is expected that this growth rate is maintained at least for the following decades. This sustained growth is mainly due to the technology's high success in accomplishing the energy and climate objectives [*37*]. This success is also related with the unique cost effective solution that wind turbines offer: high endurance machinery, lowest cost of green energy production and an entire mature industry developed around this topic. As a product of this, wind energy has become one of the most competitive technologies that nowadays can almost face fossil fuels technologies by itself. Still, there is a large room for improvement in terms of optimization and reliability.

To achieve this, a communal effort has been done in terms of technology. One small part of that collective work is modern hydraulic drivetrains. Although today these drivetrains might look as barely competitive with other already mass produced technologies; it might be the case that in a near future this drivetrains overcome their current limitations and become more competitive.

This chapter is dedicated to present general conclusions (and related recommendations) about the work presented in this document. For that purpose, this chapter had been subdivided in some sections. These subdivisions are aimed to present and support the same reasoning line that eventually will be used to directly answer the research questions presented in 1.2. To do so, first some general conclusions and recommendations are drawn for variable ratio transmissions and hydraulic power transfer; then conclusions and recommendations about analytical and computer model will be presented; to finalize directly answering research questions based on evidence presented in chapter 5.

6.1. Variable ratio transmissions and hydraulics power transfer

This section will draw some conclusions about hydraulic variable ratio transmissions, their advantages and their limitations. Furthermore, some recommendations are made for some topics that are considered to require future research (differential systems like DSgen-set®).

6.1.1. Conclusions

Variable ratio transmissions can be used to transform a variable angular speed input into a constant speed output. Variable ratio transmissions are especially attractive for wind turbine because they allow the use of a synchronous generator directly connected to the grid (overriding the function of electronic converters). There are several kinds of variable ratio transmissions. Those that incorporate fluid power can be hydrodynamic, hydrostatic or hybrid. In those hydraulic transmissions, power transfer can be controlled by means of the fluid in three different ways: built in mechanism, external control circuit and fluid properties.

There are currently several *successful* modern examples of wind turbine drivetrains that incorporate variable ratio hydraulic transmission. Some of them are already available in the market while some others are just in experimental or development stage. This document focuses on the application of hydrostatic variable ratio transmissions based on radial piston machines in a wind turbine. This kind of transmission is not new in the wind turbine industry. In the late 1970s and early 1980s some experimental drivetrains that incorporated this technology were built. At that time, the use of this transmission reported prohibitive efficiencies that impeded the arrival to the market of this alternative.

Nevertheless, in current times, increased computing power and more controllable machinery had achieved that some wind turbine manufacturers started to look back again into hydraulic variable ratio transmissions. The main motivation for this is number of components reduction aiming for a reliability increase. Some advantages of using this kind of transmission versus geared or direct driven system can be found: weight reduction, lack of geared machinery, compatibility with synchronous generators, and highly developed parallel industries.

Although hydrostatic variable ratio transmissions must be comprehended in stage A from Figure 1.5, their function in a wind turbine drivetrain should be considered equivalent to the combined action of a gearbox with an electronic converter.

Furthermore, these transmissions can provide a kind of mechanical power insulation between rotor shaft and generator shaft due to the integration of one different type of power transfer mechanism (something like optic coupling protection in electronic circuits). This *insulating* feature might reduce the impact of one component failure into another (i.e. gearbox failure might impact generator lifetime because uncontrolled vibrations).

6.1.2. Recommendations

In the first two chapters of this thesis fundamentals of hydraulic systems and their advantages in wind turbine drivetrains were boarded on a qualitative basis. Most of the attention was paid to hydraulic variable ratio transmissions. Still, as mentioned before, there are some other kind of variable ratio transmissions especially suitable for the wind turbine industry.

These variable ratio transmissions are entirely based on mechanic and electric power transfer; still they are also capable to override the function of the electronic converter. These transmissions do not incorporate any different kind (like hydraulic) of power transfer mechanism, which make them have several similarities with current geared drivetrains. Their operating principle is similar to the one presented in here for the Wikov W2000 or the LS1 (section 2.3.2). The incorporation of this controllable reaction gear enables them to transform a variable angular speed – variable torque input into a constant speed - variable torque output shaft. This electromechanical approach is very interesting too because it does not demand a radical jump of currently available technology (in the wind turbine industry) as hydraulic variable ratio transmission might demand. Therefore, it would be recommendable to study what are the possibilities in this branch and find out if this parallel technology is more prone to jump into mass production than hydraulic transmissions. Examples as the LS1 (section 2.3.2) or the DSGen-Set® from SET GmbH [*38*] might offer significant competence for hydraulic variable ratio transmissions. Consulting these and similar options are considered as valuable.

6.2. Monocylinder machine model

This section presents some general conclusions about the dynamic model for a monocylinder conventional machine and further comments on chapter 3. Furthermore, some recommendations are mentioned to improve the future performance of this model.

6.2.1. Conclusions

Among the different possibilities of hydraulic drivetrains presented in this document, the 1.6 MW Artemis drivetrain was selected to make further study. This drivetrain is considered as representative of the state of the art in hydrostatic variable ratio transmissions. Therefore, the performance of this drivetrain should be quantitatively evaluated. To do so, and aimed to extend the contribution of this document, a conventional monocylinder machine dynamic model was developed.

The monocylinder machine model presented in section 3.2 can be used to represent any kind of piston based hydraulic machine. The detailed study of such dynamic model showed that conventional hydraulic machines were subjects of several kinds of losses; being the most relevant volumetric leaks and transition regions (introduced in section 3.2.5). Abate losses due to volumetric efficiency is very hard since endurance of the system relies in lubrication. However, an optimized design, high tech materials and enhanced manufacturing processes might lead to further improvements. On the other hand, transition regions can be overcome by using different flow control mechanism independent of angular displacement of input shaft. Digital machines are optimized conventional machine that gets rid of the transition regions losses by integrating software directed valves. Software controlled valves increases machine controllability by making possible the operation in three modes for any cylinder at any time: motoring, pumping and idling. This feature decrease losses in partial load conditions at the cost of high software dependence.

The applicability of the monocylinder model was proven by modeling two different radial piston machines based on this model: ring cam digital pump and high speed digital motor. The study case, as mentioned before, corresponds to the 1.6 MW Artemis drivetrain.

6.2.2. Recommendations

This document focused primarily in the application of the monocylinder model for radial piston machines. Because of similar operating principle, other piston based hydraulic machines (i.e. fixed and variable axial piston machines) can be also represented by this monocylinder model. It would be recommendable to document the translating process from lobes in a swash plate (in a variable displacement axial piston pump) to camshaft geometry (used by the monocylinder model).

Furthermore, the present monocylinder model used the simplest case to approach the physics behind the system: radial cam with aligned followers. This simplest case is actually a particular case where cam curvature is constant and eccentricity is equal to zero. Then, it would be advisable to work in a more general case so more complex geometries can be modeled too.

Furthermore, this monocylinder model did not model thermodynamic nor drag losses. For the present document, these losses were considered as neglectable. However, it would be advisable to determine how large these losses are.

6.3. Computer model

This section will mention general conclusion for the computer model and simulation results presented in this document. Furthermore, some recommendations to improve the model accuracy are mentioned by the end of this section.

6.3.1. Conclusions

Computer models are valuable tools that can offer an *idea* about the performance of a real system. The quality of such *idea* is directly related with the detailed knowledge about principle of operation and geometry of the modeled system. On the other hand, this document presents computer models for two different types of radial piston machines (ring cam digital pump and high speed digital motor). Such models are based on the monocylinder model discussed before. The particular study case corresponds to the 1.6 MW Artemis drivetrain.

Electrically controlled valves and software control are the main commercial features of Artemis Digital Displacement systems. So, in order to model Artemis hydraulic machines, some considerations were applied to the monocylinder model (trying to reflect these commercial features). Because of intellectual and commercial property restraints, it was not possible to have accurate information about the real system. Still the purpose of this document was achieved by estimating a range of values to describe geometry of Artemis machines based on careful visual inspection of some pictures plus available literature. Based on that, the results were considered accurate enough for the steady state.

In general, it was proven that is possible to model a multicylinder machine by several monocylinder models connected in parallel to the same data input. Still, some careful considerations are required so the model can represent accurately what is intended. This approach is extremely useful for digital machines, where discrete cylinder operation is part of the main features of the real system. Nevertheless, there is an important price to pay in terms of software quality. Although this emulates the real system (in a very simple way); an optimized activation sequence is no easy thing and the performance of the system is as good as software quality (software sensibility). Still, conventional machines can be modeled by considering the adequate activation sequence (all active at all times).

In terms of the computer model, the model presented in here represents the steady state condition. In that condition, results of simulations seems to be very similar to those published by the manufacturer.

6.3.2. Recommendations

Since this document focused in the physics behind the hydrostatic transmission, there are several areas of improvement that can be made to the drivetrain computer model. The most important of them is model validation. Since there was barely factual information of the real system, a lot of assumptions were done. It is believed that those assumptions were in the range of desired accuracy; nevertheless, a computer model worth very few without the means to validate it. Still, the monocylinder model already will provide an ahead start for future projects in which experimental setup and factual information is available.

Secondly, another important improvement can be achieved by increasing the degree of complexity of complementary models (rotor and synchronous generator in section 3.5). By improving these models (i.e. including dynamic models) a better appreciation of the interaction of the hydrostatic transmission with the rest of the drivetrain system can be achieved. Furthermore, is advisable to include inertial considerations (currently not integrated) between the interconnection among components (i.e. rotor shaft with hyd. pump, hyd. motor with synch. generator, lines inside hydrostatic transmission, etc.). By including these two upgrades, new research questions can be established to study some interesting topics.

One major topic is related with the effect of the torque ripple (motor shaft) in the stator current of the synchronous generator. By assessing this topic it might be possible to further assessing software sensibility and determine when this torque ripple can drive the generator out of synchronism. Furthermore, these can be used to determine the optimal software commands.

Another major topic worth to study is to quantify the (dis)advantages of a braking algorithm implemented by software to limit the angular speed of the rotor shaft. Quantify the impact in hydrostatic machine wear and fatigue in the blades is only achievable by the implementation of dynamic models.

The past two are only examples of the possible reach of this computer model; still, it is truly believed that the most important thing is to have an experimental setup that can provide with factual information to later validate the model.

6.4. Research question: Hydraulic drivetrain in wind turbines

This section presents conclusions about the results obtained when comparing the 1.6 MW Artemis drivetrain with some other topologies currently available reported in Polinder & et.al. [*27*]. Furthermore, some recommendations are presented by the end of this section

6.4.1. Conclusions

In general for the wind turbine industry, it is possible to say that there is nothing like conventional in terms of drivetrains. Several possibilities (Figure 1.7) make this highly competitive industry fertile terrain for innovation in terms of drivetrain technologies. Among those alternatives, hydraulic drivetrains can be found.

As mentioned before, the 1.6 MW Artemis drivetrain is considered as current state of the art in hydraulic drivetrains. This drivetrain incorporate a digital hydrostatic transmission based in a low speed ring cam pump and a high speed motor. This document presented a specific case of study for this drivetrain trying to asses research questions presented in section 1.2. The computer model is based on a more general dynamic model applicable to any kind of piston based hydraulic machines. Although factual information about Artemis drivetrain system was scarce; results presented in here are mostly product of educated guesses based on available information. Still, those values were never confirmed by the manufacturer but, because the results, they are considered as representative of the system.

In this scheme and for based on the indicator estimated in chapter 5, it is possible to say that this drivetrain can be considered as competitive versus some other current available technologies in terms of levelized cost of energy production.

Furthermore, similar drivetrain to the case of study might offer a low cost per megawatt of installed power. Additionally, there are some other associated parallel advantages for this type of technologies: low drivetrain weight, compactness, use of conventional materials and manufacturing processes, modular configuration, discrete operation, etc. The influence of these advantages in the levelized cost of energy can be enhanced by increasing machinery size; but for a 1.6 MW system the advantages are still scarce making this drivetrain barely competitive and too radical.

Although this drivetrain offers a *cheap* solution; efficiency levels in the case of study are still lower than other popular systems (~2 to 5 % below). This is the main reason than this technology is just competitive. Nevertheless Artemis drivetrain use standardized components (i.e. synch. generators, pistons, valves, etc.) that might improve their production rate decreasing even further production costs.

Despite the Artemis drivetrain requires few subassemblies (hydrostatic transmission and generators) to perform its task; the number of parts in those components is still very similar to the one in a geared drivetrain that uses an electronic converter. This is due to the fact that the hydrostatic transmission has larger number of parts than a gearbox, but makes possible to override the electronic converter.

Finally, summarizing the answer to the main research question:

How large are the advantages and tradeoffs that a hydraulic based drivetrain system has over a non hydraulic drivetrain system in a wind turbine?

It can be said that the main advantages that hydraulic systems offer is stress concentration reduction. This fact solves problems due to small misalignments between shafts that might lead to excessive wear in components. Furthermore, this same idea allows the use of compact (and sometimes standardized) machinery that can be fabricated with standard materials and well known manufacturing processes. These features translate in cheaper systems with smaller dimensions and weight.

Another important feature of hydraulic systems is angular speed regulation. This feature is also shared by all variable ratio transmissions and allows the use of off-the-shell machinery which potentially can abate production cost.

On the other hand, although hydraulic drivetrains are competitive (barely for nominal power ~1.6 MW); they do present lower efficiency levels (~2-5% lower) than non hydraulic solutions. Furthermore, since today there is also no commercial history about these drivetrains; this solution still looks very *radical* for the wind turbine industry. Additionally, some potential issues for the public perception (i.e. leaks and machine endurance) can severely damage their reputation. Therefore, it is necessary to make further study about weak points and possible upsides (i.e. reliability, reparability, etc.) to keep them competitive.

6.4.2. Recommendations

Although in Artemis drivetrain components had been reduced by employing a highly evolved hydrostatic transmission, there are still some big issues that demand further research: lifetime and control of potential leaks. These two topics are considered very important since they might damage the public perception of this kind of drivetrains. Now, some other more positive aspects (i.e. reliability, decrease of down time, reparability and quality of energy - section 5.3) are required to be assessed too. Because lack of quantitative proof for now, it was not possible to draw conclusions about those topics; nevertheless, there is a strong believe that the key factor of this type of drivetrain is related with reliability (i.e. 68 independent monocylinder machines working in parallel in the Artemis pump) and maintenance (i.e. in situ repairs). Still, for now this is just a strong feeling and requires scientific proof. So it would be advisable to retake these topics in a future.

On the other hand, once again becomes evident that more specific information is required to narrow down results. Although it is believed that the used numerical values are in the range than those in the real system; there is neither solid evidence nor validation about that. Therefore this is a strong weak point to be criticized at any point. To avoid risking the effort put in the work summarized in this document, experimental validation is encouraged.

7. Appendices

Appendix A. Forces & Moments in radial piston pumps

In this subsection, an overview of the forces and moments nature will be described based on the operating principle of a radial piston pump. Recalling the idea that the positive displacement pumps (like radial piston pumps) are devices oriented to supply flow of fluid (not pressure); but still should be capable to handle large pressures, the operating principle of a radial piston pump is as follows:

The mechanical power input (a rotating shaft) is transformed to hydraulic power. To do this, mechanical energy is transmitted from a rotating camshaft to a piston-rod assembly. The angular displacement of the camshaft is transformed to linear displacement of the piston. Such displacement produces a change of volume in the pressure chamber, the change of volume leads to change of pressure and eventually flow of fluid. This flow of fluid is controlled by the flow valves. These valves allow loading (or evacuating) the fluid to (or from) the pressure chamber and therefore transmit power to the connected load.

Ideally, it is desired that there is a lossless transfer or mechanical to hydraulic; nevertheless, this is hardly achievable when having an operating principle as presented above. The most significant losses in a radial piston pump can come either from friction or undesired fluid flow. For instance, ideally is intended that only fluid flows through the valves from and to the environment. For practical reasons (geometry, manufacturing tolerances, wear and friction), this is not always possible. Sometimes is required to allow an undesired (but required) parasitic flow of fluid that eventually will pay back in terms of reliability, endurance and efficiency. A clear example of this is found within the piston ring. The piston ring is designed to minimize leaks, include an expendable part, but also to allow the right amount of lubrication during the load cycle. To join all these specification in practice, piston rings normally have to offer some degree of interference over its entire cylindrical contact surface. Interference leads to friction, friction to wear, power dissipation, and eventually to excessive losses and failure. To minimize these effects, lubrication is introduced by allowing deliberated *leaks* between the piston ring and the cylinder sleeve in every load cycle. These leaks will guarantee system endurance and performance at the cost of a parasitic flow. A similar phenomenon occurs with the piston-cylinder sleeve surface, where the piston has smaller diameter than inner diameter of cylinder sleeve (no interference between these components so the piston ring can perform as expendable part). The remaining gap between piston and cylinder sleeve is left to allow thermal expansion (due to normal operating conditions) and lubrication to other mobile parts. Within this section, forces presented in Figure 3.6 will be described and modeled in delay targeting to build, and eventually simplify, Eq. 3.19.

Dissipative loads

In Figure 3.6, all the non conservative forces presented are related with friction forces. Normally, friction forces (F_{fX}) are modeled by the use of the associated normal force (N_{fX}) and a friction coefficient (μ_{fX}) as depicted in Eq. 7.1. This empirical model can be adjusted to several different scenarios (wet or dry friction) by selecting a different μ_{fX}. For wet friction the μ_{fX} is commonly modeled in four different regimes: static friction, boundary lubrication, partial lubrication and full lubrication (or hydrodynamic). Hydrodynamic lubrication is the phenomenon that occurs when a thin film of fluid is formed between two contact surfaces reduces friction forces. In Figure 3.6, there is two friction forces in the piston-ring assembly: friction force between the ring and the cylinder sleeve (F_{fr}) and the friction force between the piston body and the cylinder sleeve (F_{fp}). Both forces can be modeled as presented in Eq. 7.1. According with Zweri [*39*], friction coefficient for cylinder sleeve-ring and cylinder sleeve-piston can be modeled as static friction (μ_{fs}) when *r* is equal to R_{TDC} and R_{BDC} (points at which $\dot{r} = 0$) , and hydrodynamic (μ_{fh}) for the remaining range. This is summarized in Eq. 7.2 and Eq. 7.3. The value for μ_{fh} is mostly depending on speed ($\dot{r}$), fluid viscosity (η_{oil}) and associated load (N_{fr}, N_{fp}), operating conditions (pressure P_{op} and temperature T_{op}). For the purpose of this document (model Artemis Digital Displacement system as a component for a wind turbine drivetrain), the value of such coefficients will be considered as similar to simplify a first approach. This is presented in Eq. 7.4. Finally, Eq. 7.5 presents a simple model applicable for lumped elements where the friction coefficients can be represented as the product of a constant c_1 by the speed of displacement $\dot{r}$. The value for c_1 T should be estimated based on empirical measurements [*39*].

$$F_{fX} = \mu_{fX} N_{fX}$$ **Eq. 7.1**

$$F_{fr} = \begin{bmatrix} \mu_{fh,r} N_{fr} \ , & r \neq R_{TDC} \ or \ R_{BDC} \\ \mu_{fs,r} N_{fr} \ , & r = R_{TDC} \ or \ R_{BDC} \end{bmatrix}$$ **Eq. 7.2**

$$F_{fp} = \begin{bmatrix} \mu_{fh,p} N_{fp} \ , & r \neq R_{TDC} \ or \ R_{BDC} \\ \mu_{fs,p} N_{fp} \ , & r = R_{TDC} \ or \ R_{BDC} \end{bmatrix}$$ **Eq. 7.3**

$$\mu_{fh} = f\left(\dot{r}, \eta_{oil}, N_{fX}, P_{op}, T_{op}, \ldots\right)$$
$$\mu_{fh,r} \approx \mu_{fh,p} \approx \mu_{fs,r} \approx \mu_{fs,p} \mu_f$$ **Eq. 7.4**

$$F_{fN} = (c_1 \dot{r}) N_{fN} = \mu_f N_{fN}$$ **Eq. 7.5**

Finally, in the camshaft free body diagram, there is a parasitic torque due to operation of disc's valves (T_V). This parasitic torque is the consequence of a tight fitting between the low and high pressure disc's valves intended to minimize leakages. T_V models the effective losses due to friction forces while *dragging* both disc's valves; so, it is the a function of the kinetic friction coefficient $\mu_{k,V}$, a geometry function G_V (number of cylinders, radius, drag coefficient, etc), and an effective normal load function N_V (function of the interference, area of ports, number of blocked ports, working pressure of pump, thermal expansion, etc.). This is expressed in Eq. 7.6.

$$T_V = f\left(\mu_{k,p}, G_V, N_V, P, T, \ldots\right)$$ **Eq. 7.6**

Conservative loads

Inertial and conservative forces are modeled by Eq. 7.7. Inertial loads makes reference to those loads due to the own mass of the system that produces a natural resistance of the system to change of speed. For these purposes, the following parameters are used: the combined mass of the piston-ring-rod-bearing set m_p; the combined mass of rotating components m_{rc} (camshaft, valve's discs, etc), g is the gravity force; K_{sp} is the return spring stiffness and ϵ_0 is the pretensioning deformation present in the spring to avoid separation of the roller-cam surfaces. m_p and m_{rc} are located at the particular center of mass for each subassembly (G_{gpr} and G_{grc} respectively).

$$\begin{gathered} F_{gp} = m_p g \\ F_{grc} = m_{rc} g \\ F_{sp} = K_{sp}(\epsilon_0 + r) \end{gathered} \quad \textbf{Eq. 7.7}$$

External excitations

In Figure 3.6 there are some loads that represents power transmission (on blue).The net input torque T_{IN} is direct function of the prime mover transmitted net power W_{IN}. This is presented in Eq. 7.8. Then force is transmitted from camshaft to piston-rod-ring assembly by the force F_{IN}. This generates a reciprocating motion of the piston and eventually the change of volume of the pressure chamber. This change of pressure will eventually lead to some resistance by the fluid leaving (or arriving) the chamber. This is modeled by force F_P. $F_P$is the resultant force due to mechanic power conversion to hydraulic power; and it function of several parameters as geometry, fluid properties and operating conditions. For now, let's consider that F_P can also be estimated as function of the cross section area of the piston (A_p) and the pressure inside the chamber (p_{Cn}). This is presented by Eq. 7.9.

$$T_{IN} = \frac{W_{IN}}{\dot{\theta}} \quad \textbf{Eq. 7.8}$$

$$F_P \approx A_p p_{Cn} \approx \frac{\pi D_c^2}{4} p_{Cn} \quad \textbf{Eq. 7.9}$$

Appendix B. Wind Turbine Basics

The purpose of this section is to give a fast overview about the power flow through the wind turbine drivetrain that documents some ranges and parameters used in Chapter 0

Rotor angular speed

According with Artemis Intelligent Power Ltd, the nominal power for the drivetrain system is about 1.5-2MW [*2*]. Currently there is no mass production of a wind turbine that integrates such technology; therefore the available information is still scarce. This scenario worsened after December 2010, when Mitsubishi Heavy Industry Ltd. acquired Artemis Intelligent Power Ltd. So, in order to model the system and having as starting point very limited information, some assumptions will be made. The assumptions made will be based on similar power plants. One of those assumptions is the one for the angular speed presented on next.

The power input to the drivetrain was expressed in Eq. 3.41. This expression should provide input parameters to be used in chapter 0To make possible the analysis of the t is important to define some ranges of $\dot{\theta}_{RT}$ which are more or less expected for a 1.5-2 MW wind turbine. Such values were estimated by looking at the parameters of some of the most commercial wind turbines currently available. These *popular* wind turbines are presented in Table 7.1. Based on the information presented in there, the last row was built. In there, some *inside the range* values were used to be employed in the model presented in Chapter 0

Make	**Model**	W_{Rated}	$\dot{\theta}_{RT,Rated}$	$\dot{\theta}_{RT}$**(Range)**	D_{rotor}	$U_{a,R}$	$U_{a,cut-in}$	$U_{a,cut-out}$
		[kW]	[rpm]	Range[rpm]	[m]	[m/s]	[m/s]	[m/s]
Siemens	SWT2.3	2300	~15	6.0 – 18.0	82.4	13.5	4	25
Enercon	E70	2300	~18	6.0 - 21.5	70	15.0	4	28
Vestas	V90	2000	16.7	10.8 - 19.1	90	16.0	4	25
Wikov Wind	W2000	2000	19.0	13.0 - 21.9	76.5	13.0	4	25
DeWind	D8.2	2000	18.0	11.1 - 20.7	80	13.5	3	25
Gamesa	G90	2000	17.0	9.0 - 19.0	80	15.0	4	25
Enercon	E82	2000	~16	6.0 - 17.5	82	13.0	3	28
Vestas	V100	1800	14.5	9.3 -16.6	100	12.5	3	20
AVERAGE	**ADD**	**1600**	**~17**	**4.0 – 20.0**	**74**	**13.5**	**3**	**25**

Table 7.1 Popular wind turbine parameters.

Appendix C. Hydraulic Parameters

Losses in suction manifold

To explain further the power dissipation in the suction manifold and its relation with low efficiency levels in partial load conditions let's said that, when the fluid arrives here; the pressure P_S-mostly hydrostatic pressure- is smaller than discharge manifold pressure (P_D). The incoming mass of fluid leaves the suction port at *high* speed due to the large pressure difference ($P_D - P_S$). This large kinetic content is rapidly dissipated inside the suction manifold (mostly as friction with other oil particles) and therefore unrecoverable. Energy is a function of time (Eq. 3.26). So, the larger time the condition of Region 2 and 5 is held, the larger the energy leaks the system has. The amount of time that transient conditions are hold is determined by the angular speed $\dot{\theta}$ at which the machine is operated. The lower the speed, the larger the time that transient conditions are hold. Therefore, the faster the machine is operated, the smaller the leaks due to Region 2 and 5 are; nevertheless, larger values of $\dot{\theta}$ also leads to larger dissipative forces, mechanical stresses and thermal expansion (halting condition). Then, the optimal point of operation for conventional radial piston pumps is given at rated speed; where the best deal for this tradeoff between power leaks, losses and endurance is obtained. Operating these machines above rated speed cannot be hold for long times (excessive wear); but operate them below rated speeds turns out to be very inefficient [*5*].

Electric solenoid valves response times

The response time for electrically triggered valves is the elapsed time that involves changing from fully closed to fully open condition. This parameter depends on the valve's geometry, operating principle, electric service, temperature, fluid type, inlet pressure and pressure drop [*40*]. For technical purposes, approximate values for different types of valves are presented in TABLE.

Operating principle	Type	Liquid fluid [ms]
Direct acting valve	Small	7.5-20
	Large	30-80
Internal pilot operated valves	Small diaphragm	23-100
	Large diaphragm	75-150
	Small piston	112-200
	Large piston	150-300

Table 7.2 Estimated response times for electric fluid valves

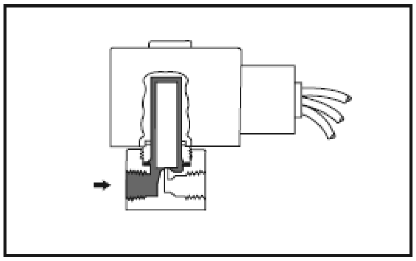

Figure 1A:
Direct Acting,
Normally Closed Valve,
De-Energized

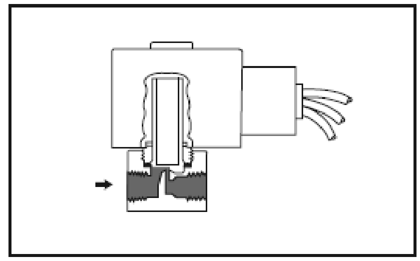

Figure 1B:
Direct Acting,
Normally Closed Valve,
Energized

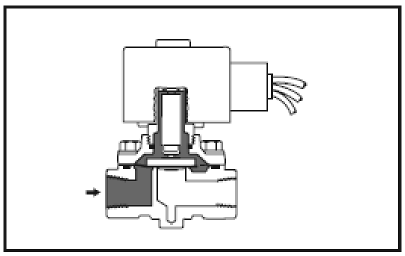

Figure 2A:
Pilot Operated, Normally
Closed Valve,
De-Energized

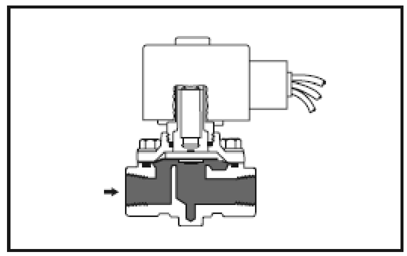

Figure 2B:
Pilot Operated,
Normally Closed Valve,
Energized

Idling losses estimation in Artemis Digital Displacement machines

The manufacturer of this kind of machines claims that idling losses are proportional to the magnitude of the net idled flow (Q_{idled}) [5]. According to the manufacturer, the losses can be estimated by using an empirical loss constant ($K_{LossIdl}$) presented in Eq. 7.10. Then, losses can be estimated according with Eq. 7.11. The net idled flow is the sum of the rated flow for all idling cylinders (also presented in Eq. 7.11).

$$K_{LossIdl} = 7\frac{W}{l/min} = 420\,000\frac{W}{m^3/s} \qquad \textbf{Eq. 7.10}$$

$$W_{LossIdl} = K_{LossIdl}\, Q_{idled}$$
$$Q_{idled} = (N-n)q_{RTDC1} \qquad \textbf{Eq. 7.11}$$

Appendix D. Angle to time domain

The angle domain (or crank domain) relates the basic motion equations with the angular displacement of a particular rotating body. It is commonly used for the study of rotating and reciprocating machines. Although this domain can offer a clear perspective on the evolution of a specific DOF in one revolution, when more complex machinery is being analyzed this domain can become impractical. This is the case of drivetrains, where there might be more than one rotating machine.

For the current case of study (hydraulic drivetrains in wind turbines), the crank domain provided the initial steps to review the motion equations of both reciprocating machines (pump and motor); nevertheless, when studying the interaction of both components, it was required to jump from the crank domain to the time domain, where a common ground for the interaction of the systems was found. This section describes the considerations required to change from the crank domain to the time domain.

Relation between angle and time

Consider a DOF θ that defines rotation of a shaft (i.e. the camshaft in the hydraulic pump). The rotation of such shaft is measured in [rad]. θ is related with the time (t) according with Eq. 7.12, where $\dot{\theta}$ represents the rate of change of θ respect to time (or angular speed). Comparably, $\ddot{\theta}$ (presented in Eq. 7.13) represents the change of angular speed respect to time (also called angular acceleration).

$$\frac{d\theta}{dt} = \dot{\theta} \qquad \textbf{Eq. 7.12}$$

$$\frac{d^2\theta}{dt^2} = \ddot{\theta} \qquad \textbf{Eq. 7.13}$$

Now, consider a generic variable called A that represents any other parameter that is directly related with θ (i.e. displacement of a piston inside a cylinder, volume, pressure, etc.). Also, the rate of change of A respect of θ is already known (presented in Eq. 7.14). It is possible to relate the DOF A with the time domain using the relations presented in Eq. 7.12 and Eq. 7.13. This is presented in Eq. 7.15

$$\begin{gathered} A = f(\theta) \\ \frac{d(A)}{d\theta} \end{gathered} \qquad \textbf{Eq. 7.14}$$

$$\frac{d(A)}{dt} = \frac{d(A)}{dt}\left(\frac{d\theta}{d\theta}\right) = \frac{d(A)}{d\theta}\ \dot{\theta} = \frac{d(A)}{d\ t} = \dot{A} \qquad \textbf{Eq. 7.15}$$

Similarly, this can be done successively to estimate the derivatives of higher order like acceleration of A ($\ddot{A}$), which is presented in Eq. 7.16.

$$\begin{aligned} \frac{d^2(A)}{dt^2} = \frac{d}{dt}\left(\frac{d(A)}{d\theta}\dot{\theta}\right) &= \frac{d}{dt}\left(\frac{d(A)}{d\theta}\right)\frac{d\theta}{dt}\left(\frac{d\theta}{d\theta}\right) + \frac{d(A)}{d\theta}\ \frac{d}{dt}\left(\frac{d\theta}{dt}\right) \\ &= \frac{d^2(A)}{d\theta^2}\ \dot{\theta}^2 + \ \frac{d(A)}{d\theta}\ \ \ddot{\theta} = \ddot{A} \end{aligned} \qquad \textbf{Eq. 7.16}$$

The presented model is simulated in the θ (angular displacement) domain for convenience. To take from the θ domain to the t (time) domain, the following relationship must be considered.

$$dt = \frac{d\theta}{\dot{\theta}}$$

In this way, it is possible to take change between domains at will.

Appendix E. Activation Sequence

Digital radial piston pump

This section presents the one possible activation sequence for the Artemis Digital Displacement pump. The goal of the activation sequence is to determine which cylinder is brought to operation during a particular load condition. This sequence does not represent the timing for the inlet and outlet valves. In fact, this firing order assumes that when a cylinder is active, the timing of the valves is optimal so best operation of every single cylinder (alone) is achieved.

Bear in mind that the activation sequence presented in Table 7.3 **is just one possibility** for bracing cylinders. The possibilities for activation sequences of 17 different type of cylinders are as large as 17! (only valid for the model). In fact, for the real system this is much worse: for a 68 cylinder machine, the possible permutations are 68!. Therefore, the permutation presented in here might not be the optimal. The optimal permutation for activation sequence is out of the scope of this document as well as the valve timing.

The present activation sequence was built based on the following principle. From pump banks presented in Figure 3.12a, before activate the first cylinder of bank 2, all 34 cylinders on bank 1 must be already active. Now, in each bank, the order of activation is intended to balance mechanical load. This means, that the first cylinder in being activated must be followed by the exactly opposite cylinder. For instance, recalling Figure 3.13, cylinder C1 must be followed by cylinder C1b (shifted mechanically 180 degrees but in phase for output flow). Although this algorithm *balances* mechanical load, it worsens the hydraulic performance by having two characteristic cylinders' flow in phase (cylinder C1 and cylinder C1b belongs to the same kind of characteristic cylinder type). This is a tradeoff must be considered by a *optimal* algorithm.

$P_{IN,mech}$ [kW]		***Active cylinders***		***Pump activation sequence per type of cylinder***																
From	***To***	***ON***	***OFF***	***C1***	***C2***	***C3***	***C4***	***C5***	***C6***	***C7***	***C8***	***C9***	***C10***	***C11***	***C12***	***C13***	***C14***	***C15***	***C16***	***C17`***
0	**1**	0	68	0	0	0	0	0	0	0	0	0	0	0	0	0	0	0	0	0
1	**24**	1	67	1	0	0	0	0	0	0	0	0	0	0	0	0	0	0	0	0
24	**47**	2	66	2	0	0	0	0	0	0	0	0	0	0	0	0	0	0	0	0
47	**71**	3	65	2	0	0	0	0	1	0	0	0	0	0	0	0	0	0	0	0
71	**94**	4	64	2	0	0	0	0	2	0	0	0	0	0	0	0	0	0	0	0
94	**118**	5	63	2	0	0	0	0	2	0	0	0	0	0	0	1	0	0	0	0
118	**141**	6	62	2	0	0	0	0	2	0	0	0	0	0	0	2	0	0	0	0
141	**165**	7	61	2	0	1	0	0	2	0	0	0	0	0	0	2	0	0	0	0
165	**188**	8	60	2	0	2	0	0	2	0	0	0	0	0	0	2	0	0	0	0
188	**212**	9	59	2	0	2	0	0	2	0	0	0	0	0	0	2	0	0	1	0
212	**235**	10	58	2	0	2	0	0	2	0	0	0	0	0	0	2	0	0	2	0
235	**259**	11	57	2	0	2	0	0	2	0	0	0	1	0	0	2	0	0	2	0
259	**282**	12	56	2	0	2	0	0	2	0	0	0	2	0	0	2	0	0	2	0
282	**306**	13	55	2	0	2	0	0	2	0	0	1	2	0	0	2	0	0	2	0
306	**329**	14	54	2	0	2	0	0	2	0	0	2	2	0	0	2	0	0	2	0
329	**353**	15	53	2	0	2	0	0	2	0	0	2	2	0	0	2	0	0	2	1
353	**376**	16	52	2	0	2	0	0	2	0	0	2	2	0	0	2	0	0	2	2

376	**400**	17	51	2	1	2	0	0	2	0	0	2	2	0	0	2	0	0	2	2
400	**424**	18	50	2	2	2	0	0	2	0	0	2	2	0	0	2	0	0	2	2
424	**447**	19	49	2	2	2	0	0	2	1	0	2	2	0	0	2	0	0	2	2
447	**471**	20	48	2	2	2	0	0	2	2	0	2	2	0	0	2	0	0	2	2
471	**494**	21	47	2	2	2	0	0	2	2	0	2	2	0	1	2	0	0	2	2
494	**518**	22	46	2	2	2	0	0	2	2	0	2	2	0	2	2	0	0	2	2
518	**541**	23	45	2	2	2	0	0	2	2	0	2	2	0	2	2	1	0	2	2
541	**565**	24	44	2	2	2	0	0	2	2	0	2	2	0	2	2	2	0	2	2
565	**588**	25	43	2	2	2	0	1	2	2	0	2	2	0	2	2	2	0	2	2
588	**612**	26	42	2	2	2	0	2	2	2	0	2	2	0	2	2	2	0	2	2
612	**635**	27	41	2	2	2	1	2	2	2	0	2	2	0	2	2	2	0	2	2
635	**659**	28	40	2	2	2	2	2	2	2	0	2	2	0	2	2	2	0	2	2
659	**682**	29	39	2	2	2	2	2	2	2	0	2	2	0	2	2	2	1	2	2
682	**706**	30	38	2	2	2	2	2	2	2	0	2	2	0	2	2	2	2	2	2
706	**729**	31	37	2	2	2	2	2	2	2	0	2	2	1	2	2	2	2	2	2
729	**753**	32	36	2	2	2	2	2	2	2	0	2	2	2	2	2	2	2	2	2
753	**776**	33	35	2	2	2	2	2	2	2	1	2	2	2	2	2	2	2	2	2
776	**800**	34	34	2	2	2	2	2	2	2	2	2	2	2	2	2	2	2	2	2
800	**824**	35	33	3	2	2	2	2	2	2	2	2	2	2	2	2	2	2	2	2
824	**847**	36	32	4	2	2	2	2	2	2	2	2	2	2	2	2	2	2	2	2
847	**871**	37	31	4	2	2	2	2	3	2	2	2	2	2	2	2	2	2	2	2
871	**894**	38	30	4	2	2	2	2	4	2	2	2	2	2	2	2	2	2	2	2
894	**918**	39	29	4	2	2	2	2	4	2	2	2	2	2	2	3	2	2	2	2
918	**941**	40	28	4	2	2	2	2	4	2	2	2	2	2	2	4	2	2	2	2
941	**965**	41	27	4	2	3	2	2	4	2	2	2	2	2	2	4	2	2	2	2
965	**988**	42	26	4	2	4	2	2	4	2	2	2	2	2	2	4	2	2	2	2
988	**1012**	43	25	4	2	4	2	2	4	2	2	2	2	2	2	4	2	2	3	2
1012	**1035**	44	24	4	2	4	2	2	4	2	2	2	2	2	2	4	2	2	4	2
1035	**1059**	45	23	4	2	4	2	2	4	2	2	2	3	2	2	4	2	2	4	2
1059	**1082**	46	22	4	2	4	2	2	4	2	2	2	4	2	2	4	2	2	4	2
1082	**1106**	47	21	4	2	4	2	2	4	2	2	3	4	2	2	4	2	2	4	2
1106	**1129**	48	20	4	2	4	2	2	4	2	2	4	4	2	2	4	2	2	4	2
1129	**1153**	49	19	4	2	4	2	2	4	2	2	4	4	2	2	4	2	2	4	3
1153	**1176**	50	18	4	2	4	2	2	4	2	2	4	4	2	2	4	2	2	4	4
1176	**1200**	51	17	4	3	4	2	2	4	2	2	4	4	2	2	4	2	2	4	4
1200	**1224**	52	16	4	4	4	2	2	4	2	2	4	4	2	2	4	2	2	4	4
1224	**1247**	53	15	4	4	4	2	2	4	3	2	4	4	2	2	4	2	2	4	4
1247	**1271**	54	14	4	4	4	2	2	4	4	2	4	4	2	2	4	2	2	4	4
1271	**1294**	55	13	4	4	4	2	2	4	4	2	4	4	2	3	4	2	2	4	4
1294	**1318**	56	12	4	4	4	2	2	4	4	2	4	4	2	4	4	2	2	4	4
1318	**1341**	57	11	4	4	4	2	2	4	4	2	4	4	2	4	4	3	2	4	4
1341	**1365**	58	10	4	4	4	2	2	4	4	2	4	4	2	4	4	4	2	4	4
1365	**1388**	59	9	4	4	4	2	3	4	4	2	4	4	2	4	4	4	2	4	4
1388	**1412**	60	8	4	4	4	2	4	4	4	2	4	4	2	4	4	4	2	4	4
1412	**1435**	61	7	4	4	4	3	4	4	4	2	4	4	2	4	4	4	2	4	4
1435	**1459**	62	6	4	4	4	4	4	4	4	2	4	4	2	4	4	4	2	4	4
1459	**1482**	63	5	4	4	4	4	4	4	4	2	4	4	2	4	4	4	3	4	4
1482	**1506**	64	4	4	4	4	4	4	4	4	2	4	4	2	4	4	4	4	4	4
1506	**1529**	65	3	4	4	4	4	4	4	4	2	4	4	3	4	4	4	4	4	4
1529	**1553**	66	2	4	4	4	4	4	4	4	2	4	4	4	4	4	4	4	4	4
1553	**1576**	67	1	4	4	4	4	4	4	4	3	4	4	4	4	4	4	4	4	4
1576	**1600**	68	0	4	4	4	4	4	4	4	4	4	4	4	4	4	4	4	4	4

Table 7.3 One possibility of activation sequence for 68 cylinder pump model(based on 17 characteristic cylinders).

Digital radial piston motor

Similar considerations to those made for digital radial piston pump are followed for the motor. In here, **one possibility** (out of 6! for the model, or 24! or the system) of activation sequence is presented in Table 7.4.

Once again, this permutation sequence here might not be the optimal. The optimal permutation for activation sequence is out of the scope of this document as well as the valve timing.

The activation algorithm is similar to that used for the pump. This is as follows: Before activate the first cylinder of bank 3 on Figure 3.12b, all cylinders in bank 1 and bank 2 must be already operating. For every bank, the firing order is C1, C4, C2, C5, C3 and C6 in Figure 3.1. In this machine, already is possible to think in a better firing sequence for each bank intended to reduce load and hydraulic ripple. For instance, minimum load by C1; then C1 and C4; then C1, C3 and C5; then C1, C2, C4 and C5; then add C3, to finally have all active. This *optimized* version is presented in Table 7.5. In there, the most important changes were highlighted (in Table 7.4 and Table 7.5) to stress the influence in software dependence. The effect of the activation sequence can was presented in section 0 only in the motor case, since the simpler geometry allows a better understanding.

$P_{IN,hyd}$ [kW]		*Active cylinders*		*Motor activation sequence per type of cylinder*					
From	***To***	***ON***	***OFF***	***C1***	***C2***	***C3***	***C4***	***C5***	***C6***
0	**1**	0	24	0	0	0	0	0	0
1	**33**	1	23	1	0	0	0	0	0
33	**67**	2	22	1	0	0	1	0	0
67	**100**	3	21	1	1	0	1	0	0
100	**133**	4	20	1	1	0	1	1	0
133	**167**	5	19	1	1	1	1	1	0
167	**200**	6	18	1	1	1	1	1	1
200	**233**	7	17	2	1	1	1	1	1
233	**267**	8	16	2	1	1	2	1	1
267	**300**	9	15	2	2	1	2	1	1
300	**333**	10	14	2	2	1	2	2	1
333	**367**	11	13	2	2	2	2	2	1
367	**400**	12	12	2	2	2	2	2	2
400	**433**	13	11	3	2	2	2	2	2
433	**467**	14	10	3	2	2	3	2	2
467	**500**	15	9	3	3	2	3	2	2
500	**533**	16	8	3	3	2	3	3	2
533	**567**	17	7	3	3	3	3	3	2
567	**600**	18	6	3	3	3	3	3	3
600	**633**	19	5	4	3	3	3	3	3
633	**667**	20	4	4	3	3	4	3	3
667	**700**	21	3	4	4	3	4	3	3
700	**733**	22	2	4	4	3	4	4	3
733	**767**	23	1	4	4	4	4	4	3
767	**800**	24	0	4	4	4	4	4	4

Table 7.4 One possibility of activation sequence for 24 cylinder motor model (based on 6 characteristic cylinders).

$P_{IN,hyd}$ [kW]		Active cylinders		Motor activation sequence per type of cylinder					
From	***To***	***ON***	***OFF***	***C1***	***C2***	***C3***	***C4***	***C5***	***C6***
0	**1**	0	24	0	0	0	0	0	0
1	**33**	1	23	1	0	0	0	0	0
33	**67**	2	22	1	0	0	1	0	0
67	**100**	3	21	1	0	1	0	1	0
100	**133**	4	20	1	1	0	1	1	0
133	**167**	5	19	1	1	1	1	1	0
167	**200**	6	18	1	1	1	1	1	1
200	**233**	7	17	2	1	1	1	1	1
233	**267**	8	16	2	1	1	2	1	1
267	**300**	9	15	2	1	2	1	2	1
300	**333**	10	14	2	2	1	2	2	1
333	**367**	11	13	2	2	2	2	2	1
367	**400**	12	12	2	2	2	2	2	2
400	**433**	13	11	3	2	2	2	2	2
433	**467**	14	10	3	2	2	3	2	2
467	**500**	15	9	3	2	3	2	3	2
500	**533**	16	8	3	3	2	3	3	2
533	**567**	17	7	3	3	3	3	3	2
567	**600**	18	6	3	3	3	3	3	3
600	**633**	19	5	4	3	3	3	3	3
633	**667**	20	4	4	3	3	4	3	3
667	**700**	21	3	4	3	4	3	4	3
700	**733**	22	2	4	4	3	4	4	3
733	**767**	23	1	4	4	4	4	4	3
767	**800**	24	0	4	4	4	4	4	4

Table 7.5 Optimized activation sequence for 24 cylinder motor

Appendix F. Geometric parameters

This section complements section 0 with further explanation on some concepts used in there.

Geometric ratios by visual inspection

Parameter	Description	Expression
Geometrical ratio 1 (G_1)	Estimated ratio of TDC over external machine radius	$\frac{R_{TDC,P}}{R_{P,ext}}$
Geometrical ratio 2 (G_2)	Estimated ratio of BDC over external machine radius	$\frac{R_{BDC,P}}{R_{P,ext}}$
Geometrical ratio 3 (G_3)	Estimated ratio of lower point of ring cam respect to the center of rotation over external machine radius	$\frac{R_{bs,P}}{R_{P,ext}}$
Geometrical ratio 4 (G_4)	Estimated ratio of distance between center of rotation and center of geometry (l_e) in the equivalent camshaft model over external machine radius	$\frac{l_{e,P}}{R_{P,ext}}$
Geometrical ratio 5 (G_5)	Estimated ratio of rod length(l_r) over external external machine radius	$\frac{l_{r,P}}{R_{P,ext}}$
Geometrical ratio 6 (G_6)	Estimated ratio of piston height(l_p) over external external machine radius	$\frac{l_{p,P}}{R_{P,ext}}$
Geometrical ratio 7 (G_7)	Estimated ratio of roller radius(R_{rlr}) over external external machine radius	$\frac{R_{rlr,P}}{R_{P,ext}}$

Table 7.6 Geometrica ratios estimation for 1.6 MW – 68 cylinder Artemis Digital displacement ring cam pump.[32]

Estimating specific machine parameters using available data.

For instance, the cylinder diameter ($D_{c,P}$) and rated cylinder displacement ($\Delta V_{C1,P}$) for this machine can be estimated according the following reasoning: there is a 1.60 MW rated power 24 lobes ring cam, 68 cylinder pump. If the rated power of the hydrostatic transmission is achieved when pressure between stages is ~300 bar (conservative value below ~400 bar reported by Rampen [5]), then expressions presented in Eq. 7.17 can be followed. In there, sub indexes P for pump, Net stands for net, $1min$ for one minute or 60 seconds, Out for outgoing, $perRev$ for per revolution, and Rat for rated .

$$\begin{aligned}
Q_{Net,Out,P} &= \frac{P_{Rat,P}}{p_{oper}} \\
&= \frac{1.60 \times 10^6}{300 \times 10^5} \sim 0.053\, m^3/s \\
Q_{Net,1min,P} &= Q_{Net,Out,P} \cdot t_{1\mathrm{min}} \\
&= 0.053(60) \sim 3.2\, m^3 \\
Q_{perRev,P} &= \frac{Q_{Net,1min,P}}{\theta_{Rat,P}} \\
&= \frac{3.2}{16.7} \sim 0.19 \frac{m^3}{rev} \\
\Delta V_{C1,perRev,P} &= \frac{Q_{perRev,P}}{N_P}
\end{aligned} \qquad \text{Eq. 7.17}$$

[32] All these parameters were estimated based on visual inspection of figures on [25].

$$= \frac{0.19}{68} \sim 0.0028 m^3$$

$$\Delta V_{C1,perLobe,P} = \frac{\Delta V_{C1,perRev,P}}{Lo_P}$$

$$= \frac{0.0028}{24} \sim 1.17 \times 10^{-4} m^3$$

$\Delta V_{C1,Rat,P} = \Delta V_{C1,perLobe,P}$ (Eq. 3.5)

$D_{c,P} > 0.071 \sim 7.5\ cm$

References

[1] GWEC, "Global wind report - annual market update 2010," 2010.

[2] Arthur Akers and et.al., *Hydraulic Power System Analysis*. New York, NY, USA: Taylor and Francis Group, 2006, vol. I, hydraulic pump and motor analysis.

[3] Vestas Americas Inc, V80-2.0 MW, April 2009.

[4] Giorgio Rizzoni, *Principles and Applications of Electrical Engineering*, 5th ed.: Mc Graw Hill, 2007.

[5] William Rampen, "Gearless Transmissions for Large Wind Turbines - The history and future of hydraulic drives," , Bremen, November 2006, pp. 1-5.

[6] Wikov Wind, "Wind Ligth and reliable gearboxes for eind turbine drives," Wind, Wikov, Hronov, Brochure 2011.

[7] Ray J. Hicks, "Optimized gearbox design for modern wind turbines," Orbital2 Ltd, Wales, 2004.

[8] Wikov Wind, "W2000 2MW Wind Turbine," Wikov Wind, Business brochure 2010.

[9] Ray Hicks, "Experience with compact orbital gears in service," *Proceedings of the Institution of Mechanical Engineers*, vol. 184, no. 30, pp. 85-94, April 1970.

[10] Jan van der Tempel, "Delft Offshore Turbine," DUWind, Delft University of Technology, Delft, October October 2011.

[11] Robert L. Norton, *Cam design and manufacturing handbook*, 2nd ed. New York, NY, USA: Industrial Press inc., 2009, cam, follower, radial cam.

[12] Keith Mobley, *Fluid Power dynamics*, Butterworth-Heinemann, Ed. Boston, MA, USA: Newnes, 2000, vol. I.

[13] Rabie Galal, *Fluid Power Engineering*. New York, NY, USA: McGraw Hill, 2009.

[14] Perry Kavanagh, "The dynamic modelling of an axial piston hydraulic pump," Department of Mechanical Engineering, University of Saskatchewan, Saskatoon, MSc. Thesis 1987.

[15] D McCloy and H Martin, *Control of Fluid Power Analysis and Design*, 2nd ed. Chichester, West Sussex, England: Ellis Horwood Limited, 1980.

[16] Terry Henshaw, *Reciprocating Pumps*. New York, NY, USA: Reinhold, 1987.

[17] John Miller, *The Reciprocating Pump*, 2nd ed. Malabar, Florida, USA: Krieger Publishing Company, 1995.

[18] Andrea Catania and Alessandro Ferrari, "Experimental Analysis, Modeling, and Control of Volumetric Radial Piston Pumps," *Journal of Fluids Engineering*, vol. 133, pp. (081103)1-12, August 2011.

[19] Artemis Intelligent Power Ltd. (2010, December) Artemis Intelligent power. [Online]. www.artemisip.com

[20] J. Manwell, J McGowan, and A. Rogers, *Wind Energy Explained*, 2nd ed. Amherst, Massachusetts , USA: John Wiley & Sons, Ltd., 2002.

[21] ENERCON, ENERCON Wind energy converters, July 2010.

[22] Siemens AG, Siemens Electric Machines s.r.o., Factory Drasov, 2010, Generator with cylindrical rotor Type 1DB.

[23] P Sen, *Principles of Electrical Machines and Power Electronics*, 2nd ed. Delhi, India: Wiley and Sons, 2009, reprinted version.

[24] Stephen Chapman, *Electric MachineryFundamentals*, 3rd ed. New York, NY, USA: McGraw Hill, 1999.

[25] Artemis Intelligent Power Ltd; Mitsubishi Power Systems Europe Ltd., Digital Displacement Technology, November 2011, Refference figures and parameters.

[26] William Rampen. (2009, October) Developing a Gearless Wind Transmissionwith Assistance from The Carbon Trust. [Online]. http://www.uhi.ac.uk/en/research-enterprise/energy/knowledge-bank/documents/Artemis_transmission_innovation.pdf

[27] Md. Ehsan, W. Rampen, and S. Salter, "Modeling of a Digital-Displacement Pump-Motors and Their Application as hydraulic drives for Nonuniform Loads," *Journal of Dynamic Systems, Measurement, and Control*, vol. 122, pp. 210-215, March 2000.

[28] H. Polinder, F. van der Pijl, G. de Vilder, and P. Tavner, "Comparison of Direct Drive and Geared Generator concepts for wind turbines," *IEEE Transactions on energy conversion*, vol. 21, pp. 725-732, September 2006.

[29] William Lovejoy, Sebastian Fixson, and Shaun jackson, "Product Costing Guidelines," Integrated Product Development, University of Michigan, Dearborn, 2009.

[30] CustomPartNet. (2009) Cost Estimator Machining. [Online].

http://www.custompartnet.com/estimate/machining/

[31] Brown & Sharpe Mfg. Company, *Brown & Sharpe Automatic Screw Machine Handbook*. Providence, Rhode Island, USA: Brown and Sharpe.

[32] John Sorensen, *Wind Energy Systems*, Jens Sorensen, Ed. United Kingdom: Woodhead Oublishing, 2010.

[33] Artemis Intelligent Power Ltd.- Mitsubishi Power Systems Europe Ltd., "The Artemis Digital transmission a lightweight, network supporting, powertrain for Sea Angel," in *EWEA 2012 Conference Proceedings*, Copenhaguen, DK, 2012.

[34] Allen Gears. (2012) The Allen Gears Epicyclic Efficiency benefits. [Online]. http://www.allengears.com/html/calculate-the-benefits.php

[35] Sauer Danfoss, "Section 2: Pressure and Speed Limits for Hydrostatic Units," in *Applications Manual*. Ames, Iowa, USA: Sauer Danfoss, 1997, p. 14.

[36] Thomas Akerman, *Wind Power in Power Systems*. New York: John Wiley & Sons, 2005.

[37] European Wind Energy Association, "Green Growth - The impact of wind energy on jobs and economy," European Wind Energy Association, Brussels, Internal Report 978-2-930670-00-3, 2012.

[38] SET Sustainable Energy Technologies GmbH. (2012, April) Electro-Mechanical diferential systems. [Online]. http://www.ghp-set.com/solutions/electro-mechanical-differential-systems

[39] Y Zweri, J Widborne, and L Sevneviratne, "Dynamic simulation of a single cylinder diesel engine including dynamometre and friction," *Proc Instn Mech Engrs*, vol. 213, no. Part D, pp. 391-402, 1999.

[40] ASCO Valve, Inc., *Engineering Information. Solenoid valves*, 2012th ed. California, USA: ASCO Valve, Inc., 2012. [Online]. http://www.ascovalve.com/

[41] W. Durfee and Z. Sun, *Fluid Power system dynamics*, University of Minnesota, Ed. Minneapolis, MN, USA: Center for Compact and Efficient Fluid Power, 2009, vol. I.

[42] ExxonMobil, "Mobil Aero Hf series - Aviation hydraulic fluids," Fairfax, VA, USA, Technical information 2011.

[43] Robert D Richardson and William L Erdman, "Variable speed wind turbine," 5,083,039, January 21, 1992.

[44] Gary Johnson, *Wind Energy Systems*. New York: Prentice Hall, 2001, vol. I.

[45] Y Zweri, J Whidborne, and L Seneviratne, "Detailed analytical model of a single cylinder diesel

engine in the crank domain," *Proc Instn Mech Engrs*, vol. 215, no. Part D, pp. 1197-1216, 2001.

[46] EngineersHandbook.com. (2006) EngineersHandbook.com. [Online]. http://www.engineershandbook.com/Tables/frictioncoefficients.htm

[47] De Wind UK, "DeWind D8.2 Technical Brochure," Technology House, Central Milton Keyness, Commercial Brochure 2011.

[48] K. Patra, *Engineering Fluid Mechanics and Hydraulic Machines*. Oxford, UK: Alpha Science, 2011.